



**HAL**  
open science

# Physiological and multi-omics studies of microbial sulfur metabolisms present in hydrothermal ecosystems

Maxime Allioux

► **To cite this version:**

Maxime Allioux. Physiological and multi-omics studies of microbial sulfur metabolisms present in hydrothermal ecosystems. Microbiology and Parasitology. Université de Bretagne occidentale - Brest, 2021. English. NNT: 2021BRES0113 . tel-03789624

**HAL Id: tel-03789624**

**<https://theses.hal.science/tel-03789624>**

Submitted on 27 Sep 2022

**HAL** is a multi-disciplinary open access archive for the deposit and dissemination of scientific research documents, whether they are published or not. The documents may come from teaching and research institutions in France or abroad, or from public or private research centers.

L'archive ouverte pluridisciplinaire **HAL**, est destinée au dépôt et à la diffusion de documents scientifiques de niveau recherche, publiés ou non, émanant des établissements d'enseignement et de recherche français ou étrangers, des laboratoires publics ou privés.

# THESE DE DOCTORAT DE

L'UNIVERSITE  
DE BRETAGNE OCCIDENTALE

ECOLE DOCTORALE N° 598  
*Sciences de la Mer et du littoral*  
Spécialité : *Microbiologie*

Par

**Maxime ALLIOUX**

**Physiological and multi-omics studies of microbial sulfur metabolisms present in hydrothermal ecosystems**

**Études physiologiques et multi-omiques de métabolismes du soufre présents dans les écosystèmes hydrothermaux**

Thèse présentée et soutenue à Plouzané, le 16 décembre 2021

Unité de recherche : Laboratoire de Microbiologie des Environnements Extrêmes (UMR 6197)

## **Rapporteurs avant soutenance :**

Ken TAKAI  
Directeur de recherche, JAMSTEC, Yokosuka  
(Japon)

Kai FINSTER  
Professeur, Aarhus University, Aarhus  
(Danemark)

## **Composition du Jury :**

Gwennola ERMEL (Présidente du jury)  
Professeure, Université de Rennes 1, Rennes

Ken TAKAI  
Directeur de recherche, JAMSTEC, Yokosuka (Japon)

Kai FINSTER  
Professeur, Aarhus University, Aarhus (Danemark)

Claire PRIGENT-COMBARET  
Directrice de recherche, CNRS, Lyon

Alexander SLOBODKIN  
Directeur de recherche, Winogradsky Institute of Microbiology,  
Moscou (Russie)

Karine ALAIN (Directrice de thèse)  
Directrice de recherche, CNRS, Plouzané

Mohamed JEBBAR (Co-directeur de thèse)  
Professeur, Université de Bretagne Occidentale, Plouzané

*Pour Titi et Francis*

## Acknowledgements/Remerciements

Cette thèse a été effectuée dans le Laboratoire de Microbiologie des Environnements Extrêmes (LM2E, UMR6197) au sein de l'IUEM de Plouzané, sous la direction de Karine Alain, Mohamed Jebbar et Zongze Shao. Ce travail a été financé par la Région Bretagne (allocation de recherche doctorale), l'École Doctorale des Sciences de la Mer et du Littoral ainsi que par l'IRP MICROBSEA.

L'aspect collaboratif est mis en avant dans cette courte prémisses car il a fait partie intégrante de la thèse et a permis de faire avancer le sujet ainsi que la réflexion scientifique. Il sera donc nécessaire de remercier les personnes concernées une ou plusieurs fois.

J'aimerais premièrement remercier mes trois directeurs de thèse avec une particulière attention à l'égard de Karine qui a su me guider au cours de ces trois années de travail toute en me laissant une grande part de liberté en vue d'un nouveau sujet prometteur et qui aura probablement pour vocation de s'installer en tant que thématique pérenne au laboratoire.

Mes deuxièmes remerciements vont aux membres de mon jury de thèse qui ont accepté l'évaluation de mes travaux de thèse : Ken Takai, Kai Finster, Gwennola Ermel, Claire Prigent-Combaret ainsi qu'Alexander Slobodkin.

Il m'est important de remercier les membres de l'équipe Kulturomics. Ce groupe nous a permis de collaborer et avancer sur nos thématiques respectives : Karine, Erwann, Sophie, Stéven, Marc et les stagiaires.

Une mention particulière est adressée aux anciens doctorants du laboratoire des deux côtés du grillage qui ont su partager leur bienveillance, sagesse, aide, bonne humeur, et moments de folies : Seb, Yang, Jordan, Sarah, Florian, Clarisse, Marc, Blandine, Marion, Pierre et Ashley.

De plus, j'aimerais remercier mes stagiaires qui ont pu accroître ma motivation durant la progression de ma thèse et qui ont apporté une aide significative au projet ainsi qu'une agréable atmosphère riche en péripéties et humour, Stéven, Solenne, Mélanie et Mila.

J'aimerais ensuite remercier tous les membres du laboratoire du côté IUEM avec qui il a été agréable de partager ces années au sein de la vie de laboratoire, tels que les vendredis « viennoiseries », les mardis « burger » partis trop tôt, les tant attendus repas de Noël et autres événements : Erwann, Yann, Karine, Stéphanie, Nadège, Jordan, Sarah, Marc, Florian, Clarisse, Blandine, Ashley, Jie, Stéven, Fabien, Loïs ainsi que les nombreux stagiaires. J'aimerais également remercier nos collègues de l'autre côté de la barrière à l'Ifremer, qui ont été d'une aide significative pour le projet et l'ouverture scientifique, Cas, Sébastien, Erwan, Joanne, Françoise, Anne, Didier, Yang, David, Maurane, Elodie ainsi que les autres avec un petit clin d'œil particulier à l'attention de Xavier.



J'aimerais également remercier toute l'équipe du Sebimer de l'Ifremer pour leur aide et mise à disposition afin de faire avancer les projets de chacun.

I would like to thank our colleagues from the laboratory of Diversity and Ecology of Extremophilic Microorganisms in Moscow and part in NEPTUNE project, Alexander Slobodkin, Galina Slobodkina, Alexander Merkel, Anastasia Frolova, Tatyana Sokolova and Elizaveta Bonch-Osmolovskaya, which always welcomed us for the best in Moscow and which was as a great and productive collaboration among those three years.

I would like also to thank our colleagues from the IRP MICROBSEA, Zongze Shao and Xiang Zeng. It was very unfortunate that we didn't manage to meet in Xiamen due to the pandemia.

Furthermore, I would like to thank Heidi Aronson and Jan Amend from the Amend lab of University of Southern California for the new exciting collaboration about sulfur disproportionation and thermodynamics.

Je remercie également mes membres de CSI, Anne Godfroy, Erwan Roussel, Loïs Magnien, Anne Postec et Stefan Lalonde pour leurs conseils durant ces trois années.

Je remercie de plus une merveilleuse partie de la communauté scientifique qui a fait du partage de connaissances, de données et de méthodologie un fondement, en particulier Alexandra Elbakyan, la créatrice de SciHub ainsi que les créateurs de logiciels Open Access, notamment Ryan Wick pour les assemblages de génome, qui ont permis l'aboutissement de cette thèse.

Un petit merci est adressé à mes sponsors non officiels, Nostalgie, l'ancien Baroom, et Bibus.

Et pour finir j'aimerais remercier tous mes proches.

# TABLE OF CONTENTS

<b>Acknowledgements/Remerciements</b>	p. 3
<b>Table of contents</b>	p. 5
<b>List of figures</b>	p. 8
<b>List of tables</b>	p. 10
<b>Abbreviations</b>	p. 11
<b>Chapter 1: Introduction</b>	p. 12
<b>1. Microbial sulfur cycle overview</b>	p. 12
1.1. Generalities about the sulfur cycle	p. 12
1.2. ISC reduction: reduction of sulfate, sulfite, thiosulfate and sulfur	p. 21
1.3. Inorganic sulfur compounds oxidation	p. 23
1.4. Inorganic sulfur compounds disproportionation	p. 24
1.5. Organic sulfur compounds	p. 39
1.6. Inorganic sulfur compounds comproporationation	p. 44
<b>2. Hydrothermal and geothermal environments, and their associated sulfur cycles</b>	p. 46
2.1. Preamble	p. 46
2.1.1. Deep-sea hydrothermal vents	p. 47
2.1.2. Shallow-sea hydrothermal vents	p. 54
2.1.3. Geothermal hot springs	p. 55
2.3. Generalities about sulfur compounds and sulfur cycling in hydrothermal and geothermal systems	p. 56
2.4. Diversity of ISC-reducers in marine hydrothermal vents	p. 59
2.5. Diversity of sulfur-oxidizers in marine hydrothermal vents	p. 60
2.6. Sulfur-disproportionators from hydrothermal vents	p. 61
2.7. Organic sulfur compounds in hydrothermal vents and microorganisms degrading them	p. 62
2.8. Sulfur comproporationation in marine hydrothermal vents	p. 65
<b>3. PhD initial goals and scientific questions</b>	p. 66
3.1. Characterization of new microorganisms involved in the sulfur cycle by culture and genomics	p. 67
3.2. Inorganic sulfur compound disproportionation understanding by multi-omics comparative approaches	p. 68
3.3. Investigation of the microbial sulfur cycle in an ecological context	p. 68

<b>Chapter 2: Tentative attempts to isolate deep-sea hydrothermal microorganisms able to use organic sulfur compounds</b>	p. 69
<b>1. Preamble</b>	p. 69
<b>2. Materials and Methods</b>	p. 69
<b>3. Results and Discussion</b>	p. 71
<b>4. Conclusions and Perspectives</b>	p. 71
<b>Chapter 3: Exploring inorganic sulfur compound disproportionation in hydrothermal vents</b>	p. 72
<b>1. Preamble</b>	p. 72
<b>2. Materials and Methods</b>	p. 73
2.1. <i>Collection of samples and pure strains</i>	p. 73
2.2. <i>Culture media</i>	p. 74
2.3. <i>Enrichment cultures, isolation of microorganisms and growth conditions for pure strains</i>	p. 76
2.4. <i>DNA extraction</i>	p. 77
2.5. <i>16S rRNA gene sequence analyses</i>	p. 78
2.6. <i>Genomic sequencing and assembly</i>	p. 79
2.7. <i>Genomic analyses</i>	p. 80
2.8. <i>Comparative genomics</i>	p. 82
2.9. <i>Comparative proteomics trial experiment</i>	p. 83
2.10. <i>Chemical monitoring, growth kinetics and proteomics</i>	p. 85
<b>3. Results and Discussion</b>	p. 88
3.1. <i>Physiology and genomics of ISC-disproportionators</i>	p. 88
3.1.1. <i>Cultivation of marine hydrothermal microorganisms able to disproportionate inorganic sulfur compounds</i>	p. 88
3.1.2. <i>Analyses of microbial genomes from hydrothermal species able to disproportionate inorganic</i>	p. 92
3.2. <i>Search for genomic markers of ISC disproportionation</i>	p. 163
3.3. <i>Monitoring of the S<sup>0</sup>-dismutation reaction by proteomics and chemical analysis: a preliminary study</i>	p. 172
<b>4. Discussion, conclusions and perspectives</b>	p. 184

<b>Chapter 4: Investigation of sulfur comproportionation in hydrothermal and geothermal samples, and with pure strains</b>	p. 192
<b>1. Preamble</b>	p. 192
<b>2. Materials and Methods</b>	p. 192
<b>3. Results and Discussion</b>	p. 195
<b>4. Conclusions and Perspectives</b>	p. 196
<b>Chapter 5: Investigation of the microbial sulfur cycle in geothermal springs</b>	p. 197
<b>1. Preamble</b>	p. 197
<b>2. Article section</b>	p. 197
<b>3. Conclusions and Perspectives</b>	p. 233
<b>General Conclusion</b>	p. 234
<b>Additional Works</b>	p. 236
<b>References</b>	p. 238
<b>Abstract/Résumé</b>	p. 263

## List of figures

<i>Figure 1: Inorganic sulfur compounds oxidation states (Suzuki et al., 1999).</i>	p. 13
<i>Figure 2: General sulfur cycle associated to redox reactions driven by the microorganisms (Madigan et al., 2015).</i>	p. 14
<i>Figure 3: Dsr-dependent dissimilatory sulfur species reduction and oxidation in prokaryotes (Neukirchen and Sousa, 2021).</i>	p. 16
<i>Figure 4: The biogeochemical sulfur cycle of marine sediments (Jørgensen et al., 2019).</i>	p. 17
<i>Figure 5: The dissimilatory conversions within the marine sulfur cycle (Van Vliet et al., 2021).</i>	p. 19
<i>Figure 6: The sulfate respiratory pathway (Santos et al., 2015).</i>	p. 22
<i>Figure 7: Overview of the putative pathways of oxidative sulfur metabolism in green sulfur bacteria (Gregersen et al., 2011).</i>	p. 23
<i>Figure 8: Diagram representing the simplified marine sedimentary sulfur cycle (Amend, 2004).</i>	p. 24
<i>Figure 9: Proposed pathways for thiosulfate and sulfur disproportionation in cultures of <i>Desulfocapsa sulfoexigens</i> (Finster, 2008).</i>	p. 31
<i>Figure 10: Envisaged mechanisms towards <math>S_0</math> uptake by <math>S_0</math> respiring bacteria (Zhang et al., 2021).</i>	p. 34
<i>Figure 11: Proposed pathway of chemolithotrophic sulfide oxidation and sulfur disproportionation by <i>Desulfurivibrio alkaliphilus</i> (Thorup et al., 2017).</i>	p. 35
<i>Figure 12: Arrangement of the YTD gene cluster in genomes of SDB (sulfur disproportionating bacteria) and SRB (sulfate reducing bacteria) (Umezawa et al., 2020).</i>	p. 38
<i>Figure 13: Schematic representation of the major pathways of DMS production and transformation in marine environment (Schäfer et al., 2010).</i>	p. 40
<i>Figure 14: Biochemical and chemical interconversions of C1-sulfur compounds and key intermediates in carbon and sulfur metabolism that have been observed across a wide range of microorganisms (Schäfer et al., 2010).</i>	p. 40
<i>Figure 15: Metabolic pathways involved in DMS degradation/transformation, one-carbon and sulfur oxidation annotated with presence/absence of specific genes in the genomes of Methylophaga. (Kröber and Schäfer, 2019).</i>	p. 44
<i>Figure 16: Values of <math>\Delta Gr</math> for sulfur comproportionation as a function of temperature and pH (Amend et al., 2019).</i>	p. 46

<i>Figure 17: Map of known vent sites and sites thought to exist from the detection of chemical signals in the water column, adapted from the InterRidge Vents Database (Humphris and Klein, 2018).</i>	p. 47
<i>Figure 18: Deep-sea hydrothermal environments simplified diagram (Flores and Reysenbach, 2007).</i>	p. 48
<i>Figure 19: General microbial habitats at deep-sea hydrothermal vents (Dick, 2019).</i>	p. 51
<i>Figure 20: Various pathways of autotrophic CO<sub>2</sub> fixation in Bacteria and Archaea (Hugler &amp; Sievert, 2011).</i>	p. 53
<i>Figure 21: Schematic representation of the hydrothermal processes at shallow-water hydrothermal vents and the additional dynamic driver's characteristic of their depth range distribution (Price and Giovannelli, 2017).</i>	p. 55
<i>Figure 22: Comparison of the synteny of the three candidate CDSs discovered by comparative genomics.</i>	p. 165
<i>Figure 23: TmHMM statistics and Phyre2 predictions diagrams for Thermosulfuriphilus ammonigenes longest central protein obtained by comparative genomics</i>	p. 168
<i>Figure 24: Structural representation of the polysulfide reductase with bound quinone inhibitor, pentachlorophenol (PCP) of Thermus thermophilus HB27 from RCSB PDB database.</i>	p. 170
<i>Figure 25: Model for the role of TorD in the TorA maturation pathway with bis(MGD)Mo cofactor (Ilbert et al., 2003).</i>	p. 171
<i>Figure 26: Growth curves of T. atlanticus and D. thermophilus under S<sup>0</sup> disproportionation and dissimilatory sulfate reduction growth conditions based on three replicates.</i>	p. 175
<i>Figure 27: Hydrogen sulfide production over time for the three replicates of T. atlanticus and D. thermophilus and associated negative controls incubated under dissimilatory sulfate reduction conditions.</i>	p. 176
<i>Figure 28: Chromatograms from LC-MS/MS analyses of cellular soluble protein extracts of T. atlanticus, D. thermophilus and T. dismutans under S<sup>0</sup> disproportionation and sulfate reduction growth conditions.</i>	p.177

## List of tables

---

<i>Table 1: The genes of sulfur metabolism proteins in elemental sulfur-disproportionating microorganisms (Slobodkin and Slobodkina, 2019).</i>	p. 37
<i>Table 2: Reactions involved in the sulfidogenic and methanogenic degradation of various methylated sulfur compounds (Scholten et al., 2003).</i>	p. 42
<i>Table 3: Energetically favorable redox reactions available to chemolithotrophic microorganisms in deep-sea hydrothermal environments (Takai et al., 2006).</i>	p. 52
<i>Table 4: Thermophilic and hyperthermophilic species isolated from deep-sea hydrothermal vents according to the electron donor and acceptor they use for growth (Godfroy et al., in press).</i>	p. 54
<i>Table 5: Results of the genomic annotation of the three candidate CDSs of sulfur disproportionation obtained with various software (MaGe platform, blast against NCBI and UniprotKB database and functional prediction by InterProScan) for the 6 species: Dissulfuribacter thermophilus, Thermodesulfatator atlanticus, Thermosulfurimonas dismutans, Thermosulfurimonas marina, Thermosulfuriphilus ammonigenes and Dissulfurirhabdus thermomarina.</i>	p. 166
<i>Table 6: BUSCA prediction of GO-terms and protein features for each of the 3 CDSs of Dissulfuribacter thermophilus, Thermodesulfatator atlanticus, Thermosulfurimonas dismutans, Thermosulfurimonas marina, Thermosulfuriphilus ammonigenes and Dissulfurirhabdus thermomarina.</i>	p. 168
<i>Table 7: Mean cell concentration between the four replicates of cultures carried out under <math>S^0</math> dismutation and sulfate reduction, in T. atlanticus and D. thermophilus cultures, before and after a short centrifugation to remove the ferrihydrite.</i>	p. 173
<i>Table 8: Protein concentrations for each culture condition, and each protein fraction.</i>	p. 173
<i>Table 9: Results and associated statistics of LC-MS/MS analyses for cellular soluble protein extracts of T. atlanticus, D. thermophilus and T. dismutans under <math>S^0</math> disproportionation and sulfate reduction conditions based on PGAP annotations and predictions.</i>	p. 178
<i>Table 10: Spectra annotation analyses and comparison of D. thermophilus grown under <math>S^0</math> disproportionation and sulfate reduction conditions.</i>	p. 179
<i>Table 11: Spectra annotation analyses and comparison of T. atlanticus grown under <math>S^0</math> disproportionation and sulfate reduction conditions.</i>	p. 180
<i>Table 12: Spectra annotation analyses and comparison of T. dismutans grown under <math>S^0</math> disproportionation and sulfate reduction conditions.</i>	p. 181
<i>Table 13: Composition of sulfur comproportionation media and incubation conditions, for each inoculum type.</i>	p. 194

---

## Abbreviations

AAI: Average Amino acid Identity  
ANI: Average Nucleotide Identity  
AprAB: Adenylylsulfate or APS reductase  
AsrABC: Anaerobic sulfite reductase  
CBB: Calvin-Benson-Bassham  
CDS: Coding DNA Sequence  
CRISPR: Clustered Regularly Interspaced Short Palindromic Repeats  
DDH: DNA–DNA hybridization  
DHPS: 2,3-dihydroxypropane-1-sulfonate  
DMS: Dimethylsulfide  
DMSO: Dimethyl sulfoxide  
DMSP: Dimethylsulfoniopropionate  
DNA: Deoxyribonucleic acid  
DNRA: Dissimilatory Nitrate Reduction to Ammonia  
DSMZ: Deutsche Sammlung von Mikroorganismen und Zellkulturen GmbH  
Dsr: Dissimilatory sulfite reductase  
FccAB: Flavocytochrome C/sulfide dehydrogenases  
Fsr: F<sub>420</sub> dependent sulfite reductase  
GSB: Green Sulfur Bacteria  
GTDB: Genome Taxonomy Database  
HydDACB: Sulfhydrogenase/hydrogenase I  
HPLC: High-Performance Liquid Chromatography  
ISC: Inorganic Sulfur Compounds  
JGI IMG: Integrated Microbial Genomes & Microbiomes  
LC-MS/MS: Liquid chromatography–mass spectrometry  
MAG: Metagenome-Assembled Genome  
MaGe: Magnifying Genomes platform  
MccA/SirA: Sulfite reductase cytochrome  
NCBI: National Center for Biotechnology Information  
Npsr: NADH-dependent persulfide reductase  
NSAF: Normalized Spectral Abundance  
Otr: octoheme Tetrathionate reductase  
PAI: Protein Abundance Index  
PCR: Polymerase Chain Reaction  
PIPES: Piperazine-N,N'-bis(2-ethanesulfonic acid)  
PGAP: NCBI Prokaryotic Genome Annotation Pipeline  
PhsABC: Thiosulfate reductase  
Prokka: Rapid prokaryotic genome annotation  
PsrABC: Polysulfide reductase  
QmoABC: Quinone-interacting membrane-bound oxidoreductase  
RAST: Rapid Annotation of microbial genomes using Subsystems Technology  
Rhd-TusA-DsrE2: Rhodanase-like protein-sulfurtransferase gene cluster  
rRNA: Ribosomal ribonucleic acid  
rTCA: Reverse tricarboxylic  
SAT: Adenylyltransferase  
SDB: sulfur disproportionating bacteria  
ShyCBDA/SuDh: Sulfhydrogenase/hydrogenase II  
Sqr: Sulfide:quinone-oxidoreductase  
SOR: Sulfur oxygenase reductase  
SRB: Sulfate reducing bacteria  
SreABC: Sulfur reductase  
UBO: Université de Bretagne Occidentale  
UBOCC: UBO Culture Collection  
TetH: Tetrathionate hydrolase  
TsdA: Thiosulfate dehydrogenase  
TtrABC: Tetrathionate reductase



# Chapter 1: Introduction

## 1. Microbial sulfur cycle overview

### *1.1 Generalities about the sulfur cycle*

Sulfur is estimated to be the sixth most abundant element in microbial biomass. On Earth, sulfur is residing naturally in minerals such as metal sulfides, in gases such as SO<sub>2</sub>, H<sub>2</sub>S, in aqueous solutions such as SO<sub>4</sub><sup>2-</sup> and HS<sup>-</sup> and could be present as elemental sulfur (Klotz et al., 2011). Chemical studies of sulfur are relatively ancient (Meyer, 1976). Sulfur have been used across human history for various purposes, while sulfur chemistry and microbiology have changed our views on many aspects of microbially driven biogeochemical cycles and led to advances in new methods, techniques, and discoveries.

Sulfur is highly redox sensitive, occurring in a variety of oxidation states from -2 in sulfide to +6 in sulfate. The common intermediate oxidation states are 0 in elemental sulfur (S<sup>0</sup>) and +4 in sulfite (SO<sub>3</sub><sup>2-</sup>) (Fig.1). Because of its abundance, its range of oxidation states, and its chemical reactivity, sulfur plays an important role in biogeochemical and metabolic processes in a wide diversity of microorganisms. Sulfur cycling in open ocean, marine sediments, and continental environments is getting better and better established, and the isotopic fractionations, redox intermediates, related enzymes, organisms involved, and symbiotic relationships have largely been studied and reviewed (Amend et al., 2004; Rabus et al., 2013; Madigan et al., 2015; Wasmund et al., 2017; Avetisyan et al., 2019; Jørgensen et al., 2019; Wu et al., 2021). A recent prospective article by Jørgensen (2021) provides an extensive introduction to the biochemical cycle of sulfur in marine sediments and perspectives in this field.

-2	0	+2	+4	+6
H <sub>2</sub> S	S	(SO)	SO <sub>2</sub>	SO <sub>3</sub>
Hydrogen sulfite	Elemental sulfur	Sulfur monoxide	Sulfur dioxide	Sulfur trioxide
HS <sup>-</sup>	S <sub>8</sub> /S <sup>0</sup>	H <sub>2</sub> SO <sub>2</sub>	H <sub>2</sub> SO <sub>3</sub>	H <sub>2</sub> SO <sub>4</sub>
		Sulfoxylic acid	Sulfurous acid	Sulfuric acid
			SO <sub>3</sub> <sup>2-</sup>	SO <sub>4</sub> <sup>2-</sup>
			Sulfite	Sulfate
	S		SO <sub>3</sub> <sup>2-</sup>	
		Thiosulfate		
	S		SO <sub>3</sub> <sup>2-</sup>	
		Tetrathionate		
	S			SO <sub>3</sub>
	<sup>-2</sup> S	S <sub>n</sub>		
		Polysulfide		

Figure 1: Oxidation states of inorganic sulfur compounds (ISC) (Suzuki et al., 1999).

Sulfur is present in amino acids such as cysteine and methionine, and also in several vitamins, including thiamin, biotin, and lipoic acid, and is commonly supplied to cells as sulfate (Madigan et al., 2015). Elemental sulfur is one of the most ubiquitous sulfur species in sediments and can be formed by biological and chemical oxidation of H<sub>2</sub>S (Rabus et al., 2013). Sulfur can be found in inorganic forms such as hydrogen sulfide (H<sub>2</sub>S), elemental sulfur (S<sup>0</sup>), sulfite (SO<sub>3</sub><sup>2-</sup>), thiosulfate (S<sub>2</sub>O<sub>3</sub><sup>2-</sup>), tetrathionate (S<sub>4</sub>O<sub>6</sub><sup>2-</sup>), polythionates (S<sub>n</sub>(SO<sub>3</sub>)<sub>2</sub><sup>2-</sup>), sulfate (SO<sub>4</sub><sup>2-</sup>) and polysulfides (S<sub>n</sub><sup>2-</sup>), or organic forms such as methanethiol (CH<sub>3</sub>SH), dimethyl sulphide ((CH<sub>3</sub>)<sub>2</sub>S), carbon disulfide (CS<sub>2</sub>) and more complex molecules such as taurine C<sub>2</sub>H<sub>7</sub>NO<sub>3</sub>S and its derivatives notably.

Currently, the global sulfur cycle is relatively well described, especially, the reactions of sulfo-oxidation, sulfo-reduction and sulfate-reduction, and the taxa carrying out these reactions are identified for most of them (Fig.2) (Klotz and al., 2011; Madigan et al., 2015). The sulfur cycle is particularly well known in marine sediments (Wasmund et al., 2017; Jørgensen et al., 2019; Jørgensen, 2021).

### Key Processes and Prokaryotes in the Sulfur Cycle

Process	Organisms
<b>Sulfide/sulfur oxidation</b> ( $\text{H}_2\text{S} \rightarrow \text{S}^0 \rightarrow \text{SO}_4^{2-}$ )	
Aerobic	Sulfur chemolithotrophs ( <i>Thiobacillus</i> , <i>Beggiatoa</i> , many others)
Anaerobic	Purple and green phototrophic bacteria, some chemolithotrophs
<b>Sulfate reduction</b> (anaerobic) ( $\text{SO}_4^{2-} \rightarrow \text{H}_2\text{S}$ )	<i>Desulfovibrio</i> , <i>Desulfobacter</i> <i>Archaeoglobus</i> (Archaea)
<b>Sulfur reduction</b> (anaerobic) ( $\text{S}^0 \rightarrow \text{H}_2\text{S}$ )	<i>Desulfuromonas</i> , many hyperthermophilic Archaea
<b>Sulfur disproportionation</b> ( $\text{S}_2\text{O}_3^{2-} \rightarrow \text{H}_2\text{S} + \text{SO}_4^{2-}$ )	<i>Desulfovibrio</i> , and others
<b>Organic sulfur compound oxidation or reduction</b> ( $\text{CH}_3\text{SH} \rightarrow \text{CO}_2 + \text{H}_2\text{S}$ ) ( $\text{DMSO} \rightarrow \text{DMS}$ )	Many organisms can do this
<b>Desulfurylation</b> (organic-S $\rightarrow$ $\text{H}_2\text{S}$ )	Many organisms can do this

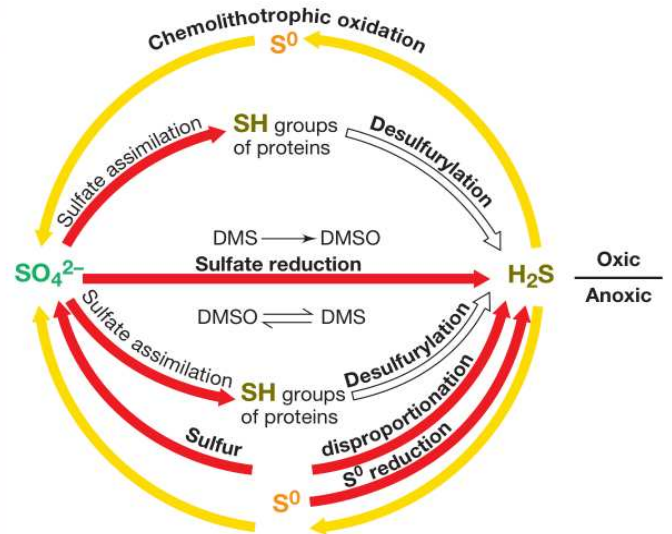


Figure 2: General sulfur cycle associated to redox reactions driven by the microorganisms. Oxidations are indicated by yellow arrows and reduction by red arrows. Reactions without redox changes are in white. DMS: dimethylsulfide, DMSO: dimethylsulfoxide. The up-half circle on the diagram are the reactions carried out under oxic conditions, and the down half circle those performed under anoxic conditions (Madigan et al., 2015).

Metabolic reactions of the microbial sulfur cycle can be subdivided into five main categories. Firstly, reactions of sulfur compound reduction, generally associated to sulfate, sulfite and elemental sulfur. Secondly, reactions of sulfur compound oxidation, generally associated to sulfide such as hydrogen sulfide, and elemental sulfur. Thirdly, reactions of sulfur disproportionation, generally associated to thiosulfate, elemental sulfur and sulfite. Fourthly, the use of organic sulfur species such as methanethiol or dimethylsulfide which can be reduced or oxidized and used as carbon sources. Finally, the microbes have specific pathways for sulfur assimilation required for diverse cellular functions, but there is no production of energy associated to this process. A wide range of bacterial and archaeal phyla are involved in the sulfur cycle. The sulfur cycle also includes abiotic reactions that are also important in certain environments, such as volcanic environments, but this introduction will be focused on the biotic reactions, specifically the microbial ones.

The microorganisms using sulfur compounds can be classified by different ways. They can be classified based on their taxonomic position but also based on their physiological characteristics. Historically they have been classified into taxonomic groups with an associated function, called: colorless sulfur bacteria, purple sulfur bacteria, green sulfur bacteria, sulfate reducing microorganisms and elemental sulfur reducing microorganisms (De Anda et al., 2018).

#### Methods to study the sulfur cycle

The microbial sulfur cycle can be studied with various approaches, based on physics, chemistry, and biology, with several techniques listed in the review by Jørgensen (2021), such as microbial activity measurements with radiolabelled tracers, cultivation, molecular ecology approaches (qPCR, metagenomics, metabarcoding), measurements of chemical species (isotopes, HPLC, modeling). During this PhD, the main approaches used were cultivation and genomics. Among the cultivation approaches targeting different metabolisms, the cultivation of sulfur disproportionators is not the easiest one. Culture allows to investigate in details the physiology of a microorganism, such as for example its range of temperature or pH for growth, its spectrum of used electron donors and acceptors, and much more.

Genomics and metagenomics approaches are interesting in order to determine a genetic potential, but must be implemented with an awareness of their limitations. They can be independent for some cases of culture and are of a great use for studying especially microorganisms difficult to grow. Some analyses could then be performed with genomic annotation to investigate microbial genomes. New tools are developed relying on sequence homology and database which are getting more and more complete every day.

The review of Ayling et al., 2020 shows the current trends and approaches in metagenomics.

It is also interesting to note that, in contrast to the early days of bioinformatics, there is now an increasing number of bioinformaticians and interest in the discipline, as well as bioinformatics software for broad application panels. However, researchers may now be confronted with too much software, with comparison becoming difficult due to the phenomenal number of software packages available with deep scientific knowledge and specificity. Genome annotation software and pipelines such as Prokka (Rapid prokaryotic genome annotation), RAST (Rapid Annotation of microbial genomes using Subsystems Technology), MaGe (Magnifying Genomes) platform, JGI IMG (Integrated Microbial Genomes & Microbiomes) and PGAP (NCBI Prokaryotic Genome Annotation Pipeline) can be used to identify and analyze specific

enzymes associated to sulfur cycle (Seemann, 2014; Brettin et al., 2015; Tatusova et al., 2016; Chen et al., 2017; Vallenet et al., 2017). Nevertheless, these approaches their own limitations. As a kind of example, enzymes such as the ones encoded by the Dsr (Dissimilatory sulfite reductase subunits) genes are not necessarily linked to reductive processes, they can also be associated to oxidative process and possibly to sulfur compound disproportionation (Fig. 3). The sulfur cycle could also be investigated through culture independent methods, combining for example isotopic fractionations of sulfur compounds, metagenomics and metaproteomics (Bell et al., 2021).

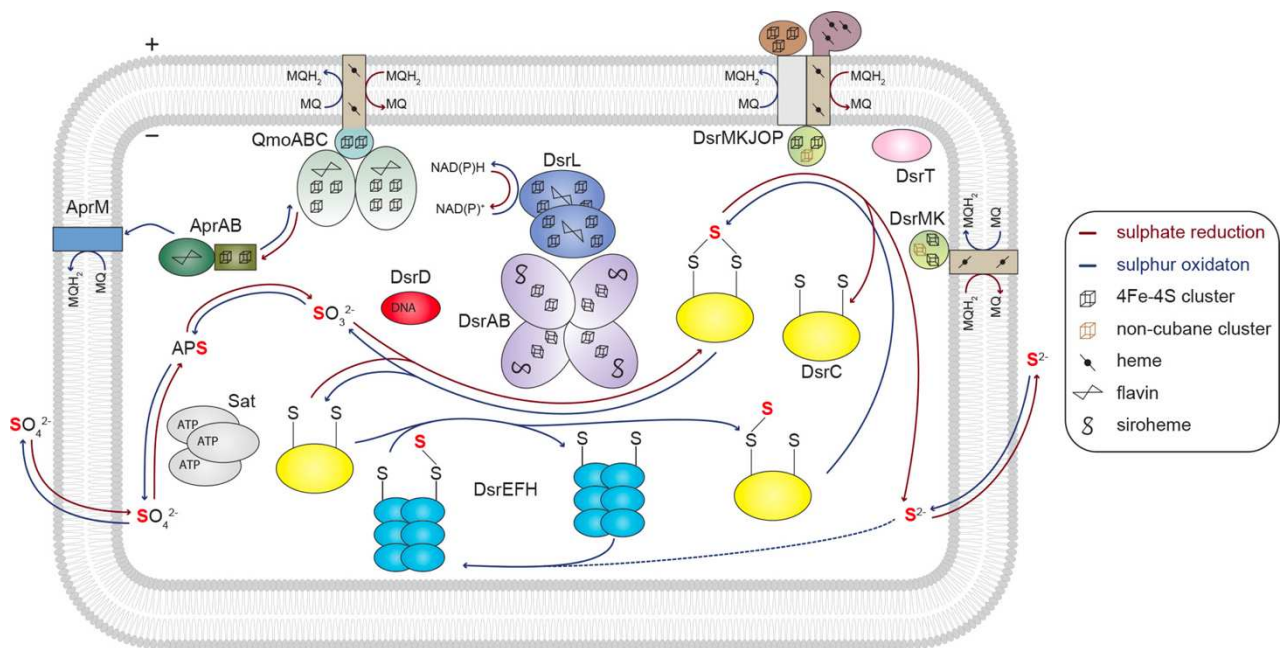


Figure 3: Dsr-dependent dissimilatory sulfur species reduction and oxidation in prokaryotes. Schematic representation of the main complexes and reactions involved in Dsr-dependent dissimilatory sulfate reduction (red arrows) and/or sulfur oxidation (blue arrows). Homologous proteins are represented with the same colour code. MQ – Menaquinone (Neukirchen and Sousa, 2021).

### The microbial sulfur cycle in natural environments

The sulfur cycle is best documented in marine sediments. Diverse microorganisms are present in various niches in marine sediments, and derive their energy by transforming sulfur compounds of various redox states (Fig. 4). The sedimentary sulfur cycling is primarily driven by sulfate reduction, associated to other geochemical cycles and consequently has a significant implication for cellular and ecosystem level processes, especially in organic rich sediments (Wasmund et al., 2017). At a global scale, it was predicted that the remineralization of up to 29% of the organic matter deposited on the seafloor is carried out by sulfate reducers and that

11.3 teramoles of sulfate are reduced to  $\text{H}_2\text{S}$  in marine sediments every year (Bowles et al., 2014). Anaerobic oxidation of methane coupled to sulfate reduction is also present in marine sediments. Sulfide resulting from sulfate reduction process is used by sulfide oxidizers, and it is estimated that 80 to 90% of this sulfide is re-oxidized by sulfide oxidizers (Wasmund et al., 2017; Jørgensen et al., 2019). Sulfide oxidizers are restricted to upper sediment where they depend on electron acceptors with high redox potentials such as oxygen and nitrate. Several metabolisms lie on sulfur intermediates, including sulfite,  $\text{S}^0$ , polysulfides, and polythionates, for reduction but also oxidation, and disproportionation metabolisms. Some microorganisms are also able to consume or produce organic sulfur compounds in marine sediments, and to derive their energy from the transformation of these organosulfur compounds, but these reactions are much less documented. Nitrogen and sulfur microbial cycles are also connected through specific metabolisms such as sulfide and sulfur oxidation coupled to nitrate reduction, or dissimilatory nitrate reduction to ammonia (DNRA).

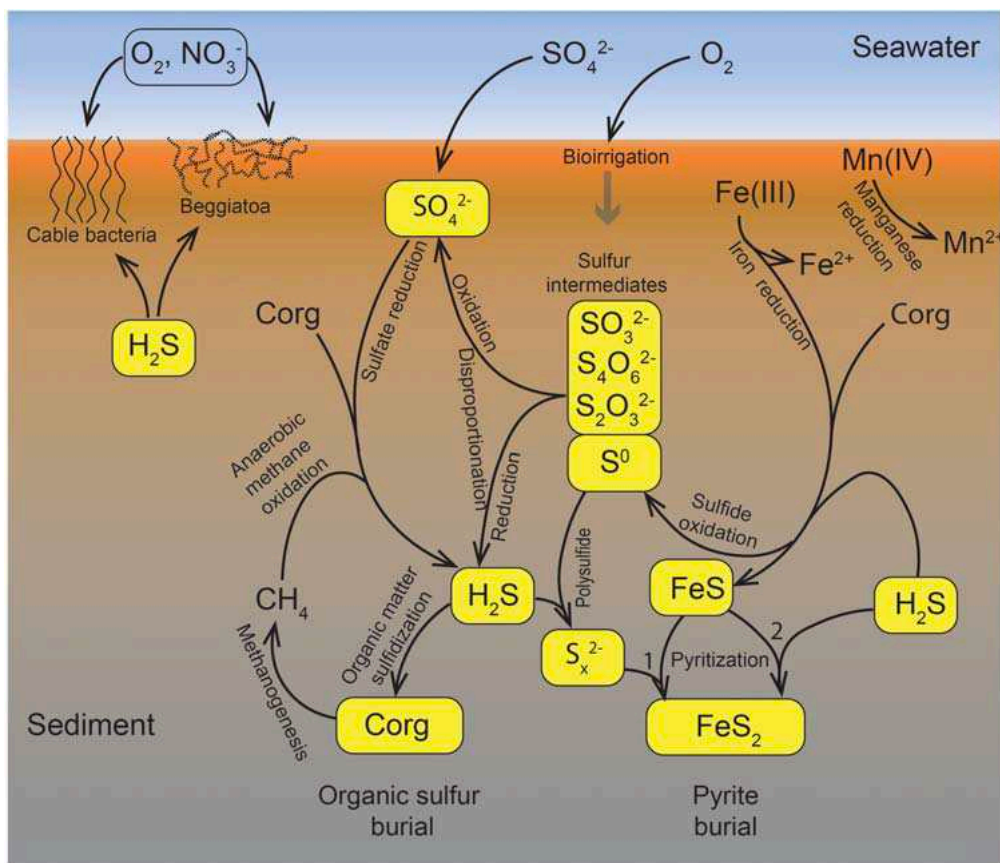


Figure 4: The biogeochemical sulfur cycle of marine sediments. Arrows indicate fluxes and pathways of biological or chemical processes (Jørgensen et al., 2019).

The microbial sulfur cycle has also been investigated in other natural environments. For example, it is documented in the terrestrial deep subsurface (Bell et al., 2020), in oceanic oxygen minimum zones (Callbeck et al., 2021), and in expanding dysoxic and euxinic marine waters (Van Vliet et al., 2021). The study of Van Vliet et al. (2021) well describe the complexity of the sulfur cycle in marine sediments in their recent study (Fig. 5). As geochemical cycles are connected, the sulfur cycle is directly connected to carbon, hydrogen, nitrogen, iron, manganese cycles and others, which complicates its understanding (Fig. 4) (Jørgensen et al., 2019; Wu et al., 2021).



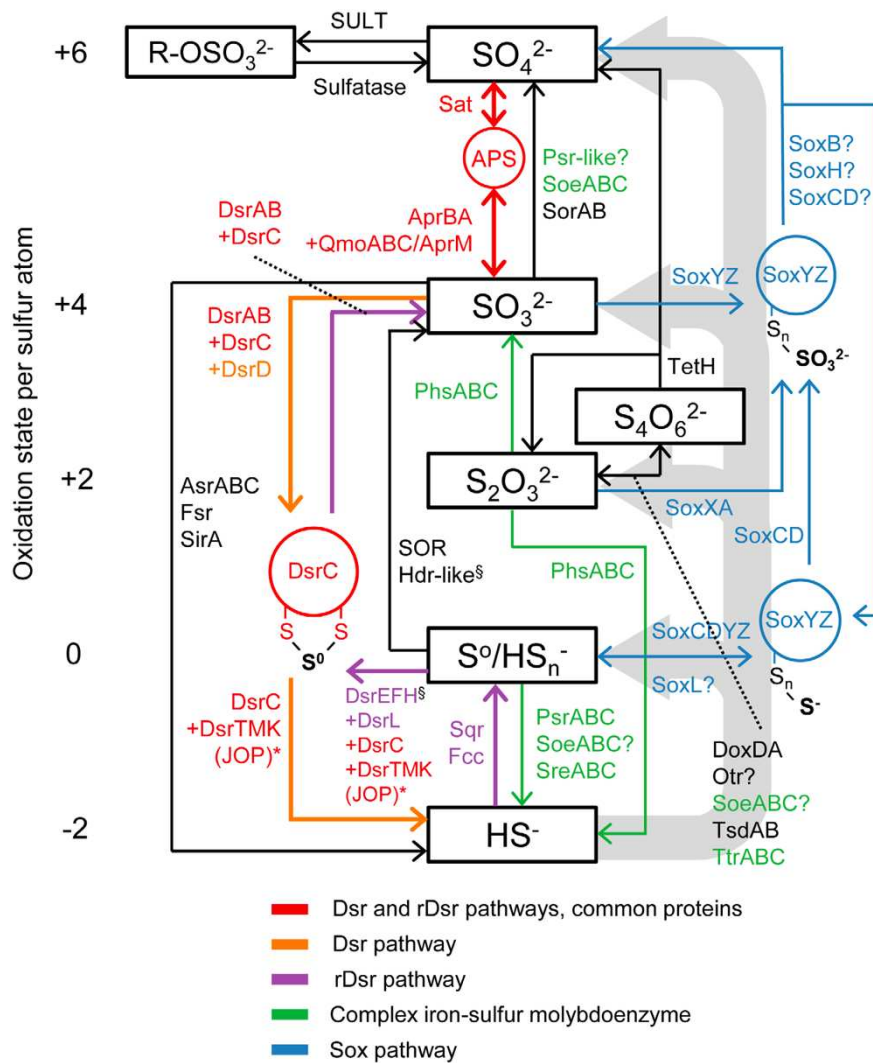


Figure 5: The dissimilatory conversions within the marine sulfur cycle. The oxidation state of the inorganic species is indicated on the left. Abiotic and assimilatory reactions are not indicated, except for the abiotic oxidation of sulfide which is illustrated by wide grey arrows. The  $S^0$  in DsrC-trisulfide is considered zerovalent. The sulfur atom in APS has an oxidation state of +6, and those in tetrathionate have an oxidation state of +2.5. A question mark symbol (?) shows that involvement is uncertain. The asterisk symbol (\*) indicates that DsrT is required for sulfide oxidation in green sulfur bacteria, but is also found in sulfate reducing bacteria. Protein complexes other than DsrTMK(JOP) can also transfer electrons to DsrC to enable this reaction. The section symbol (§) indicates that the rhodanese sulfurtransferases Rhd-TusA-DsrE2 are also essential in the reaction mediated by this complex. Apr, APS reductase; Asr, anaerobic sulfite reductase; Dox, thiosulfate:quinone oxidoreductase; Dsr, dissimilatory sulfite reductase; Fcc, flavocytochrome c sulfide dehydrogenase; Fsr, F420-dependent sulfite reductase; Hdr, heterodisulfide reductase; Otr, octaheme tetrathionate reductase; Phs, thiosulfate reductase; Psr, polysulfide reductase; Qmo, quinone-interacting membrane-bound oxidoreductase; Sat, sulfate adenylyltransferase; Sir, sulfite reductase; Soe, sulfite-oxidizing enzyme; SOR, sulfur oxygenase/reductase; Sor, sulfite-acceptor oxidoreductase; Sox, sulfur-oxidizing multienzyme complex; Sqr, sulfide: quinone oxidoreductase; Sre, sulfur reductase; SULT, sulfotransferase; Tet, tetrathionate hydrolase; Tsd, thiosulfate dehydrogenase; Tr, tetrathionate reductase (Van Vliet et al., 2021).



## The genomic markers of the microbial sulfur cycle reactions and their limits

The main enzymes associated with the sulfur cycle and genomic markers of specific pathways are detailed in the review by Wasmund et al. (2017). They are also detailed in §1.2, 1.3, 1.4 and 1.5 of this PhD thesis.

Nevertheless, knowledge in this field is in constant evolution, new putative enzymes associated to sulfur cycle are often found and studied, for example thiosulfate quinones (Kanao et al., 2020), thiosulfate oxidation enzymes (Zhang et al., 2020), sulfate transporters (Marietou et al., 2018), sulfane reductases (Wu et al., 2018), SQR (sulfide:quinone reductase) genes (Lahme et al., 2020), making the understanding of the microbial sulfur cycle using gene/protein markers very difficult. In addition, it was demonstrated that some enzymes, such as Dsr associated proteins can perform reductive or oxidative processes depending various parameters which complicates the use of these genes as markers of a specific metabolism (Crane, 2019). At the cell and community scales, all sulfur reactions within all *Archaea* and *Bacteria* are not fully documented, with the intervention of several known and unknown enzymes (Wu et al., 2018; Wang et al., 2019; Camacho et al., 2020). In conclusion, the understanding of the microbial-mediated sulfur cycle is constantly evolving and can help us to think about new hypotheses at different scales, molecular, physiological and ecological.

## Potential biotechnological applications

Microbial reactions of the sulfur cycle could find various biotechnological applications. For example, for acid mine drainage bioremediation, to remediate the black-odorous urban rivers, in processes for sewage treatments, for removal of halogenated organic pollutants, and to limit sulfide associated corruptions (Wu et al., 2021). Moreover, S<sup>0</sup>-based biotechnologies and applications already exist in water and wastewater treatment. They are reviewed in the study by Zhang et al. (2021). As stated by Zhang et al. (2021), sulfur disproportionation could also be employed to provide readily bioavailable electron donors and acceptors for water and wastewater treatment, but the engineering application of S<sup>0</sup> disproportionation processes has not yet been reported.

## Exobiology of the sulfur cycle

Sulfur may be associated with the earliest metabolisms on Earth and the ancient sulfur cycle is the subject of ongoing research (Fike et al., 2015; De Anda et al., 2018; Ollivier et al., 2018; Fakhraee and Katsev, 2019; Morrison and Mojzsis, 2020). A possible interaction between sulfate-reducing microorganisms and anaerobic methane oxidizers in 2.72 Ga old stromatolites and a potential trace of sulfur-utilizing microorganism 3.5 Ga ago have been considered (Schoft et al., 2018; Lepot et al., 2019). Since the late 1980s, extraterrestrial microbial life has even been hypothesized on other planets: for example, anaerobic and chemoautotrophic microorganisms using different sulfur sources on Europa and early Mars (Oró and Mills, 1989; Amend et al., 2004). The study of sulfur isotopes can also provide information on the potential presence of a microbial (*versus* abiotic) process and even on the nature of the process, i.e., reduction, oxidation, or dismutation. It has recently become possible to study sulfur isotopes on Mars and then to develop hypotheses. This was achieved, for example, in the study by Szykiewicz et al. (2018), which focused solely on geological features.

This first part introduction aims at overviewing most of the sulfur metabolisms currently known, i.e. inorganic sulfur compound (ISC) reduction, ISC oxidation, ISC disproportionation, the still hypothetical metabolism of ISC comproportionation and the use of organic sulfur as an energy source. However, from the current extensive literature and taking into account the work done in this PhD thesis, it was decided to put more emphasize on ISC disproportionation, ISC comproportionation and on the use of organic compounds. ISC reduction and oxidation independent processes will only be briefly described in this introduction.

### 1.2 ISC reduction: reduction of sulfate, sulfite, thiosulfate and sulfur

The reduction of inorganic sulfur compounds is relatively well known in various ecosystems due to intensive research and its ubiquity in anoxic environments. Among the reactions studied, the reduction of sulfates is among the best documented (Pereira et al., 2011; Madigan et al., 2015; Wasmund et al., 2017; Anantharaman et al., 2018; Jørgensen et al., 2019; Kushkevych et al., 2020; Tang et al., 2021; Wu et al., 2021; Wójcik-Augustyn et al., 2021). Sulfate reduction pathway associated genes and proteins are shown in Figure 5 and 6. Dissimilatory sulfite

reductase proteins (DsrAB, DsrC, DsrMKJOP, DsrD, and DsrN), sulfate adenylyltransferase (Sat), adenylylsulfate or APS reductase (AprAB), and quinone-interacting membrane-bound oxidoreductase complex (QmoABC) are required for dissimilatory sulfate reduction.

Other dissimilatory reductive processes are sulfite, thiosulfate, sulfur and polysulfides reduction which couple additional proteins to the dissimilatory sulfate reduction pathway (Wasmund et al., 2017; Wu et al., 2021). For sulfite reduction, sulfite reductase cytochrome (MccA/SirA), anaerobic sulfite reductase (AsrABC) and F<sub>420</sub> dependent sulfite reductase (Fsr) are specific enzymes. For thiosulfate, thiosulfate reductase (PhsABC), thiosulfate dehydrogenase (TsdA), octoheme tetrathionate reductase (Otr), tetrathionate reductase (TrABC), and tetrathionate hydrolase (TetH) are specific enzymes of thiosulfate reduction. For S<sup>0</sup> and polysulfides, polysulfide reductase (PsrABC), NAD(P)H sulfur oxidoreductase, sulfhydrogenase/hydrogenase I (HydDACB), sulfhydrogenase/hydrogenase II (ShyCBDA/SuDh), sulfur reductase (SreABC) and NADH-dependent persulfide reductase (Npsr) are specific enzymes.

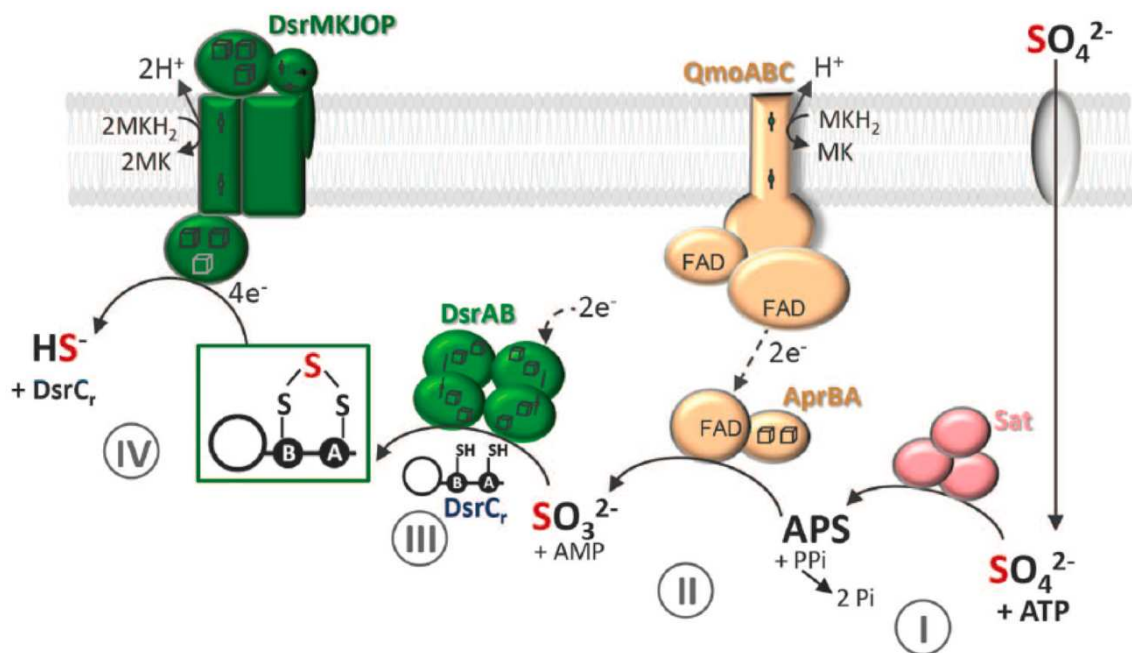


Figure 6: The sulfate respiratory pathway, involving import of sulfate, activation by sulfate adenylyl transferase (SAT) to adenosine 5'-phosphosulfate (APS) (I), reduction of APS to sulfite by the APS reductase (II), reduction of sulfite to the DsrC trisulfide by DsrAB/DsrC (III), and last, reduction of the trisulfide to sulfide and reduced DsrCr by the DsrMKJOP complex (IV) (Santos et al., 2015).

### 1.3 *Inorganic sulfur compounds oxidation*

Succinctly, sulfide and sulfur oxidation are the most described reactions of inorganic sulfur compound oxidation (Gregersen et al., 2011; Madigan et al., 2015; Wasmund et al., 2017; Jørgensen et al., 2019; Wu et al., 2021). Associated pathways are shown in Figure 5, and Figure 7 on the example of green sulfur bacteria (GSB). Sulfur-oxidation pathways include sulfide:quinone-oxidoreductase (Sqr), Sox multisystem (SoxXA, SoxYZ, SoxB, SoxCD, and SoxL), flavocytochrome C/sulfide dehydrogenases (FccAB), rhodanese-like protein-sulfurtransferase gene cluster (Rhd-TusA-DsrE2) and the reverse sulfate reduction pathway.

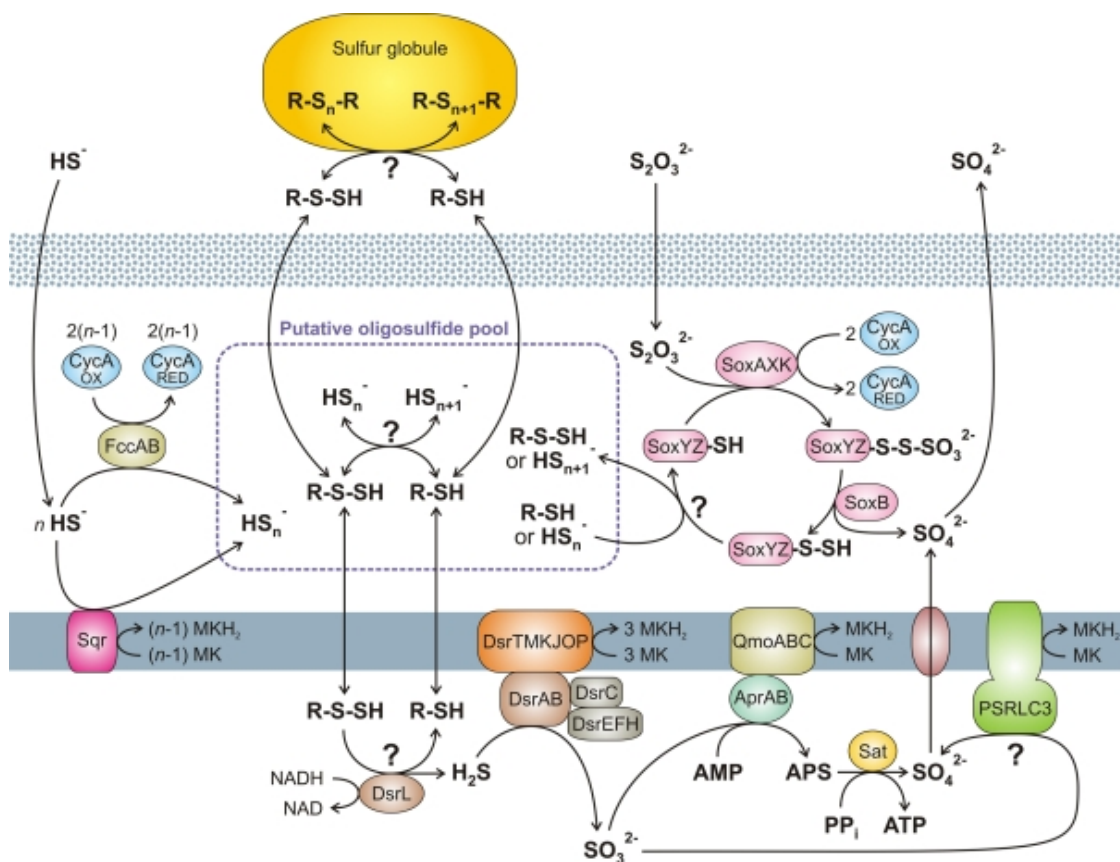


Figure 7: Overview of the putative pathways of oxidative sulfur metabolism in green sulfur bacteria (GSB). All oxidative enzyme systems shown in the periplasm (SOX, SQR, and FCC systems) as well as extracellular sulfur globules contribute to a putative pool of oligosulfides (and possibly organic  $R-S_n-H$ ). Complete oxidation of this pool to sulfate is dependent on the DSR system. MK, menaquinone (Gregersen et al., 2011).

## 1.4 Inorganic sulfur compounds disproportionation

### Definition, reactions and thermodynamic considerations

A disproportionation corresponds to a chemical or biological reaction where the same mineral or organic compound serves both as an electron donor and as an electron acceptor. In the case of inorganic sulfur compounds such as thiosulfate ( $\text{S}_2\text{O}_3^{2-}$ ), sulfite ( $\text{SO}_3^{2-}$ ), and elemental sulfur ( $\text{S}^0$ ), each one may be oxidized to  $\text{SO}_4^{2-}$  and reduced to  $\text{HS}^-$  and then “disproportionated”. In other words, disproportionation, also called dismutation or inorganic fermentation, is a redox reaction in which a compound of intermediate oxidation state turns into two different compounds, one of higher and one of lower oxidation state. Diverse inorganic sulfur compounds can be disproportionated: generally, the most studied forms for sulfur disproportionation are elemental sulfur, thiosulfate and sulfite (Finster, 2008; Slobodkin and Slobodkina, 2019). Figure 8 schematizes the reactions of sulfur cycle taking place in marine sediments, the dismutation reactions being indicated by dotted arrows on the left of the diagram.

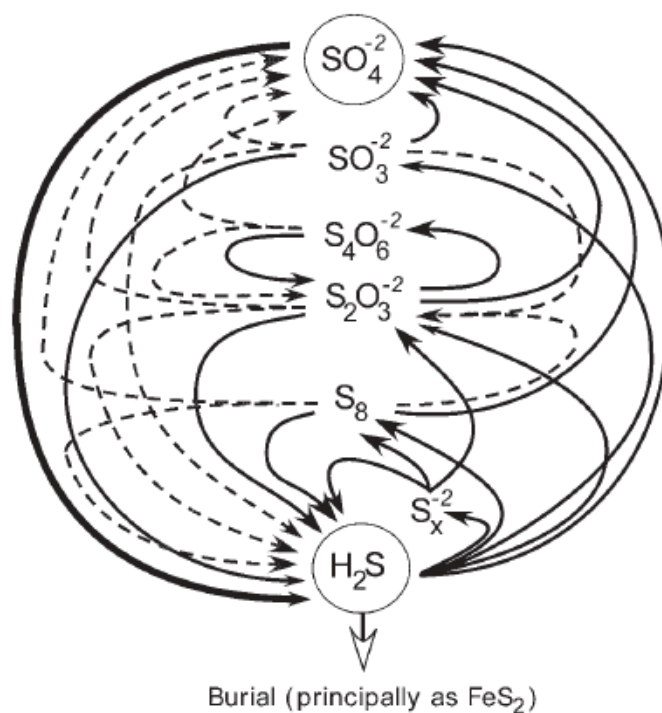
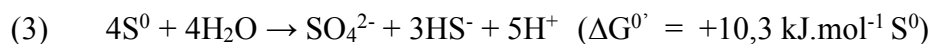
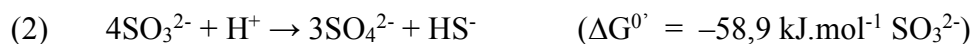
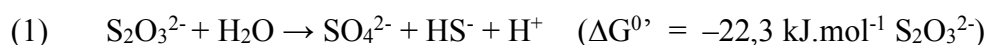
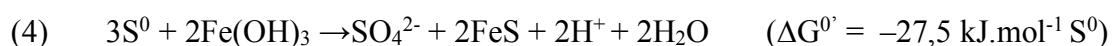


Figure 8: Diagram representing the simplified marine sedimentary sulfur cycle. Reductive pathways are represented by left-side down arrows, oxidative pathways are represented by right-side upward arrows. Broken lines on the left represent disproportionation reactions. The thick arrow on the left represent the degradation of organic compounds coupled to the reduction of sulfate by sulfate reduction microorganisms. Burial of iron sulfur minerals, mostly  $\text{FeS}_2$  represents the dominant sink for reduced sulfur in marine sediments (Amend, 2004).

Disproportionation reactions are given below, with their Gibbs free energy values under standard conditions (Reactions 1, 2 and 3) (Finster, 2008; Ollivier et al., 2018):



Under standard conditions, disproportionation reactions have a mainly low energy yield except for sulfite. Elemental sulfur disproportionation is even endergonic under standard conditions.  $\text{S}^0$  disproportionation can become exergonic depending on the physical and chemical conditions. The presence of a sulfide scavenging chemical species can turn the reaction exergonic (Finster, 2008; Ollivier et al., 2018). Moreover, the pH and temperatures could also influence disproportionation, higher alkaline pH and higher temperatures being related to higher Gibbs free energy in the case of  $\text{S}^0$  disproportionation (Belkin et al., 1985). Thus, the three bacteria (*Desulfurivibrio alkaliphilus* AHT 2<sup>T</sup>, *Desulfurivibrio* sp. AMeS2, and *Dethiobacter alkaliphilus* AHT 1<sup>T</sup>) that have been characterized by Poser et al. (2008) can grow by  $\text{S}^0$  disproportionation without any sulfide scavenger, under highly alkaline conditions. Nevertheless, a sulfide scavenging species seems to be required under neutrophilic conditions because microbial growth will be inhibited by high sulfide concentrations. Inhibition of disproportionation is proportional to the sulfide concentration at different temperatures (Finster, 2008). Sulfide scavengers can be for example iron oxides such as ferric hydroxides ( $\text{Fe(II)CO}_3$ ,  $\text{Fe(III)OOH}$ ) or manganese oxides such as manganese oxide ( $\text{Mn(IV)O}_2$ ), two natural chemicals acting as scavengers for  $\text{H}_2\text{S}$  in environmental sediments. In the case of ferrihydrite, the disproportionation will result in the production of  $\text{FeS}$  or  $\text{FeS}_2$  such as iron monosulfide or pyrite (Reaction 4) (Finster, 2008; Ollivier et al., 2018):



Disproportionation has been firstly described as a chemical abiotic process related to specific physical and chemical conditions such as high temperatures. It is demonstrated, for example, that elemental sulfur can be disproportionated abiotically at temperatures between 50 to 200°C, producing sulfate and sulfides (Belkin et al., 1985; Smith, 2000). Thiosulfate and sulfite can also be potentially abiotically disproportionated.

## Discovery of the ISC disproportionation

The biological inorganic sulfur compounds disproportionation has been officially described for the first time in the late 80's by Bak and Cypionka (1987) and Bak and Pfennig (1987). By studying *Desulfovibrio sulfodismutans*, they discovered this new metabolic reaction. Indeed, *D. sulfodismutans* was able to grow in a mineral medium with thiosulfate or sulfite as sole electron donor and acceptor, and CO<sub>2</sub> as sole carbon source, under anaerobic conditions. The first report of elemental sulfur disproportionation was then made by Thamdrup et al. (1993). In 1974, a study suggested that a *Chlorobium* bacterium may be able to perform a photochemical disproportionation of sulfur, thus light-dependent (Paschinger et al., 1974).

From the literature, we could elaborate the following list of 43 bacterial strains disproportionating inorganic sulfur compounds (independent of the sulfur oxygenase reductase enzyme (SOR) and of light) (Bak and Cypionka, 1987; Tasaki et al., 1991; Cypionka et al., 1998; Jackson and McCinerney, 2000; Obratsova et al., 2002; Finster et al., 2008; Slobodkin et al., 2012; Slobodkin et al., 2013; Finster et al., 2013; Poser et al., 2013; Slobodkina et al., 2016; Slobodkin et al., 2016; Kojima et al., 2016; Florentino et al., 2016; Slobodkina et al., 2017; Frolova et al., 2018; Slobodkin and Slobodkina, 2019; Kawai et al., 2019; Umezawa et al., 2021): *Desulfobulbus propionicus* 1pr3<sup>T</sup>, *Desulfocapsa thiozymogenes* Bra2<sup>T</sup>, *Desulfocapsa* sp. Cad626, *Desulfovibrio sulfodismutans* ThAc01<sup>T</sup>, *Desulfurella amilsii* TR1<sup>T</sup>, *Desulfovibrio desulfuricans* CSN, *Desulfocapsa sulfoexigens* SB164P1<sup>T</sup>, *Desulfofustis glycolicus* PerGlyS<sup>T</sup>, *Pantoea agglomerans* SP1, *Desulfovibrio brasiliensis* LVform1<sup>T</sup>, *Desulfovibrio oxycliniae* P1B<sup>T</sup>, *Desulfonatronospira delicata* AHT 6<sup>T</sup>, *Desulfonatronospira thiodismutans* ASO3-1<sup>T</sup>, *Desulfonatronovibrio magnus* AHT22<sup>T</sup>, *Desulfonatronovibrio thiodismutans* AHT9<sup>T</sup>, *Desulfonatronum lacustre* Z-7951<sup>T</sup>, *Desulfonatronum thioautotrophicum* ASO4-1<sup>T</sup>, *Desulfonatronum thiodismunans* MLF1<sup>T</sup>, *Desulfonatronum thiosulfatophilum* ASO4-2<sup>T</sup>, *Desulfonatronum parangueonense* PAR180<sup>T</sup>, *Desulfurivibrio alkaliphilus* AHT 2<sup>T</sup>, *Desulfurivibrio* sp. AMeS2, *Dethiobacter alkaliphilus* AHT 1<sup>T</sup>, *Desulfomonile tiedje* DCB-1<sup>T</sup>, *Desulfotomaculum salinum* 435<sup>T</sup>, *Desulfotomaculum salinum* 781, *Desulfotomaculum thermobenzoicum* TSB<sup>T</sup>, *Caldimicrobium thiodismutans* TF1<sup>T</sup>, *Caldimicrobium rimae* FM8, *Caldimicrobium rimae* 76, *Dissulfuribacter thermophilus* S69<sup>T</sup>, *Dissulfurimicrobium hydrothermale* Sh68<sup>T</sup>, *Dissulfurirhabdus thermomarina* SH388<sup>T</sup>, *Thermosulfurimonas dismutans* S95<sup>T</sup>, *Thermosulfurimonas marina* S872<sup>T</sup>, *Thermosulfuriphilus ammonigenes* ST65<sup>T</sup>, *Desulfobacter curvatus* DSM 3379, *Desulfobacter hydrogenophilus* DSM 3380,

*Desulfococcus multivorans* DSM 2059, *Desulfotomaculum nigrificans* DSM 574, *Desulfovibrio mexicanus* DSM 13116, *Desulfovibrio aminophilus* DSM 12254, *Dissulfurispira thermophila* T55J<sup>T</sup>.

#### Taxonomic and functional diversity of ISC-disproportionators

Most of the strains (36 strains out of the 43) were rigorously listed as a function of their optimum temperature and pH, isolation environments and conditions, taxonomic position and metabolic characteristics in the review by Slobodkin and Slobodkina (2019). Other strains (6 strains out of the 43) were observed to perform disproportionation for energy production but not for growth and were listed in the review by Finster (2008). Finally, a new species, *Dissulfurispira thermophila*, was shown to disproportionate thiosulfate or S<sup>0</sup> (Umezawa et al., 2021). Additionally, some microorganisms not isolated in culture are very likely to perform sulfur disproportionation as demonstrated for cable bacteria, with high sensitivity to sulfides (Müller et al., 2020).

In the current state of knowledge and with recent discoveries, ISC-disproportionating microorganisms appear to be phylogenetically widespread, particularly in the bacterial domain. Disproportionation was initially thought to be related to *Deltaproteobacteria*, but the identification of new species has broadened its positions in phylogenies. The study by Obraztsova et al. (2002) showed that *Pantoea agglomerans*, a *Gamaproteobacteria*, can disproportionate sulfur and thus that disproportionation is not restricted to strict anaerobes (Ollivier et al., 2018). Afterwards, ISC-disproportionating microorganisms belonging to *Thermodesulfobacteria*, *Aquificae*, *Firmicutes* and recently *Nitrospirae* have been identified (Jackson and McCinerney, 2000; Guiral et al., 2012; Slobodkin et al., 2012; Slobodkin and Slobodkina, 2019; Umezawa et al., 2021).

The diversity of *Deltaproteobacteria* and their participation in various geochemical cycles, in particular the sulfur cycle, are of special interest as they are essential and not yet fully understood, but new studies are expanding our understanding of phylogeny and metabolism (Wait et al., 2020; Langwig et al., 2021; Ward et al., 2021). Up to date, 28 sulfur-disproportionating species of *Deltaproteobacteria* are known and important to consider according to the results of this PhD project.



As said before, this reaction is not necessarily associated with the growth of the microorganism that implements it. Some species are able to disproportionate inorganic sulfur compounds but only for producing energy, and not to grow (Finster, 2008). In some cases, it could be a maintenance process, that could increase survival under limiting conditions. *Desulfobacter curvatus*, *Desulfobacter hydrogenophilus*, *Desulfococcus multivorans* and *Desulfotomaculum nigrificans* can produce energy but cannot grow *via* thiosulfate disproportionation. In the same way, *Desulfovibrio mexicanus* and *Desulfovibrio aminophilus* cannot grow on thiosulfate and sulfite disproportionation but can be sustained by these compounds (Finster, 2008). Moreover, most of the sulfur-disproportionating bacteria are known to use other energy production pathways, which are based on other electron donors and acceptors, and produce more energy.

Thiosulfate and sulfite disproportionation seem to be common among sulfate-reducers, but not in sulfur and sulfide oxidizers (Finster, 2008). As said previously, these reactions have a relatively low energy yield under standard conditions, and is probably not used in priority by cells if more energetic processes can be implemented.

Furthermore, it is possible that  $S^0$  (as cyclooctasulfur) could be converted into polysulfides and/or polythionates, depending on various ecophysiological conditions and be used as an energy source (Berg et al., 2014; Slobodkin and Slobodkina, 2019). In their article, Slobodkin and Slobodkina (2019) reported the different energy yields associated to different polysulfide species ( $\Delta G^{0'} = -15.3 \text{ kJ mol}^{-1} S_2^{2-} / \Delta G^{0'} = +26.9 \text{ kJ mol}^{-1} S_5^{2-}$ ). Polysulfide species ( $S_x^{2-}$ ) are notoriously difficult to quantify in natural systems due to their reactivity, sensitivity to sample handling and the analytical complexity associated with their measurement. The review by Findlay (2016) summarizes current knowledge about polysulfides.

The microbial sulfur disproportionation could be more widespread than initially suspected. Sulfur disproportionators could even be more widespread among prokaryotes. However, it is very important to differentiate aerobic from anaerobic sulfur disproportionation. The anaerobic microbially mediated sulfur disproportionation process, which is investigated in this PhD work and described above, is strictly distributed among anaerobic bacteria. To date, no archaea is known to perform sulfur compounds disproportionation under strict anaerobic conditions. The pathways and enzymes of the process are only partially elucidated.

The sulfur disproportionation can also proceed through another way, with the SOR (sulfur oxygenase reductase) enzyme, which disproportionates sulfur in the presence of oxygen (Kletzin, 1989; Kletzin et al., 2004; Liu et al., 2012). This enzyme is present in several archaea and few bacteria, such as the archaeon *Acidianus ambivalens* (or *Desulfurolobus ambivalens*) from a continental solfataric field, and the bacterium *Aquifex aeolicus* whose SOR have been well studied (Kletzin, 1989; Pelletier et al., 2008). In this PhD project, we decided to focus our investigations on the SOR-independent sulfur compound disproportionation. However, the SOR presence among hydrothermal/geothermal vent taxa is also not well documented and should deserve investigations. To date, the hydrothermal bacterium *Aquifex aeolicus* isolated from a shallow-sea hydrothermal vent and the two archaea *Sulfurisphaera tokodaii* and *Acidianus tengchongensis* isolated from acidic hot springs have been reported to have a SOR (UniprotKb database). Therefore, it might also be interesting to investigate the presence of the SOR enzyme in microorganisms from hydrothermal and geothermal habitats. It should be noted, however, that Blast comparisons of the SOR genes from *Aquifex aeolicus* and *Acidianus ambivalens* that I performed against the NCBI nucleotide collection and UniprotKb genomic databases failed to find similar sequences other than terrestrial homologs from acidic hot spring environments.

#### Habitats, environmental significance and dating

ISC-disproportionators are originating from a large panel of environments such as marine sediments, freshwater sediments, anaerobic digestors, terrestrial, shallow and deep-sea hydrothermal vents, geothermal hot springs, and acidic, neutral and alkaline lakes (Tasaki et al., 1991; Canfield and Thamdrup, 1996; Cypionka et al., 1998; Finster et al., 2008; Slobodkin et al., 2012; Poser et al., 2013; Slobodkina et al., 2016; Florentino et al., 2016; Ihara et al., 2019; Slobodkin and Slobodkina, 2019; Umezawa et al., 2021).

After the first descriptions of ISC-disproportionating microorganisms, researchers studied whether this metabolism can have an impact on the whole marine sulfur cycle and how important it is. Jørgensen (1990) used <sup>35</sup>S-labeled isotopes to show that thiosulfate disproportionation is a key process in the transformation of intermediately oxidized/reduced sulfur compounds in both marine and freshwater sediments. This study provided experimental evidence that thiosulfate is a central intermediate in the oxidation of hydrogen sulfide *in situ* (Finster, 2008). Another study showed that ISC-disproportionators would be abundant, with an

estimate of up to  $10^7$  cells capable of disproportionating thiosulfate per  $\text{cm}^3$  of marine sediment (Jørgensen and Bak, 1991). In general, there are very few comprehensive ecological studies on the microbial sulfur disproportionation in natural environments, as results of sulfur isotope fractionations signatures and stable isotope composition of sulfur species are difficult to interpret regarding to disproportionation reactions (Jørgensen et al., 2019). Distribution of sulfur disproportionators has been poorly investigated, and most of the strains isolated are from sediments. Such investigation remains very difficult as there are no specific markers for this reaction, which is for example very complex in stratified lakes (Avetisyan et al., 2019).

Isotopes analyses can be used to follow the disproportionation process. The sulfur isotopes can indicate various biological or abiotic processes in different environments (Amend et al., 2004). Stable isotopes can be used especially for geobiological studies over time as they provide important information about the current and past processes, or natural fractionation reactions of ongoing processes of sulfate reduction, sulfide oxidation and ISC disproportionation (Böttcher and Thamdrup, 2001; Philippot et al., 2007). Use of radiolabeled substrates but also analyses of stable sulfur isotopes allows to follow chemical and biological reactions as well as to the evolution of a substrate in an ecosystem (Jørgensen et al., 1990). The study of isotopes can even distinguish between abiotic and biotic fractionation. Böttcher et al. (2005) combined for the first-time sulfur and oxygen isotopes applied to the dismutation of sulfur compounds by studying the ratios  $^{34}\text{S}/^{32}\text{S}$  and  $^{18}\text{O}/^{16}\text{O}$  which is a valuable method to distinguish microbial from abiotic sulfur disproportionation.

Disproportionation of elemental sulfur could date back up to 3.5 Ga. Sulfur isotope data from early Archaean rocks and the presence of microfossils from 3.4 billion-year-old geological formations suggest that sulfur disproportionation could be one of the earliest modes of microbial metabolism. This metabolism could be associated to the production of sulfate in the sea (Canfield and Thamdrup, 1994; Philippot et al., 2007; Wacey et al., 2011). Some others studies suggest rather that this process became significant between 1.45 to 1.3 Ga (Johnston et al., 2005). The sulfur and polysulfide metabolisms remain good theories for the origin of life but are still very controversial (Ollivier et al., 2018).

## Pathways of ISC disproportionation

Genetic and biochemical processes of sulfite and thiosulfate disproportionation were studied in great details in the bacterium *Desulfocapsa sulfoexigens*. These experiments demonstrated that sulfite is reduced to sulfide and oxidized to sulfate. Based on enzymatic activity measurements, ATP is likely to be produced by phosphorylation *via* an ATP sulfurylase-like system that may be completely independent of any proton gradient and ATP synthase (Figure 9) (Krämer and Cypionka, 1989; Frederiksen and Finster, 2003).

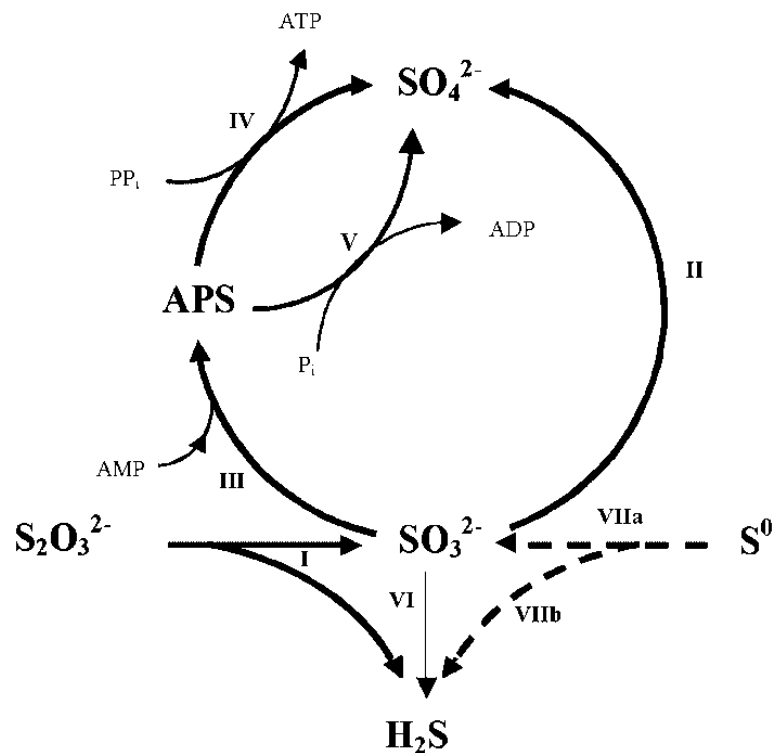


Figure 9: Proposed pathways for thiosulfate and sulfur disproportionation in cultures of *Desulfocapsa sulfoexigens*. The enzyme activities were measured in cell-free extracts of cultures that were grown in a batch fermenter in the absence of a sulfide scavenger. Hydrogen sulfide was removed by continuously flushing of the culture with a gas mixture of 10%  $\text{CO}_2$  and 90%  $\text{N}_2$ . Activities of the following enzymes could be determined: I. Thiosulfate reductase, II. Sulfite oxidoreductase, III. APS reductase, IV. ATP sulfurylase, V. Adenylylsulfate-phosphate adenylyltransferase, VI. Sulfite reductase. VIIa and VIIb: unresolved reactions that may proceed via unidentified intermediates. Full bold lines indicate reactions that are involved in the disproportionation process. The rates that were measured in the enzyme assays were high enough to explain the disproportionation rates measured in the cultures used for cell extract preparation. Thin lines indicate that the strain possesses the enzyme but that the activity was too low to explain the measured overall disproportionation rates. Dotted bold lines indicate tentative pathways for which no enzyme activity could be measured (Finster, 2008).

In this bacterial model, inorganic sulfur compounds appear to be converted *via* a reverse sulfate reduction pathway to produce directly ATP. These results may indicate that sulfite is an intermediate for elemental sulfur and thiosulfate disproportionation process, in this bacterium. Thiosulfate can be split into sulfide and sulfite by a thiosulfate reductase and then follow the sulfite disproportionation route. Sulfite can be formed from different substrates such as sulfate, thiosulfate and sulfur. However, these results may not be universal for all taxa as some species are capable of disproportionating S<sup>0</sup> and/or thiosulfate but not sulfite (Slobodkin and Slobodkina, 2019). Cypionka et al. (1998) determined that thiosulfate might be an intermediate in the bacterium *Desulfovibrio desulfuricans* because they did not find a direct formation of sulfide and sulfate from the thiosulfate even if it had been previously described that the thiosulfate reductase can produce sulfide and sulfite. As a conclusion, it may be potentially possible that it exists at least three independent mechanisms for the disproportionation of sulfur, thiosulfate and sulfite. Krämer and Cypionka (1989) suggested also that the capacities to reduce sulfate and to disproportionate sulfite or thiosulfate are present simultaneously and thus that the capacity to disproportionate could be constitutive. However, given that this study was conducted on a small number of microorganisms, this conclusion is not generalizable to all ISC-disproportionators.

There are very few studies focusing on the genomics of ISC disproportionation, particularly on the anaerobic microbial sulfur disproportionation which this PhD project focuses on. When the PhD started, articles by Finster et al. (2013), Mardanov et al. (2016), Florentino et al. (2017), Thorup et al. (2017) were among the ones studying the genomic capital of ISC-disproportionators. At the end point of PhD, at least all the additional studies below were published, Bertran et al. (2019), Florentino et al. (2019), Slobodkin and Slobokina (2019), Allieux et al. (2020), Slobodkina et al. (2020), Ward et al. (2020a); Ward et al. (2020b), Allieux et al. (2021), Müller et al. (2020), Umezawa et al. (2020), Bell et al. (2021) and Umezawa et al. (2021) showing a renewed interest in this issue.

Finster et al. (2013) annotated for first time the genome of a S<sup>0</sup> disproportionating bacterium called *Desulfocapsa sulfoexigens*, but did not find any specific markers for S<sup>0</sup> disproportionation. Nevertheless, this work provided a basis for the analysis of ISC-disproportionating microorganisms.

Mardanov et al. (2016) provided an extensive and precise genome analysis of *Thermosulfurimonas dismutans*. They sequenced, described and annotated *T. dismutans* complete genome and focused on sulfur disproportionation related genes. This genome analysis revealed previously described characteristics such as a possible reverse reduction of sulfate to produce ATP and a potential ability to disproportionate tetrathionate. However, their study also did not identify genes or pathways specific for S<sup>0</sup> disproportionation. They suggested that S<sup>0</sup> could be oxidized to sulfite by an adenylylsulfate reductase and a heterodisulfide reductase enzyme and then, the sulfite could potentially be oxidized to sulfate and produce ATP. S<sup>0</sup> would then be the first intermediate, which may be a plausible hypothesis as they interestingly found that *T. dismutans* can grow without a direct cell contact with S<sup>0</sup>. In addition, they proposed that molybdopterins could be involved.

Comparative genomics and proteomics under various physiological conditions have been carried out on the family *Desulfurellaceae*, by Florentino et al. (2017 and 2019). To our knowledge, it was the first time that comparative genomics was carried out on sulfate-reducing microorganisms capable of growing under different metabolic conditions and in particular *via* sulfur disproportionation, which should make it possible to deduce the specific genes of this pathway. Comparative genomics was carried out on several species of the family *Desulfurellaceae* which includes two sulfur disproportionating species among six species. The comparative proteomics was carried out on *Desulfurella amilsii* only, grown under different metabolic conditions. First of all, this study demonstrated, similarly to the study by Mardanov et al. (2016), that a direct cellular contact with S<sup>0</sup> is not strictly required but beneficial to the reaction. However, as stated by Florentino et al. (2019), elemental sulfur could be used by different hypothetical ways. Envisaged mechanisms towards S<sup>0</sup> uptake by S<sup>0</sup> respiring bacteria, and potentially sulfur disproportionators, are listed in Figure 10 (Florentino et al., 2019; Lahme et al., 2020; Zhang et al., 2021). Elemental sulfur could form sulfur nanoparticles which could enter directly the membranes (Mardanov et al., 2016; Florentino et al., 2019). It cannot also be excluded that elemental sulfur is only a temporary intermediate and that polysulfides can be used for energy purposes; indeed, nucleophilic attack of sulfur by sulfide can generate polysulfides. Alternatively, elemental sulfur which is poorly soluble would not enter the cell, but would penetrate in the form of soluble sulfane-sulfur compound glutathione persulfide. Strategies involving pili or flagella could also be considered.

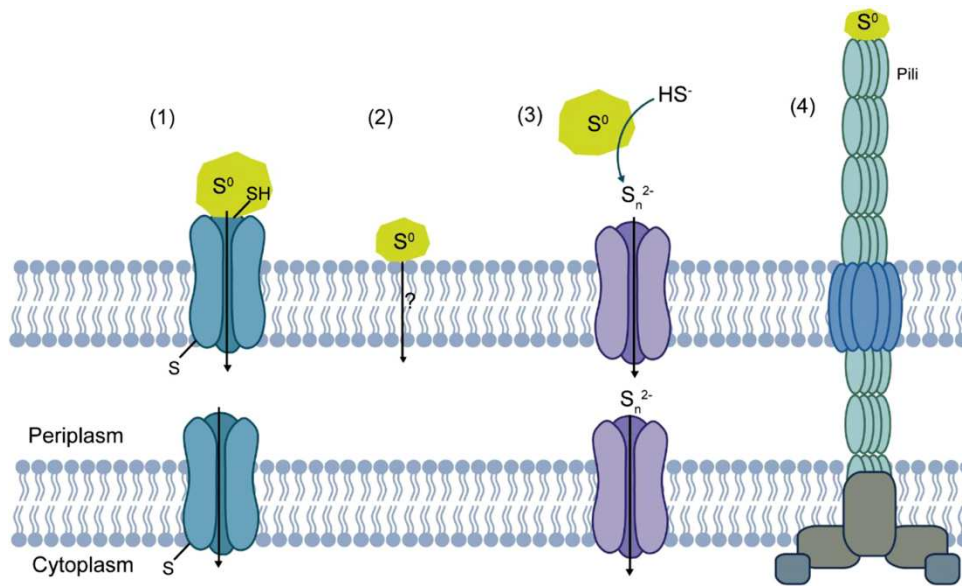


Figure 10: Envisaged mechanisms towards  $S^0$  uptake by  $S^0$  respiring bacteria. (1) attachment of cell-  $S^0$  and interaction between  $S^0$  and thiol-containing outer-membrane proteins to generate soluble polysulfanes; (2) direct uptake of polymeric sulfur; (3) Nucleophilic attack of  $S^0$  by sulfide to generate polysulfide; (4) pili formation resulting in extracellular electron transport (Zhang et al., 2021).

Regarding comparative proteomics, 16 unique proteins out of the 698 total proteins were associated to the  $S^0$  disproportionation process, as compared to thiosulfate and sulfur reduction processes (with  $H_2$  or acetate as electron donors, at pH of 3.5 and 6.5). The genome of *D. amilsii* does not encode any ATP sulfurylase and any adenylyl-sulfate reductase, but encodes a dissimilatory sulfite reductase (Florentino et al. 2017; Slobodkin and Slobodkina, 2019). Under sulfur disproportionation conditions, a rhodanese like sulfurtransferase was synthesized in large quantities. Interestingly, this protein was only present under growth conditions targeting  $S^0$  disproportionation and in low pH cultures. In summary, the two studies by Florentino developed very interesting approaches that were implemented also in this PhD project. In Florentino's study, two protein candidates for sulfur disproportionation have been highlighted using this approach, namely molybdopterins and rhodanese-like proteins (Mardanov et al., 2016; Florentino et al., 2017; Florentino et al., 2019).

The study by Thorup et al. (2017) focused on *Desulfurivibrio alkaliphilus*. It demonstrated that this strain possesses all the genomic potential to perform dissimilatory sulfate reduction but in fact was growing by sulfide oxidation. Interestingly, they also made a comparative study focused on sulfur disproportionation. By comparing gene expression under  $S^0$  disproportionation and DNRA growth conditions, they observed that some genes were over-expressed under sulfur disproportionation conditions. Those selected genes were NrfD-like

protein, rhodanese type protein, molybdopterin oxidoreductase, sulfide:quinone oxidoreductase and hypothetical proteins. They described a new putative polysulfide reductase gene cluster which integrates some of the cited enzymes. No genes were expressed only under  $S^0$  disproportionation conditions when compared to DNRA conditions, which could suggest that there is a potential overlap between these two metabolic pathways. Finally, they proposed a model for  $S^0$  disproportionation, in which  $S^0$  would be converted to DsrC-trisulfide, a key intermediate which would be ultimately reduced to sulfide and oxidized to sulfate. This hypothesis is a second interesting hypothesis on the possible intermediates of the reaction, in addition to the other one based on sulfite as a main intermediate (Fig. 11). However, it is important to keep in mind that the study was performed only on *D. alkaliphilus*.

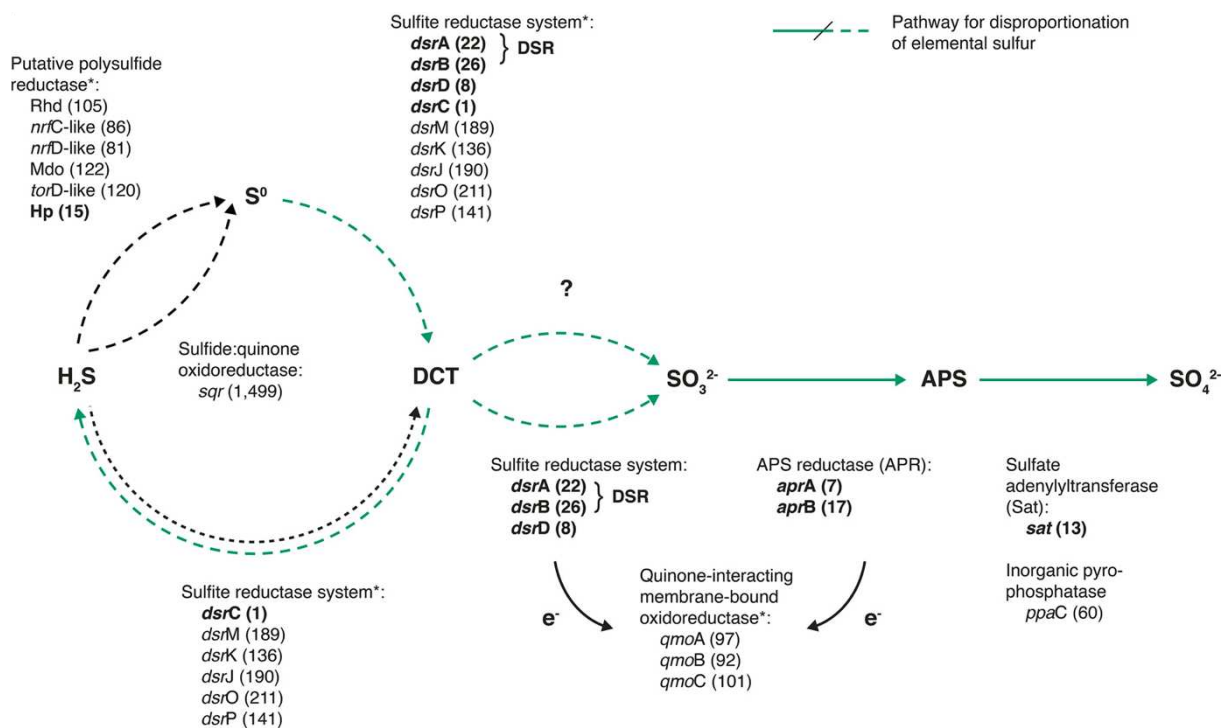


Figure 11: Proposed pathway of chemolithotrophic sulfide oxidation and sulfur disproportionation by *Desulfurivibrio alkaliphilus*. Shown are the enzymes proposed to be involved and the associated genes. Gene expression rank during growth by sulfide oxidation is shown in parentheses. Highly expressed genes are in bold type. The pathway for sulfur disproportionation is in green. Asterisks indicate that electrons transferred to these membrane-associated enzyme complexes are used to reduce menaquinone and are presumably consumed by DNRA. Abbreviations used for the putative polysulfide reductase operon: Rhd, rhodanese; Mdo, molybdopterin oxidoreductase; Hp, hypothetical protein. DTC, DsrC-trisulfide (Thorup et al., 2017).



In the review by Slobodkin and Slobodkina (2019), ISC-disproportionators genomes were compared with each other *via* comparative genomics. Comparative genomics was performed on 10 genomes of S<sup>0</sup> disproportionators, by targeting genes and gene clusters associated to dissimilatory sulfate reduction, sulfur activation and sulfur transfer into the cells and membrane-bound molybdopterin oxidoreductases involved in sulfur metabolism (Table 1). None of the genomes contained the *sox*, *sor*, or *sqr* genes associated to sulfur-oxidizing microorganisms. Most genomes contained the key genes for dissimilatory sulfate reduction but none of the studied genomes contained all the genes chosen for the screening. Surprisingly, *Dethiobacter alkaliphilus* lacks *dsrABD*, *dsrC*, *dsrMK*, and *qmoABC*, and *Desulfurella amilsii*, lacks *aprAB*, *qmoABC*, and *sat* genes. Most microorganisms share the genes associated with activation of insoluble sulfur compounds and their transfer into the cells (*tusA*, *dsrE*, *dsrE2*). Sulfur transferases with two rhodanese-domains (*SseA*) and cytoplasmic NAD(P)-dependent hydrogenase or sulfide dehydrogenase (*sudh*) were absent in all genomes as opposed to molybdopterin-containing thiosulfate and polysulfide reductases (*phsA/psrA*) present in all genomes except in *Dethiobacter alkaliphilus*. Once again, no genomic marker of ISC disproportionation could be found. However, the main conclusion was that a complete set of genes of dissimilatory sulfate reduction is potentially not required for S<sup>0</sup> disproportionation. The second main conclusion was that the proteins transferring the sulfur-containing groups and the enzymes reducing S<sup>0</sup> and/or polysulfides (sulfur transferases and polysulfide reductases) may be key components in the sulfur disproportionation process.

Table 1: The genes of sulfur metabolism proteins in elemental sulfur-disproportionating microorganisms. Designations: *sat*, sulfate adenylyl transferase; *aprAB*, adenylyl-sulfate reductase subunits alpha and beta; *dsrABD*, sulfite reductase, dissimilatory-type subunits alpha, beta and clustered protein *DsrD*; *dsrC*, dissimilatory sulfite reductase, small protein *DsrC*; *dsrMK*, sulfite reduction-associated electron transfer complex, proteins *DsrM* and *DsrK*; *qmoABC*, APS reductase-associated electron transfer complex *QmoABC*; *dsrE*, *DsrE* sulfur-transporting protein; *tusA*, sulfur relay protein *TusA*; *dsrE2*, transmembrane sulfur-transporting protein; *dsrL*, non-sulfur flavoprotein with proposed NAD(P)H: acceptor oxidoreductase; *phsA/psrA*, polysulfide reductase / thiosulfate reductase chain A; *sudhAB*, sulfide dehydrogenase subunit A and B; *DESAMIL20\_2007*, thiosulfate sulfurtransferase, rhodanese from *Desulfurella amilsii* *TR1<sup>T</sup>*; *sseA*, 3-mercaptopyruvate sulfurtransferase *SseA*, contains two rhodanese domains. *Cat*, *Caldimicrobium thiodismutans* *TF1<sup>T</sup>*; *Dbp*, *Desulfobulbus propionicus* *lpr3<sup>T</sup>*; *Des*, *Desulfocapsa sulfoexigens* *SB164P1<sup>T</sup>*; *Det*, *Desulfocapsa thiozymogenes* *Bra2<sup>T</sup>*; *Dva*, *Desulfurivibrio alkaliphilus* *AHT 2<sup>T</sup>*; *Dam*, *Desulfurella amilsii* *TR1<sup>T</sup>*; *Dfg*, *Desulfofustis glycolicus* *PerGlyS<sup>T</sup>*; *Dta*, *Dethiobacter alkaliphilus* *AHT 1<sup>T</sup>*; *Dit*, *Dissulfuribacter thermophilus* *S69<sup>T</sup>*; *Tsd*, *Thermosulfurimonas dismutans* *S95<sup>T</sup>* (*Slobodkin and Slobodkina, 2019*).

Gene or gene cluster	Microorganism									
	Cat	Dbp	Des	Det	Dva	Dam	Dfg	Dta	Dit	Tsd
<i>sat</i>	+	+	+	+	+	None	+	+	+	+
<i>aprAB</i>	+	+	+	+	+	None	+	+	+	+
<i>qmoABC</i>	+	+	+	+	+	None	+	None	+	+
<i>dsrABD</i>	+	+	+	AB	+	AB	+	None	+	+
<i>dsrC</i>	+	+	+	+	+	+	+	None	+	+
<i>dsrMK</i>	+	+	+	M	+	+	+	None	+	+
<i>dsrL</i>	None	None	None	None	None	+	None	None	None	None
<i>tusA</i>	+	+	+	+	+	None	+	+	+	+
<i>dsrE</i>	+	+	+	+	+	None	+	None	+	+
<i>dsrE2</i>	+	+	+	+	+	None	+	+	+	+
<i>DESAMIL20_2007</i>	None	None	None	None	None	+	None	None	+	+
<i>sseA</i>	None	None	+	None	+	+	+	None	+	+
<i>phsA/psrA</i>	+	+	+	+	+	+	+	None	+	+
<i>sudhAB</i>	None	None	None	None	None	+	+	+	None	None

Another interesting hypothesis about putative genomic markers of S<sup>0</sup> disproportionation was proposed by Bertran (2019) in her PhD thesis. By comparing protein sequences of the gene *aprB* they observed some disparities. Hypothesis was that different length of *aprB* gene could be correlated with disproportionation ability, as shorter sequences were observed in sulfur disproportionators (Bertran, 2019; Ward et al., 2020a; Ward et al., 2020b).

Finally, the recent study by Umezawa et al. (2020) suggested the potential involvement of the YTD gene cluster in sulfur disproportionation, based on a comparative genomic analysis. The YTD cluster is a genomic cluster composed of genes *yedE* (inner membrane protein), *dsrE* (putative sulfurtransferase) and *tusA* (sulfur carrier protein) and followed by hypothetical genes (Hp1 and Hp2). It has been proposed that it may serve as a genomic marker for sulfur disproportionation due to its presence in several sulfur disproportionators and its syntenic arrangement (Figure 12).



Figure 12: Arrangement of the YTD gene cluster in genomes of SDB (sulfur disproportionating bacteria) and SRB (sulfate reducing bacteria). Sulfur disproportionation ability was demonstrated for bacteria shown in red (Umezawa et al., 2020).

This gene cluster YTD seems to be a good candidate but its involvement in sulfur disproportionation needs to be confirmed. It was found in the genomic comparative study by Slobodkin and Slobodkina (2019) that these genes were absent from the genome of *Desulfurella amilsii*.

In summary, sulfur inorganic compounds disproportionation pathways are not totally resolved. In some taxa, the reducing branch of the microbial sulfur disproportionation pathway involves enzymes of the sulfate-reduction pathway (Sat, AprAB, DsrAB, DsrC, DsrMKJOP) and it could very likely exist different pathways among prokaryotes.

### *1.5 Organic sulfur compounds*

Organic sulfur compounds are organic molecules which contain at least one sulfur molecule. These molecules are widespread and very diverse on Earth. They can be produced abiotically within specific conditions, or biotically especially by microorganisms. Organic sulfur compounds are present in living organisms such as certain amino acids, vitamins, co-factors, and metalloproteins. Here is a non-exhaustive list of such organosulfur compounds: methanethiol ( $\text{CH}_3\text{SH}$ ), dimethyl sulfide or DMS ( $\text{CH}_3\text{SCH}_3$ ), dimethyl sulfoxide or DMSO ( $(\text{CH}_3)_2\text{SO}$ ), 2,3-dihydroxypropane-1-sulfonate (DHPS), carbon disulfide ( $\text{CS}_2$ ), carbonyl sulfide (OCS), Acetyl methyl sulfide ( $\text{CH}_3\text{COSCH}_3$ ), cysteine ( $\text{C}_3\text{H}_7\text{NO}_2\text{S}$ ), cystine ( $\text{C}_6\text{H}_{12}\text{N}_2\text{O}_4\text{S}_2$ ) and methionine ( $\text{C}_5\text{H}_{11}\text{NO}_2\text{S}$ ). It has been proved that  $\text{CS}_2$ , OCS,  $\text{CH}_3\text{SH}$ , and  $\text{CH}_3\text{SCH}_3$  especially are and have been involved in the past in important gas fluxes on our planet, associated to climate change. Their generation depends on  $\text{CH}_4$  and  $\text{CO}_2$  concentrations (Charlson et al., 1987; Arney et al., 2018). DMS and methanethiol play an important role in the atmosphere (Loveloock et al., 1972; Charlson et al., 1987; Barnes et al., 2006). In regular aqueous environment, organic sulfur compounds such as thiols, small amounts of  $\text{CS}_2$  and dimethyldisulfide (DMDS), can be produced abiotically. They can be produced very basically from  $\text{FeS}/\text{H}_2\text{S}/\text{CO}_2$  or  $\text{FeS}/\text{HCl}/\text{CO}_2$  molecular trios in natural environment and are dependent on compound concentrations and environmental temperature (Heinen and Lauwers, 1996). In their paper, Heinen and Lauwers (1996) review all abiotic production processes of organic sulfur compounds.

Organic sulfur compounds and associated transformation pathways and intermediates in natural environments are relatively well documented and studied. These organosulfur species play an important role in the global sulfur budget (Fig. 13 and Fig. 14) (De Zwart and Kuenen, 1992; Lomans et al., 1997; Schäfer et al., 2010; Wasmund et al., 2017; Jørgensen et al., 2019). In anoxic freshwater sediments for example, there is formation of DMS and methanethiol, and their concentrations are significantly higher in sediments than at water surface (Lomans et al., 1997).

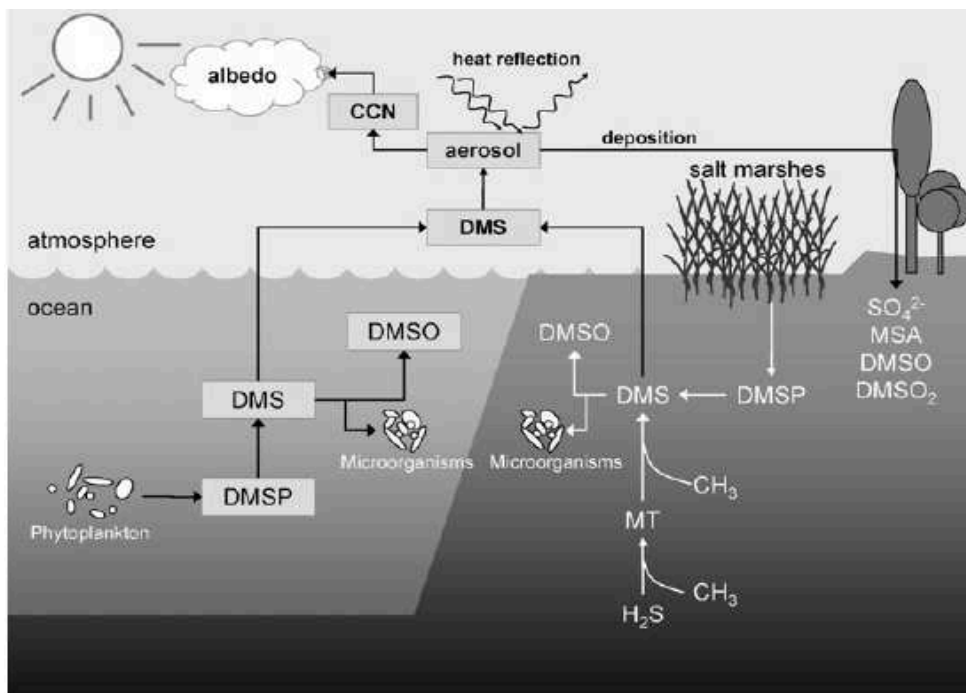


Figure 13: Schematic representation of the major pathways of DMS production and transformation in marine environment (Schäfer et al., 2010).

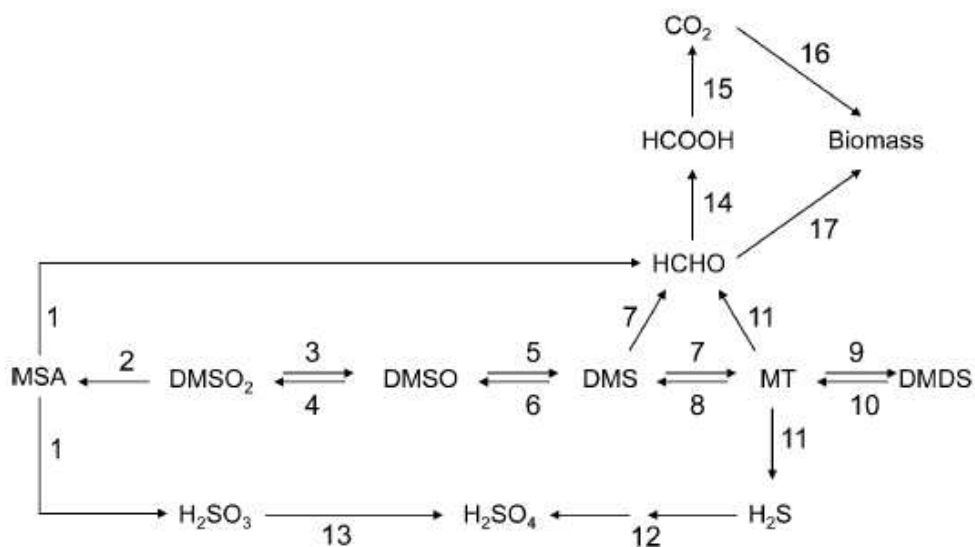


Figure 14: Biochemical and chemical interconversions of C1-sulfur compounds and key intermediates in carbon and sulfur metabolism that have been observed across a wide range of microorganisms. Either enzymes, processes or an organism in which the conversion has been observed are given as an example. 1: MSA monooxygenase; 2: FMNH<sub>2</sub>-dependent DMSO<sub>2</sub> monooxygenase; 3: DMSO<sub>2</sub> dehydrogenase; 4: Rhodococcus SY1 (Omori et al., 1995); 5: DMSO reductase; 6: DMS dehydrogenase; 7: DMS monooxygenase/DMS methyltransferase; 8: Methylation of MT; 9: Chemical oxidation of MT to DMDS; 10: DMDS reductase; 11: MT oxidase; 12: Bacterial inorganic sulfur oxidation pathways; 13: Sulfite oxidase; 14: Formaldehyde oxidation (various enzymes); 15: Formate dehydrogenase; 16: Calvin-Benson-Bassham cycle; 17: Serine cycle or ribulose monophosphate cycle (Schäfer et al., 2010).

It has been proposed that organic sulfur may have played an important role in ancient ecosystems and sulfur cycle, and may be related to origin of life and primitive metabolic cycles (Schulte and Rogers, 2004; Fakhraee and Katsev, 2019). Methanethiol, which can be produced abiotically, could be a precursor of acetyl thioester, directly related to Acyl-coenzyme A and acetate, and could have been used in primitive microbial metabolic pathways (Huber and Wachtershauser, 1997; Chen and Chen, 2005; Reeves et al., 2014). Environmental organic sulfur compounds could then be related to the first organic amino acids used by primitive microorganisms. Furthermore, metabolic networks and modeling have converged to the hypothesis that an organo-sulfur-based proto-metabolism could be likely, more likely than a proto-metabolism based on nitrogen for example (Goldford et al., 2019).

It has been shown that sulfate-reducing bacteria, methylotrophic bacteria and methylotrophic methanogenic archaea can use organic sulfur compounds as a carbon and energy source (Table 2) (Kiene et al., 1986; Finster et al., 1992; Tanimoto and Bak, 1994; Jordan et al., 1995; Scholten et al., 2003; Visscher et al., 2003; Moran et al., 2008; Schäfer et al., 2010; Rosenberg, 2013; Vanwonterghem et al., 2016). Reviews by Scholten et al. (2003) and Schäfer et al. (2010) greatly summarized reactions, associated microorganisms, mechanisms and related enzymes, free energy of formation, cultures with methylated sulfur compounds and all associated references. In addition, diversity and ecology of dimethylsulfide degrading methanogens and sulfate reducing bacteria are still being studied, especially in sediments (Tsola et al., 2021).

Table 2: Reactions involved in the sulfidogenic and methanogenic degradation of various methylated sulfur compounds. (DMS Dimethylsulfide, DMDS dimethyldisulfide, DMSP dimethylsulfoniopropionate, MMPA 3-S-methylmercaptopropionate, MPA-3-mercaptopropionate, MT methanethiol (Scholten et al., 2003).

S-compound	Reaction number	Reaction	Reference
<b>Sulfidogenic degradation</b>			
DMS	1	$(\text{CH}_3)_2\text{S} + 1/2 \text{SO}_4^{2-} \rightarrow 2\text{HCO}_3^- + 2/2 \text{HS}^- + 1/2 \text{H}^+$	Tanimoto and Bak (1994)
DMDS	2	$(\text{CH}_3)_2\text{S}_2 + 1/2 \text{SO}_4^{2-} \rightarrow \text{CH}_3\text{SH} + \text{CO}_2 + 1/2 \text{HS}^- + 1/2 \text{H}^+$	This study
DMSP	3	$(\text{CH}_3)_2\text{-S}^+\text{-CH}_2\text{-CH}_2\text{-COO}^- \rightarrow (\text{CH}_3)_2\text{S} + \text{CH}_2=\text{CH-COO}^- + \text{H}^+$	Van der Maarel et al. (1996)
DMSP	4	$(\text{CH}_3)_2\text{-S}^+\text{-CH}_2\text{-CH}_2\text{-COO}^- + 3/4 \text{SO}_4^{2-} \rightarrow \text{CH}_3\text{-S-CH}_2\text{-CH}_2\text{-COO}^- + \text{HCO}_3^- + 3/4 \text{HS}^- + 1/4 \text{H}^+$	Van der Maarel et al. (1993)
MMPA	5	$\text{CH}_3\text{-S-CH}_2\text{-CH}_2\text{-COO}^- + 3/4 \text{SO}_4^{2-} \rightarrow \text{HS-CH}_2\text{-CH}_2\text{-COO}^- + \text{HCO}_3^- + 3/4 \text{HS}^- + 1/4 \text{H}^+$	This study
MPA	6	$\text{HS-CH}_2\text{-CH}_2\text{-COO}^- + 1/2 \text{SO}_4^{2-} + \text{H}^+ \rightarrow \text{CH}_3\text{COO}^- + \text{CO}_2 + 1/2 \text{H}_2\text{S}$	This study
MT	7	$\text{CH}_3\text{SH} + 3/4 \text{SO}_4^{2-} \rightarrow \text{HCO}_3^- + 3/4 \text{HS}^- + 1/4 \text{H}^+$	Tanimoto and Bak (1994)
<b>Methanogenic degradation</b>			
DMS	8	$(\text{CH}_3)_2\text{S} + 1/2 \text{H}_2\text{O} \rightarrow 1/2 \text{CH}_4 + 1/2 \text{HCO}_3^- + \text{HS}^- + 1/2 \text{H}^+$	Finster et al. (1992)
DMDS	9	$(\text{CH}_3)_2\text{S}_2 + 1/2 \text{H}_2\text{O} \rightarrow 1/4 \text{CH}_4 + 3/4 \text{CO}_2 + 2\text{HS}^- + 2\text{H}^+$	This study
DMSP	10	$(\text{CH}_3)_2\text{-S}^+\text{-CH}_2\text{-CH}_2\text{-COO}^- + 1/2 \text{H}_2\text{O} \rightarrow 1/2 \text{CH}_4 + \text{CH}_2=\text{CH-COO}^- + 1/2 \text{HCO}_3^- + \text{HS}^- + 1/2 \text{H}^+$	This study
DMSP	11	$(\text{CH}_3)_2\text{-S}^+\text{-CH}_2\text{-CH}_2\text{-COO}^- + 4/7 \text{H}_2\text{O} \rightarrow \text{CH}_3\text{-S-CH}_2\text{-CH}_2\text{-COO}^- + 5/7 \text{CH}_4 + 2/7 \text{CO}_2 + \text{H}^+$	This study
MMPA	12	$\text{CH}_3\text{-S-CH}_2\text{-CH}_2\text{-COO}^- + 3/4 \text{H}_2\text{O} \rightarrow \text{HS-CH}_2\text{-CH}_2\text{-COO}^- + 3/4 \text{CH}_4 + 1/4 \text{HCO}_3^- + 1/4 \text{H}^+$	Van der Maarel et al. (1995)
MPA	13	$\text{HS-CH}_2\text{-CH}_2\text{-COO}^- + 2/2 \text{H}_2\text{O} \rightarrow 1/2 \text{CH}_4 + 1/2 \text{HCO}_3^- + \text{HS}^- + 1/2 \text{H}^+$	This study
MPA	14	$\text{HS-CH}_2\text{-CH}_2\text{-COO}^- + \text{H}_2\text{O} \rightarrow 1/2 \text{CH}_4 + 1/2 \text{CO}_2 + \text{HS}^- + \text{H}^+ + \text{CH}_3\text{COO}^-$	This study
MT	15	$\text{CH}_3\text{SH} + 3/4 \text{H}_2\text{O} \rightarrow 3/4 \text{CH}_4 + 1/4 \text{HCO}_3^- + \text{HS}^- + 1/4 \text{H}^+$	Finster et al. (1992)

DMS and methanethiol can be synthesized *via* biogenic hydrogen sulfide derived from sulfate reduction or other processes. The study by Visscher et al. (2003) considers that S-containing amino acids are the dominant precursors of DMS in intertidal sediment systems. Moreover, DMSP for example which is produced by several microorganisms, such as algae, can be degraded to DMS. These organosulfur compounds can be used, not only as carbon and sulfur sources, but also as energy sources or as terminal electron acceptors. As a kind of example, DMS can be used as a carbon and energy source, DMSO can be reduced by heterotrophic or phototrophic microorganisms, and both compounds can be used as sulfur sources. It was shown that few prokaryotes, and notably methanogens, from other natural environments than hydrothermal systems, can grow with methanethiol under mesophilic and thermophilic conditions (Van Leerdam et al., 2008).

DMS can be produced abiotically and be used by microorganisms as carbon and sulfur sources and also as energy source. From Schäfer et al. (2010) review, DMS can be involved in three catabolic pathways referenced as DMS monooxygenase pathway, methyltransferase pathway and DMS oxidation (Fig. 14). DMSO can be used as a terminal electron acceptor for respiration

by several mesophilic microorganisms and be reduced to DMS for example. For example, DMSO can be used as an alternative terminal electron acceptor in several species of *Desulfovibrio* (which are sulfate reducing bacteria) (Rosenberg, 2013). DMSO is not easy to handle for cultural purposes, because when it is mixed with water, it can be abiotically disproportionated into sulfite and sulfone (Wood, 1981). DMSO can also be fermented by microorganisms. Vogt et al. (1997) study, showed few prokaryotes able to respire DMSO. For example, the marine bacterium *Rhodowulum euryhalinum* is able to reduce DMSO to DMS chemotrophically and phototrophically with sulfide as an electron donor. The marine bacterium *Chlorobium vibrioforme* is able to reduce DMSO to DMS phototrophically with sulfide and thiosulphate as electron donors, but less efficiently in the dark (Vogt et al., 1997).

Some genomic markers for the oxidation of these organosulfur compounds have been identified. They are shown in Figure 14. Genes associated to the degradation of DMS have also been studied in details in the bacterium *Methylophaga thiooxydans* (Kröber and Schäfer, 2019). In this latter study, proteomics and transcriptomics were used to identify genes expressed during growth on dimethylsulfide and methanol in *M. thiooxydans* (Fig. 15).



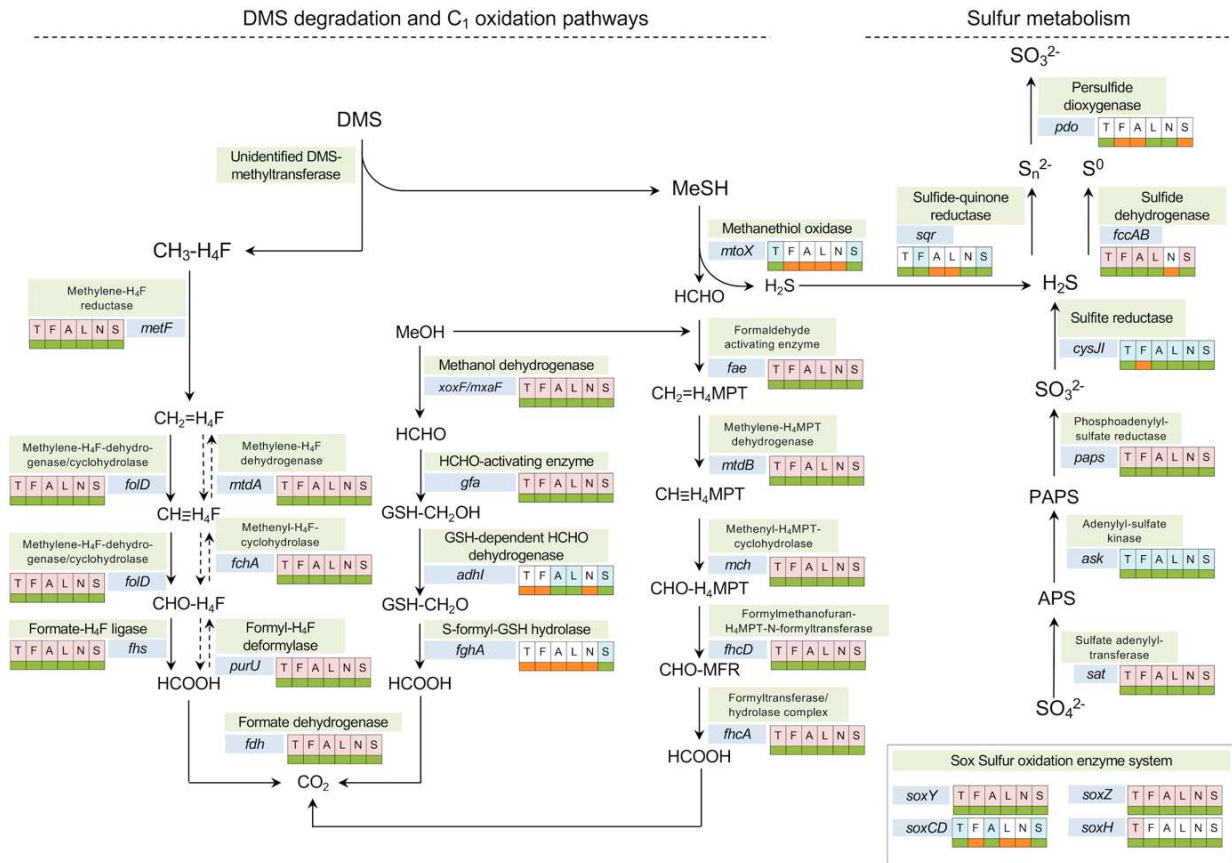


Figure 15: Metabolic pathways involved in DMS degradation/transformation, one-carbon and sulfur oxidation annotated with presence/absence of specific genes in the genomes of Methylophaga. The analysis was based on a six-way comparison among *M. thiooxydans* (T), *M. frappieri* (F), *M. aminisulfidivorans* (A), *M. lonarensis* (L), *M. nitratireducenticrescens* (N), and *M. sulfidovorans* (S). The shadings behind the letters indicate presence in core (light red) or accessory (light blue) genome. The color-coded boxes next to the genes indicate the presence (green) or absence (orange) of a gene in each genome (Kröber and Schäfer, 2019).

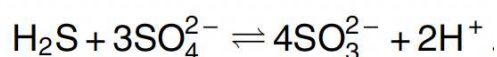
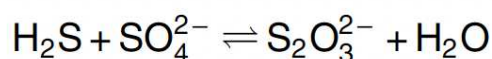
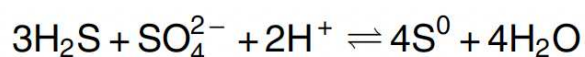
Moreover, methanethiol and DMS cycling have been studied in saltmarsh (Carrion et al., 2019). They used *mddA* (S-adenosyl-Met-dependent methyltransferase), *ddhA* (DMS dehydrogenase gene), *dmoA* (DMS monooxygenase gene), *tmm* (trimethylamine monooxygenase), *megL* (methionine gamma lyase that cleaves Met to MeSH), and *mtoX* (MeSH oxidase) gene markers for metagenomic analyses.

Organic sulfur compounds are an integral part of the microbial sulfur cycle and should not be ignored. They could be studied in other natural environments based on the search for the genetic markers described above.

## 1.6 Inorganic sulfur compounds comproportionation

New putative metabolisms can be predicted based on thermodynamics calculations. This approach allows to estimate the associated yields and to determine under which potential environmental conditions this putative metabolism could be discovered (Amend and LaRowe, 2019). This approach has been implemented in a few studies, and has led to the discovery of new putative metabolisms such as the sulfur comproportionation and new metabolisms involving manganese (Amend et al., 2020; LaRowe et al., 2021). However, thermodynamics also has its limitations and even though the free energy of a reaction may be strongly negative, this doesn't mean that the process will occur, for example for biological issues. These new putative metabolisms can be then investigated in environmental samples by cultural approaches.

Inorganic sulfur compound comproportionation is a new theoretical metabolism which has been predicted by thermodynamics, by Amend et al. (2020). It is the reverse reaction of a disproportionation, which could produce elemental sulfur, thiosulfate or sulfite from sulfate and sulfide. The reactions are as follows:



This metabolism would be more energetical at acidic pH and low temperatures (Fig. 16).

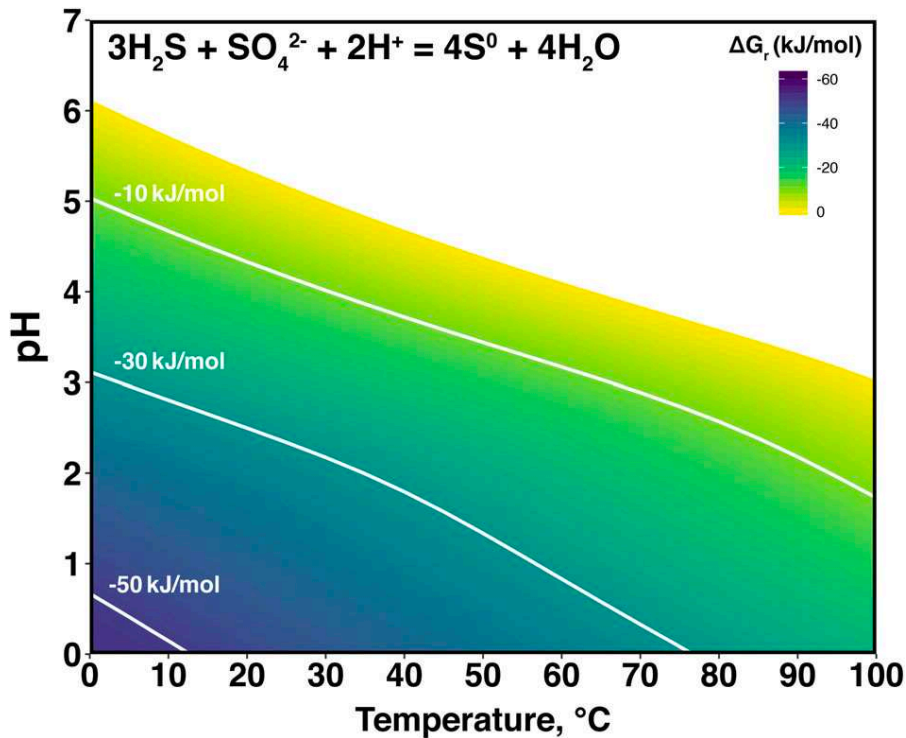


Figure 16: Values of  $\Delta G_r$  for sulfur disproportionation as a function of temperature and pH. Values of  $\Delta G^0_r$  were computed with the SUPCRT92 software package. Activities of aqueous  $\text{H}_2\text{S}$  and  $\text{SO}_4^{2-}$  across the temperature and pH space represented here were calculated with equilibrium speciation among  $\text{H}_2\text{S}$  and  $\text{HS}^-$  given a total sulfide activity of  $10^{-3}$ , and among  $\text{HSO}_4^-$  and  $\text{SO}_4^{2-}$  given a total sulfate activity of  $10^{-2}$  (Amend et al., 2020).

This metabolism is totally putative. There is still no evidence of its existence by culture or genomics up to date, making this part difficult to discuss. However, it opens many new perspectives and could increase the complexity of sulfur cycle.

## **2. Hydrothermal and geothermal environments, and their associated sulfur cycles**

### *2.1 Preamble*

During this PhD project, investigations were done with natural samples or strains from deep-sea hydrothermal vents, shallow hydrothermal vents and geothermal hot springs. However, as the initial goal of the PhD was focused on deep-sea hydrothermal vents, the section dedicated to deep-sea hydrothermal vents will be more detailed in the manuscript than shallow-sea hydrothermal vents and geothermal hot springs.

### 2.1.1 *Deep-sea hydrothermal vents*

Deep-sea hydrothermal vents are ancient and unique ecosystem located at the bottom of the ocean. These ecosystems are characterized by “extreme” conditions from an anthropocentric perspective, steep gradients, and unique chemistry. They were discovered in 1977 by Corliss and Ballard who observed for the first time the presence of life at such depth in the ocean (Corliss and Ballard, 1977; Lonsdale, 1977). Soon after the first descriptions of black smokers, the hydrothermal vent environment began to be described by the scientific community, describing its biological, geological, physical and chemical parameters (Corliss and Ballard, 1977; Lonsdale, 1977; Corliss and al., 1978; Corliss and al., 1979). However, deep-sea hydrothermal vents present such scientific potential for new discoveries that they are still intensely studied our days.

Hydrothermal vents are located in a broad range of depths, down to 4960 m at the Mid-Cayman Rise (Connelly et al., 2012). The repartition of submarine hydrothermal vents and inferred sites can be found on the InterRidge Vents Database (<https://vents-data.interridge.org/>) (Fig. 17).

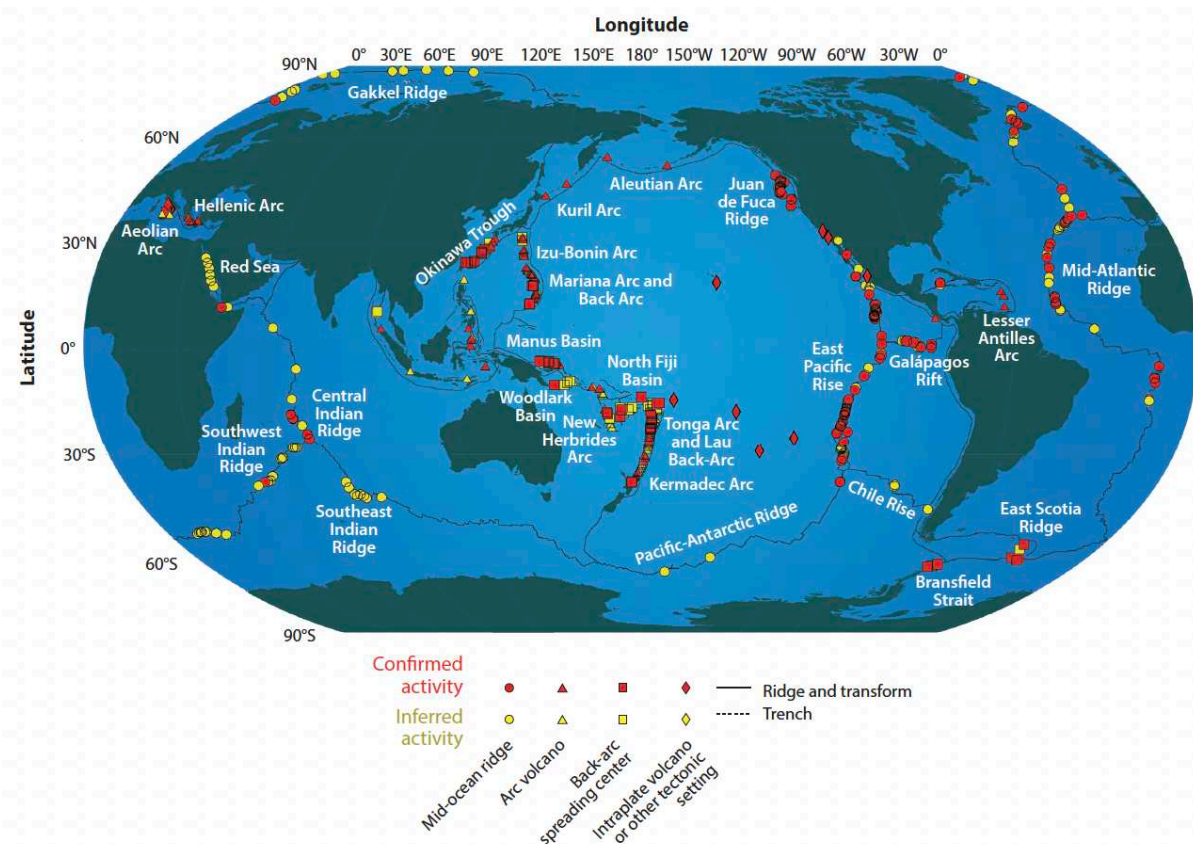


Figure 17: Map of known vent sites (red symbols) and sites thought to exist from the detection of chemical signals in the water column (yellow symbols), adapted from the InterRidge Vents Database (Humphris and Klein, 2018).

Hydrothermal vents are located at mid-ocean ridges, volcanic arcs and back-arc spreading centers or on volcanic hotspots where magmatic heat sources drive the hydrothermal circulation. Venting systems can also be located distantly from spreading centers, driven by exothermic, mineral-fluid reactions or remnant lithospheric heat (Wheat et al., 2004; Kelley et al., 2005). Most seafloor hydrothermal vent systems are associated with extension of tectonic activity and heated by magmatic heat. Hydrothermal vents geological structures are formed by the convergence of tectonic plates or their divergence. Close to the oceanic drift, the tectonic plates divergence causes a magma uprising which will be cooled down by sea water and form very porous rocks. Sea water will then infiltrate the oceanic crust, and then charge the magma close to the magmatic chamber with chemical elements that will be released to the surface of hydrothermal vents (Fig. 18) (Kelley et al., 2002; Flores and Reysenbach, 2007).

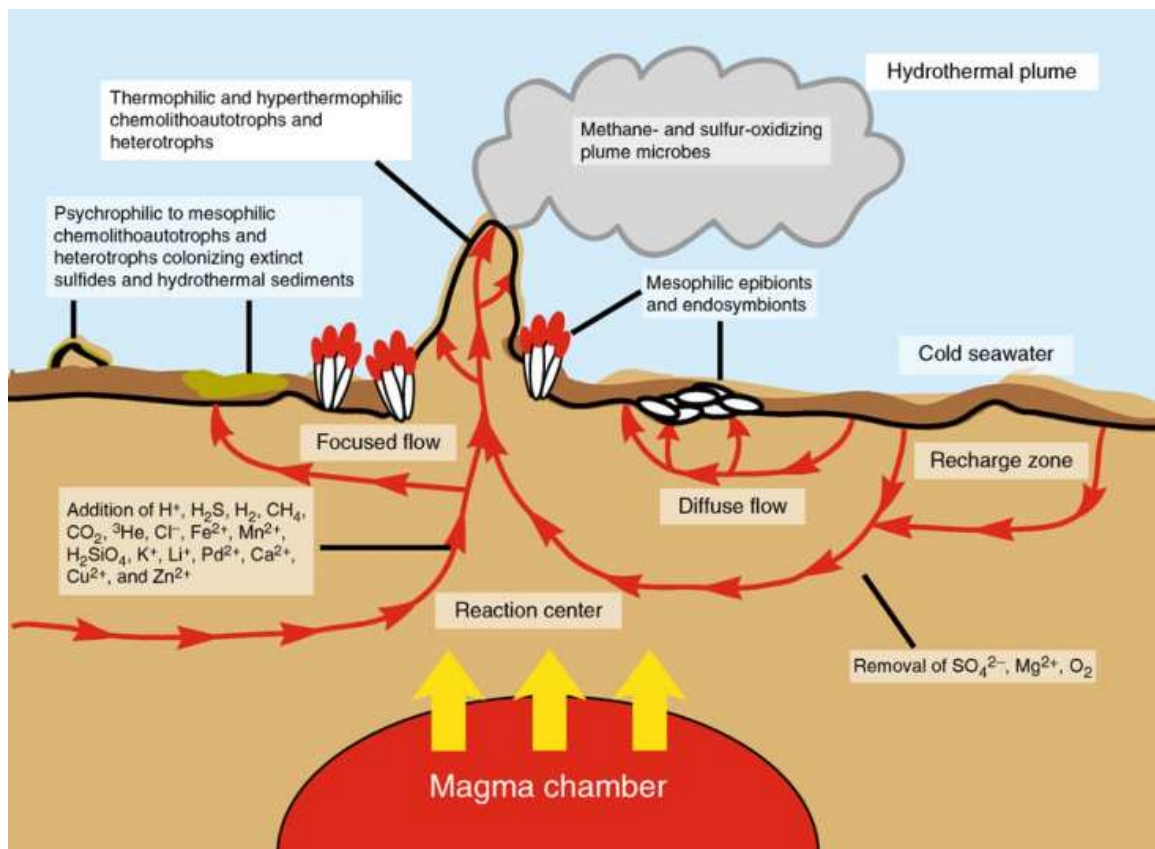


Figure 18: Deep-sea hydrothermal environments simplified diagram. Hydrothermal circulation along a mid ocean rift depicting compositional changes of seawater and microbial habitats supported by hydrothermal fluids (small arrows indicate fluid flow while large arrows indicate heat transfer from magmatic source) (Flores and Reysenbach, 2007).

Most end-member fluids from spreading centers around the world share some common chemical features. They are generally anoxic, highly reduced, often acidic (pH from 2 to 4), and are enriched in silica, carbon dioxide, hydrogen sulfide, methane, dihydrogen, iron, zinc,

copper, and other transition metals, in various concentrations (Von Damm, 1995). Geochemistry of hydrothermal fluids are getting better and better documented (Humphris and Klein, 2018). Different types of hydrothermal vents can be described based on the substratum, plume color, temperature and associated chemistry of the end members fluids. They have been classified as black and white smokers with a wide variety of intermediates. The white smokers are in general cooler, more alkalized and richer in elements such as barium, calcium and silicon. However, all hydrothermal fluids which rise at the oceanic crust at hydrothermal vent sites are cooled, and oxygenized by the sea water and form polymetallic precipitates such as metallic sulfides, calcium or barium sulfates which will participate in the hydrothermal vent chimney structure (Callac, 2013).

The first discoveries of hydrothermal vents led to the identification of chemoautotrophic symbiosis and forced biologists to reassess the contribution that chemosynthesis makes to marine primary production, particularly in the deep sea, where it can support a high biomass in a food-limited ecosystem (Corliss and al., 1979; Rogers et al., 2012). Hydrothermal vents are considered as marine oasis of life supplying energy for the development of microorganisms and macro-organisms structured into an ecosystem. The existence of life in these extremely harsh conditions has stimulated an increasing research effort on the diversity, ecology, and physiology of hydrothermal vent organisms, as well as new avenues of research into the origins of life on Earth (Rogers et al., 2012).

Several studies are focusing on hydrothermal vent environmental conditions in order to make some hypothesis on the first living organism and on the hypothetical LUCA (Last Universal Common Ancestor) (Holm, 1992; Martin and Russel, 2007; Martin et al., 2008; Loison et al., 2010; Weiss et al., 2016). The biochemistry of hydrothermal vent's chemolithotrophs might give some clues about the first potential microorganisms and biochemical pathways related to the chemistry of life. The book's chapter from De Anda et al., 2018 summarizes interestingly current trends about the origin of life.

Because of the characteristics of hydrothermal vent communities, they are regarded as unique, especially by the high levels of species endemism. Ecologists recognize that the unusual characteristics of deep-sea vents compared to other deep-sea habitats, coupled with the ephemeral nature of hydrothermal circulation, have probably important implications for the composition, diversity, and biogeography of their communities and then for the dispersal and



the genetic population structure of vent species. Several decades of exploration have resulted in the detection of numerous vent sites and faunal assemblages at many mid-ocean ridges and back-arc basins (Rogers, et al., 2012).

Hydrothermal vents are a rich source of microorganisms, at the taxonomic and metabolic point of views. We can find very diverse microbial metabolisms in these singular ecosystems. Chemolithoautotrophs, chemoorganoautotrophs, chemoorganoheterotrophs and chemolithomixotrophs have been identified, within *Bacteria* and *Archaea* (Cao, 2016; Zeng et al., 2021). The recent review by Dick (2019) introduces greatly the general characteristics of deep-sea hydrothermal vents microbiomes. Temperature plays especially, a significant role on hydrothermal vent microbial communities (Lagostina et al., 2021). Hydrothermal environments present different sources of energy especially for chemoautotrophic growth. Chimneys minerals, hydrothermal fluids, hydrothermal sediments and surrounding sea water present an important difference of redox potential. Microorganisms can use this redox differential to produce energy. The most emblematic source of energy for chemolithoautotrophy growth is the use of chemicals from the hydrothermal fluid as electron donors and chemicals from the sea water as electron acceptors with specific niches for microorganisms (Fig. 19) (Flores and Reysenbach, 2007; Dick, 2019).

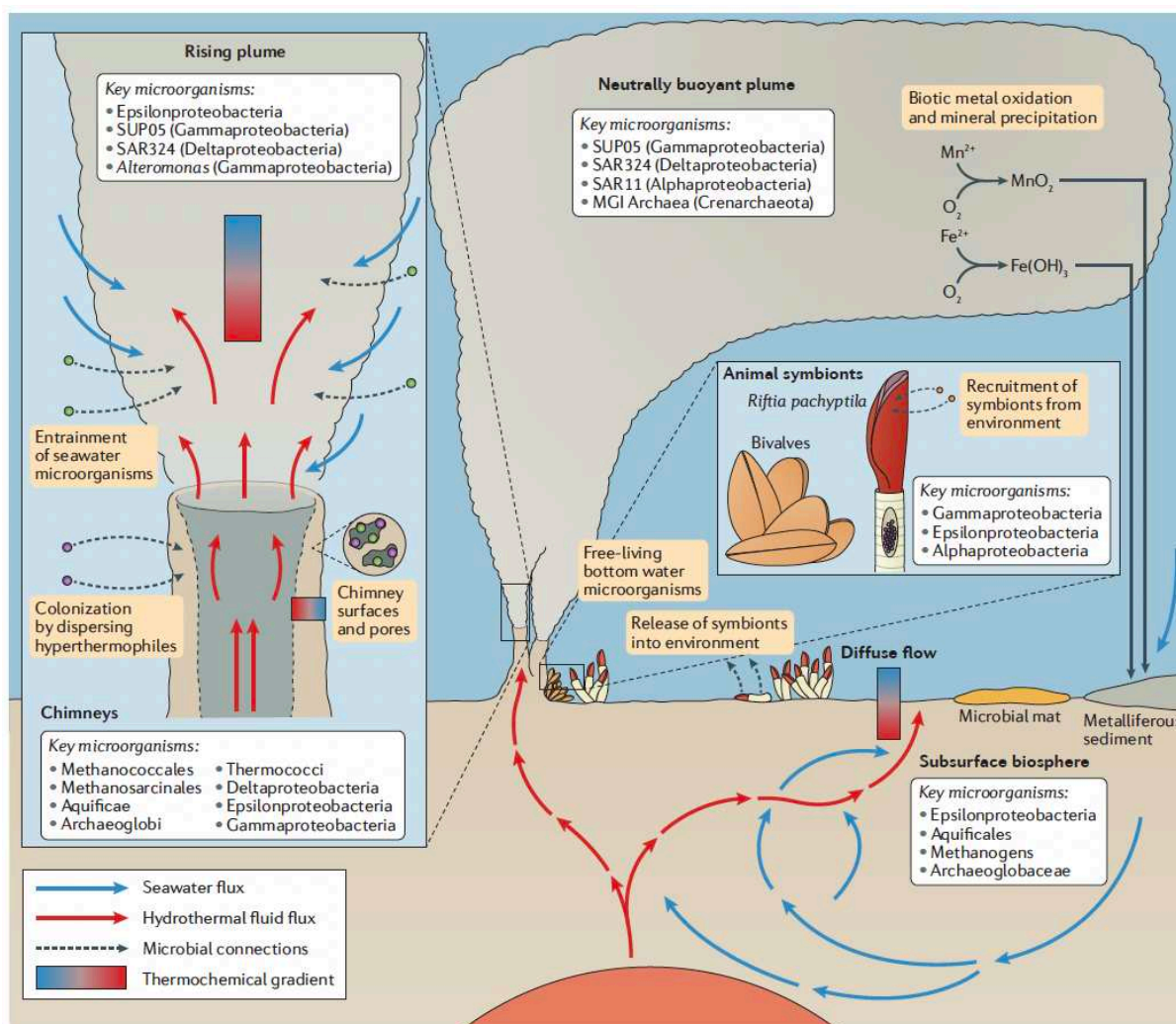


Figure 19: General microbial habitats at deep-sea hydrothermal vents. The main habitats at hydrothermal vents are chimneys, the surrounding subsurface, animals and rising plumes. Hydrothermal fluids move between habitats and mix with cold seawater. Key microorganisms for each habitat represent abundant taxa observed across multiple vent fields by various cultivation-independent approaches. The red–blue rectangle indicates a thermochemical gradient between anoxic, chemically reducing, hot hydrothermal fluids and oxic, cold seawater (Dick, 2019).

Chemolithotrophic microorganisms are the base of the whole hydrothermal vents' ecosystem. They are the microorganisms able to generate energy by exploiting the chemical disequilibria resulting from inorganic reaction kinetics of many redox reactions that can occur at the interface between oxidized seawater and reduced hydrothermal vent fluids (Fig. 19). Hydrogen sulfide, dihydrogen, elemental sulfur, thiosulfate and methane from the hydrothermal fluids can be used as electron donors, in combination with a variety of electron acceptors (Flores and Reysenbach, 2007; Renshaw, 2007). The main electron donors and electron acceptors pairs used by hydrothermal microorganisms are summarized in Table 3.



Table 3: Energetically favorable redox reactions available to chemolithotrophic microorganisms in deep-sea hydrothermal environments (Takai et al., 2006).

Type of metabolism	Electron donor	Electron acceptor	Redox reaction
Methanotrophy	CH <sub>4</sub>	O <sub>2</sub>	CH <sub>4</sub> + 2O <sub>2</sub> = CO <sub>2</sub> + 2H <sub>2</sub> O
Methanotrophy	CH <sub>4</sub>	SO <sub>4</sub> <sup>2-</sup>	CH <sub>4</sub> + SO <sub>4</sub> <sup>2-</sup> = HCO <sub>3</sub> <sup>-</sup> + HS <sup>-</sup> + H <sub>2</sub> O
Methanogenesis	H <sub>2</sub>	CO <sub>2</sub>	H <sub>2</sub> + 1/4CO <sub>2</sub> = 1/4CH <sub>4</sub> + 1/2H <sub>2</sub> O
S reduction (sulfate reduction)	H <sub>2</sub>	SO <sub>4</sub> <sup>2-</sup>	H <sub>2</sub> + 1/4SO <sub>4</sub> <sup>2-</sup> + 1/2H <sup>+</sup> = 1/4H <sub>2</sub> S + H <sub>2</sub> O
S reduction (sulfur reduction)	H <sub>2</sub>	S <sup>0</sup>	H <sub>2</sub> + S <sup>0</sup> = H <sub>2</sub> S
S oxidation	H <sub>2</sub> S	O <sub>2</sub>	H <sub>2</sub> S + 2O <sub>2</sub> = SO <sub>4</sub> <sup>2-</sup> + 2H <sup>+</sup>
S oxidation	S <sup>0</sup>	O <sub>2</sub>	S <sup>0</sup> + H <sub>2</sub> O + 31/5O <sub>2</sub> = SO <sub>4</sub> <sup>2-</sup> + 2H <sup>+</sup>
S oxidation	S <sub>2</sub> O <sub>3</sub> <sup>2-</sup>	O <sub>2</sub>	S <sub>2</sub> O <sub>3</sub> <sup>2-</sup> + 10OH <sup>-</sup> + O <sub>2</sub> + 4H <sup>+</sup> = 2SO <sub>4</sub> <sup>2-</sup> + 7H <sub>2</sub> O
S oxidation/denitrification	S <sub>2</sub> O <sub>3</sub> <sup>2-</sup>	NO <sub>3</sub> <sup>-</sup>	S <sub>2</sub> O <sub>3</sub> <sup>2-</sup> + 6OH <sup>-</sup> + 4/5NO <sub>3</sub> <sup>-</sup> + 4/5H <sup>+</sup> = 2SO <sub>4</sub> <sup>2-</sup> + 17/5H <sub>2</sub> O + 2/5N <sub>2</sub>
S oxidation/denitrification	S <sup>0</sup>	NO <sub>3</sub> <sup>-</sup>	S <sup>0</sup> + 32/5H <sub>2</sub> O + 6/5NO <sub>3</sub> <sup>-</sup> = SO <sub>4</sub> <sup>2-</sup> + 34/5H <sup>+</sup> + 3/5N <sub>2</sub> + 6OH <sup>-</sup>
S oxidation/denitrification	H <sub>2</sub> S	NO <sub>3</sub> <sup>-</sup>	H <sub>2</sub> S + 36/5H <sub>2</sub> O + 16/5NO <sub>3</sub> <sup>-</sup> = 2SO <sub>4</sub> <sup>2-</sup> + 84/5H <sup>+</sup> + 8/5N <sub>2</sub> + 16OH <sup>-</sup>
H <sub>2</sub> oxidation	H <sub>2</sub>	O <sub>2</sub>	H <sub>2</sub> + 1/2O <sub>2</sub> = H <sub>2</sub> O
Fe reduction	H <sub>2</sub>	Fe(III)	H <sub>2</sub> + 2Fe <sup>3+</sup> = 2Fe <sup>2+</sup> + 2H <sup>+</sup>
Fe oxidation	Fe(II)	O <sub>2</sub>	Fe <sup>2+</sup> + 1/4O <sub>2</sub> + H <sup>+</sup> = Fe <sup>3+</sup> + 1/2H <sub>2</sub> O
Fe oxidation/denitrification	Fe(II)	NO <sub>3</sub> <sup>-</sup>	Fe <sup>2+</sup> + 1/5NO <sub>3</sub> <sup>-</sup> + 2/5H <sub>2</sub> O + 1/5H <sup>+</sup> = 1/10N <sub>2</sub> + Fe <sup>3+</sup> + OH <sup>-</sup>
Mn reduction	H <sub>2</sub>	MnO <sub>2</sub>	H <sub>2</sub> + MnO <sub>2</sub> + 2H <sup>+</sup> = Mn <sup>2+</sup> + 2H <sub>2</sub> O
Nitrification	NO <sub>2</sub> <sup>-</sup>	O <sub>2</sub>	NO <sub>2</sub> <sup>-</sup> + 1/2O <sub>2</sub> + 2OH <sup>-</sup> + 2H <sup>+</sup> = NO <sub>3</sub> <sup>-</sup> + 2H <sub>2</sub> O
Nitrification	NH <sub>3</sub>	O <sub>2</sub>	NH <sub>3</sub> + 3OH <sup>-</sup> + 4O <sub>2</sub> = 3NO <sub>3</sub> <sup>-</sup> + 2H <sub>2</sub> O
Denitrification	H <sub>2</sub>	NO <sub>3</sub> <sup>-</sup>	H <sub>2</sub> + 2/5NO <sub>3</sub> <sup>-</sup> + 2/5H <sub>2</sub> O = 1/5N <sub>2</sub> + 8/5H <sup>+</sup> + 2OH <sup>-</sup>

Autotrophic microorganisms use an inorganic carbon source such as carbon dioxide (CO<sub>2</sub>), bicarbonates (HCO<sub>3</sub><sup>-</sup>) or carbonates (CO<sub>3</sub><sup>2-</sup>) to produce organic carbon, which is fixed using a carbon fixation pathway (Fig. 20) (Nakagawa and Takai, 2008; Hügler and Sievert 2011; Sánchez-Andrea et al., 2020). The less energy consuming carbon fixation pathways seem to be deployed at very high temperatures: Wood-Ljungdhal and dicarboxylate-4-hydroxybutyrate in microorganisms with T<sup>o</sup> opt. >90°C, rTCA cycle at 20-90°C, and Calvin-Benson-Bassham at <20°C (Hugler and Sievert, 2011).

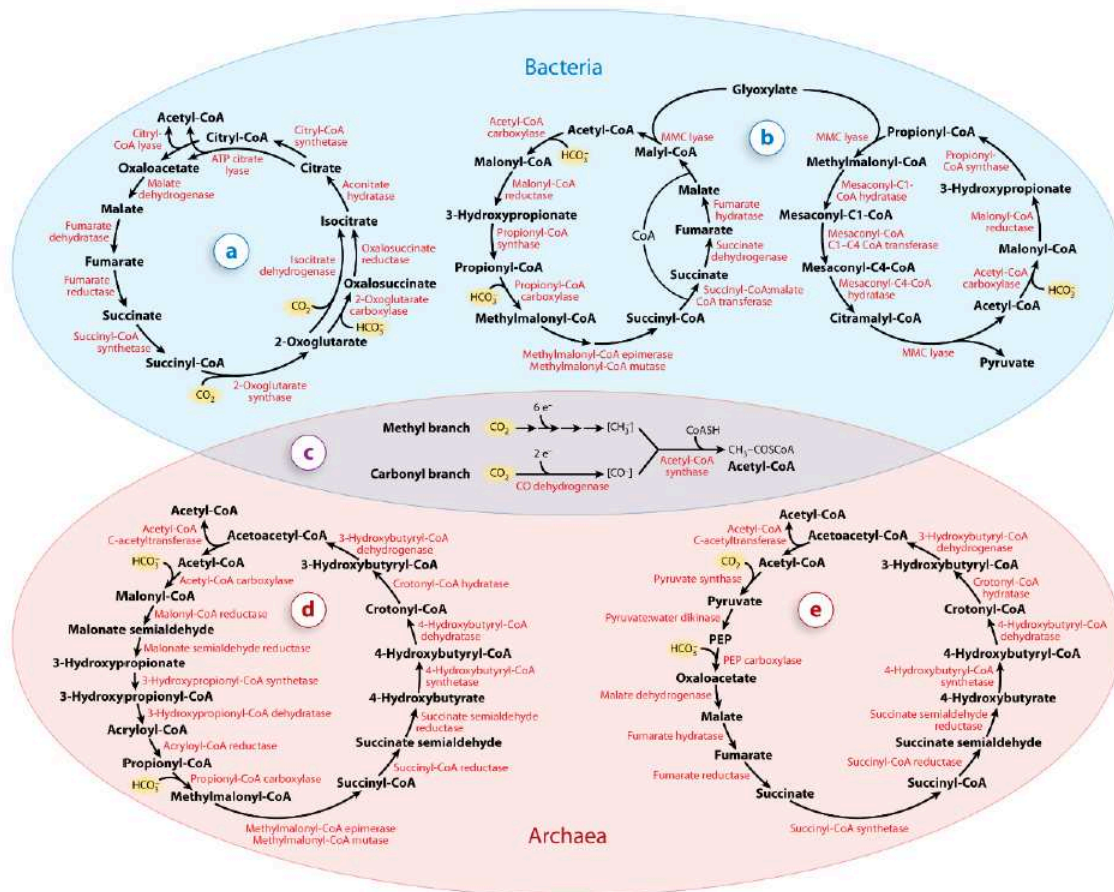


Figure 20: Various pathways of autotrophic CO<sub>2</sub> fixation in Bacteria and Archaea: (a) reductive tricarboxylic acid cycle, (b) 3-hydroxypropionate bicycle, (c) reductive acetyl-CoA pathway, (d) 3-hydroxypropionate/4-hydroxybutyrate cycle, and (e) dicarboxylate/4-hydroxybutyrate cycle. The biochemical reactions involved, as well as the enzymes (red) catalyzing the reactions, are depicted. Note that the reductive acetyl-CoA pathway is so far the only known CO<sub>2</sub> fixation pathway used by bacteria as well as archaea. (Hugler & Sievert, 2011).

A change in the level of activity of inorganic carbon-binding metabolic pathways has also been observed *via* functional studies, thus shifting from the reverse tricarboxylic pathway (rTCA) on an active hydrothermal pathway to the Calvin-Benson-Bassham (CBB) pathway on an inactive chimney (Hou et al., 2020).

Mixotrophic and heterotrophic microorganisms are also present at deep-sea hydrothermal vents (Table 4) (Godfroy et al., in press). Heterotrophs can grow either *via* microbial fermentation or/and *via* respiration of inorganic species such as oxygen, nitrate, sulfur, sulfite, thiosulfate, sulfate or ferric iron, for example.

Table 4: *Thermophilic and hyperthermophilic (underlined) species isolated from deep-sea hydrothermal vents according to the electron donor and acceptor they use for growth. (S): use sulfur as electron sink; (sp): only some species/strains of the genus perform the reaction; (M): some strains are mixotroph and also use organic matter for growth; (H): use inorganic electron donor but organic matter as carbon source; (F): perform fermentation but is also able to use inorganic electron acceptor; (CO): also able to oxidize carbon monoxide for autotrophic growth (Godfroy et al., in press).*

Electron Donor	Electron Acceptor	Genera
Organic matter (also used as carbon source)	S <sup>0</sup>	<i>Thermococcus (S), Palaeococcus (F), Pyrococcus (S), Pyrodictium (sp, F), Aciduliprofundum, Marinitoga (S), Mesoaciditoga, Kosmotoga, Thermotomaculum, Oceanithermus, Anoxybacter (F), Tepidibacter (F), Deferrisoma, Hippea</i>
	SO <sub>4</sub> <sup>2-</sup>	<i>Palaeococcus (sp, F), Desulfothermus</i>
	NO <sub>3</sub> <sup>-</sup>	<i>Vulcanibacillus, Piezobacter, Geothermobacter, Alcanivorax (F) Oceanithermus</i>
	Fe <sup>3+</sup>	<i>Aciduliprofundum, Anoxybacter (F), Caloranaerobacter (F), Deferrisoma, Geothermobacter</i>
	Fermentation	<i>Thermococcus (S), Pyrococcus (S) Caloranaerobacter, Caminicella, Carboxydoobranchium (CO), Marinitoga (S), Clostridium, Exilispira</i>
H <sub>2</sub>	O <sub>2</sub>	<i>Aeropyrum, Marinithermus, Oceanithermus, Rhabdothermus, Thermus, Vulcanithermus, Bacillus, Geobacillus, Rhodothermus, Piezobacter</i>
	S <sup>0</sup>	<i>Iqnicoccus, Pyrodictium (sp, H), Methanocaldococcus, Methanococcus, Persephonella (sp), Balnearium, Desulfurobacterium (sp), Phorcysia, Thermosulfidibacter, Thermovibrio, Thermosipho, Deferribacter (M), Hippea, Hydrogenimonas, Caminibacter (M), Cetia, Lebetimonas, Nautilia</i>
	S <sub>2</sub> O <sub>3</sub> <sup>2-</sup>	<i>Pyrolobus, Archaeoglobus (sp), Desulfurobacterium (sp), Thermosipho, Nautilia (sp)</i>
	SO <sub>4</sub> <sup>2-</sup>	<i>Archaeoglobus (M), Desulfurobacterium (sp), Thermodesulfatator (M), Thermodesulfobacterium</i>
	SO <sub>3</sub> <sup>2-</sup>	<i>Archaeoglobus (sp, M)</i>
	NO <sub>3</sub> <sup>-</sup>	<i>Pyrodictium (sp), Pyrolobus, Desulfurobacterium (sp), Persephonella, Phorcysia, Thermovibrio, Caldithrix (M), Oceanithermus (sp, M), Vulcanithermus (H), Deferribacter (M), Piezobacter, Hydrogenimonas, Nitratiruptor, Caminibacter (M), Cetia, Lebetimonas (sp), Nautilia (sp)</i>
	Fe <sup>3+</sup>	<i>Pyrodictium (sp), Geoglobus (M), Thermosipho (sp), Deferribacter (M)</i>
	CO <sub>2</sub>	<i>Methanocaldococcus, Methanococcus, Methanopyrus, Methanothermococcus, Methanotorris</i>
	O <sub>2</sub>	<i>Pyrolobus, Persephonella, Vulcanithermus (H), Piezobacter, Hydrogenimonas, Nitratiruptor</i>
	S <sup>0</sup>	Disproportionation
NO <sub>3</sub> <sup>-</sup>		<i>Hydrogenivirga, Thermosulfuriphilus, Piezobacter, Thioprofundum</i>
O <sub>2</sub>		<i>Hydrogenivirga, Persephonella, Piezobacter, Thioprofundum</i>
S <sub>2</sub> O <sub>3</sub> <sup>2-</sup>	Disproportionation	<i>Thermosulfuriphilus, Dissulfuribacter</i>
	NO <sub>3</sub> <sup>-</sup>	<i>Hydrogenivirga, Piezobacter, Thioprofundum</i>
	O <sub>2</sub>	<i>Hydrogenivirga, Persephonella, Piezobacter, Thioprofundum</i>
SO <sub>3</sub> <sup>2-</sup>	Disproportionation	<i>Thermosulfuriphilus, Dissulfuribacter</i>

### 2.1.2 Shallow-sea hydrothermal vents

Shallow-sea hydrothermal vents share characteristics with deep-sea hydrothermal vents but also display differences. They are subjected to low pressures close to atmospheric pressure and are subject to terrestrial inputs. Light is present in these systems and is an additional source of energy (Fig. 21). Shallow hydrothermal vents are generally located at a water depth of less than 200 m and, like deep-sea hydrothermal vents, they are characterized by wide redox, temperature and pH gradients, allowing chemotrophs to grow on chemical energy, in addition to phototrophs developing from light energy (Tarasov et al., 2005). These ecosystems are often rich in various sulfur compounds and have been demonstrated to be inhabited by sulfur-oxidizing bacteria, and various chemotrophic microorganisms using alternative electron donors such as sulfide, thiosulfate, molecular hydrogen and electron acceptors such as oxygen, sulfur, manganese, iron, nitrite and nitrate (Price and Giovannelli, 2017). The reviews by Tarasov et al. (2005), Price and Giovannelli (2017) and book chapter 25 by Rajasabapathy et al. (2021) greatly summarize geochemistry and especially microbiology of shallow-marine hydrothermal vents and provide comparison with deep-sea hydrothermal vents.

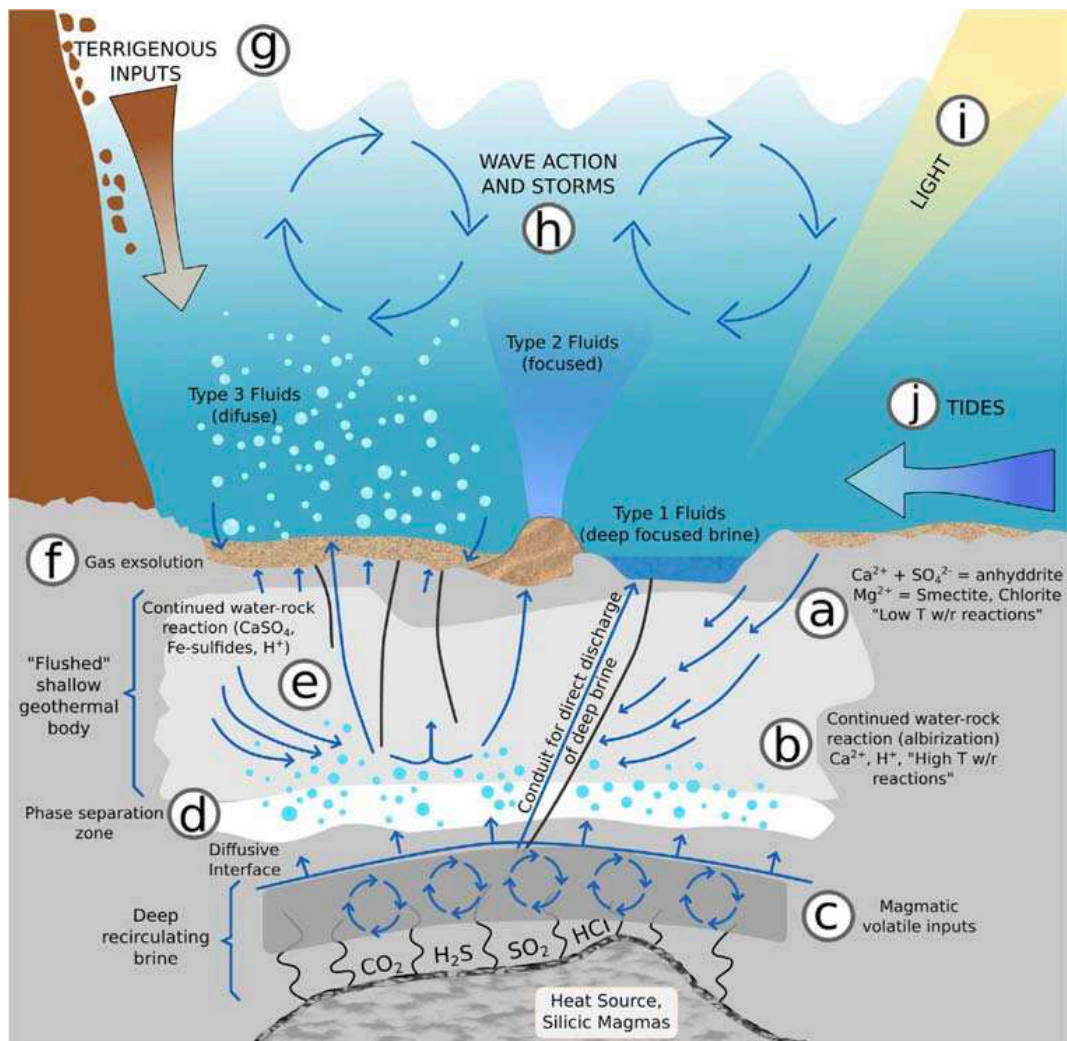


Figure 21: Schematic representation of the hydrothermal processes at shallow-water hydrothermal vents and the additional dynamic driver's characteristic of their depth range distribution. (A) Low temperature water–rock reactions, (B) high temperature water–rock reactions, (C) magmatic volatile inputs, (D) phase separation, (E) continued water–rock reactions, and (F) degassing of dissolved volatiles, (G) terrigenous input of labile organic matter and phytodetritus, (H) wave action and storms, (I) penetration of light, and (J) tidal cycles (Price and Giovannelli, 2017).

### 2.1.3 Geothermal hot springs

Geothermal sources or terrestrial hot springs are created from geothermally heated groundwater on the earth's surface. Such as shallow-sea hydrothermal vents, light and terrestrial inputs are present. Hot springs are chemically diverse environments characterized by high temperatures. They are found all over the world, and especially abundant in volcanic areas. They harbor particular microbial cohorts including endemic taxa. Hot springs are present in various



countries such as USA, Iceland, Japan, Russia, Chile, Algeria, India or New Zealand (Mehta and Satyanarayana, 2013; Schuler et al., 2017; Poddar and Das, 2018; Power et al., 2018; DesMarais and Walter, 2019). Most of the terrestrial hot springs have been the subject of numerous microbiological investigations, including the study of the microbial community composition, isolation and physiological characterization of new microorganisms, investigation of adaptive mechanisms, and searching for new enzymes, activities or molecules of biotechnological interest (Brock et al., 1972; Meyer-Dombard et al., 2005; Kublanov et al., 2009; Reigstad et al., 2010; Wemheuer et al., 2013; Merckel et al., 2017; Wilkins et al., 2019). Studies of microorganisms living in geothermal systems are also essential for exobiology purposes, as these environments are also considered as early Earth analogs and one of the possible cradles of life (DesMarais and Walter, 2019; Lezcano et al., 2019).

## 2.2 Generalities about sulfur compounds and sulfur cycling in hydrothermal and geothermal systems

Sulfur compounds are present and abundant in different parts of the hydrothermal ecosystem. They play an important role in energy production in these ecosystems. At deep-sea hydrothermal vents, inorganic sulfur compounds are present in the surrounding sea water, which contains some sulfate that could be used as a terminal electron acceptor. Seawater contains on average 28 mmol/kg of sulfate but during seafloor hydrothermal circulation, most sulfate precipitates as anhydrite ( $\text{CaSO}_4$ ) because of the temperature, and then only a small fraction of sulfate enters to the deep hydrothermal system (Ono and al., 2007). In the case of young chimneys especially, the structures are sulfate-dominated, sulfate which precipitates mainly into anhydrite, forms the first stage of chimney formation. Older chimneys are formed and composed of copper and iron sulfides especially in the chimney center (notably pyrite and chalcopyrite), forming what is called a second stage chimney (Haymon, 1983; Fouquet, 1988). Metallic sulfides establish the chimney structure, which is composed of minerals such as pyrite ( $\text{FeS}_2$ ), marcasite ( $\text{FeS}_2$ ), baryte ( $\text{BaSO}_4$ ) and sphalerite ( $\text{ZnS}$ ) for the external and central part of the chimney, and chalcopyrite ( $\text{CuFeS}_2$ ) for the inner center of the chimney (Haymon, 1983; German and Von Damm, 2004). The study by McCollom (2000) estimated the potential metabolic energy available from chemolithoautotrophic reactions in a submarine hydrothermal plume. Focusing on the vent fluid chemistry from the East Pacific Rise, they estimated that most of the energy available from potential oxidations is related to sulfur compounds, especially

from solid substrates such as the elementary sulfur and then from the sulfur-based minerals such as pyrite, sphalerite and other minerals cited before.

Hydrothermal fluids are also a source of sulfur compounds. Fluid composition differs from one geographical site to another, based on the lithological settings. Fluid properties has also a direct impact on the microbial communities' structure, especially on the chemoautotrophs that will influence the whole hydrothermal ecosystem (Flores and Reysenbach, 2011). In the hydrothermal fluid, the sulfur is present in its most reduced form which is sulfide, especially as hydrogen sulfide ( $\text{H}_2\text{S}$ ) or  $\text{HS}^-$  or  $\text{S}^{2-}$  depending on the pH. However, concentration of hydrogen sulfide, as well as that of other chemicals, can vary between hydrothermal sites (Callac, 2013).

Sulfur is also present in organic forms in hydrothermal ecosystems. As said previously, sulfur is present in living beings, for example in amino acids such as methionine and cysteine, in ferredoxins and vitamins. Other molecules such as DMS come from plankton degradation or can be abiotically produced. DMSP is present in some plankton and bacteria, and methanethiol could originate from animal feces or be abiotically produced such as in other ecosystems (Schäfer et al., 2010; Rogers and Schulte, 2012; Wasmund et al., 2017). Hypotaaurine ( $\text{C}_2\text{H}_7\text{NO}_2\text{S}$ ) and thiotaurine ( $\text{C}_2\text{H}_7\text{NO}_2\text{S}_2$ ) are also quantitatively important, notably in hydrothermal vent bivalves and worms' tissues (Rosenberg et al., 2006).

Associations of microorganisms with fauna are also found at deep-sea hydrothermal vents, and it is worth to note that their symbiotic associations are mainly based on sulfur compounds oxidation or reduction, coupled to  $\text{CO}_2$  fixation (Van Dover, 2000; Nakagawa and Takai, 2008; Hügler et al., 2010; Zeng et al., 2021).

Sulfur compounds are very interesting sources of energy and could be related to the first traces of life. In the current theories related to the origin of life based on hydrothermal vents and primitive soup theories, sulfur compounds could have played an essential role in microbial development (Raulin and Toupance, 1977; Holm, 1992; Chen and Chen, 2005; Philippot et al., 2007; Weiss et al., 2016; Ollivier et al., 2018). The biogeochemical cycling of sulfur is of special interest in the evolutionary history of electron transfers reactions. Thus, sulfur is likely to have played a key role in the history of microbial metabolisms. The book chapters by De Anda et al. (2018) and by Ollivier et al. (2018), and the review by Fike et al. (2015) summarize

and provide relevant hypotheses on primitive microorganisms and the sulfur cycle applied to the origin of life.

With the advances of metabarcoding and metagenomics techniques, our knowledge of microorganisms involved in the sulfur cycle has progressed phenomenally. A non-exhaustive list of the prokaryotes involved in the sulfur cycle isolated from deep-sea hydrothermal vents can be found in the PhD thesis of Cao (2016), in the book chapter by Godfroy et al. (in press) and in the recent review by Zeng et al. (2021).

The sulfur cycle is currently studied through ecogenomics approaches such as metabarcoding, metagenomics and metatranscriptomics. However, metabolic processes at work are more difficult to predict than thought. For example, the Dsr genes can be associated to sulfur compounds reduction, oxidation and disproportionation (Thorup et al., 2017; Anantharaman et al., 2018; Crane, 2019). Moreover, there are alternative pathways for different processes such as sulfur oxidation which could be dependent or independent from the Sox genes for some deep-sea vent chemoautotrophs (Nakagawa and Takai, 2008). As said before, the paper by Crane (2019) underlines that analyses based on genetic markers (metabarcoding, metagenomics) are biased in the case of ISC oxidation and reduction. Indeed, some enzymes can be reversible depending on the conditions or cannot guarantee the real metabolic ability. This means that metabolic predictions from such analyses remain difficult. Furthermore, in deep-sea hydrothermal vents as in other natural habitats, the sulfur cycling is also indirectly driven by viruses due to their auxiliary metabolic genes such as genes associated with sulfur and thiosulfate oxidations (Kieft et al., 2021).

In shallow-sea hydrothermal vents, the sulfur cycle is less documented. Some studies focused on chemistry, isotopy and geology (Gilhooly et al., 2014; Houghton et al., 2019). Microbiological investigations by culture-dependent and -independent methods have been performed at Eolian Islands (Italy), Kueishan Island and Kueishantao Islet (Taiwan) shallow-sea hydrothermal vents sites with their sulfur cycle insights (Maugeri et al., 2009; Wang et al., 2017, Li et al., 2018). Sulfur rich sediments of shallow hydrothermal vents of Kueishan Island (Taiwan) were composed mostly by *Sulfurovum* and *Sulfurimonas* taxa (Wang et al., 2017). Moreover, most microorganisms involved in sulfur cycle isolated from shallow-sea hydrothermal vents have been listed in the reviews by Price and Giovannelli (2017) and chapter 25 by Dhanasekaran et al. (2021).

Regarding geothermal hot springs, they are characterized by a wide diversity of geological and physicochemical conditions and of microbial taxa. For example, among the 20 hot springs of the Kamchatka area, temperatures range from 54°C to 90°C, pH range from 3.5 to 7.0 and sulfide concentrations range from 0 to 630 µM from one hot spring to another (Merkel et al., 2017). In India, from about 400 hot springs, 28 were reported with temperature from 37°C to 99 °C and pH from 6.8 to 10.0 (Poddar and Das, 2018). Sulfur is a central chemical species for energy production in some hot springs. Sulfide- and sulfur-oxidizers, sulfate-, thiosulfate-, sulfite- and sulfur-reducers, sulfur disproportionators and even symbiotic growth based on sulfur compounds have been reported in hot springs (Merkel et al., 2017; Kawai et al., 2019).

Below, we present more detailed information on ISC disproportionation, ISC-comproportionation, and the use of organic sulfur compounds in deep-sea hydrothermal vents, and succinctly summarize the state of knowledge on these microbial processes in shallow hydrothermal vents and geothermal hot springs.

### 2.3 Diversity of ISC-reducers in marine hydrothermal vents

Sulfur-, thiosulfate-, sulfite- and sulfate-reducing prokaryotes are listed in two books (Amend et al., 2004; Dahl and Friedrich, 2008) and a PhD thesis (Cao, 2016). They are also detailed in the recent review by Zeng et al. (2021). They belong to the following bacterial and archaeal phyla or families: *Campylobacterota*, *Proteobacteria*, *Nitrospirae*, *Firmicutes*, *Aquificae*, *Thermotogae* and *Deferribacteres*, for the domain *Bacteria*, and *Euryarchaeota* and *Crenarchaeota*, for the domain *Archaea*. Among those phyla or families, some genera, orders and classes are better described. Members of the orders *Thermococcales* and *Thermotogales* for example, are anaerobic heterotrophic sulfur-reducing thermophiles. Members of *Desulfurococcales*, *Desulfurobacterales*, *Nautiliales*, and *Deferribacteres* are hydrogen-oxidizing, and sulfur-reducing autotrophs and mixotrophs. Members of the genera *Caminibacter*, *Nautilia*, *Lebetimonas*, and *Cetia* are sulfur-reducing autotrophs and mixotrophs. Members of the genera *Pseudodesulfobacterium*, *Desulfobacterium*, and *Desulfonauticus* are sulfate-, thiosulfate-, sulfite- reducers and members of the genus *Desulfothermus* are sulfate reducers. Representatives of the genera *Desulfobacterium* and *Thermovibrio* are sulfur-reducing chemolithoautotrophs using hydrogen as sole electron donor. Finally, members of the class *Thermodesulfobacteria* are sulfate reducers and taxa of the genus *Deferribacter* are sulfur reducers.



In shallow-sea hydrothermal vents, numerous thermophilic microorganisms couple the oxidation of organic matter or H<sub>2</sub> and to the reduction of sulfur (Tarasov et al., 2005). List of involved prokaryotes are available in the review by Price and Giovannelli (2017). Sulfur reducers belong to the phyla *Euryarchaeota* (*Pyrococcus*, *Thermococcus*), *Crenarchaeota* (*Acidianus*, *Pyrodictium*, *Staphylothermus*, *Stetteria* and *Ignicoccus*), *Aquificae* (*Thermovibrio*), *Proteobacteria* (*Desulfurella*, *Hipaea*), *Planctomycetes* (*Thermostilla*), *Thermotogae* (*Kosmotoga*), and *Firmicutes* (*Bacillus*). Sulfate-, sulfite- and thiosulfate-reducers are represented by *Euryarchaeota* (*Archaeoglobus*) and *Proteobacteria* (*Desulfacinum*). Finally, sulfite reducers include only the species *Thermus thermophilus*.

#### 2.4 Diversity of sulfur-oxidizers in marine hydrothermal vents

Likewise, ISC-oxidizers are listed in two books (Amend et al., 2004; Dahl and Friedrich, 2008), in the PhD thesis of Cao (2016) and in the review by Zeng et al. (2021). These microorganisms belong to the phyla *Campylobacterota*, *Proteobacteria*, *Aquificae*, and *Thermodesulfobacteria*. Members of the genera *Sulfurimonas*, *Sulfurovum* and *Lebetimonas* are mesophilic sulfur-oxidizers commonly found in these habitats. Members of the order *Thiotrichales* are sulfur-oxidizers and representatives of the genus *Aquifex* genus are thermophilic hydrogen- and/or sulfur-oxidizers.

Sulfur-oxidizers can be free-living or symbiotic. Sulfide can notably be oxidized by some bacteria present in several species of tube worms, mussels or shrimps for example (Van Dover, 2000; Nakagawa and Takai, 2008; Hügler et al., 2010; Zeng et al., 2021). Thiosulfate can also be oxidized by bacteria within invertebrate symbioses, especially within the bivalve mollusks. Elemental sulfur can moreover be oxidized by tubeworm's symbionts, and may serve as a short-term energy storage (Van Dover, 2000).

In shallow-sea hydrothermal vents, prokaryotes are highly involved in the oxidative phase of sulfur cycle, for example at the Panarea shallow marine vents (Maugeri et al., 2009). Sulfur oxidizers comprise *Crenarchaeota* (*Acidianus* genus), *Aquificae* (*Hydrogenivirga* genus), and *Proteobacteria* (*Hydrogenobacter* and *Thiobacillus* genus), while thiosulfate oxidizers include various genera of *Proteobacteria* (*Hydrogenobacter*, *Galenea*, *Halothiobacillus*, *Inmirania* and *Sulfurivirga* genus) (Price and Giovannelli, 2017).

*Thiomicrospira*, *Thiomicrothrix*, *Thiothrix*, *Sulfurovum*, and *Arcobacter* were identified as key genera in the Kueishantao Islet shallow vents, deriving their energy from the oxidation of reduced sulfur compounds and fixing dissolved inorganic carbon (Li et al., 2018). Sox-dependent and reverse sulfate reduction were identified as main pathways of energy generation, and thought to be probably coupled to denitrification by providing electrons to nitrate and nitrite (Li et al., 2018).

### 2.5 Sulfur-disproportionators from hydrothermal vents

Among the 43 prokaryotes strains identified as sulfur compounds disproportionators, 9 bacterial species have been isolated from hydrothermal ecosystems, and do not rely on the SOR enzyme.

The species *Thermosulfuriphilus ammonigenes*, *Dissulfuribacter thermophilus*, and *Thermosulfurimonas dismutans* originate from deep-sea hydrothermal vents (Slobodkin et al., 2012; Slobodkin et al., 2013; Slobodkina et al., 2017). Sulfur-disproportionators might also possibly be present in the microbiome associated with the deep-sea hydrothermal shrimp *Rimicaris exoculata*, such as *Candidatus* “*Desulfobulbus rimicarenis*” (Jiang et al., 2020). The species *Thermosulfurimonas marina* and *Dissulfurirhabdus thermomarina* originate from shallow hydrothermal vents (Slobodkina et al., 2016; Frolova et al., 2018). The species *Dissulfurispira thermophila*, *Caldimicrobium rimae* (strains FM8 and 76), *Caldimicrobium thiodismutans* and *Dissulfurimicrobium hydrothermale* originate from terrestrial hot springs (Kojima et al., 2016; Slobodkin et al., 2016; Merkel et al., 2017; Umezawa et al., 2021).

As said before, sulfur-disproportionators can use alternative catabolic pathways associated with higher energetical yields. For example, *T. ammonigenes*, *D. thermophilus*, *T. dismutans*, and *T. marina* can perform DNRA (Dissimilatory Nitrate reduction to Ammonium). *D. thermomarina* can reduce sulfite with H<sub>2</sub> as an electron donor, but does not reduce sulfate while its genome encodes a complete set of genes necessary for the dissimilatory reduction of sulfates (including the *sat* gene). However, in the current state of knowledge, *Dissulfurimicrobium hydrothermale* and potentially *Caldimicrobium thiodismutans* and *Caldimicrobium rimae* (strains FM8 and 76) might only be able to grow by ISC disproportionation, which makes them very interesting genomic models (Slobodkin and Slobodkina, 2019). Main physiological characteristics and taxonomic position of those ISC-disproportionators are reported in Slobodkin and Slobodkina (2019), and in the study by Umezawa et al. (2020) for hot spring's taxon *Dissulfurispira*

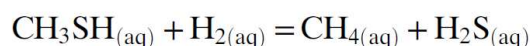
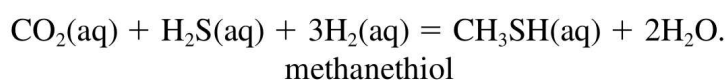
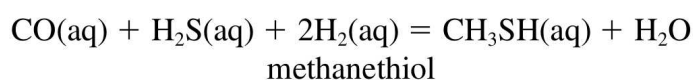
*thermophila*. Currently, genomes of 7 species out of the 9 have been sequenced and deposited in public databases, and their genomic contents have been investigated (Kojima et al., 2016; Mardanov et al., 2016; Slobodkina et al., 2017b; Allieux et al., 2020; Allieux et al., 2021; Slobodkina et al., 2021; Umezawa et al., 2021).

As ISC disproportionation is sensitive to sulfides and becomes energetically more favorable in the presence of sulfide scavengers, this catabolic reaction might be favorable in hydrothermal ecosystems. Indeed, iron and manganese oxides are present in high concentration at some deep-sea hydrothermal sites, which should favor their presence (Chavagnac et al., 2018).

## 2.6 Organic sulfur compounds in hydrothermal vents and microorganisms degrading them

From an analysis of the current scientific literature, we concluded that there is an important lack of data, on this issue. Indeed, very few studies focused on sulfur organic compounds in hydrothermal environments, especially in deep-sea hydrothermal vents (Schulte and Rogers, 2004; Dias et al., 2009; Schulte, 2010; Rogers and Schulte, 2012; McDermott et al., 2015; Longnecker et al., 2018). Furthermore, no prokaryote able to grow on organic sulfur compounds as sole energy or carbon source has been isolated to date from this ecosystem (Rogers and Schulte, 2012). Organosulfur compounds are diverse, so we decided to focus mainly on methanethiol and DMS, which are the molecules the best known in other ecosystems.

Under deep-sea hydrothermal vents conditions, methanethiol could be theoretically produced abiotically from dissolved elements according to the three reactions described below (Schulte and Rogers, 2004; Reeves et al., 2014):



Methanethiol can also originate from biological sources such as microorganisms which can produce this molecule. It can also derive from biological degradation of organics, particularly thermal degradation. However, some studies indicated that there are no significant evidences for abiotic methanethiol synthesis from inorganic precursors in hydrothermal fluids (Reeves et al., 2014). The main source of methylated organic compounds was demonstrated to derive from the pyrolysis of subsurface organic matter in crustal mixing zones (Reeves et al., 2014).

Methanethiol and DMS have been speculated to be present at concentrations ranging from  $10^{-9}$  to  $10^{-3}$  M in hydrothermal systems (Reeves, 2010; Rogers et al., 2012; Reeves and al., 2014). However, concentrations of these organosulfur compounds could be more important in some hydrothermal sites (Reeves, 2011; Reeves et al., 2014). These estimates of methanethiol and DMS concentrations found at deep-sea vents were then further revised to be more probably comprised between  $10^{-9}$  and  $10^{-6}$  M (Reeves, 2010; Reeves and al. 2014). The highest concentration of methanethiol was reported in the Guaymas basin, with a value over  $10^{-5}$  M of methanethiol in the hydrothermal fluid endmember. The areas the most enriched in methanethiol are probably subsurface mixing of high temperature endmember fluids with seawater (Reeves et al., 2014). It seems that there are is no correlation with the chemical species present at a given site and the methanethiol concentration that is measured, while methanethiol can be produced abiotically with  $\text{CH}_4$ ,  $\text{CO}_2$ ,  $\text{H}_2\text{S}$  and  $\text{H}_2$ . In hydrothermal systems, methanethiol could be more likely derived from a biological degradation or from other geological and chemical parameters (Reeves, 2010).

2,3-dihydroxypropane-1-sulfonate (DHPS) seems to be abundant in the ocean, and maybe also at deep-sea hydrothermal vents (Longnecker et al., 2018). This organosulfur compound can be produced by bacteria and diatoms. In the study by Longnecker et al. (2018), it was still the most abundant organic sulfur compounds compared with 3-mercapto-propionate, 5'-deoxy-5'(methylthio)adenosine and dimethylsulfoniopropionate (DMSP). The DHPS metabolism has been recently investigated in the *Roseobacter* genus (Chen et al., 2021).

Neil and al. (1988) discovered that the bacterium *Thiobacillus thioparus* is able to grow on carbon disulfide. However, we didn't find any information relative to carbon disulfide in deep-sea hydrothermal vents apart abiotic synthesis of organic compounds from carbon disulfide under hydrothermal conditions (Rushdi and Simoneit, 2005).

Interestingly, metabolic modelling based on thermodynamics indicated that the oxidation of methanethiol and DMS with various electron acceptors would be exergonic at deep-sea hydrothermal vents (Rogers and Schulte, 2012). Rogers and Schulte (2012) calculated potential free energy yields from the oxidation of these organosulfur compound, at various temperatures and with diverse electron acceptors such as sulfate, nitrate and oxygen. They moreover, suggest different utilization according to the temperature and oxygen availability of these compounds (Rogers and Schulte, 2012).

The only concrete information we found in the literature is that several prokaryotes from hydrothermal vents can use cystine as a terminal electron acceptor or as an amino acid source (Erauso et al., 1993; L'Haridon et al., 2019). Instead of trying to enrich or isolate taxa that oxidize or reduce organosulfur compounds, it would be interesting to test isolates of hydrothermal origin for their ability to oxidize or reduce organic sulfur compounds. For example, the deep-sea hydrothermal vent bacterium *Marinithermus hydrothermalis* is a strictly aerobic heterotroph that can utilize a variety of organic compounds, perhaps it could grow on organic sulfur compounds (Sako et al., 2003).

Prokaryotes using organosulfur compounds can also be studied by molecular and genome-based approaches. Microorganisms able to use methanethiol or/and DMS can be analyzed by studying few specific genes, such as in the study of Carrión et al. (2019). As a kind of example, the study of Kröber and Schäfer (2019) focusing on organic sulfur pathway, and especially DMS, is very complete and interesting and could inspire future work on hydrothermal vents. If we merge data from Carrión et al. (2019) and of Kröber and Schäfer (2019) studies, we could have relevant leads to study methanethiol and DMS metabolisms by omics approaches. Moreover, Smeulders et al. (2011) study is related to carbon disulfide genes and proteins sequences that could be used.

Based on such an approach, Zhou et al. (2020) reconstructed MAGs from deep-sea hydrothermal plume metagenomes which code the genetic potential to use organosulfur compounds. For the first time, hydrothermal MAGs with associated transcriptional activities were investigated regarding organic sulfur compounds. They predicted methanethiol oxidation in *Methanococcales* and *Cycloclasticus* MAGs because of the presence of *mto* operons and gene expression observed and other associated enzymes (Zhou et al., 2020). From these results,

perspectives to find new prokaryotes using organic sulfur compounds in deep-sea hydrothermal vents are promising.

Finally, it could be interesting to evaluate potential biotechnological applications if we discover new prokaryotes able to degrade organosulfur compounds. The study of Yao et al. (2019) is focused on methanethiol removal. It is an interesting subject because methanethiol is a toxic molecule and it can have high ecological impacts, especially associated to waste management. In theory, it should be very useful to describe new thermophilic species able to degrade methanethiol fast and efficiently.

### 2.7 Sulfur comproportionation in marine hydrothermal vents

As seen before, sulfur comproportionation metabolism is not documented and is theoretical. This is the reason why it is difficult to discuss perspectives on such a topic. However, from thermodynamics, it was observed that cold and acidic environment, and high concentration of sulfate and sulfide increase energy yield of the reaction and then should increase the probability to find such microorganisms with this potential metabolism (Amend et al., 2020). It was listed in the article of Amend et al. (2020) probable environments favorizing presence of sulfur compounds comproportionators. Shallow-sea and surficial hydrothermal systems, interfaces between acidic, sulfidic vent fluids and cooler, sulfate rich seawater and acid-sulfate crater lakes could be environments of interest to search for sulfur comproportionation. Moreover, by hypothesis, cold sediments close to deep-sea hydrothermal vents could also be considered.

### **3. PhD initial goals and scientific questions**

The sulfur cycle is relatively well known in environments such as soil, marine and freshwater systems, especially sediments. It is less documented at shallow and deep-sea hydrothermal vents or geothermal hot springs, despite the importance of sulfur in these ecosystems. The biogeochemical cycling of sulfur in hydrothermal environments includes aerobic and anaerobic prokaryotic activities related to the reduction and oxidation of sulfur compounds. These metabolisms are relatively well documented, but other sulfur metabolisms are less known and studied and even hypothetical for some of them. It is the case for ISC disproportionation, sulfur organic compounds metabolisms and sulfur comproportionation. The initial focus of this PhD thesis was to address these three metabolisms in order to increase our knowledge of these reactions, and even to find genetic markers to estimate their importance in natural environments by combining cultural and functional approaches. The idea was to put more emphasis on sulfur disproportionation and to consider the use of organo-sulfur compounds and the sulfur comproportionation as side projects. Disproportionation of inorganic sulfur compounds deserves further study because there are currently no specific genomic markers for this reaction, making impossible to study the distribution of taxa that carry it out. Moreover, it is very likely that there are several disproportionation pathways and therefore several markers for disproportionation. Finding such markers could help us test one of our hypotheses that ISC disproportionation is more prevalent than previously thought in diverse ecosystems.

After three years, the PhD project has evolved significantly based on initial results and technical issues. The main objective of this PhD project was redirected towards understanding the microbial disproportionation of elemental sulfur based on the search for genomic markers in hydrothermal microorganisms using comparative genomics and then comparative proteomics combined with chemical monitoring of substrates and products of metabolism. Side projects were also addressed: namely, the cultivation of microorganisms oxidizing or reducing organic sulfur compounds and the cultivation sulfur comproportionators. Finally, a global study was conducted using metagenomic approaches to place the sulfur cycle in an environmental context. Results of this PhD thesis conducted over three years are presented in four chapters. The original project was ambitious, as was the revised project. In addition, significant time was lost due to numerous tweaks, cultural and molecular concerns, as is certainly the case in all research work, so that not all experiments resulted in publishable results.

In summary this PhD thesis was organized as follows, into four chapters:

- (i) Cultivation of deep-sea hydrothermal microorganisms able to use organic sulfur compounds
- (ii) Exploring inorganic sulfur compound disproportionation at deep-sea hydrothermal vents
  - a. *Genomic and Physiological characterization of new marine hydrothermal microorganisms able to disproportionate inorganic sulfur compounds*
  - b. *Understanding the metabolic pathway of microbial elemental sulfur disproportionation*
- (iii) Investigation about sulfur comproportionation
- (iv) Investigation of the microbial sulfur cycle in hydrothermal vents and geothermal springs; example of the Kerguelen hot springs

The different angles of study implemented in this work are summarized below.

### 3.1 Characterization of new microorganisms involved in the sulfur cycle by culture and genomics

The first scientific approach used was the characterization of new microorganisms able to perform ISC disproportionation, sulfur comproportionation and use organosulfur compounds *via* cultural/physiological approaches and genomics. Culture-based approach allow the isolation and physiological characterization of taxa. Genomics allow to study these microorganisms with no or very limited culture, which is advantageous for microorganisms difficult to grow. This is the reason why a special effort was made during this PhD to design and optimize a complete procedure to go from genomic DNA extraction to genome annotation with most accurate bioinformatics tools. Genomic approaches have been focused on the study of sulfur-disproportionators. By this approach, we sequenced and analyzed the genome of three already characterized bacteria, *Thermosulfurimonas marina*, *Thermosulfuriphilus ammonigenes* and *Dissulfurirhabdus thermomarina* in order to gain insight on their genomic potential. Moreover, we sequenced the genome of a new isolate, *Thermosulfurimonas* strain F29, we analyzed its genomic content and also predicted some physiological features.



These results that have been included in this thesis as three published and one submitted scientific articles.

### 3.2 Inorganic sulfur compound disproportionation understanding by multi-omics comparative approaches

Then, efforts were made in order to decipher the genes, proteins and catabolic pathways of elemental sulfur disproportionation by implementing multi-omics approaches and analytical methods. Comparative genomics carried out with genome of taxa from hydrothermal habitats allowed the discovery of a cluster composed of 3 genes that could be potentially involved in sulfur disproportionation. Then, an experiment was carried out by implementing proteomics and chemical analyses of substrates and products of metabolism, with strains grown on one hand under sulfur disproportionation conditions, and on the other hand under sulfate-reduction conditions, in order to investigate the pathways of sulfur disproportionation. However, due to technical issues we were not able to complete the experiment of comparative proteomics and then discussed only the preliminary results in the manuscript. No genomic markers clearly specific of the process of sulfur disproportionation could be retrieved but several hypotheses can be proposed from our work.

### 3.3 Investigation of the microbial sulfur cycle in an ecological context

Finally, a last study was done in order to replace the knowledge about sulfur cycle into an ecological context. The oceanographic mission in which I was supposed to participate having been cancelled due to the worldwide pandemic in Covid-19, this study was carried out from four samples of terrestrial hot springs of Kerguelen Islands which were available in the laboratory and which were particularly interesting because the microbial communities that they host are very poorly documented.

## **Chapter 2: Tentative attempts to isolate deep-sea hydrothermal microorganisms able to use organic sulfur compounds**

### **1. Preamble**

As seen in the introduction, no prokaryote able to grow on organic sulfur compounds as sole energy or/and carbon source has been isolated to date from deep-sea hydrothermal ecosystem. We found in the literature that organic sulfur compounds are naturally present in this singular habitat and potentially at high concentrations from some species. In addition, the presence of genes involved in DMS and methanethiol catabolism was recently reported in deep-sea hydrothermal vent metagenomes, (Zhou et al., 2020). As a conclusion it is very likely that prokaryotes using these compounds could be discovered in deep-sea hydrothermal samples.

The tentative enrichment and isolation of strains using organic sulfur compounds was carried out at the beginning of the PhD and passed through several issues. As the appropriate equipment were not present in our lab to work with DMS and methanethiol (dangerous for human health), we decided to focus on harmless molecules such as DMSO, cystine and cysteine. No growth was observed in these experiments probably due to the fact that we did not work with fresh hydrothermal samples. We then decided to abort any experiments based on culture or bioinformatics in order to focus exclusively on inorganic sulfur disproportionation. The goal of this succinct chapter is mainly to summarize the experiments that were carried out, despite of their failures, in order to be improve for future projects and especially to be performed with fresh samples to isolate new microorganisms able to use organic sulfur compounds from those ecosystems.

### **2. Materials and Methods**

#### Hydrothermal samples used as inocula

Two samples were used for these enrichment cultures in the presence of organic sulfur compounds, collected from previous oceanographic cruises:

- Hydrothermal sulfide rock sample from the TAG vent field, at the Mid Atlantic Ridge, collected during the Bicose 2 cruise (N 26° 8' 12.42" W 44° 49' 33.959") (2018).
- Hydrothermal chimney fragments from the Von Damm Vent Field at the Mid-Cayman Rise, collected during the cruise QUELLE2013 (Hole to Hell; N 22° 35' 2.76" W 47° 53' 32.64") (2013).

### Culture media

This medium contained (per liter distilled water): 0.3 g NH<sub>4</sub>Cl, 0.5 g KCl, 0.15 g CaCl<sub>2</sub>.6H<sub>2</sub>O, 0.2 g KH<sub>2</sub>PO<sub>4</sub>, 20.00 g NaCl, 3.00 g MgCl<sub>2</sub>.6H<sub>2</sub>O, 10 mM PIPES buffer, two drops of resazurin at 1% (w/v) and 1 ml trace element solution (SL-10). The mineral medium was then boiled to remove dissolved oxygen, pH was adjusted to 6.0 before to be autoclaved at 121°C for 20 minutes. We used penicillin flasks of 50 mL for cultures with 25 mL of media. Different combinations of electron donors and acceptors were then added to the mineral medium. Gaseous phase was then replaced with N<sub>2</sub> (100%) or N<sub>2</sub>/CO<sub>2</sub> (80%/20%) by flush to obtain 1 bar in the flasks and 0.1 mL of 5% Na<sub>2</sub>S solution was added in some cases to reduce the medium, depending on conditions.

Added organic sulfur compounds were DMSO (20 mM), cysteine (20 mM) or *L*-cystine (10 g/l), as electron acceptors, or DMSO (20mM) for unique substrate for fermentation. Cultures were incubated at 22, 50°C, 65°C, 80°C and 95°C. Unless stated otherwise, the gaseous phase consisted of 1 bar of 100% N<sub>2</sub> and, excepted when the tested electron donor was H<sub>2</sub> (80% H<sub>2</sub>, 20% CO<sub>2</sub> gaseous phase).

Incubation times are not reported because of experimental issues with cultures. Cultures were moreover observed by epifluorescence microscopy with SYBR®Green. Inoculation was performed at 1/10th, and subcultures were performed up to four times with a transfer ratio of 4% (v/v).

### **3. Results and Discussion**

No significant growth was ever observed under any of the conditions. No growth could be maintained for any of the conditions described above after four subcultures under the same conditions.

Absence of microbial growth could be related to the long storage of the sample from the Mid-Cayman Rise. As a conclusion, under our experimental conditions, it was not possible to get any isolate using organic sulfur compounds from the collected samples.

### **4. Conclusions and Perspectives**

Culture with organic sulfur compounds were performed during this PhD but were finally aborted because of the lack of results and of access to other fresh deep-sea hydrothermal samples. Presence of those microorganisms could be significantly site-dependent, present on some specific sites only, associated to high biological degradation or abiotic production of organic sulfur compounds. Culture could be performed with known species, available from microorganisms' collections (*e.g.* DSMZ, UBOCC) from analyzing their genomes if available in public database. Different molecules as substrates could also be considered for culture perspectives. DSMP molecule is very abundant in the ocean and could be potentially interesting to test (Gonzalez et al., 2002; Curson et al., 2017). Moreover, thiocyanate molecule could be use as energy source and could be interesting to study because it was not intensely studied, but it is as well a very dangerous molecule for human health (Tsallagov et al., 2019). Moreover, metagenomics approach could be interesting to perform as a first step in deep-sea and shallow-sea hydrothermal vents and geothermal hot springs to search for associated genomic markers and then use a cultural approach. Such a metagenomic approach could give interesting results as genetic markers are known from strains from other environments (Schäfer et al., 2010; Carrión et al., 2019; Kröber and Schäfer 2019; Zhou et al., 2020).

Finally, the cycling of organic sulfur in hydrothermal systems is poorly understood. It would be interesting to conduct additional geochemical studies to determine the species of organosulfur compounds present in hydrothermal ecosystems and their concentrations in different sites.

## **Chapter 3: Exploring inorganic sulfur compound disproportionation in hydrothermal vents**

### **1. Preamble**

The main goal of this PhD thesis was to investigate the sulfur disproportionation process at deep-sea hydrothermal vents. This metabolism could be more common than thought and could be present in a large spectrum of ecosystems.

- The first approach consisted in isolating new sulfur-disproportionators from deep-sea hydrothermal vents and to characterize their physiology and genomic content *via* cultivation and genomic approaches.
- The second step consisted in merging and comparing all available data from these microorganisms and other known sulfur-disproportionators to search for potential similarities and shared features and to try to decipher the genomic pathways of sulfur disproportionation by comparative genomics. In parallel, we also carried out comparative proteomics and chemical monitoring of sulfur disproportionation and sulfate reduction on few bacterial models, as already described elsewhere (Florentino et al., 2017; Florentino et al., 2019 and Kröber and Schäfer, 2019).
- Thirdly, the goal was to study the full sulfur cycle at a given deep-sea hydrothermal vent site and to search for genomic markers of sulfate reduction, sulfur oxidation and sulfur disproportionation, but this study was not carried out.

## **2. Materials and Methods**

### *2.1 Collection of samples and pure strains*

Deep-sea hydrothermal samples were collected and stored by Anne Godfroy, Françoise Lesongeur and David Francois during the MoMARSAT 2019 and MoMARSAT 2020 oceanographic cruises, from the deep-sea hydrothermal vent field Lucky strike, at the Mid-Atlantic Ridge. Samples were collected with the clamp of the Nautilie submersible and brought to the surface into a decontaminated insulated box. Once onboard, the sample was ground in a sterile mortar inside an anaerobic chamber under a N<sub>2</sub>/H<sub>2</sub> (90%/10%) gas atmosphere to homogenize it, and then stored into Schott flasks under anaerobic conditions. Samples were stored at 4°C until subsequent use for enrichment culture. Protocol had been detailed in the PhD manuscript of D. Francois (2021).

Enrichment cultures targeting S<sup>0</sup> disproportionators were carried out with the five following samples, three from MoMARSAT 2019 and two from MoMARSAT 2020 campaigns:

- Three hydrothermal samples were collected in 2019 during the MoMARSAT 2019 oceanographic cruise at the Lucky strike vent field, and were referenced as: **1939** (sample MOM19 Aisics 2 PL1939-1-PBT3; Aisics chimney; N 37° 17' 20.34" W 32° 16' 33.899"; 1690 m depth), **1945** (sample MOM19 Cap2 PL1945-7; Capelinhos vent; N 37° 17' 20.34" W 32° 16' 33.899"; 1663 m depth), and **1947** (sample MOM19 PL1947-PBT2-DEAFS; Montségur vent; N 37° 17' 20.34" W 32° 16' 33.899"; 1699 m depth). These samples were composed of chimney rocks, sediments and sea water.
- Two hydrothermal samples were collected in 2020 during the MoMARSAT 2020 oceanographic cruise at the Lucky strike vent field, from the Aisics chimney, and were referenced as, **MOM20h** for the top of the chimney (sample MOM20 PL762-10, cheminée Aisics 1, partie haute; chimney rock fragments), and **MOM20b** for the bottom of the chimney (sample MOM20 PL762-10, cheminée Aisics 2, partie basse; chimney rocks and sediments) (Aisics chimneys; N 37° 17' 20.34" W 32° 16' 31.739"; 1688 m depth).

In addition, about 30 deep-sea hydrothermal samples stored in our lab since 2013-2014, and collected from the Atlantic, Indian and Pacific Oceans, and 5 samples of sediments from “Rade de Brest” have also been tested. They are not detailed here as they did not provide any positive results.

Further investigations were also performed with pure strains deposited in public collections such as the DSMZ (Deutsche Sammlung von Mikroorganismen und Zellkulturen, Leibniz, Germany) and the UBOCC (University of Brest Culture Collection, Plouzané, France) hosted by our laboratory. These strains are *Thermodesulfatator atlanticus* DSM 21156<sup>T</sup>, *Thermodesulfatator indicus* DSM 15286<sup>T</sup> and *Thermodesulfatator autotrophicus* S606<sup>T</sup>. We also obtained strains from our collaborators of the Laboratory of Diversity and Ecology of Extremophilic Microorganisms of the Winogradsky Institute of Moscow: *Thermosulfurimonas marina* SU872<sup>T</sup>, *Thermosulfurimonas dismutans* S95<sup>T</sup>, *Thermosulfuriphilus ammonigenes* ST65<sup>T</sup>, *Dissulfuribacter thermophilus* S69<sup>T</sup> and *Dissulfurirhabdus thermomarina* SH388<sup>T</sup>.

## 2.2 Culture media

### DNRA (Dissimilatory Nitrate Reduction to Ammonium) medium

This medium is composed of a mineral basis, and includes nitrate as a terminal electron acceptor, elemental sulfur as an electron donor, and a gas phase of CO<sub>2</sub> (100%) as a carbon source.

The medium for enrichment contained (per liter distilled water): 0.33 g NH<sub>4</sub>Cl, 0.50 g KCl, 0.5 g CaCl<sub>2</sub>·6H<sub>2</sub>O, 0.33 g KH<sub>2</sub>PO<sub>4</sub>, 25.00 g NaCl, 4.40 g MgCl<sub>2</sub>·6H<sub>2</sub>O, two drops of resazurin at 1% (w/v), and 1 mL of trace elements (SL-10). The mineral medium was boiled for less than 5 minutes to remove the dissolved oxygen, and its pH was adjusted between 6.5 to 7.0. Then, 20 mM of PIPES (piperazine-*N,N'*-bis(2-ethanesulfonic acid)) buffer and 10 ml/L of vitamin solution according to the composition of DSMZ medium 461 (Nagel and Andreesen) were added and the pH was checked again to be adjusted between 6.5 to 7.0. A small amount of sulfur flower was then added (5 to 10 g/L) before closing the flasks and changing its gaseous phase to 100% (v/v) N<sub>2</sub> (0.5 bars). The medium was then tyndallized twice at 2 atm 105°C (30 min.). Just before inoculation, 20 mM of NaNO<sub>3</sub> was added from a sterile stock solution and the gaseous phase was replaced by 1 bar of 100% (v/v) CO<sub>2</sub> by flushing (relative pressure).

### Dissimilatory sulfate reduction medium

This medium consisted of a mineral basis and included sulfate as an electron acceptor, and a gas phase of H<sub>2</sub>/CO<sub>2</sub> (80%/20%) as energy and carbon sources. The medium for enrichment contained (per liter distilled water): 0.33 g NH<sub>4</sub>Cl, 0.50 g KCl, 0.5 g CaCl<sub>2</sub>·6H<sub>2</sub>O, 0.33 g KH<sub>2</sub>PO<sub>4</sub>, 25.00 g NaCl, 4.40 g MgCl<sub>2</sub>·6H<sub>2</sub>O, 12.888 g Na<sub>2</sub>SO<sub>4</sub>·10H<sub>2</sub>O (about 20 mM), two drops of resazurin at 1% (w/v), 1 mL of trace elements (SL-10), and 1 mL of selenite-tungstate solutions. The mineral medium was boiled for less than 5 minutes to remove the dissolved oxygen and its pH was adjusted between 6.5 to 7.0. Then, 20 mM of PIPES buffer and 10 ml/L of vitamin solution (according to the composition of DSMZ medium 461) were added and the pH was checked again to be adjusted between 6.5 to 7.0. The flasks were then closed and their gaseous phases were replaced by 100% N<sub>2</sub> (0.5 bars). The medium was then tyndallized twice at 2 atm 105°C for 30 minutes. Before inoculating the media, media were reduced by adding 0.5 g/L Na<sub>2</sub>S·9H<sub>2</sub>O and gaseous phase was replaced by flushing with 1 bar of H<sub>2</sub>/CO<sub>2</sub> (80%/20%) (relative pressure).

### Inorganic sulfur compound disproportionation medium

We used a recipe and a preparatory mode learned from Russian collaborators (laboratory of Diversity and Ecology of Extremophilic Microorganisms in Moscow, headed by A. Slobodkin). The medium targeting this singular metabolism is based on the mixing of a standard mineral medium with a ferrihydrite solution (Slobodkin et al., 1999).

Firstly, the ferrihydrite solution is prepared from a 60 g/L of FeCl<sub>3</sub>·6H<sub>2</sub>O (pH = 2.0) solution which is titrated slowly with NaOH 10% (w/v) according to a ratio about 75%/25%, in order to reach a pH of about 8.0 to 9.0. The solution is then left overnight for ferrihydrite formation.

The mineral fraction contains (per liter distilled water): 0.33 g NH<sub>4</sub>Cl, 0.50 g KCl, 0.5 g CaCl<sub>2</sub>·6H<sub>2</sub>O, 0.33 g KH<sub>2</sub>PO<sub>4</sub>, 25.00 g NaCl, 4.40 g MgCl<sub>2</sub>·6H<sub>2</sub>O, 1 mL of trace elements (SL-10) and 1 mL of selenite-tungstate solutions. The mineral medium is boiled for less than 5 minutes to remove dissolved oxygen and cooled on ice. Ferrihydrite is then added to the mineral solution, in order to get a final concentration of about 90 mM in the medium. After an overnight precipitation at room temperature, ferrihydrite solution is then centrifuged in 50 mL Falcon tubes at 3000 rpm for 10 minutes and supernatants are discarded. The ferrihydrite pellets are directly added to the mineral solution. The solution is bubbled afterwards with pure CO<sub>2</sub> to adjust the pH due to the alkaline pH of ferrihydrite pellets, at values between 6.5 to 7.0. Then,



20 mM PIPES buffer and 10 ml/L of vitamin solution (according to the composition of DSMZ medium 461) are added. The medium is directly added into penicillin vials, Bellco tubes, or 1-liter Schott glass bottles with the addition of a small amount of sulfur flower (5 g/L) if  $S^0$  disproportionation is tested. The vials are then closed with butyl rubber stoppers and their gaseous phases are replaced by 100%  $N_2$  at 0.5 bars. The vials are then tyndallized twice at 2 atm and 105°C (30 min). Prepared vials are stored at 4°C, and their gaseous phases is changed by flushing to 1 bar of 100%  $CO_2$  just before inoculation

Sulfite or thiosulfate can also be used instead of elemental sulfur by adding 10 mM of sodium thiosulfate or 5 mM sodium sulfite from sterile stock solutions.

The medium can also be prepared without ferrihydrite to check that growth is due to sulfur disproportionation and not to iron reduction.

The specificity of this medium is that when sulfides are produced, they interact directly with the ferrihydrite and then form iron sulfide species. The purpose of using ferrihydrite is to scavenge the sulfides as they inhibit the disproportionation of sulfur compounds (Finster, 2008; Slobodkin and Slobodkina, 2019). Ferrihydrite turns from brown to dark-brown or dark in colour, which is convenient for monitoring microbial growth.

### 2.3 Enrichment cultures, isolation of microorganisms and growth conditions for pure strains

Enrichment cultures targeting  $S^0$  disproportionation were carried out with the hydrothermal samples referenced as 1939, 1945, 1947, MOM20h, and MOM20b. Inoculation and subcultures were performed at 1/10<sup>th</sup> (v/v).

Moreover, in order to try to isolate *Archaea* able to perform  $S^0$  disproportionation, replicates of these enrichment cultures were also carried out in the presence of antibiotics, respectively ampicillin (from 25 to 250  $\mu\text{g}/\text{mL}$ ) and Streptomycin (from 50 to 100  $\mu\text{g}/\text{mL}$ ). Cultures were incubated at various temperatures, from 19°C to 80°C. Enrichment cultures and subcultures were performed in the same conditions than for the initial enrichment step. Serial dilutions to extinction at 1/10<sup>th</sup> were carried out in order to isolate strains from positive cultures. In order to confirm that growth was due to  $S^0$  disproportionation, each isolate was transferred onto  $S^0$  disproportionation medium prepared without ferrihydrite with a ratio of 2% (v/v) and subcultured three times under these conditions.

*Thermosulfurimonas marina* and *Thermosulfuriphilus ammonigenes* were grown under DNRA conditions, in order to get their genome sequenced and annotated. *Thermosulfuriphilus ammonigenes* was incubated at 65°C and *Thermosulfurimonas marina* at 75°C until we got a sufficient quantity of cells for molecular investigations (Slobodkina et al., 2017; Frolova et al., 2018).

At the request of our colleagues Alexander Slobodkin and Galina Slobodkina, we tested the ability of *Thermodesulfatator* species to disproportionate inorganic sulfur compounds and to perform DNRA, in order to confirm results, they had also obtained in their laboratory. *Thermodesulfatator atlanticus*, *Thermodesulfatator indicus* and *Thermodesulfatator autotrophicus* were incubated at 70°C under sulfite, thiosulfate and S<sup>0</sup> disproportionation conditions and additionally into DNRA medium (Moussard et al., 2004; Alain et al., 2010; Lai et al., 2016). Subcultures were performed at 1/10<sup>th</sup> (v/v) and subcultures were carried out three times under these conditions

Moreover, for comparative proteomics experiments, we incubated the three species *Thermosulfurimonas dismutans*, *Dissulfuribacter thermophilus*, and *Thermodesulfatator atlanticus* in media targeting dissimilatory sulfate reduction and S<sup>0</sup> disproportionation. Each strain was “acclimatized” for about four subcultures into growth conditions in which no growth had previously been reported (Alain et al., 2010; Slobodkin et al., 2012; Slobodkin et al., 2013). *Thermosulfurimonas dismutans* was acclimatized at 70°C to sulfate reduction, *Dissulfuribacter thermophilus* was acclimatized at 60°C to sulfate reduction, and *Thermodesulfatator atlanticus* was acclimatized at 65°C, to S<sup>0</sup> disproportionation. Subcultures were performed with a ratio of 2% (v/v).

#### 2.4 DNA extraction

Genomic DNA was extracted with a standard PCI (Phenol: Chloroform: Isoamyl Alcohol (25:24:1)) protocol, as described elsewhere (Charbonnier et al., 1995). Cells were first pelleted by centrifugation, for 20 minutes, at 8000 rpm. Pellets were then resuspended in 800 µL of TE-Na-1× lysis buffer (TRIS 100 mM pH = 8.0, EDTA 50 mM pH = 8.0 and NaCl 100mM). 40 µL of Sarkosyl (10%), 40 µl of SDS (10%) and 5 µL of proteinase-K (20 mg/mL) were added to the suspension, and incubated for 2 hours at 55°C. 1 volume of PCI solution was then added to 1 volume of lysis solution, gently inverted, and then centrifuged for 15 minutes at 13000 rpm

(4°C). The upper liquid phase was then transferred to 1 volume of PCI and extraction was repeated until there were no cellular debris anymore at the interface between the 2 liquid phases. The upper phase was collected, 2 µL of RNase One (Promega) was added to it, and the suspension was then incubated for 1 hour at 37°C. 1 volume of chloroform was then added to it and centrifuged for 15 minutes at 13000 rpm at 4°C. The upper liquid phase was then collected and 40 µL of sodium acetate (3M pH = 5.2) added to it. Finally, 1 volume of isopropanol was added and precipitation of nucleic acids proceeded overnight at -20°C. The next morning, the DNA pellet was collected after centrifugation for 10 minutes at maximum speed. DNA was washed with 70% (v/v) ethanol and dried to be resuspended afterwards in 20 to 50 µL of Qiagen EB buffer (similar to 10 mM Tris-Cl buffer, pH 8.5). DNA was stored at 4°C for short term storage or -20°C for long term storage.

However, at some point, some problems arose. DNA extractions from the dismutation media were affected by interactions with iron precipitates, or interaction between iron and phenol. Additional DNA extraction kits were tested: DNeasy® PowerMax® Soil Kit, DNeasy® PowerLyzer® Microbial Kit and FastDNA™ SPIN Kit (MP Biomedicals). Finally, we found 2 solutions to improve DNA extractions: (i) to prepare the lysis buffer without EDTA; (ii) to use a dithionite solution to dissolve iron precipitates, as described elsewhere (Thamdrup et al., 1993).

Double-strand DNA concentration was measured using the kit Quantifluor™ dsDNA system (Promega), following the manufacturer's instructions and quality/purity was assessed with a spectrophotometer NanoDrop (ThermoFisher). Genomic DNA quality was then doublechecked by the sequencing companies.

### 2.5 16S rRNA gene sequence analyses

16S rRNA gene sequences were amplified from genomic DNA extracts with the primers Bac8F and 1492Runi targeting bacterial 16S rRNA gene sequences or Arc8F and Arc1492R targeting archaeal 16S rRNA gene sequences:

Bac8F: 5'-AGAGTTTGATCATGGCTCAG-3' (Tm: 55°C)

1492Runi: 5'-CGGTTACCTTGTTACGACTT-3' (Tm: 55.3°C)

Arc8F: 5'-TCCGGTTGATCCTGCC-3' (Tm: 46.7°C)

Arc1492R: 5'- GGCTACCTTGTTACGACTT- 3' (Tm: 55.3°C)

16S rRNA gene sequence amplifications followed by Sanger sequencing were carried out to identify the isolated strains and also to check the purity of the strains before proteomic experiments.

The PCR reaction mixture, for a final volume of 25  $\mu\text{L}$ , was composed of 18.18  $\mu\text{L}$  of ultrapure water, 5  $\mu\text{L}$  of 5 $\times$  *Taq* buffer (GreenGoTaq® buffer, Promega, Madison, USA), 0.5  $\mu\text{L}$  of dNTPs (10 mM of each dNTP), 0.1  $\mu\text{L}$  of each primer (10  $\mu\text{M}$ ), 0.12  $\mu\text{L}$  of polymerase GoTaq®G2 DNA Polymerase (5 U  $\mu\text{L}^{-1}$ , Promega), 0.4  $\mu\text{L}$  of  $\text{MgCl}_2$ , and 0.5  $\mu\text{L}$  of DNA template (diluted or not). The program was adjusted to 1 cycle of 3 min at 95°C, 30 cycles of 1 min at 94°C, 1.5 minutes at 53°C (Bac8F-1492Runi) or 50°C (Arc8F- Arc1492R), 2 min at 72°C and 1 cycle of 6 min at 72°C. DNA quantification and purity could also be estimated with a NanoDrop spectrophotometer or by quantification onto a Quantus fluorimeter after staining with PicoGreen™ as described above. Migration onto an agarose gel (at 1% w/v) containing ethidium bromide was then performed at 90 V for 45 minutes, and observation was done with a UV transilluminator (Avantec, Thermo Fisher Scientific, equipped with a camera and the software Infinity version 15.08, Capt®). Amplicons of the expected size (~1500 bp) were sent to the German sequencing company Genewiz (<https://www.genewiz.com>) for Sanger sequencing with both reverse and forward primers. The sequencing quality and purity of the sequenced products was evaluated by visualizing the sequence chromatograms using Chromas and Geneious (v11) software. The sequences were organized into contigs using the *de novo assemble* command of the Geneious software. The complete sequences of the genes encoding the 16S rRNAs were then compared to the GenBank database using the BLAST program, blastn command (<https://blast.ncbi.nlm.nih.gov/Blast.cgi>), and to the sequences of the cultured strains recognized by the International Systematics Committee using the 16S-based ID tool on EZBioCloud (<https://www.ezbiocloud.net/>).

## 2.6 *Genomic sequencing and assembly*

Two approaches were used for sequencing, a short read sequencing based on the Illumina technology and a coupled short and long reads sequencing. Short read DNA sequencing was carried out by the company Fasteris (<https://www.fasteris.com/dna/>) or by the company

Molecular Research (<https://www.mrdnalab.com/>) using Illumina MiSeq (nano or micro) V2 technology with 2x150 bp paired reads. Long read DNA sequencing was carried out by the company Molecular research MrDNA (<http://www.mrdnalab.com/>) using the PacBio Sequel technology or by MinIon (Oxford Nanopore), in our laboratory, with the rapid sequencing kit (SQK-RAD004) and with R9.4.1 flow cells.

Post-quality controls were performed by sequencing facilities and checked also with FastQC (v0.11.8 - <https://www.bioinformatics.babraham.ac.uk/projects/fastqc/>). Reads were filtered with fastp (v0.20.1 - <https://github.com/OpenGene/fastp>) (Chen et al., 2018). Genome were assembled by using the Unicycler pipeline for *de novo* short reads and hybrid assembly (<https://github.com/rrwick/Unicycler>), and its associated dependencies (Wick et al., 2017). Genome assembly statistics were obtained with Quast (v5.0.2; <https://github.com/ablab/quast>) and used to compare different assemblies. Genome assembly visualization was plotted with Bandage (v0.8.1 - <http://rrwick.github.io/Bandage/>) in order to detect potential plasmids from obtained contigs and afterwards checked with plasmidVerify or viralVerify python script which predict plasmid and virus sequences (<https://github.com/ablab/viralVerify>) based on HMMs (Wick et al., 2015; Antipov et al., 2019). Genome completeness and potential contamination were controlled with CheckM (v1.1.2 - <https://ecogenomics.github.io/CheckM/>), and whole genome average coverage was calculated using BMap (v38.87 - BMap – Bushnell B. – [sourceforge.net/projects/bbmap/](https://sourceforge.net/projects/bbmap/)) against short reads sequences.

## 2.7 *Genomic analyses*

Genomes were analyzed and annotated with the fast annotation software Prokka (<https://github.com/tseemann/prokka>), Dfast (v1.2.5 - [https://github.com/nigyta/dfast\\_core](https://github.com/nigyta/dfast_core)), MicroScope microbial genome annotation analysis platform (MaGe) (<https://mage.genoscope.cns.fr/microscope/home/index.php>), using KEGG and BioCyc database, the NCBI integrated PGAP pipeline (<https://github.com/ncbi/pgap>), and RAST server (v2.0 - <https://rast.nmpdr.org/>), with default parameters and databases (Seemann, 2014; Brettin et al., 2015; Tatusova et al., 2016; Vallenet et al., 2017; Tanizawa et al., 2018). Functional annotation of predicted CDSs was further blasted with UniProtKB + Swiss-Prot database. Hydrogenase classification has been checked using the HydDB webtool (<https://services.birc.au.dk/hyddb/>). All dsr genes were extracted and analyzed with the DiSCo

perl script (<https://github.com/Genome-Evolution-and-Ecology-Group-GEEG/DiSCo>) from Prokka protein output sequences (Neukirchen and Sousa, 2021).

Identification and classification of the CRISPR-Cas systems were performed by using CRISPRCas Finder webserver, with default parameters (<https://crisprcas.i2bc.paris-saclay.fr/>) (Couvin et al., 2018). Prediction of laterally transferred gene clusters (genomic islands) was performed with IslandViewer4 webserver (<http://www.pathogenomics.sfu.ca/islandviewer/>) based on GenBank files generated by Prokka, and IslandPath-DIMOB and SIGI-HMM predictions were taken in account (Bertelli et al., 2017). To study the taxonomic position of the strain, 16S rRNA gene sequences were extracted from assembled genomes using Barrnap (<https://github.com/tseemann/barrnap>) and sequences were compared to the NCBI nucleotide collection. Pairwise 16S rRNA gene sequence similarity was then determined using the EzTaxon-e server (<https://www.ezbiocloud.net/>) (Kim et al., 2012). Estimated *in silico* DNA–DNA hybridization (DDH) were determined using the Genome-to-Genome Distance Calculator (GGDC 2.1) using formula 2 (<http://ggdc.dsmz.de/home.php>) (Meier-Kolthoff et al., 2013). Moreover, GTDB-Tk was also used (<https://github.com/Genome-Evolution-and-Ecology-Group-GEEG/GTDBTk>) with associated database to assess taxonomy and to place the genome on a tree made of concatenated reference proteins (Chaumeil et al., 2019). For a more accurate classification, average nucleotide identity (ANI) scores were also calculated, using default parameters of the software. OrthoANLu scores were calculated against genomes using ANI calculator tool provided by EzBioCloud web server (<https://www.ezbiocloud.net/tools/ani>) (Lee et al., 2016; Yoon et al., 2017). Average amino acid identity (AAI) was calculated using the AAI calculator of the Enveomics collection (<http://enve-omics.ce.gatech.edu/>) with Prokka output (Rodriguez & Konstantinidis, 2016). We considered the following thresholds for classification: for 16S rRNA sequences, identity <98.7% for a new species and <94.5% for a new genus (Stackebrandt & Ebers 2006; Yarza et al., 2014). For digital DDH, score <70% for a new species (Wayne et al., 1987). For ANI, score <94–96% for a new species (Richter & Rosselló-Móra, 2009), and <70.85–76.56% for a new genus with alignment fraction (Barco et al., 2020). For AAI, scores comprised 95% and 100% for a same species, and between 65% and 95% for a same genus (Konstantinidis et al., 2017).

## 2.8 *Comparative genomics*

Firstly, a collection of microbial genomes was made from public databases, and notably GenBank (<https://www.ncbi.nlm.nih.gov/genbank/>). It is important to note that we searched for the genomes of sulfur-disproportionating microorganisms, at the exception of the SOR (sulfur oxygenase reductase) depending ones. We found 23 genomes of mesophilic ISC-disproportionators, and 5 genomes of thermophilic ISC-disproportionators. In addition, we had 3 genomes of thermophilic ISC-disproportionators that we sequenced and assembled in this work or in collaboration with our Russian partner. Thus, we collected a total of 31 genomes of ISC-disproportionators, among which 8 are from thermophilic ISC-disproportionators and 6 are from marine hydrothermal thermophilic ISC-dismutators.

In order to search for potential marker genes of sulfur disproportionation, we used the MaGE platform (<https://mage.genoscope.cns.fr/microscope/home/index.php>). Its comparative genomics section allows to compare up to 30 genomes and also to exclude genomes from the analysis (Vallenet et al., 2017). This software is based on a clustering algorithm (SiLiX: <http://lbbe.univ-lyon1.fr/-SiLiX-.html>) and can allow clustering by 50% amino-acid identity and 80% amino-acid alignment coverage with permissive parameters.

In order to identify genes specific to the dismutation of inorganic sulfur compounds, we performed genome comparisons considering different parameters: the sulfur species that is dismutated, the taxonomic affiliation of the species and its associated natural environment. It was also important to keep in mind that several pathways could exist for a same process. These comparative genomic analyses were performed with the 31 genomes collected from public databases or generated by ourselves. Comparisons were performed at first according to the physiology of the microorganisms (sulfur, sulfite or/and thiosulfate disproportionation ability), then according to their original environment (marine sediments, freshwater sediments, anaerobic digestors, terrestrial, shallow and deep-sea hydrothermal vents, acidic and alkaline lakes) and third according to their taxonomic affiliation, and then to their phylogenetic relationships (*Deltaproteobacteria*, *Thermodesulfobacteria*, *Thermodesulfobacteriaceae*, etc.).

Afterwards, we tried to better understand the potential functions and associated protein structures of the resulting CDS extracted from this comparative genomic analysis, by using HMMpred (<https://toolkit.tuebingen.mpg.de/tools/hhpred>), NCBI blast, UniprotKB blast, and InterProScan (<http://www.ebi.ac.uk/interpro/search/sequence/>).

For the prediction of secondary structures and cellular subcellular localization, we used for each of the three CDS extracted using this approach, the tools TMHMM (<http://www.cbs.dtu.dk/services/TMHMM/>), Quick2D (<https://toolkit.tuebingen.mpg.de/tools/quick2d>), Phyre2 (<http://www.sbg.bio.ic.ac.uk/~phyre2/html/page.cgi?id=index>) with intensive search and finally BUSCA server (<http://busca.biocomp.unibo.it/>) (Savojardo et al., 2018).

## 2.9 Comparative proteomics trial experiment

Cultures of *Thermosulfurimonas dismutans*, *Dissulfuribacter thermophilus*, and *Thermodesulfatator atlanticus* were performed under both dissimilatory sulfate reduction and S<sup>0</sup> disproportionation conditions. The goal was to analyze and compare the proteomes obtained by LC-MS/MS (Liquid Chromatography coupled to tandem Mass Spectrometry) under S<sup>0</sup> disproportionation and dissimilatory sulfate reduction (with H<sub>2</sub> as an energy source). In this preliminary experiment whose objective was to verify that the extraction of proteins, their quantification and identification by LC-MS/MS were working well, comparative proteomics was carried out from cultures without replicates, and only on the soluble cytosolic fraction of proteins. This experiment was performed with the help of Sébastien Laurent, and main LC-MS/MS spectra analyses were performed by my master intern Solenne Giardi and by Sébastien Laurent.

For this experiment, 60 mL of culture of *T. dismutans*, *D. thermophilus*, and *T. atlanticus* in the late exponential phase of growth, were collected from dissimilatory sulfate reduction and S<sup>0</sup> disproportionation growth conditions. For cultures got under S<sup>0</sup> disproportionation conditions, slow centrifugation at 500g for 3 minutes was done and followed by an additional filtration by syringe filters of 5 µm in order to remove iron compounds and residual elemental sulfur. Samples were then centrifuged at 8,000g for 20 minutes at room temperature. Pellets were recovered into 500 µL of lysis buffer (40 ml of PBS 1x pH 7.4 with one tablet of Protease inhibitor cocktail cComplete™) and transferred to 2 mL Eppendorf tubes®. Samples were then conserved on ice during the rest of experiment. Ultrasound sonication was then performed in ice during 5 minutes of 0.5 second ON and 0.5 second OFF intermittence at an amplitude of 40% (Vibra-Cell™ 72408, Bioblock) for each sample. In order to potentially split up soluble and non-soluble proteins, samples after sonication were centrifuged at 15,000g for 1 hour at 4°C, and only supernatants were recovered with expected soluble cytosolic and periplasmic



proteins. Protein extracts were then concentrated onto Amicon Ultra-0.5mL centrifugal filter units with 3kDa filtration cut-off (Millipore®) by centrifugation at 14,000g for 1 hour at 4°C. Protein concentrates were then quantified using the Bradford method with Quick Start Bradford Mix (Bio-Rad) and a bovine serum albumin reference range, thanks to an Uvikon-XL spectrophotometer (Bio-Tek Instruments) at 595 nm absorbance (Bradford, 1976). Recommended quantity of protein for analyses at PAPPSSO platform is between 10 and 20 µg of proteins. Protein extracts were then quantified in mg/mL and then about 10 µg of proteins with associated volume were added into a reducing (4/5) and blue marking (1/5) Bio-Rad mixed solution (XT reducing Agent) homogenized by vortex and incubated at 95°C for 7 minutes. Samples were then migrated into electrophoresis agarose gels (Criterion XT Precast Gel, Bio-Rad) with associated MOPS 1x buffer, for long and short migrations at 150V and 0,16A. Long migration was done for 45 minutes for visual observation and short migration was done for 8 minutes for LC-MS/MS application. Migration gels were then cleaned with milliQ water, incubated for 48 hours into Coomassie blue solutions and discolored with an ethanol and acetic acid washing solution for about 3 hours. For LC-MS/MS applications, pieces of gel associated to short migrations were collected under clean conditions in order to avoid contaminations such as keratin, and transferred into Eppendorf tubes®. Tubes were then sent to the PAPPSSO platform (<http://pappso.inrae.fr/>) for LC-MS/MS analyses.

During LC-MS/MS, the peptides resulting from an enzymatic hydrolysis are separated by reverse phase liquid chromatography according to their hydrophobicity and arrive sequentially in the source of the mass spectrometer (nanospray) where they are ionized. In a second step, the peptides are analyzed in the mass spectrometer. This instrument allows to measure the peptide masses and also, if necessary, to fragment the peptides in the gas phase to obtain elements of primary structure (<http://pappso.inrae.fr/en/analyses/principe/>). MS spectra resulting from the fragmentation are then processed with X!TandemPipeline C++ software and annotated from Prokka and PGAP proteome output sequences of *T. dismutans*, *D. thermophilus*, and *T. atlanticus*. Spectra analyses were based on percentage of specific spectra (relative abundance), PAI (Protein Abundance Index) and NSAF (Normalized Spectral Abundance) indexes.

## 2.10 Chemical monitoring, growth kinetics and proteomics

*Dissulfuribacter thermophilus* and *Thermodesulfatator atlanticus* were grown under dissimilatory sulfate reduction and S<sup>0</sup> disproportionation conditions in order (i) to follow the evolution of the cell concentration in these cultures, (ii) to follow the chemical intermediates of the metabolism and in particular the sulfur compounds and (iii) to analyze the proteomes. For this experiment, two sets of cultures of 300 mL with four or three replicates under each condition were launch in parallel. The first set was used to perform a chemical monitoring of the culture and to follow cell density (three replicates) and the second set was used to analyze total proteomes (four replicates), i.e. cellular soluble and insoluble proteins, and extracellular proteins. This experiment was performed with the help of my master intern Solenne Giardi, Sébastien Laurent (proteomics) and Xavier Philippon (chemical analyses).

### Chemical monitoring and growth kinetics

Between t<sub>0</sub> and 288 hours of incubation, a regular sampling (15 to 17 points) had been carried out from *T. atlanticus* and *D. thermophilus* cultures, grown under S<sup>0</sup> disproportionation and sulfate reduction conditions, in order to perform the following analyses:

First, the headspaces of the cultures were analyzed by gas chromatography in order to monitor the concentrations of H<sub>2</sub>, CO<sub>2</sub>, and H<sub>2</sub>S. these analyses were done with a Micro GC FUSION Gas Analyser (INFICON, Bâle, Switzerland) with pressure analyzer (CTE80005AY0, Sensortech GmbH). Gas concentrations were then calculated from ideal gas law formula. Second, a chemical analysis of the aqueous phase was carried out by ionic chromatography. 800 µL of culture were collected and centrifuged at 15,000g for 10 minutes at room temperature. Supernatants were transferred with pipettes and stored at -20°C. Because of high salt medium concentration, samples were diluted in sterile filtered milliQ water (100 µL sample into 900 µL of water) and transferred into Chromacol (Thermo Scientific™) before analysis. Chemical analyses were performed using a Dionex ICS-900 Ion Chromatography System (Dionex, Camberley, UK) equipped with an IonPac CS16 column maintained at 60°C in an UltiMate™3000 Thermostated Column Compartment (Thermo Scientific, Waltham, MA, USA).

Third, to determine cell numbers, 100  $\mu\text{L}$  of cultures were collected and fixed into 25  $\mu\text{L}$  of 25% glutaraldehyde solution, and stored at  $-80^{\circ}\text{C}$  before cell counting. Additional stocks of 100  $\mu\text{L}$  of cultures were collected and fixed into 2  $\mu\text{L}$  of 25% glutaraldehyde solution and stored at  $-80^{\circ}\text{C}$  for safety. Samples were then mixed into 100  $\mu\text{L}$  of acridine solution (0.1% m/v), vortexed and kept 10 minutes in the dark. Samples were diluted with sterile filtered milliQ water with a dilution coefficient (F), adapted regarding growth phase. Samples were then filtered onto 0.22  $\mu\text{m}$  black polycarbonate membrane filters Whatman®. Filters were then deposited between slide and slip, with a drop of mineral oil for the adhesion, and observed with a BX-60 Olympus fluorescence microscope (1000 $\times$ ) under green light excitation (577-492 nm) and cell counts were performed on 10 ranges. Cellular density was then calculated with the formula below:

$$\text{Cellular density} = \frac{\text{Average number of cells}}{\text{Filtered volume of sample}} \times \frac{\text{Filtered surface (189.81 mm}^2\text{)}}{\text{Range surface (0.0025 mm}^2\text{)}} \times F$$

### Proteomics

For proteomics, the four replicates of *T. atlanticus*  $\text{S}^0$  (disimutation), *T. atlanticus*  $\text{SO}_4^{2-}$  (sulfate reduction), *D. thermophilus*  $\text{S}^0$  and *D. thermophilus*  $\text{SO}_4^{2-}$  were stopped respectively after 148 hours, 54 hours 30 min, 45 hours 30 min and 97 hours 30 min of incubation in late exponential growth phase (based on growth kinetics data).

For the extraction of extracellular proteins, 90 mL of culture of *D. thermophilus*, and *T. atlanticus* in each condition were collected and were then centrifuged at 8,000g for 20 minutes at  $4^{\circ}\text{C}$ . Supernatants were collected and conserved into ice during the whole rest of experiment. Supernatants were then filtered by syringe filters (pores: 0.45  $\mu\text{m}$ ) in order to remove residues. Because of the important iron precipitation after one hour, only the supernatants of the cultures carried out under sulfate reduction growth conditions were then concentrated with Amicon Ultra-15mL centrifugal filtration units, with 3kDa filtration cut-off (Millipore®) (10,000g centrifugation for 40 minutes at  $4^{\circ}\text{C}$ ). Supernatants of cultures obtained under  $\text{S}^0$  disproportionation conditions were centrifuged at 14,000g for 15 minutes at  $4^{\circ}\text{C}$  in order to remove iron precipitates but without success.

For the extraction of soluble cytosolic proteins, another 90 mL aliquot of each culture was also collected. For samples got under  $S^0$  disproportionation conditions, a slow centrifugation at 500g for 1 minute at 4°C was done to remove iron compounds and residual elemental sulfur. Cell densities were determined before and after centrifugation. Samples were then centrifuged at 8,000g for 20 minutes at 4°C. Pellets were then resuspended into 500  $\mu$ L of lysis buffer (40 ml of PBS 1x pH 7.4 with one tablet of Protease inhibitor cocktail cOmplete™) and transferred to 2 ml Eppendorf tubes®. Samples were conserved on ice during the whole rest of experiment. Ultrasound sonication was then performed in ice during 5 minutes of 0.5 second ON and 0.5 second OFF intermittence at an amplitude of 20% (Vibra-Cell™ 72408, Bioblock) for each sample. In order to potentially split up soluble and non-soluble proteins, samples were centrifuged at 15,000g for 1 hour at 4°C after sonication. Supernatants were recovered with expected soluble cytosolic proteins and then concentrated with Amicon Ultra-0.5ml with 3kDa filtration cut-off (Millipore®) by centrifugation at 14,000g for 1 hour at 4°C. Pellets expected to contain insoluble membrane proteins were collected and resuspended into 500  $\mu$ L of lysis buffer (40 ml of PBS 1x pH 7.4 with one tablet of Protease inhibitor cocktail cOmplete™) and stored on ice.

All protein extracts, with the exception of extracellular protein extracts associated to  $S^0$  disproportionation, were then quantified by Bradford method with Quick Start Bradford Mix (Bio-Rad) and a bovine serum albumin reference range with a Uvikon-XL (Bio-Tek Instruments) at 595 nm absorbance (Bradford, 1976). Proteins extracts were then quantified in mg/mL for each condition. Afterwards about 20  $\mu$ g of proteins with associated volume, or 20  $\mu$ L of protein extracts, were added into 6.25  $\mu$ L of reducing agent and 1.5  $\mu$ L of blue marking Bio-Rad mixed solution (XT reducing Agent) homogenized by vortex and incubated at 95°C for 7 minutes. Samples were then put into an electrophoresis agarose gel (Criterion XT Precast Gel, Bio-Rad) in MOPS 1x buffer, for only long migrations at 150V and 0,16A. Long migration was done for 1 hour for visual observation application. Migration gels were then cleaned with milliQ water, incubated for 48 hours into Coomassie blue solutions and discolored with an ethanol and acetic acid washing solution for about 3 hours.

### **3. Results and Discussion**

#### *3.1 Physiology and genomics of ISC-disproportionators*

##### *3.1.1 Cultivation of marine hydrothermal microorganisms able to disproportionate inorganic sulfur compounds*

###### Considerations regarding cultivation of elemental sulfur disproportionators

The cultivation of ISC-disproportionators is quite delicate to manage. We observed for example that it is important to subculture strains when they are in the mid exponential growth phase, because cultures in a stationary growth phase are difficult to grow again. As already described elsewhere, color change of ferrihydrite from brown to black are not always associated with bacterial growth. Ferrihydrite can also turn black to brown after a specific amount of time of incubation, correlated to potential sulfide species releasing or degradation. Among the different sulfide scavengers tested, ferrihydrite is among the most efficient scavengers and is easy to prepare. Nevertheless, high concentrations of ferrihydrite affect downstream applications such as DNA extraction, protein extraction and also chemical monitoring. It was tried to decrease the concentration of ferrihydrite at 45 mM in cultures of strains *T. dismutans*, *T. atlanticus* and *D. thermophilus* but lower growth with 45 mM ferrihydrite than with 90 mM was observed. Other tests were also performed by Stéven Yvenou, another PhD student in the lab, with various intermediates concentrations, and good growth of *Thermosulfurimonas* strain F29 was obtained with 59 mM ferrihydrite. Addition of non-toxic sulfate scavengers could also increase kinetics of reaction, reduced species of barium or calcium could be interesting to consider (Benatti et al., 2009). We then tested this idea by increasing  $\text{CaCl}_2 \cdot 6\text{H}_2\text{O}$  concentration, up to 45 mM but no significant differences were observed. Furthermore, from stated hypotheses that sulfur disproportionation could be associated to molybdopterins, about 5 mM of sodium molybdate as a molybdenum source (which could also inhibit sulfate reduction), were added to cultures of strains *T. dismutans*, *T. atlanticus*, and *D. thermophilus* but without significant better growth (Tanaka and Lee, 1997; Slobodkin and Slobokina, 2019). Finally, we tried and kept as reported in Umezawa et al. (2020), the addition of selenite-tungstate solution. It is also important to note that at temperatures close to 100°C, sulfur disproportionation to sulfide and thiosulfate can occur abiotically (Belkin et al., 1985). For optimal growth, temperature, pH, salinity, sulfide and sulfate scavenger concentration are also important to consider and it is the reason why

sulfur disproportionators are so difficult to grow *in vitro*. It is very likely that every strain requires its own specific adjustments of growth medium.

Several problems caused by these specific culture conditions interfere with downstream applications, including DNA extraction due to iron compounds, in pure strain genome sequencing perspectives because sequencing requires very pure DNA. We obtained brown DNA pellets during some extractions with PCI. It is documented that dissolved iron can interact with phenol during DNA extraction (Moeller and Shellman, 1953). By removing the EDTA from the lysis buffer, we circumvented this inconvenient. When the lysis buffer was composed only of pure water, NaCl and TrisHCl, the brown color of the DNA pellet disappeared. Furthermore, the addition of sodium dithionite (Thamdrup et al., 1993), to dissolve iron precipitates also proved efficient to increase DNA yield and quality, even if a low quantity of dissolved iron was still potentially present (light pink color). Electrophoretic migration of the DNA might also be useful to purify the DNA, as the iron will migrate in the reverse direction than DNA but such an approach will decrease the final DNA yield.

#### Enrichment cultures from deep-sea hydrothermal vents samples

It was possible to enrich/isolate four new strains able to disproportionate  $S^0$ , from the Lucky Strike vent field at the Mid-Atlantic Ridge. These strains belong to the genus *Thermosulfurimonas* and to the class *Deltaproteobacteria*.

- A new strain, representing a new species of the genus *Thermosulfurimonas*, was isolated at 60°C from the sample “1945” and referenced as strain F29. It was found that this strain has an optimal temperature for growth at 70°C. A physiological characterization is currently in progress in the framework of the PhD thesis of Stéven Yvenou and won't be detailed in this manuscript. Moreover, the genome of this strain was sequenced and analyzed, and is described a little further.
- A new strain, representing a new genus of the family *Dissulfuribacteraceae*, was isolated from the sample “1945” at 45°C with 50 µg/mL of ampicillin. It was referenced as strain M45. The genome of this strain was sequenced but no physiological characterization is planned.

- A new strain, referenced as strain M19, and representing a new genus in the family *Desulfobulbaceae* was isolated from the sample “1945”, at 19°C. Strain M19 genome was then sequenced and its physiological characterization is in progress in the lab, by Erwann Vince (technician).
- A new strain, strain B35, representing a new genus in the family *Desulfobulbaceae* family was isolated from the sample “MOM20b”, at 45°C with 250 µg/mL of ampicillin. This strain grows better at 35°C than at 45°C. Its genome was sequenced but because of time issue, no physiological characterization was planned.

Furthermore, from culture performed with “1939” sample and incubated at 45°C with 100 µg/mL of ampicillin, we identified from 16 rRNA gene amplification and sequencing, a sequence belonging to *Dissulfurirhabdaceae* family. But we were not able to maintain the potential isolate after 8 subcultures since its transfer after serial dilution experiment.

As a result, we isolated new sulfur disproportionators that belong to taxonomic branches already encompassing sulfur disproportionators and especially *Deltaproteobacteria*. However, for reasons of culture and time, only two of the four new strains will be characterized physiologically. The following strains will be characterized: *Thermosulfurimonas* strain F29 which is part of another PhD project; *Desulfobulbaceae* strain M19 which has just started to be characterized, and which is particularly difficult to grow but represents the first mesophilic sulfur-disproportionator isolated from a deep-sea hydrothermal vent.

#### Physiological investigations of representatives of the genus *Thermodesulfatator*: DNRA and S<sup>0</sup> disproportionation

We tested three strains of *Thermodesulfatator* (*Thermodesulfatator atlanticus*, *Thermodesulfatator indicus* and *Thermodesulfatator autotrophicus*) for their capacity to grow through DNRA and ISC disproportionation, which had not been tested in the original publications. Among the strains studied, only *T. atlanticus* could grow *via* DNRA and *via* S<sup>0</sup> disproportionation metabolism. However, *T. atlanticus* could not be grown by sulfite (5 mM) and thiosulfate (20 mM) disproportionation. Furthermore, those experiments were performed in parallel by our colleagues from the laboratory of Diversity and Ecology of Extremophilic Microorganisms and gave the same results. In addition, *T. atlanticus* cultivated under DNRA conditions was associated to a high acidification of the medium despite the presence of PIPES

buffer, which has not been observed as such for any other strain under these conditions. Acidification could indicate that another pathway is at work, associated to nitrate reduction and leading to acid production. It is still not elucidated if the absence of growth by sulfite disproportionation is artefactual or not. It should be interesting to carry out new tests with lower sulfite concentrations, for example 1 to 3 mM (5 mM tested), to conclude definitely, as sulfite is toxic and the tested concentration might have skewed our results. It however questions the fact that sulfite could be the key intermediate for sulfur compound disproportionation, because other strains in other taxa can grow by S<sup>0</sup> or/and thiosulfate disproportionation but not with sulfite (Slobodkin and Slobodkina, 2019).

In conclusion, we have thus demonstrated that the already known species *T. atlanticus* can disproportionate S<sup>0</sup> to sulfate and sulfide and perform DNRA. From those results, we can see that *T. atlanticus* can be a very pertinent model for studying associated genes, transcripts and proteins associated to S<sup>0</sup> disproportionation if compared to *T. indicus* and *T. autotrophicus*, very close strains with similar metabolisms but unable to grow by S<sup>0</sup> disproportionation (Moussard et al., 2004; Alain et al., 2010; Lai et al., 2016).

#### Cultures targeting elemental sulfur disproportionation and sulfate reduction for proteomic purposes

We demonstrated that *Dissulfuribacter thermophilus* was able to grow by dissimilatory sulfate reduction. In addition, as detailed above, we also showed that *Thermodesulfatator atlanticus* was able to grow by S<sup>0</sup> disproportionation after several subcultures under these conditions.

- *Thermosulfurimonas dismutans* could be subcultured 19 times under sulfate reduction conditions but growth was very weak (less than one cell per field of view) and might be only maintenance. As biomass was extremely low, we decided not to retain this strain for proteomics testing.
- *Thermodesulfatator atlanticus* grew slowly by S<sup>0</sup> disproportionation than the other thermophilic S<sup>0</sup> disproportionators that I worked with. It took two weeks to reach the end of the exponential growth phase. This might mean that *T. atlanticus* uses a different biological system to perform S<sup>0</sup> disproportionation associated to lower yield, which could be investigated by genomics or proteomics.



- *Dissulfuribacter thermophilus* showed fast growth under both sulfate reduction (with H<sub>2</sub> as an electron donor) and sulfur disproportionation conditions, and provided high amounts of cell required for protein extractions. In this work, we demonstrated the ability of this strain to perform sulfate reduction with H<sub>2</sub> as electron donor.

### 3.1.2 Analyses of microbial genomes from hydrothermal species able to disproportionate inorganic sulfur compounds

During this PhD, a complete methodology was developed and perfected from DNA extraction to deep genome analysis; genome sequencing, assembly, annotation and taxonomical analysis were optimized and were finally very valuable. Genome annotation is especially of interest for S<sup>0</sup> disproportionating microorganisms because of their relative difficulty to be cultivated. A recent script developed and called DISCO (<https://github.com/Genome-Evolution-and-Ecology-Group-GEEG/DiSCo>) was used, making the analysis of genomes and MAGs simpler and faster of Dsr specific enzymes for sulfate reduction and sulfide oxidation but stays however unverified information for disproportionation process in particular (Neukirchen and Sousa, 2021). However, depending on the application, results should be verified mandatory by culture. It is important to retain, as said the authors, the goal of this software is not to differentiate Dsr genes associated to sulfate reduction or disproportionation.

Four genomes of ISC-disproportionators have been analyzed in collaboration with our colleagues from the laboratory of Diversity and Ecology of Extremophilic Microorganisms of Moscow. Three out of the four bacteria whose genomes have been annotated had already been the subject of a physiological characterization. Our objectives were then to explore the genomes of these taxa to better understand their genetic potential and deduce putative ecological features and investigate sulfur disproportionation pathways, while generating more genomic data for future functional studies and comparative approaches. Annotation can help to better understand metabolisms, and also to think about and elaborate new hypotheses about the metabolic routes of S<sup>0</sup>, thiosulfate, and sulfite disproportionation for example.

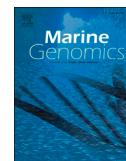
### Genome analyses of strains with known physiology

The genomes of *Thermosulfurimonas marina* strain SU872<sup>T</sup>, *Thermosulfuriphilus ammonigenes* strain ST65<sup>T</sup> and *Dissulfurirhabdus thermomarina* strain SH388<sup>T</sup> were sequenced, assembled and analyzed in three independent scientific publications integrated bellow.



Contents lists available at ScienceDirect

Marine Genomics

journal homepage: [www.elsevier.com/locate/margen](http://www.elsevier.com/locate/margen)

## Complete genome sequence of *Thermosulfurimonas marina* SU872<sup>T</sup>, an anaerobic thermophilic chemolithoautotrophic bacterium isolated from a shallow marine hydrothermal vent

Maxime Allieux<sup>a</sup>, Mohamed Jebbar<sup>a</sup>, Galina Slobodkina<sup>b</sup>, Alexander Slobodkin<sup>b</sup>, Yann Moalic<sup>a</sup>, Anastasia Frolova<sup>b</sup>, Zongze Shao<sup>c</sup>, Karine Alain<sup>a,\*</sup>

<sup>a</sup> Univ Brest, CNRS, IFREMER, LIA 1211 MicrobSea, Laboratoire de Microbiologie des Environnements Extrêmes LM2E, IUEM, Rue Dumont d'Urville, F-29280 Plouzané, France

<sup>b</sup> Winogradsky Institute of Microbiology, Research Center of Biotechnology of the Russian Academy of Sciences, Moscow, Russia

<sup>c</sup> Key Laboratory of Marine Genetic Resources, Third Institute of Oceanography, Ministry of Natural Resources, Xiamen 361005, China

### ARTICLE INFO

#### Keywords:

Thermophilic  
*Thermosulfurimonas*  
 Shallow-sea hydrothermal vents  
 Sulfur compounds disproportionation  
 DNRA metabolism

### ABSTRACT

*Thermosulfurimonas marina* strain SU872<sup>T</sup> is a thermophilic, anaerobic, chemolithoautotrophic bacterium, isolated from a shallow-sea hydrothermal vent in the Pacific Ocean near Kunashir Island, that is able to grow by disproportionation of inorganic sulfur compounds and dissimilatory nitrate reduction to ammonium. Here we report the complete genome sequence of strain SU872<sup>T</sup>, which presents one circular chromosome of 1,763,258 bp with a mean G + C content of 58.9 mol%. The complete genome harbors 1827 predicted protein-encoding genes, 47 tRNA genes and 3 rRNA genes. Genes involved in sulfur and nitrogen metabolism were identified. This study expands our knowledge of sulfur and nitrogen use in energy metabolism of high temperatures areas of shallow-sea hydrothermal environments. In order to highlight *Thermosulfurimonas marina* metabolic features, its genome was compared with that of *Thermosulfurimonas dismutans*, the only other species described within the *Thermosulfurimonas* genus.

### 1. Introduction

*Thermosulfurimonas marina* strain SU872<sup>T</sup> had been discovered and characterized by Frolova et al. (2018) as a novel thermophilic, anaerobic, chemolithoautotrophic bacterium. *T. marina* was isolated from a shallow-sea hydrothermal vent located off the Kunashir Island in the Sea of Okhotsk. It is likely to be involved in the nitrogen and sulfur cycles of this ecosystem through its metabolic activities. Shallow hydrothermal vents are generally located at a water depth less than 200 m and, like deep-sea hydrothermal vents, they are characterized by wide redox, temperature and pH gradients, allowing chemotrophs to grow on chemical energy, in addition to phototrophs developing from light energy (Tarasov et al., 2005). This complex ecosystem is rich in various sulfur compounds and had been demonstrated to be inhabited by sulfur-oxidizing bacteria, and various chemotrophic microorganisms using

alternative electron donors such as sulfide, thiosulfate, molecular hydrogen and electron acceptors such as oxygen, sulfur, manganese, iron, nitrite and nitrate (Price and Giovannelli, 2017). As suggested by Price and Giovannelli (2017), nitrate reducers may represent a significant fraction of the microbial community inhabiting shallow hydrothermal vents but only few nitrate reducers have been isolated to date from this habitat. Frolova et al. (2018) demonstrated that *T. marina* grows by sulfur compounds (elemental sulfur, thiosulfate and sulfite) disproportionation (= dismutation), and by utilization of these sulfur compounds as electron donors and nitrate as an electron acceptor with CO<sub>2</sub>/HCO<sub>3</sub><sup>-</sup> as sole carbon source. Besides, *T. marina* is one of the few shallow vent microorganisms known to perform DNRA metabolism (Dissimilatory Nitrate Reduction to Ammonium). This energy-yielding reaction is a little more documented within deep-sea hydrothermal vent species (Slobodkina et al., 2017). *T. marina* is a member of the

**Abbreviations:** ANI, average nucleotide identity; CDS, coding DNA sequence; CMP-KDO, cytidine 5'-monophospho-3-deoxy-D-manno-2-octulosonic acid; COG, clusters of orthologous groups; CRISPR, clustered regularly interspaced short palindromic repeats; ENA, European nucleotide archive; KEGG, Kyoto encyclopedia of genes and genomes; ORF, open reading frame; TCA, tricarboxylic acid cycle.

\* Corresponding author.

E-mail address: [Karine.Alain@univ-brest.fr](mailto:Karine.Alain@univ-brest.fr) (K. Alain).

<https://doi.org/10.1016/j.margen.2020.100800>

Received 24 April 2020; Received in revised form 18 June 2020; Accepted 18 June 2020

Available online 11 July 2020

1874-7787 /© 2020 Elsevier B.V. All rights reserved.

*Thermodesulfobacteria* phylum and the *Thermodesulfobacteriaceae* family, represented currently by five genera. Based on its 16S ribosomal RNA gene sequence, *T. marina* is phylogenetically closely related to *Thermosulfurimonas dismutans* S95<sup>T</sup>, a thermophilic, anaerobic, chemolithoautotrophic bacterium isolated from a deep-sea hydrothermal vent chimney located in the Pacific Ocean. *T. dismutans* is the first described representative of the *Thermosulfurimonas* genus whose genome has been assembled, annotated and studied by Mardanov et al. (2016), and which possesses similar physiological properties (Slobodkin et al., 2012; Slobodkina et al., 2017) (Table 1).

In this study, we analyzed the genome of *T. marina* SU872<sup>T</sup>, the second sequenced genome within the *Thermosulfurimonas* genus, and investigated its metabolic features. Genome sequence availability will promote a better understanding of metabolic traits of prokaryotes participating in sulfur, nitrogen and carbon cycles in shallow hydrothermal vents and especially sulfur compound disproportionation and DNRA metabolism. *T. marina* is the latest bacterium described to carry out sulfur compound disproportionation among thermophilic microorganisms. From evolution and adaptation perspectives, this genome sequence will also allow a better understanding of streamlined coding bacterial genomes.

## 2. Data description

### 2.1. Genome sequencing and assembly

Cultivation of *Thermosulfurimonas marina* strain SU872<sup>T</sup> was performed as described in Frolova et al. (2018), under anaerobic conditions, at 75 °C, with elemental sulfur as an electron donor (5 g/L), nitrate (10 mM) as a terminal electron acceptor and CO<sub>2</sub>/HCO<sub>3</sub><sup>-</sup> as sole carbon source. Genomic DNA was extracted with a standard PCI (Phenol: Chloroform: Isoamyl Alcohol (25:24:1)) protocol, as described elsewhere (Charbonnier et al., 1995). The complete genome sequence of strain SU872<sup>T</sup> was determined by combining short and long read sequencing. Short read DNA sequencing was performed by FASTER SA (Plan-les Ouates, Switzerland) using the Illumina nanoMiSeq technology (2 × 150 bp paired-reads, Nano V2 chemistry). Long read DNA sequencing was done by the company Molecular Research (MrDNA Shallowater, USA), using the PacBio Sequel technology. Libraries constructions and quality controls were performed by both sequencing facilities and verified with FastQC (v0.11.8 - <https://www.bioinformatics.babraham.ac.uk/projects/fastqc/>).

All sequences were high quality score estimated and then directly assembled and circularized by using the Unicycler pipeline for *de novo* hybrid assembly (v0.4.8-beta - <https://github.com/rwrick/Unicycler>), and its dependencies (spades.py v3.13.0; racon v1.3.3; makeblastdb v2.9.0+; tblastn v2.9.0+; bowtie2-build v2.3.5; bowtie2 v2.3.5; samtools v1.9; java v11.0.1; pilon v1.23) (Wick et al., 2017). Genome assembly statistics were obtained with Quast (v5.0.2 - <https://github.com/ablab/quast>). Genome completeness and potential contamination were controlled with CheckM (v1.1.2 - <https://ecogenomics.github.io/CheckM/>), and whole genome average coverage was calculated using BMap (v38.70 - BMap - Bushnell B. - [sourceforge.net/projects/bbmap/](https://sourceforge.net/projects/bbmap/)).

### 2.2. Genome annotation

Genome was analyzed and annotated with the online version of the RAST server (v2.0 - <http://rast.theseed.org/FIG/rast.cgi>), the fast annotation software Prokka (v1.13 - <https://github.com/tseeman/prokka>), Dfast (v1.2.5 - [https://github.com/nigyta/dfast\\_core](https://github.com/nigyta/dfast_core)), the MicroScope Microbial Genome Annotation and Analysis Platform (MaGe) (<https://mage.genoscope.cns.fr/microscope/home/index.php>) (supplementary material S1), using KEGG and BioCyc database, and eggNOG mapper v2 (<http://eggno-mapper.embl.de/>), with default parameters and databases for all of the five software/pipelines

**Table 1**

General features and genome sequencing information for *Thermosulfurimonas marina* strain SU872<sup>T</sup> and *Thermosulfurimonas dismutans* strain S95<sup>T</sup>, including MIGS mandatory information, based on MaGe platform.

Item	Description	
Investigation Strain	<i>Thermosulfurimonas marina</i> strain SU872 <sup>T</sup>	<i>Thermosulfurimonas dismutans</i> strain S95 <sup>T</sup>
Submitted to INSDC	GenBank	GenBank
Investigation type	Bacteria	Bacteria
Project name	CP042909	LWL001
Geographic location (latitude and longitude)	44° 29.469' N, 146° 06.247' E	22° 10.82' S, 176° 36.09' W
Geographic location (country and/or sea, region)	Sea of Okhotsk, 250 m from the Kunashir Island shore (Sakhalin oblast, Russia)	Eastern Lau Spreading Center, SW Pacific Ocean
Collection date	June 2013	June 2009
Environment (biome)	marine hydrothermal vent biome ENVO:01000030	marine hydrothermal vent biome ENVO:01000030
Environment (feature)	marine hydrothermal vent ENVO:01000122	marine hydrothermal vent ENVO:01000122
Environment (material)	marine hydrothermal vent chimney ENVO:01000129	marine hydrothermal vent chimney ENVO:01000129
Depth	-12 m	-1910 m
General features		
Classification	Domain Bacteria	Domain Bacteria
	Phylum <i>Thermodesulfobacteria</i>	Phylum <i>Thermodesulfobacteria</i>
	Class <i>Thermodesulfobacteria</i>	Class <i>Thermodesulfobacteria</i>
	Order <i>Thermodesulfobacteriales</i>	Order <i>Thermodesulfobacteriales</i>
	Family <i>Thermodesulfobacteriaceae</i>	Family <i>Thermodesulfobacteriaceae</i>
	Genus <i>Thermosulfurimonas</i>	Genus <i>Thermosulfurimonas</i>
	Species: <i>Thermosulfurimonas marina</i>	Species: <i>Thermosulfurimonas dismutans</i>
Gram stain	Negative	Negative
Cell shape	Oval to short rods	Rods
Motility	Motile	Motile
Growth temperature	Thermophilic, optimum at 74 °C	Thermophilic, optimum at 74 °C
Relationship to oxygen	Anaerobic	Anaerobic
Trophic level	Chemolithoautotroph	Chemolithoautotroph
Biotic relationship	free-living	free-living
Isolation and growth conditions	doi: <a href="https://doi.org/10.1134/S0026261718040082">https://doi.org/10.1134/S0026261718040082</a>	doi: <a href="https://doi.org/10.1099/ijs.0.034397-0">https://doi.org/10.1099/ijs.0.034397-0</a>
Sequencing technology	Illumina MiSeq + PacBio Sequel (hybrid)	454 sequencing
Assembler	Unicycler v 0.4.8-beta	Newbler v. 2.9
Contig number	1	61
N50	1,763,258	94,683
Genome coverage	116.0086×	35×
Genome assembly NCBI	ASM1231758v1	ASM165258v1
Assembly level	Complete genome	Contig
Genomic features		
Genome size (bp)	1,763,258	2,119,932
GC content (mol %)	58.90	50.12
Protein coding genes	1827	2201
Number of RNAs	54	51
tRNAs	47	48
16S-23S-5S rRNAs	1-1-1	1-1-1

(Seemann, 2014; Brettin et al., 2015; Huerta-Cepas et al., 2016; Vallenet et al., 2017; Tanizawa et al., 2018). Functional annotation of predicted CDSs was further blasted with NCBI (v2.10.0+) and UniProtKB databases (release 2020\_02). To investigate sulfur oxygenase reductases, we blasted *Aquifex aeolicus* VF5 sulfur oxygenase reductase (*sor*) sequence (ENA accession: AAC06723.1) against *T. marina*'s genome.

### 2.3. CRISPRs and genomic islands

Identification and classification of the CRISPR-Cas systems were performed by using the CRISPRCas Finder webserver, with default parameters (<https://crispr.i2bc.paris-saclay.fr/>) (Grissa et al., 2007). The prediction of laterally transferred gene clusters (genomic islands) was performed and plotted with the IslandViewer4 webserver (<http://www.pathogenomics.sfu.ca/islandviewer/>) (Bertelli et al., 2017). Genome visualization plot was carried out with the CGView Server ([http://stothard.afns.ualberta.ca/cgview\\_server/](http://stothard.afns.ualberta.ca/cgview_server/)) merged to the IslandViewer4 plot (Grant and Stothard, 2008; Bertelli et al., 2017).

### 2.4. Genome properties

The complete genome sequence of *T. marina* SU872<sup>T</sup> consisted of a single circular chromosome of 1,763,258 bp in length and a G + C content of 58.9 mol%. No plasmids were detected (Fig. 1).

CheckM estimated the genome to be 99.0398% complete (3 markers were missing) and hypothetical contamination to be 0.411523% (1 marker was duplicated). Average coverage was around 116× according to raw pair reads sequences extracted from MiSeq sequencing. Annotation with MaGe (Vallenet et al., 2017) resulted in prediction of 1881 genes, among which 1827 were protein-coding sequences (CDSs). Coding sequences are estimated to cover 95.46% of the entire genome.

However, slightly different results were obtained with other annotation software: 1778 CDSs were found with RAST (1298/1778 were not integrated to subsystem categories), 1786 CDSs with Prokka, 1794 CDSs with Dfast and 1674 CDSs with eggNOG mapper.

Genome contained one operon of 5S-16S-23S rRNA genes and 47 tRNA genes for all 20 standard amino acids and selenocysteine. *T. marina* was confirmed to be a new species based on the level of its 16S rRNA gene sequence identity and ANI score with its closest relative *T. dismutans*, which were below the cut-off values for species delineation by these approaches (<98.7% and < 95–96%, respectively) (supplementary data S2) (Richter and Rosselló-Móra, 2009). No CRISPR loci were found, while five genomic islands (GI) of a total length of 85.8 kb were detected (Fig. 1). The vast majority of genes located on these islands encoded proteins. Based on automatic annotation, one GI region demonstrated a pattern related to NADH-quinone oxidoreductase, containing subunits A1, B2, C, D1, H, I, J, K, L, M and N. Few diverse genes encoding for carbohydrate and nucleic acid related enzymes with no precise predicted functions were found, while the majority of CDSs encoded for hypothetical proteins. Most of the CDSs obtained from the MaGe annotation pipeline (85.89%, 1560/1827 CDSs) could be assigned to at least one COG group (supplementary data S2).

### 2.5. Genes related to carbon metabolism

*T. marina*, which is capable of growing autotrophically from CO<sub>2</sub>/HCO<sub>3</sub><sup>-</sup> (Frolova et al., 2018), possessed a complete Wood-Ljungdahl (reductive acetyl-CoA) pathway for carbon dioxide fixation, as well as *T. dismutans* (Mardanov et al., 2016). Seven enzymes in the pathway (out of eight) were found in KEGG (Reductive acetyl-CoA pathway) and Biocyc databases. The missing enzyme, namely the 5-methyltetrahydrofolate corrinoid/iron sulfur protein methyltransferase (EC: 2.1.1.258),

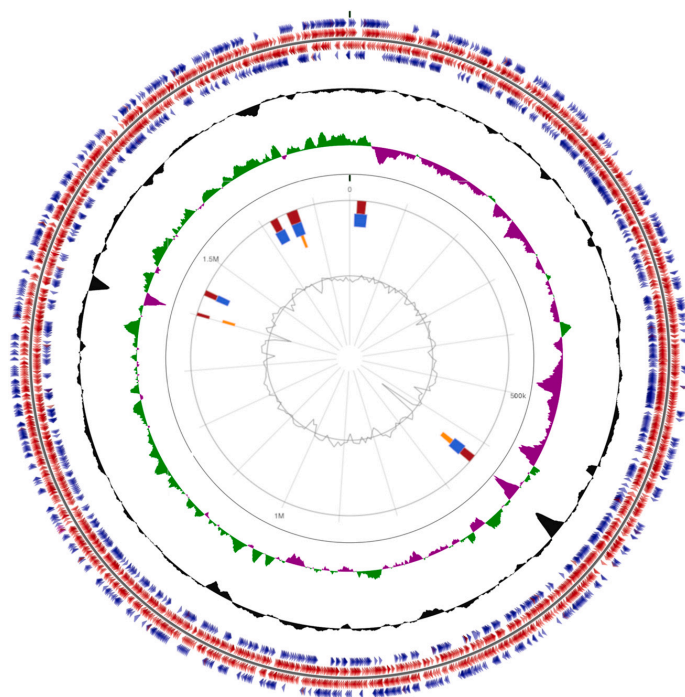


Fig. 1. Schematic representation of *Thermosulfurimonas marina* SU872<sup>T</sup> genome. Labeling from the outside to the center is as follows: circle 1, CDSs on the forward and the reverse strand in blue, ORFs on the forward and the reverse strand in red, and tRNAs in pink, rRNAs in lilac; circle 2, G + C content; circle 3, G + C skew; circle 4, genomic islands shown as red, orange and blue rectangles attributed respectively to integrated, SIGI-HMM and IslandPath-DIMOB prediction genomic islands methods; circle 5, IslandViewer4 automatic calculated G + C content. (For interpretation of the references to colour in this figure legend, the reader is referred to the web version of this article.)

was however detected with Dfast and Prokka annotations. In both *Thermosulfurimonas* species, the TCA cycle seemed highly incomplete and apparently only linking citrate to succinyl-CoA, on the basis of data from KEGG and Biocyc databases. As *T. dismutans*, *T. marina* possessed also the formaldehyde oxidation V (tetrahydrofolate pathway) pathway, but we did not find any evidence for a capacity to oxidize formate into CO<sub>2</sub>. Other known pathways for carbon fixation were lacking or partial.

*T. marina* possessed also a complete metabolic path for gluconeogenesis (Biocyc gluconeogenesis I), the reversal of glycolysis, and the three enzymes of the non-oxidative branch of the pentose phosphate pathway, respectively for the generation of glucose from non-sugar carbon substrates and for NADPH synthesis. *T. marina* possessed also the entire enzymatic set to synthesize one type of carbohydrate, CMP-KDO, a typical component of bacterial lipopolysaccharides.

As for *T. dismutans*, based on BioCyc database, we found several genes encoding for some amino acid biosynthesis in the genome of *T. marina*, namely fifteen amino acid complete biosynthetic pathways. Based on known amino acid biosynthetic pathways, four other pathways appear to be incomplete in this strain which is nevertheless described as autotrophic (Frolova et al., 2018). We also found few genes related to amino acid degradation, six complete degradation pathways and three partial ones.

#### 2.6. Genes related to nitrogen metabolism

As *T. dismutans*, *T. marina* possessed the genes encoding the nitrogenase (molybdenum-iron type) (EC: 1.18.6.1) involved in nitrogen fixation. In this way, based on Prokka annotation, five grouped CDSs were found, including two CDSs related to cofactors, one to its alpha chain and one to its beta chain. Moreover, a periplasmic Nap-type nitrate reductase CDS was found and must be involved in nitrate conversion to nitrite. It has been demonstrated *in vitro* that the conversion of nitrite to ammonium may proceed *via* a non-canonical mode, potentially through the production of hydroxylamine (Hanson et al., 2013; Slobodkina et al., 2017; Slobodkin et al., 2019). The hydroxylamine reductase (EC: 1.7.99.1) found in the genome might be involved in the reduction of hydroxylamine to ammonium. In addition, we also found a hydroxylamine oxidase, a glutamine synthetase, three ammonium transporters associated CDSs and five CDSs coding for nitrogen regulatory proteins P-II with Prokka.

#### 2.7. Genes related to sulfur metabolism

Based on the physiological work done *in vitro*, *T. dismutans* and *T. marina* are not able to reduce sulfate (Slobodkin et al., 2012; Frolova et al., 2018). Surprisingly, complete sulfate reduction pathways are present in both genomes. We found an almost complete dissimilatory sulfate reduction pathway based on Prokka annotation, respectively with a sulfate adenylyltransferase (*sat*), both subunits alpha and beta of adenylyl-sulfate reductase (*aprA*, *aprB*), a manganese-dependent inorganic pyrophosphatase, and dissimilatory sulfite reductase subunits alpha, beta and gamma (*dsvA*, *dsvB*, *dsvC*, the respective homologs of DsrA, DsrB, and DsrC). The DsrC-trisulfide reductase, also known as DsrK catalytic subunit from the DsrMKJOP complex, was not detected except with the RAST annotation pipeline, in addition of all each other subunits M, K, J, O and P. A complete APS reductase-associated electron transfer complex (QmoABC) was found with Dfast according to QmoABC operon homologies annotated in Mardanov et al. (2016) study. We found furthermore a dissimilatory sulfite reductase D (DsrD) sequence which could be involved in transcription or translation of genes catalyzing dissimilatory sulfite reduction according to the literature (Mizuno et al., 2003). It can be hypothesized that those enzymes related to dissimilatory sulfate reduction are involved in the inorganic sulfur compound disproportionation pathway. This assumption is supported by the fact that these enzymes are more similar to those present in other sulfur disproportionators (Slobodkin and Slobodkina, 2019).

This hypothesis is also reinforced by the finding of a complete hypothetical sulfite oxidation pathway in the genome (adenylylsulfate reductase and sulfate adenylyltransferase), as already found by Finster (2008). None of the marker genes for sulfur oxidation processes (based on the genes cited in the review of Wasmund et al., 2017) had been found in the genome, with any of the five annotation methods used. Furthermore, genes encoding for several hypothetical subunits of tetrathionate reductase were found based on Prokka annotation, namely two alpha subunits and four beta subunits, and also one gene encoding one chain of polysulfide reductase. The proteins encoded by these genes could as well be related to inorganic sulfur compounds disproportionation, or more generally to sulfur metabolism. However, in contrast to *T. dismutans* and to several sulfur disproportionators, *T. marina* did not harbor any thiosulfate reductase in its genome (Slobodkin and Slobodkina, 2019). Moreover, *T. marina* did not harbor any sequence related to a sulfur oxygenase reductase, suggesting that the enzymes cited before are better candidates for sulfur disproportionation in this bacterial model.

#### 2.8. Conclusion

The whole-genome annotation was generally supporting the main metabolic features demonstrated experimentally for *T. marina* SU872<sup>T</sup> (Frolova et al., 2018). However, some pathways related to specific activities (DNRA, sulfur disproportionation) could not be retrieved precisely from genomic data and need further experimental characterization. *T. marina* is the first microorganism originating from a shallow-sea hydrothermal vent to be sequenced, that is known to be able to disproportionate sulfur inorganic compounds with another enzymatic machinery than the sulfur oxygenase reductase. Analysis of genomic data of *T. marina* shows that this bacterium is likely involved in the sulfur and nitrogen cycles in shallow-sea hydrothermal vents.

#### 3. Nucleotide sequence accession number

The complete genome sequence of *Thermosulfurimonas marina* SU872<sup>T</sup> has been deposited in GenBank under the accession number CP042909. The strain is available in All-Russian Collection of Microorganisms (VKM) under the accession number VKM B-3177<sup>T</sup>.

#### Declaration of Competing Interest

The authors declare that they have no known competing financial interests or personal relationships that could have appeared to influence the work reported in this paper.

#### Acknowledgements

This work was supported by the French-Russian collaborative Project (CNRS/RFBR) Neptune (PRC Russie 2017 n°281295), by the Sino-French LIA 1211 MicrobSea, by the Russian Foundation for Basic Research, grant number 18-54-15008, and by the Ministry of Science and Higher Education of the Russian Federation. The LABGeM (CEA/Genoscope & CNRS UMR8030), the France Génomique and French Bioinformatics Institute national infrastructures (funded as part of Investissement d'Avenir program managed by Agence Nationale pour la Recherche, contracts ANR-10-INBS-09 and ANR-11-INBS-0013) are acknowledged for support within the MicroScope annotation platform.

#### Appendix A. Supplementary data

Supplementary data to this article can be found online at <https://doi.org/10.1016/j.margen.2020.100800>.



## References

- Bertelli, C., Laird, M.R., Williams, K.P., Simon Fraser University Research Computing Group, Lau, B.Y., Hoad, G., Winsor, G.L., Brinkman, F., 2017. IslandViewer 4: expanded prediction of genomic islands for larger-scale datasets. *Nucleic Acids Res.* 45 (W1), W30–W35. <https://doi.org/10.1093/nar/gkx343>.
- Brettin, T., Davis, J.J., Disz, T., Edwards, R.A., Gerdes, S., Olsen, G.J., Olson, R., Overbeek, R., Parrillo, B., Pusch, G.D., Shukla, M., Thomason, J.A., Stevens, R., Vonstein, V., Wattam, A.R., Xia, F., 2015. RASTk: a modular and extensible implementation of the RAST algorithm for building custom annotation pipelines and annotating batches of genomes. *Sci. Rep.* 5, 8365. <https://doi.org/10.1038/srep08365>.
- Charbonnier, F., Forterre, P., Erauso, G., Prieur, D., 1995. Purification of plasmids from thermophilic and hyperthermophilic archaeobacteria. In: Robb, F. T. (Editor in Chief), Place, A.R., DasSarma, S., Schreier, H.J., Fleischmann, E.M. (Eds.), *Archaea: A Laboratory Manual*. Cold Spring Harbor Laboratory Press, NY. Thermophiles, pp. 87–90, 1995.
- Finster, K., 2008. Microbiological disproportionation of inorganic sulfur compounds. *Journal of Sulfur Chemistry* 29, 281–292. <https://doi.org/10.1080/17415990802105770>.
- Frolova, A.A., Slobodkina, G.B., Baslerov, R.V., Novikov, A.A., Bonch-Osmolovskaya, E. A., Slobodkin, A.I., 2018. *Thermosulfurimonas marina* sp. nov., an autotrophic sulfur-disproportionating and nitrate-reducing bacterium isolated from a shallow-sea hydrothermal vent. *Microbiology* 87, 502–507. <https://doi.org/10.1134/S0026261718040082>.
- Grant, J.R., Stothard, P., 2008. The CGView server: a comparative genomics tool for circular genomes. *Nucleic Acids Res.* 36, W181–W184. <https://doi.org/10.1093/nar/gkn179>.
- Grissa, I., Vergnaud, G., Pourcel, C., 2007. CRISPRFinder: a web tool to identify clustered regularly interspaced short palindromic repeats. *Nucleic Acids Res.* 35, W52–W57. <https://doi.org/10.1093/nar/gkm360>.
- Hanson, T.E., Campbell, B.J., Kalis, K.M., Campbell, M.A., Klotz, M.G., 2013. Nitrate ammonification by *Nautilia profundicola* AmH: experimental evidence consistent with a free hydroxylamine intermediate. *Front. Microbiol.* 4, 180. <https://doi.org/10.3389/fmicb.2013.00180>.
- Huerta-Cepas, J., Szklarczyk, D., Forslund, K., Cook, H., Heller, D., Walter, M.C., Rattei, T., Mende, D.R., Sunagawa, S., Kuhn, M., Jensen, L.J., von Mering, C., Bork, P., 2016. eggNOG 4.5: a hierarchical orthology framework with improved functional annotations for eukaryotic, prokaryotic and viral sequences. *Nucleic Acids Res.* 44 (D1), D286–D293. <https://doi.org/10.1093/nar/gkv1248>.
- Mardanov, A.V., Beletsky, A.V., Kadnikov, V.V., Slobodkin, A.I., Ravin, N.V., 2016. Genome analysis of *Thermosulfurimonas dismutans*, the first thermophilic sulfur-disproportionating bacterium of the phylum *Thermodesulfobacteria*. *Front. Microbiol.* 7, 950. <https://doi.org/10.3389/fmicb.2016.00950>.
- Mizuno, N., Voordouw, G., Miki, K., Sarai, A., Higuchi, Y., 2003. Crystal structure of dissimilatory Sulfite reductase D (DsrD) protein-possible interaction with B- and Z-DNA by its winged-helix motif. *Structure* 11 (9), 1133–1140. [https://doi.org/10.1016/S0969-2126\(03\)00156-4](https://doi.org/10.1016/S0969-2126(03)00156-4).
- Price, R.E., Giovannelli, D., 2017. A review of the geochemistry and microbiology of marine shallow-water hydrothermal vents. In: Reference Module in Earth Systems and Environmental Sciences. <https://doi.org/10.1016/B978-0-12-409548-9.09523-3>.
- Richter, M., Rosselló-Móra, R., 2009. Shifting the genomic gold standard for the prokaryotic species definition. *Proc. Natl. Acad. Sci. U. S. A.* 106 (45), 19126–19131. <https://doi.org/10.1073/pnas.0906412106>.
- Seemann, T., 2014. Prokka: rapid prokaryotic genome annotation. *Bioinformatics* 30 (14), 2068–2069. <https://doi.org/10.1093/bioinformatics/btu153>.
- Slobodkin, A., Slobodkina, G., Allioux, M., Alain, K., Jebbar, M., Shadrin, V., Kublanov, I., Toshchakov, S., Bonch-Osmolovskaya, E., 2019. Genomic insights into the carbon and energy metabolism of a thermophilic deep-sea bacterium *Deferribacter autotrophicus* revealed new metabolic traits in the phylum *Deferribacteres*. *Genes* 10, 849. <https://doi.org/10.3390/genes10110849>.
- Slobodkin, A.I., Slobodkina, G.B., 2019. Diversity of Sulfur-Disproportionating microorganisms. *Microbiology* 88 (5), 509–522. <https://doi.org/10.1134/S0026261719050138>.
- Slobodkin, A.I., Reysenbach, A.L., Slobodkina, G.B., Baslerov, R.V., Kostrikin, N.A., Wagner, I.D., Bonch-Osmolovskaya, E.A., 2012. *Thermosulfurimonas dismutans* gen. Nov., sp. nov., an extremely thermophilic sulfur-disproportionating bacterium from a deep-sea hydrothermal vent. *Int. J. Syst. Evol. Microbiol.* 62 (11), 2565–2571. <https://doi.org/10.1099/ijs.0.034397-0>.
- Slobodkina, G.B., Mardanov, A.V., Ravin, N.V., Frolova, A.A., Chernyh, N.A., Bonch-Osmolovskaya, E.A., Slobodkin, A.I., 2017. Respiratory ammonification of nitrate coupled to anaerobic oxidation of elemental Sulfur in Deep-Sea autotrophic thermophilic Bacteria. *Front. Microbiol.* 8, 87. <https://www.frontiersin.org/article/10.3389/fmicb.2017.00087>.
- Tanizawa, Y., Fujisawa, T., Nakamura, Y., 2018. DFAS: a flexible prokaryotic genome annotation pipeline for faster genome publication. *Bioinformatics* 34 (6), 1037–1039. <https://doi.org/10.1093/bioinformatics/btx713>.
- Tarasov, V.G., Gebruk, A.V., Mironov, A.N., Moskalev, L.I., 2005. Deep-sea and shallow-water hydrothermal vent communities: two different phenomena? *Chem. Geol.* 224 (1), 5–39. <https://doi.org/10.1016/j.chemgeo.2005.07.021>.
- Vallenet, D., Calteau, A., Cruveiller, S., Gachet, M., Lajus, A., Josso, A., Médigue, C., 2017. MicroScope in 2017: an expanding and evolving integrated resource for community expertise of microbial genomes. *Nucleic Acids Res.* 45 (D1), D517–D528. <https://doi.org/10.1093/nar/gkx1101>.
- Wasmund, K., Mußmann, M., Loy, A., 2017. The life sulfuric: microbial ecology of sulfur cycling in marine sediments. *Environ. Microbiol. Rep.* 9 (4), 323–344. <https://doi.org/10.1111/1758-2229.12538>.
- Wick, R.R., Judd, L.M., Gorrie, C.L., Holt, K.E., 2017. Unicycler: resolving bacterial genome assemblies from short and long sequencing reads. *PLoS Comput. Biol.* 13 (6), e1005595. <https://doi.org/10.1371/journal.pcbi.1005595>.

**Complete genome sequence of *Thermosulfurimonas marina* SU872<sup>T</sup>, an anaerobic thermophilic chemolithoautotrophic bacterium isolated from a shallow marine hydrothermal vent.**

Maxime Allieux<sup>1</sup>, Mohamed Jebbar<sup>1</sup>, Galina Slobodkina<sup>2</sup>, Alexander Slobodkin<sup>2</sup>, Yann Moalic<sup>1</sup>, Anastasia Frolova<sup>2</sup>, Zongze Shao<sup>3</sup>, Karine Alain<sup>1\*</sup>

<sup>1</sup>Univ Brest, CNRS, IFREMER, LIA 1211 MicrobSea, Laboratoire de Microbiologie des Environnements Extrêmes LM2E, IUEM, Rue Dumont d'Urville, F-29280 Plouzané, France

<sup>2</sup>Winogradsky Institute of Microbiology, Research Center of Biotechnology of the Russian Academy of Sciences, Moscow, Russia

<sup>3</sup>Key Laboratory of Marine Genetic Resources, Third Institute of Oceanography, Ministry of Natural Resources, Xiamen 361005, China

**Supplementary Material S2: Text file providing missing information about comparative genomics, COG associations, other annotated genes of *Thermosulfurimonas marina* SU872<sup>T</sup> genome and associated gene locus tags.**

S2.1. Comparative Genomics

*Thermosulfurimonas marina*'s 16S rRNA gene sequence was extracted from our reconstructed genome using Barrnap (v0.9 - <https://github.com/tseemann/barrnap>) and compared to the sequence published with the characterization of the strain (Frolova et al., 2018). The 16S rRNA gene sequence extracted with Barrnap resulted in a percentage identity of 99.67% with a partial 16S rRNA gene published previously (GenBank accession KY953157, Frolova et al., 2018). It



also shared 97.91% sequence identity with the 16S rRNA gene sequence of *Thermosulfurimonas dismutans* strain S95<sup>T</sup>, as published previously (Mardanov et al., 2016).

Average Nucleotide Identity (ANI) was calculated using the ANI calculator tool provided by the EzBioCloud web server (<https://www.ezbiocloud.net/tools/ani>) on genomes of the strain SU872<sup>T</sup> and *T. dismutans*, its closest relative organism (GenBank accession LWLG00000000, Mardanov et al., 2016) (Yoon et al., 2017). ANI score calculated against *T. dismutans* had an OrthoANIu value of 72.35 %, with an average aligned length of 810,696 bp. This value is much lower than the threshold criterion for prokaryotic species delineation proposed to be 95–96 % (Richter and Rosselló-Móra, 2009). DNA-DNA hybridization (DDH) estimate values were calculated using the genome-to-genome distance calculator (GGDC v2.1, formula 2) (Meier et al., 2013). The digital DNA-DNA hybridization estimate value between strain SU872<sup>T</sup> and *T. dismutans* S95<sup>T</sup> was 20.2%, which is far below the standard criterion (70%) for delineation of a prokaryotic species (Wayne et al., 1987), confirming that the strain SU872<sup>T</sup> belongs to a different species than *T. dismutans*.

## S2.2. COG associations

The major predicted COG categories (encompassing more than 2% of the CDSs) were related to translation-ribosomal structure-biogenesis (J) (8.4 %), energy production and conversion (C) (8.0 %), amino acid transport and metabolism (E) (7.5 %), replication-recombination-repair (L) (6.9 %), cell wall/membrane/envelope biogenesis (M) (6.5 %), signal transduction mechanisms (T) (5.2 %), coenzyme transport and metabolism (H) (5.0 %), posttranslational modification-protein turnover-chaperones (O) (4.8 %), cell motility (N) (4.3 %), inorganic ion transport and metabolism (P) (3.8%), intracellular trafficking-secretion-vesicular transport (U) (3.6 %), transcription (K) (3.4%), and carbohydrate transport and metabolism (G) (3.4 %), nucleotide transport and metabolism (F) (2.8%) and lipid transport and metabolism (I) (2.2%).

### S2.3. Other genes

No antibiotic resistance genes have been found with Mage platform, with CARD (v3.0.2) or RGI (v5.0.0) software. With BioCyc and Prokka, we found that *T. marina* possesses an arsenate reductase suggesting the capacity for utilization of arsenate as a terminal electron acceptor. However, in our laboratory experiments *T. marina* SU872<sup>T</sup> was not able to grow with arsenate (5 mM) and with either elemental sulfur (5 g/L) or molecular hydrogen as electron donors (data not shown).

### S2.4. Gene locus summary

Gene name	Gene associated locus (NCBI PGAP)
5-methyltetrahydrofolate corrinoid/iron sulfur protein methyltransferase	FVE67_RS00220
nitrogenase (molybdenum-iron type) associated sequences	FVE67_RS04245 ; FVE67_RS04250 ; FVE67_RS04255 ; FVE67_RS04260 ; FVE67_RS04275
Periplasmic Nap-type nitrate reductase	FVE67_RS02215
hydroxylamine reductase	FVE67_RS08695
hydroxylamine oxidase	FVE67_RS00020
glutamine synthetase	FVE67_RS00930
sulfate adenylyltransferase	FVE67_RS03090
adenylyl-sulfate reductase subunit A	FVE67_RS03075
adenylyl-sulfate reductase subunit B	FVE67_RS03080
manganese-dependent inorganic pyrophosphatase	FVE67_RS08780
dissimilatory sulfite reductase subunits alpha	FVE67_RS07950
dissimilatory sulfite reductase subunits beta	FVE67_RS07955
dissimilatory sulfite reductase subunits gamma	FVE67_RS07655
DsrM	FVE67_RS01460
DsrK	FVE67_RS01455
DsrJ	FVE67_RS01450
DsrO	FVE67_RS01445
DsrP	FVE67_RS01440
QmoA	FVE67_RS03070
QmoB	FVE67_RS03065
QmoC	FVE67_RS03060
dissimilatory sulfite reductase D	FVE67_RS07960
tetrathionate reductase subunit A associated sequences	FVE67_RS06180 ; FVE67_RS06900
tetrathionate reductase subunit B associated sequences	FVE67_RS02245 ; FVE67_RS02285 ; FVE67_RS06890 ; FVE67_RS08835
polysulfide reductase chain A	FVE67_RS02290
arsenate reductase	FVE67_RS06830

Table S2.4: Correspondences between the loci of the annotations by Prokka, Dfast, RAST and UniProtKB with the CDSs of the NCBI's automated prokaryotic genome annotation pipeline (PGAP). CDSs found with their associated loci, based on the assembly repository ASM1231758v1.

**Supplementary material associated references:**

Mardanov, A.V., Beletsky, A.V., Kadnikov, V.V., Slobodkin, A.I., and Ravin, N.V., 2016. Genome analysis of *Thermosulfurimonas dismutans*, the first thermophilic sulfur-disproportionating bacterium of the phylum *Thermodesulfobacteria*. *Frontiers in Microbiology*, vol. 7, p. 950. <https://doi.org/10.3389/fmicb.2016.00950>

Meier-Kolthoff, J.P., Auch, A.F., Klenk, H.-P., Göker, M., 2013. Genome sequence-based species delimitation with confidence intervals and improved distance functions. *BMC Bioinformatics*, 14:60. <https://doi.org/10.1186/1471-2105-14-60>

Richter, M., Rosselló-Móra, R., 2009. Shifting the genomic gold standard for the prokaryotic species definition. *Proc. Natl. Acad. Sci. U. S. A.* 106 (45), 19126–19131. <https://doi.org/10.1073/pnas.0906412106>

Wayne, L.G., Brenner, D.J., Colwell, R.R., Grimont, P.A.D., Kandler, O. *et al.*, 1987. Report of the *ad hoc* committee on reconciliation of approaches to bacterial systematics. *International Journal of Systematic and Evolutionary Microbiology*, 37:463-464. <https://doi.org/10.1099/00207713-37-4-463>

Yoon, S. H., Ha, S. M., Lim, J. M., Kwon, S.J. & Chun, J., 2017. A large-scale evaluation of algorithms to calculate average nucleotide identity. *Antonie van Leeuwenhoek*, 110:1281–1286. <https://doi.org/10.1007/s10482-017-0844-4>



## Genome analysis of *Thermosulfuriphilus ammonigenes* ST65<sup>T</sup>, an anaerobic thermophilic chemolithoautotrophic bacterium isolated from a deep-sea hydrothermal vent

Galina Slobodkina<sup>a,\*</sup>, Maxime Allieux<sup>b</sup>, Alexander Merkel<sup>a</sup>, Karine Alain<sup>b</sup>, Mohamed Jebbar<sup>b</sup>, Alexander Slobodkin<sup>a</sup>

<sup>a</sup> Winogradsky Institute of Microbiology, Research Center of Biotechnology of the Russian Academy of Sciences, Leninsky Prospect, 33, bld. 2, 119071 Moscow, Russia

<sup>b</sup> Univ Brest, CNRS, Ifremer, UMR 6197, Laboratoire de Microbiologie des Environnements Extrêmes LM2E, LIA1211, MicrobSea, F-29280, Plouzané, France



### ARTICLE INFO

**Keywords:**  
Thermophile  
Chemolithoautotroph  
Extreme environment  
Deep sea  
Sulfur disproportionation  
Nap complex

### ABSTRACT

*Thermosulfuriphilus ammonigenes* ST65<sup>T</sup> is an anaerobic thermophilic bacterium isolated from a deep-sea hydrothermal vent chimney. *T. ammonigenes* is an obligate chemolithoautotroph utilizing elemental sulfur as an electron donor and nitrate as an electron acceptor with sulfate and ammonium formation. It also is able to grow by disproportionation of elemental sulfur, thiosulfate and sulfite. Here, we present the complete genome sequence of strain ST65<sup>T</sup>. The genome consists of a single chromosome of 2,287,345 base pairs in size and has a G + C content of 51.9 mol%. The genome encodes 2172 proteins, 48 tRNA genes, and 3 rRNA genes. Genome analysis revealed a complete set of genes essential to CO<sub>2</sub> fixation and gluconeogenesis. Homologs of genes encoding known enzyme systems for nitrate ammonification are absent in the genome of *T. ammonigenes* assuming unique mechanism for this pathway. The genome of strain ST65<sup>T</sup> encodes a complete set of genes necessary for dissimilatory sulfate reduction, which are probably involved in sulfur disproportionation and anaerobic oxidation. This is the first reported genome of a bacterium from the genus *Thermosulfuriphilus*, providing insights into the microbial contribution into carbon, sulfur and nitrogen cycles in the deep-sea hydrothermal vent environment.

### 1. Introduction

The deep-sea hydrothermal systems are characterized by darkness, high pressures and steep gradients of physical and chemical parameters formed in mixing zones between hot reduced hydrothermal fluid and cold oxidized ocean water. As water column prevents the penetration of the sunlight, the trophic chains in these ecosystems are based primarily on chemosynthesis with chemolithoautotrophic microorganisms as primary producers. A number of studies have shown the predominance of *Proteobacteria*, especially *Epsilonproteobacteria* in deep sea hydrothermal systems, while other bacterial groups like the *Aquificales*, *Thermales*, *Thermotogales*, *Deltaproteobacteria*, and *Thermodesulfobacteriaceae* are also often detected (Nakagawa and Takai, 2008; Orcutt et al., 2011; Flores et al., 2012). Most of the cultivated representatives of these taxa are associated with utilization of inorganic sulfur compounds.

The genus *Thermosulfuriphilus* belongs to a deep lineage in the phylum *Thermodesulfobacteria* (Slobodkina et al., 2017). Currently, the

genus comprises a sole species, *T. ammonigenes* ST65<sup>T</sup>, an extremely thermophilic, anaerobic, obligately chemolithoautotrophic bacterium that was isolated from a deep-sea hydrothermal vent at the Eastern Lau Spreading Centre in the Pacific Ocean, at a depth of 1870 m. The energy metabolism of *T. ammonigenes* ST65<sup>T</sup> is mandatorily dependent on the transformations of sulfur compounds. The strain grows due to oxidation of elemental sulfur or thiosulfate coupled to reduction of nitrate with ammonium production. It also grows by disproportionation of sulfur, thiosulfate and sulfite (Slobodkina et al., 2017).

In this study, we analyzed the genome of *T. ammonigenes* ST65<sup>T</sup>, the first sequenced complete genome within the species of genus *Thermosulfuriphilus*, and highlighted its general metabolic pathways. The availability of the genome sequence will promote the better understanding of the metabolic traits of prokaryotes participating in sulfur, nitrogen and carbon cycles in such unique types of ecosystems as deep-sea hydrothermal vents.

\* Corresponding author at: Winogradsky Institute of Microbiology, Research Center of Biotechnology of the Russian Academy of Sciences, Moscow, Russia.  
E-mail address: [gslobodkina@mail.ru](mailto:gslobodkina@mail.ru) (G. Slobodkina).

<https://doi.org/10.1016/j.margen.2020.100786>

Received 9 April 2020; Received in revised form 18 May 2020; Accepted 19 May 2020

Available online 04 June 2020

1874-7787/ © 2020 Elsevier B.V. All rights reserved.

## 2. Data description

For genomic DNA extraction, the strain was cultivated anaerobically at 65 °C with elemental sulfur (5 g/L) and potassium nitrate (10 mM) as an electron donor and an electron acceptor, respectively. Cells were harvested in the late exponential phase of growth. The DNA was extracted using a FastDNA™ Spin Kit (MP Biomedicals, USA) according to the manufacturer's instructions. The whole genome was sequenced using the Illumina nanoMiSeq technology (Fasteris, Switzerland) (2 × 150 bp paired-reads, Nano V2 chemistry) generating more than 200 Mb clean data, and using the PacBio Sequel technology (MrDNA, USA). Clean reads from long-reads and short reads sequencing were assembled and circularized using Unicycler v0.4.8-beta assembly pipeline (<https://github.com/rrwick/Unicycler>) (Wick et al., 2017). Average coverage was calculated using BBtools (BBMap – Bushnell B. – [sourceforge.net/projects/bbmap/](https://sourceforge.net/projects/bbmap/)) and was about 88 x. Gene search and annotation were performed by means of the Rapid Annotation using Subsystem Technology (RAST/SEED v2.0) pipeline (Overbeek et al., 2014), the Integrated Microbial genomes IMG/M v.5.0 analysis system (Chen et al., 2019) and NCBI's (National Center of Biotechnology Information) Prokaryotic Genome Annotation Pipeline (PAPG) (Tatusova et al., 2016). The search and analysis of transposase families was performed by ISSaga web server (Varani et al., 2011). Identification and classification of the CRISPR-Cas system was performed by the CRISPRCas Finder web server (Couvain et al., 2018). The prediction of laterally transferred gene clusters (genomic islands) was performed with the IslandViewer4 web server (Bertelli et al., 2017). Genome visualization was made with the CGView program (Grant and Stothard, 2008).

The general features of *T. ammonigenes* strain ST65<sup>T</sup> and the genome sequencing information are summarized in Table 1.

The complete genome of strain ST65<sup>T</sup> consisted of a single circular chromosome with a total length of 2,287,345 bp and a G + C content of 51.9 mol%. No plasmids were detected (Fig. 1). CheckmM v1.1.2 estimated the genome to be 99.5935% complete based on the presence of default single-copy marker genes (1 marker was missing) and hypothetical contamination to be 1.6260%. Annotation with PGAP resulted in prediction of 2236 genes, 2172 of which are protein-coding sequences (CDSs) that cover about 97% of the entire genome. Genome also contained one operon of 5S, 16S and 23S rRNA genes and 48 tRNA genes for all 20 standard amino acids. No CRISPR loci were found.

Analysis of the COG (Clusters of Orthologous Genes) functional categories was performed with the eggNOG-Mapper (v.5.0) (Huerta-Cepas et al., 2019). Majority of the CDSs (95.3%) could be assigned to at least one COG group. The main predicted COG categories (encompassing more than 100 CDSs) were energy production and conversion (11.9%); translation, ribosomal structure and biogenesis (7.97%); cell wall/membrane/envelope biogenesis (7.23%); amino acid transport and metabolism (6.92%); signal transduction mechanisms (6.81%); replication, recombination and repair (5.97%) and coenzyme transport and metabolism (5.56%).

A large number of various transposases and integrases could facilitate the transfer of adaptive genes between different microbial species, and thus contribute to the diversity of deep-sea bacteria. The search and analysis of transposases revealed the presence of 10 insertion sequences (IS) belonging to 4 different IS families (IS3\_ssr\_IS407, IS256, IS3\_ssr\_IS150 and IS630). These sequences contained putative genes of 4 transposases and 10 integrases that according to Pfam database belonged to diverse protein families (Table 2).

The prediction of laterally transferred genes showed that the *T. ammonigenes* ST65<sup>T</sup> genome possesses 5 genomic islands (GI) of 124.3 kb total length. The vast majority of the genes located on the genomic islands encode proteins annotated as hypothetical proteins. Meanwhile, one of genomic islands carried genes encoding ribosomal proteins and also genes involved in dissimilatory sulfate reduction (*sat*, *aprAB* and *qmoABC*) (Fig. 1).

**Table 1**

General features and genome sequencing information for *Thermosulfuriphilus ammonigenes* ST65<sup>T</sup> according to MIGS recommendations.

Item	Description
<b>Investigation</b>	
Submitted to INSDC	GenBank: CP048877
Investigation type	Bacteria
Project name	<i>Thermosulfuriphilus ammonigenes</i> type strain ST65 genome sequencing
NCBI BioProject	Accession: PRJNA606893 ID: 606893
NCBI BioSample	Accession: SAMN14116118 ID: 14116118
Geographic location (latitude and longitude)	21° 59'35"S, 176° 34'06"W
Geographic location (country and/or sea, region)	Eastern Lau Spreading Centre, south-west Pacific Ocean
Collection date	June 2009
Environment (biome)	marine hydrothermal vent biome ENVO:01000030
Environment (feature)	marine hydrothermal vent ENVO:01000122
Environment (material)	marine hydrothermal vent chimney ENVO:01000129
Depth	1870 m
<b>General features</b>	
<b>Classification</b>	
	Domain <i>Bacteria</i>
	Phylum <i>Thermodesulfobacteria</i>
	Class <i>Thermodesulfobacteria</i>
	Order <i>Thermodesulfobacteriales</i>
	Family <i>Thermodesulfobacteriaceae</i>
	Genus <i>Thermosulfuriphilus</i>
	Species: <i>Thermosulfuriphilus ammonigenes</i>
Gram stain	Negative
Cell shape	Rod
Motility	non-motile
Growth temperature range	Thermophilic, optimum at 65° C
Relationship to oxygen	Obligate anaerobe
Trophic level	Chemolithoautotroph
Biotic relationship	free-living
Isolation and growth conditions	DOI <a href="https://doi.org/10.1099/ijsem.0.002142">https://doi.org/10.1099/ijsem.0.002142</a>
<b>Sequencing</b>	
Sequencing platform	Illumina MiSeq + PacBio Sequel (hybrid)
Assembler	Unicycler v 0.4.8-beta
Finishing strategy	complete
Method reads	Hybrid
Contig number	1
N50	2,287,345
Genome coverage	88 x
<b>Genomic features</b>	
Genome size (bp)	2,287,345
G + C content (mol %)	51.9
Number of genes	2236
Protein coding genes	2172
Genes with COGs	1908
Number of RNAs	55
rRNAs	1, 1, 1 (5S, 16S, 23S)
tRNAs	48

The whole-genome sequence data were generally consistent with the main metabolic features experimentally demonstrated in strain ST65<sup>T</sup> (Slobodkina et al., 2017). The genome of strain ST65<sup>T</sup> possessed the genes essential for the Wood–Ljungdahl (the reductive acetyl-CoA) pathway for the fixation of CO<sub>2</sub>. In consistency with the inability of ST65<sup>T</sup> to utilize organic substances, the tricarboxylic acid cycle (TCA) was found to be incomplete (4 enzymes out of 9 were missing). The genome contained all genes for glycolysis (Embden-Meyerhof pathway) which obviously operated in the reverse direction for gluconeogenesis. The ability to use nitrate as an electron acceptor is enabled by the presence of an operon *napMADGH* encoding periplasmic Nap-type nitrate reductase. The reduction of the produced nitrite to ammonium does not proceed via the canonical Nrf system because the gene, encoding the key enzyme of this pathway (i.e., pentaheme cytochrome c

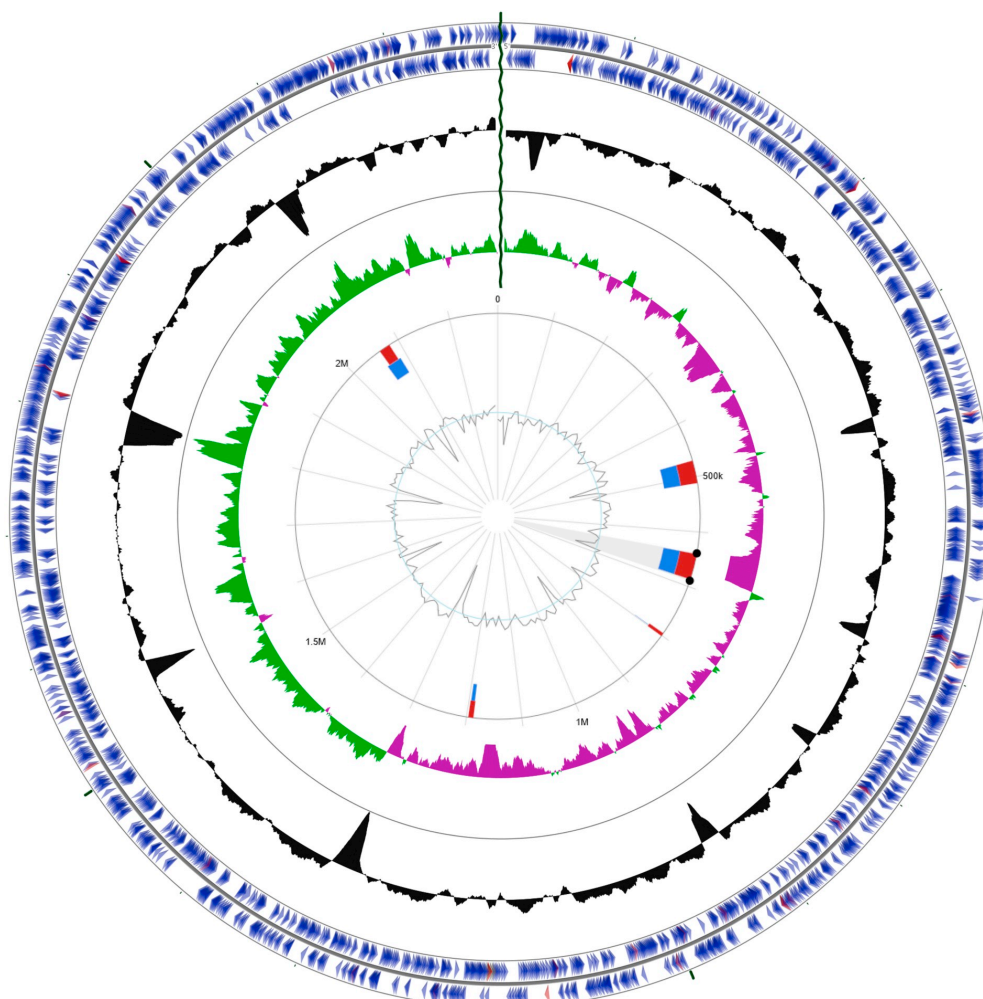


Fig. 1. Schematic representation of the *Thermosulfuriphilus ammonigenes* ST65<sup>T</sup> genome. Labeling from the outside to the center is as follows: circle 1, genes on the forward strand; circle 2, genes on reverse strand (tRNAs pink, rRNAs lilac); circle 3, G + C content; circle 4, G + C skew. Genomic islands are shown as red-and-blue trapezes, GI carrying sulfate reduction genes highlighted in black circles. (For interpretation of the references to colour in this figure legend, the reader is referred to the web version of this article.)

nitrite reductase NrfA), was not found in the genome. Yet, the genome of strain ST65<sup>T</sup> contains genes of hydroxylamine oxidoreductases (Hao) and hydroxylamine reductase (Hcp). Thus, the Nrf complex in *T. ammonigenes* could be replaced by an ammonification pathway based on Hao and Hcp enzymes as it has been proposed for several other marine bacteria (Hanson et al., 2013; Slobodkina et al., 2017a; Slobodkin et al., 2019).

Sulfur cycle is of a great importance in the deep-sea environments. It is notably the case at deep-sea hydrothermal vents where the reactions of CO<sub>2</sub> fixation, linkage to organic matter metabolism and remineralization to CO<sub>2</sub> involve especially the oxidation or reduction of inorganic sulfur species of different redox states. Homologs of genes encoding known enzyme systems of reduced sulfur compounds oxidation such as sulfide: quinone oxidoreductase (SQR), sulfite oxidizing enzyme (SOE), sulfur oxidizing (Sox) enzyme complex or sulfur oxygenase/reductase (SOR) were absent in genome of *T. ammonigenes*. The genome

of strain ST65<sup>T</sup> encodes a complete set of genes necessary for dissimilatory sulfate reduction although the ability of this microorganism to grow by sulfate respiration was not revealed in laboratory experiments (Slobodkina et al., 2017). Probably, the sulfate reduction pathway in this bacterium is involved in disproportionation of sulfur compounds as it was assumed earlier for *Desulfocapsa sulfoexigens* and *Thermosulfurimonas dismutans* (Frederiksen and Finster, 2003; Mardanov et al., 2016). Some of these genes also can be used to oxidize sulfur compounds during growth with S<sup>0</sup> or thiosulfate and nitrate as it was shown for phototrophic sulfur bacteria (Frigaard and Dahl, 2009). The detection of sulfate reducing genes on GI indicates the contribution of mobile elements in the adaptation of bacteria to the environment and in active participation in the sulfur cycle.

In conclusion, the genomic analysis of *T. ammonigenes* ST65<sup>T</sup> has revealed that despite the ability of the strain to grow by sulfur oxidation coupled to nitrate ammonification, the genes encoding the canonical



**Table 2**  
Mobile elements in the genome of *Thermosulfuriphilus ammonigenes* ST65<sup>T</sup>.

Gene ID	Gene product	Pfam ID	Number of genes
QIJ70900 (2 copies) QIJ72367 (2 copies) QIJ72678	Integrase core domain	pfam13358	5
QIJ71194 QIJ71591	Phage integrase family	pfam00589	2
QIJ71463	Phage integrase	pfam13495	1
QIJ71806 QIJ72599 QIJ72601	Transposase, Helix-turn-helix domains	pfam01527	3
QIJ71807 QIJ72907	Integrase core domain	pfam00665	2
QIJ71809	Transposase, Mutator family	pfam00872	1

enzyme systems for these pathways such as SQR, SOE, Sox, SOR and Nrf, are absent. Conversely, the presence of all genes necessary for dissimilatory sulfate reduction does not provide the ability to grow due to sulfate reduction. These genes are apparently involved in disproportionation and oxidation of reduced sulfur compounds. In accordance with the fact that *T. ammonigenes* is an obligate lithoautotroph its genome contains genes involved in CO<sub>2</sub> fixation, gluconeogenesis and incomplete set of genes participating in TCA cycle.

### 3. Genome sequence accession numbers

The genome sequence of *T. ammonigenes* ST65<sup>T</sup> has been deposited in DDBJ/ENA/GenBank under the accession number CP048877. The BioSample data is available in the NCBI BioSample database (<http://www.ncbi.nlm.nih.gov/biosample/>) under the accession number SAMN14116118. The BioProject data is available in the NCBI BioProject database (<https://www.ncbi.nlm.nih.gov/bioproject/>) under the accession number PRJNA606893. The strain is available in the German Collection of Microorganisms and Cell Cultures (DSMZ) and All-Russian Collection of Microorganisms (VKM) under the accession numbers DSM 102941<sup>T</sup> and VKM B-2855<sup>T</sup>.

### Acknowledgement

This research was funded by the Russian Foundation for Basic Research, grant number 18-54-15008, by the Ministry of Science and Higher Education of the Russian Federation, by the French–Russian collaborative project (CNRS/RFBR) Neptune (PRC Russie 2017 n°281295), and by the LIA 1211 MicrobSea.

### Declaration of Competing Interests

The authors declare that they have no known competing financial interests or personal relationships that could have appeared to influence the work reported in this paper.

### References

Bertelli, C., Laird, M.R., Williams, K.P., Lau, B.Y., Hoad, G., Winsor, G.L., Brinkman, F.S., Brinkman, F.S.L., 2017. IslandViewer 4: expanded prediction of genomic islands for

larger-scale datasets. *Nucleic Acids Res.* 45, W30–W35. <https://doi.org/10.1093/nar/gkx343>.

Chen, I.-M.A., Chu, K., Palaniappan, K., Pillay, M., Ratner, A., Huang, J., Huntemann, M., Varghese, N., White, J.R., Seshadri, R., Smirnova, T., Kirton, E., Jungbluth, S.P., Woyke, T., Eloe-Fadrosh, E.A., Ivanova, N.N., Kyrpides, N.C., 2019. IMG/M v.5.0: an integrated data management and comparative analysis system for microbial genomes and microbiomes. *Nucleic Acids Res.* 47, 666–677. <https://doi.org/10.1093/nar/gky901>.

Couvin, D., Bernheim, A., Toano-Nioche, C., Touchon, M., Michalik, J., Néron, B., Rocha, E.P.C., Vergnaud, G., Gautheret, D., Pourcel, C., 2018. CRISPRCasFinder, an update of CRISPRFinder, includes a portable version, enhanced performance and integrates search for Cas proteins. *Nucleic Acids Res.* 46, W246–W251. <https://doi.org/10.1093/nar/gky425>.

Flores, G.E., Shakya, M., Meneghin, J., Yang, Z.K., Seewald, J.S., Geoff Wheat, C., Podar, M., Reysenbach, A.L., 2012. Inter-field variability in the microbial communities of hydrothermal vent deposits from a back-arc basin. *Geobiology*, 10, 333–346. <https://doi.org/10.1111/j.1472-4669.2012.00325.x>.

Frederiksen, T.M., Finster, K., 2003. Sulfite-oxido-reductase is involved in the oxidation of sulfite in *Desulfocapsa sulfoexigens* during disproportionation of thiosulfate and elemental sulfur. *Biodegradation* 14, 189–198. <https://doi.org/10.1023/A:1024255830925>.

Frigaard, N.-U., Dahl, C., 2009. Sulfur metabolism in phototrophic sulfur bacteria. *Adv. Microb. Physiol.* 54, 103–200. [https://doi.org/10.1016/S0065-2911\(08\)00002-7](https://doi.org/10.1016/S0065-2911(08)00002-7).

Grant, J.R., Stothard, P., 2008. The cgview server: a comparative genomics tool for circular genomes. *Nucleic Acids Res.* 36, W181–W184. <https://doi.org/10.1093/nar/gkn179>.

Hanson, T.E., Campbell, B.J., Kalis, K.M., Campbell, M.A., Klotz, M.G., 2013. Nitrate ammonification by *Nautilia profundicola* AMH: experimental evidence consistent with a free hydroxylamine intermediate. *Front. Microbiol.* 4, 180. <https://doi.org/10.3389/fmicb.2013.00180>.

Huerta-Cepas, J., Szklarczyk, D., Heller, D., Hernández-Plaza, A., Forslund, S.K., Cook, H., Mende, D.R., Letunic, I., Rattei, T., Jensen, L.J., von Mering, C., Peer, Bork P., 2019. eggNOG 5.0: a hierarchical, functionally and phylogenetically annotated orthology resource based on 5090 organisms and 2502 viruses. *Nucleic Acids Res.* 47, D309–D314. <https://doi.org/10.1093/nar/gky1085>.

Mardanov, A.V., Beletsky, A.V., Kadnikov, V.V., Slobodkina, A.I., Ravin, N.V., 2016. Genome analysis of *Thermosulfurimonas dismutans*, the first thermophilic sulfur-disproportionating bacterium of the phylum *Thermodesulfobacteria*. *Front. Microbiol.* 7, 950. <https://doi.org/10.3389/fmicb.2016.00950>.

Nakagawa, S., Takai, K., 2008. Deep-sea vent chemoautotrophs: diversity, biochemistry and ecological significance: chemoautotrophy in deep-sea vents. *FEMS Microbiol. Ecol.* 65, 1–14. <https://doi.org/10.1111/j.1574-6941.2008.00502.x>.

Orcutt, B.N., Sylvan, J.B., Knab, N.J., Edwards, K.J., 2011. Microbial ecology of the dark ocean above, at, and below the seafloor. *Microbiol. Mol. Biol. Rev.* 75, 361–422. <https://doi.org/10.1128/MMBR.00039-10>.

Overbeek, R., Olson, R., Pusch, G.D., Olsen, G.J., Davis, J.J., Disz, T., Edwards, R.A., Gerdes, S., Parrello, B., Shukla, M., Vonstein, V., Wattam, A.R., Xia, F., Stevens, R., 2014. The SEED and the rapid annotation of microbial genomes using subsystems technology (RAST). *Nucleic Acids Res.* 42, D206–D214. <https://doi.org/10.1093/nar/gkt1226>.

Slobodkina, A., Slobodkina, G., Allieux, M., Alain, K., Jebbar, M., Shadrin, V., Kublanov, I., Toshchakov, S., Bonch-Osmolovskaya, E., 2019. Genomic insights into the carbon and energy metabolism of a thermophilic deep-sea bacterium *Deferribacter autotrophicus* revealed new metabolic traits in the phylum *Deferribacteres*. *Genes*, 10, 849. <https://doi.org/10.3390/genes10110849>.

Slobodkina, G.B., Reysenbach, A.L., Kolganova, T.V., Novikov, A.A., Bonch-Osmolovskaya, E.A., Slobodkina, A.I., 2017. *Thermosulfuriphilus ammonigenes* gen. nov., sp. nov., a thermophilic, chemolithoautotrophic bacterium capable of respiratory ammonification of nitrate with elemental sulfur. *Int. J. Syst. Evol. Microbiol.* 67, 3474–3479. <https://doi.org/10.1099/ijsem.0.002142>.

Slobodkina, G.B., Mardanov, A.V., Ravin, N.V., Frolova, A.A., Chernyh, N.A., Bonch-Osmolovskaya, E.A., Slobodkina, A.I., 2017a. Respiratory ammonification of nitrate coupled to anaerobic oxidation of elemental sulfur in deep-sea autotrophic thermophilic bacteria. *Front. Microbiol.* 8, 87. <https://doi.org/10.3389/fmicb.2017.00087>.

Tatsova, T., DiCuccio, M., Badretin, A., Chetverin, V., Nawrocki, E.P., Zaslavsky, L., Lomsadze, A., Pruitt, K.D., Borodovsky, M., Ostell, J., 2016. NCBI prokaryotic genome annotation pipeline. *Nucleic Acids Res.* 44, 6614–6624. <https://doi.org/10.1093/nar/gkw569>.

Varani, A.M., Siguier, P., Goubeyre, E., Charneau, V., Chandler, M., 2011. ISsaga is an ensemble of web-based methods for high throughput identification and semi-automatic annotation of insertion sequences in prokaryotic genomes. *Genome Biol.* 12, R30. <https://doi.org/10.1186/gb-2011-12-3-r30>.

Wick, R.R., Judd, L.M., Gorrie, C.L., Holt, K.E., 2017. Unicycler: resolving bacterial genome assemblies from short and long sequencing reads. *PLoS Comput. Biol.* 13, e1005595. <https://doi.org/10.1371/journal.pcbi.1005595>.



Article

# Genomic Characterization and Environmental Distribution of a Thermophilic Anaerobe *Dissulfurirhabdus thermomarina* SH388<sup>T</sup> Involved in Disproportionation of Sulfur Compounds in Shallow Sea Hydrothermal Vents

Maxime Allieux<sup>1</sup>, Stéven Yvenou<sup>1</sup>, Galina Slobodkina<sup>2</sup>, Alexander Slobodkin<sup>2</sup>, Zongze Shao<sup>3</sup> , Mohamed Jebbar<sup>1</sup> and Karine Alain<sup>1,\*</sup>

<sup>1</sup> Univ Brest, CNRS, IFREMER, LIA1211, Laboratoire de Microbiologie des Environnements Extrêmes LM2E, IUEM, Rue Dumont d'Urville, F-29280 Plouzané, France; Maxime.Allieux@univ-brest.fr (M.A.); steven.yvenou@gmail.com (S.Y.); Mohamed.Jebbar@univ-brest.fr (M.J.)

<sup>2</sup> Winogradsky Institute of Microbiology, Research Center of Biotechnology of the Russian Academy of Sciences, 117312 Moscow, Russia; gslobodkina@mail.ru (G.S.); aslobodkin@hotmail.com (A.S.)

<sup>3</sup> Key Laboratory of Marine Genetic Resources, Third Institute of Oceanography, Ministry of Natural Resources, Xiamen 361005, China; shaozongze@tio.org.cn

\* Correspondence: Karine.Alain@univ-brest.fr

Received: 5 July 2020; Accepted: 24 July 2020; Published: 27 July 2020



**Abstract:** Marine hydrothermal systems are characterized by a pronounced biogeochemical sulfur cycle with the participation of sulfur-oxidizing, sulfate-reducing and sulfur-disproportionating microorganisms. The diversity and metabolism of sulfur disproportionators are studied to a much lesser extent compared with other microbial groups. *Dissulfurirhabdus thermomarina* SH388<sup>T</sup> is an anaerobic thermophilic bacterium isolated from a shallow sea hydrothermal vent. *D. thermomarina* is an obligate chemolithoautotroph able to grow by the disproportionation of sulfite and elemental sulfur. Here, we present the results of the sequencing and analysis of the high-quality draft genome of strain SH388<sup>T</sup>. The genome consists of a one circular chromosome of 2,461,642 base pairs, has a G + C content of 71.1 mol% and 2267 protein-coding sequences. The genome analysis revealed a complete set of genes essential to CO<sub>2</sub> fixation via the reductive acetyl-CoA (Wood-Ljungdahl) pathway and gluconeogenesis. The genome of *D. thermomarina* encodes a complete set of genes necessary for the dissimilatory reduction of sulfates, which are probably involved in the disproportionation of sulfur. Data on the occurrences of *Dissulfurirhabdus* 16S rRNA gene sequences in gene libraries and metagenome datasets showed the worldwide distribution of the members of this genus. This study expands our knowledge of the microbial contribution into carbon and sulfur cycles in the marine hydrothermal environments.

**Keywords:** genome annotation; *Dissulfurirhabdus*; shallow sea hydrothermal vents; inorganic sulfur compound disproportionation

## 1. Introduction

Anaerobic microorganisms are involved in biogeochemical cycles and are vital for global ecosystem maintenance, including marine hydrothermal vents. Shallow hydrothermal vents, like deep-sea hydrothermal vents, are areas characterized by the discharge of hot, anoxic, mineral-loaded, and reduced compound-rich fluid into the cold and oxygenated water of the ocean floor [1,2]. Sulfur is a ubiquitous element in the hydrothermal environment and is very important for energy production.



It is found in various oxidation states in the mineral structures forming chimneys, in the fluid emitted from the chimneys, especially as hydrogen sulfide (H<sub>2</sub>S) and in the surrounding sea-water as sulfate. The sulfur-oxidizing and sulfur/sulfate-reducing microbial taxa of these habitats are well known [3]. However, it is only very recently that sulfur-disproportionating species from this ecosystem have been reported there, even though the physico-chemical conditions of this habitat are obviously favorable to this reaction. To date, five sulfur-disproportionating species, all thermophilic, have been isolated from marine hydrothermal environments. The bacteria *Thermosulfuriphilus ammonigenes*, *Dissulfuribacter thermophilus* and *Thermosulfurimonas dismutans* were isolated from deep-sea hydrothermal vents [4–6], and the species *Thermosulfurimonas marina* and *Dissulfurirhabdus thermomarina* from shallow hydrothermal systems [7,8].

Disproportionation, also called dismutation, corresponds to a chemical or biological reaction where the same mineral or organic compound serves as an electron donor and as an electron acceptor. The microbially-mediated disproportionation of inorganic sulfur compounds was first described in 1987 [9,10]. Diverse inorganic sulfur compounds can be disproportionated: generally, the most studied forms for sulfur disproportionation are elemental sulfur (S<sup>0</sup>), thiosulfate (S<sub>2</sub>O<sub>3</sub><sup>2-</sup>) and sulfite (SO<sub>3</sub><sup>2-</sup>), which can be both oxidized to sulfate (SO<sub>4</sub><sup>2-</sup>) and reduced to sulfide (HS<sup>-</sup>) [11]. Under standard conditions, disproportionation reactions have a mainly low energy yield or can even be endergonic for elemental sulfur, according to thermodynamics, but can shift to be more energetic depending on the physico-chemical conditions of the natural environments and/or the presence of possible sulfide scavenging species. Few species have also been reported to disproportionate sulfur compounds solely for energy production and not for growth [11], as a kind of maintenance process, which could increase survival under limiting conditions. Most of the disproportionating microorganisms are known to use alternative energetically more favorable processes, such as sulfate-reduction or dissimilatory nitrate reduction to ammonium [12]. Interestingly, the disproportionation of elemental sulfur could date back up to 3.5 Ga and could be one of the earliest modes of microbial metabolism [13,14], but this hypothesis still remains highly controversial [15].

Sulfur compounds disproportionators originate from a large panel of environments such as marine sediments, freshwater sediments, anaerobic digestors, terrestrial, shallow and deep-sea hydrothermal vents, and acidic and alkaline lakes [12]. This process has been extensively studied in marine sediments but not in other environments [12,16,17]. In the current state of knowledge, and with recent discoveries, sulfur compounds disproportionating microorganisms appear to be phylogenetically diverse, particularly in the bacterial domain. From the literature, we could elaborate a list of 42 bacterial species in total, known to be able to disproportionate inorganic sulfur compounds, and being independent of the sulfur oxygenase reductase (SOR) enzyme [11,12]. The microorganisms known so far to be capable of disproportionating sulfur compounds under anaerobic conditions belong to *Thermodesulfobacteria*, *Firmicutes*, *Deltaproteobacteria* and *Gammaproteobacteria* [12].

To date, the metabolic pathways of sulfur-compound disproportionation and the importance of this process remain poorly documented, notably due to the absence of specific genomic markers.

Pathways of the disproportionation of sulfur are unknown and different pathways are very likely to exist. Some hypotheses have been proposed, such as the use of the complete or partial dissimilatory sulfate reduction pathway (adenylylsulfate reductase, heterodisulfide reductase, dissimilatory sulfite reductase), or the involvement of rhodanese-like sulfurtransferase or molybdopterin [18–20]. As suggested by Ward et al. (2020) [21], a truncated AprB protein may also be involved in this process but this modified protein does not appear to be common in all sulfur disproportionators. Finally, Mardanov et al. (2016) [18] showed that direct cellular contact with sulfur is not required. As suggested in Florentino et al. (2019) [19], certain molecular strategies could be involved in the assimilation of sulfur in cells, such as the formation of sulfur nanoparticles that can penetrate membranes, the nucleophilic attack of sulfur by sulfides that could generate polysulfides, used as a source of energy, or strategies involving flagella or pili.

*Dissulfurirhabdus thermomarina* SH388<sup>T</sup> is an anaerobic, thermophilic, chemolithoautotrophic bacterium isolated from a shallow submarine hydrothermal vent, located off the Kuril Islands (44°29.469' N 146°06.247' E), in the Sea of Okhotsk, at a water depth of 12 m [7]. It is the first strict anaerobic thermophilic species disproportionating inorganic sulfur compounds which was isolated from a shallow sea habitat. Based on its 16S rRNA gene sequence, it belongs to the class *Deltaproteobacteria* and is closely related to *Dissulfuribacter thermophilus* S69<sup>T</sup> and *Dissulfurimicrobium hydrothermale* SH68<sup>T</sup>. Physiological experiments demonstrated that *D. thermomarina* strain SH388<sup>T</sup> grows chemolithoautotrophically with bicarbonate/CO<sub>2</sub> as a carbon source, either by the respiration of sulfite coupled to the oxidation of dihydrogen, or by the disproportionation of sulfite or elemental sulfur [7]. However, it does not grow by thiosulfate disproportionation. In this work, we analyzed the genome and the geographical distribution of *D. thermomarina* SH388<sup>T</sup>. A very recent study also looked at the genome of *D. thermomarina* and in particular at its phylogenetic positioning [21]. In this survey, we did not rely on the assembly of this genome already available in the RefSeq and GenBank databases (accession number ASM1049943v1) used in Ward et al.'s (2020) [21] study, but we sequenced this genome de novo and made our own assembly, as detailed below, with more in-depth genome assembly and annotation strategies. Based on our genome assembly, we have highlighted the general metabolic pathways of this strain, and focused in particular on the energy production pathways involving sulfur inorganic compounds. Genome sequence availability and annotation will promote a better understanding of the genomic traits of a sulfur compound disproportionating bacteria, the metabolic features related to the adaptations to the ecosystem, and will be useful for future sulfur cycle studies.

## 2. Materials and Methods

### 2.1. Genome Sequencing and Assembly

For genomic DNA extraction, the strain was cultivated anaerobically at 50 °C, with H<sub>2</sub> as an electron donor, sulfite (5 mM) as a terminal electron acceptor and CO<sub>2</sub>/HCO<sub>3</sub><sup>-</sup> as the sole carbon source. Cells were harvested in the late exponential phase of growth. Genomic DNA was extracted using a FastDNA™ Spin Kit (MP Biomedicals, Irvine, CA, USA) according to the manufacturer's instructions. The genome sequence of strain SH388<sup>T</sup> was determined by the company Molecular Research (MrDNA, Shallowater, TX, USA) using the Illumina MiSeq technology (2 × 150 bp paired-reads, MicroV2 chemistry). Libraries' constructions and quality controls were performed by both sequencing facilities and verified with FastQC (v0.11.8—<https://www.bioinformatics.babraham.ac.uk/projects/fastqc/>). Genome was assembled into contigs by using the Unicycler pipeline for the de novo assembly (version: 0.4.8-beta—<https://github.com/rrwick/Unicycler>), and its dependencies (spades.py v3.14.0; makeblastdb v2.9.0+; tblastn v2.9.0+; bowtie2-build v2.3.5.1; bowtie2 v2.3.5.1; samtools v1.10; java v11.0.1; pilon v1.23; bcftools v1.10.2) [22]. Genome assembly statistics were obtained with Quast (v5.0.2; <https://github.com/ablab/quast>) and used to compare the different assemblies. Genome assembly visualization was plotted with Bandage (v0.8.1—<http://rrwick.github.io/Bandage/>) in order to detect potential plasmids from obtained contigs and afterwards checked with plasmidVerify python script (<https://github.com/ablab/plasmidVerify>) [23,24]. Genome completeness and potential contamination were controlled with CheckM (v1.1.2—<https://ecogenomics.github.io/CheckM/>), and whole genome average coverage was calculated using BBMap (v38.70—BBMap—Bushnell B.—[sourceforge.net/projects/bbmap/](https://sourceforge.net/projects/bbmap/)).

### 2.2. Genome Annotation

Genome was analyzed and annotated with the online version of the RAST software (v2.0—<http://rast.theseed.org/FIG/rast.cgi>), the fast annotation software Prokka (v1.14.6—<https://github.com/tseemann/prokka>), Dfast (v1.2.5—[https://github.com/nigyta/dfast\\_core](https://github.com/nigyta/dfast_core)), the MicroScope Microbial Genome Annotation and Analysis Platform (MaGe) (<https://mage.genoscope.cns.fr/microscope/home/index.php>), using the Kyoto Encyclopedia of Genes and Genomes (KEGG) and BioCyc databases,

and the NCBI prokaryotic genome annotation pipeline (PGAP) (2020-03-30.build4489—<https://github.com/ncbi/pgap>) with default parameters and databases for all of the five software/pipelines [25–29]. The functional annotation of predicted coding DNA sequences (CDSs) was further blasted with NCBI (v2.10.0+), and UniProtKB database (release 2020\_04). Hydrogenase classification was checked using the HydDB webtool (<https://services.birc.au.dk/hyddb/>) [30].

### 2.3. Clustered Regularly Interspaced Short Palindromic Repeats (CRISPRs) and Genomic Islands

Identification and classification of the CRISPR–Cas systems were performed by using the CRISPRCas Finder webserver, with default parameters (<https://crisprcas.i2bc.paris-saclay.fr/>) [31]. The prediction of laterally transferred gene clusters (genomic islands) was performed with the IslandViewer4 webserver (<http://www.pathogenomics.sfu.ca/islandviewer/>) based on an EMBL file generated by Dfast [32].

### 2.4. Geographical Distribution

The geographical distribution of *D. thermomarina* was studied at species and genus level within the 16S rRNA gene sequences available in the databases and in the public metagenomes deposited at the GBIF (Global Biodiversity Information Facility) facility (<https://www.gbif.org/>) and in the NCBI database.

### 2.5. Taxonomical Analyses and Comparative Genomics

To study the taxonomic position of the strain, we used GTDB-Tk (v1.1.1—<https://github.com/Ecogenomics/GTDBTk>) to place the genome on a tree made of concatenated reference proteins, we compared by blast the 16S rRNA CDS obtained from genomic assembly to the sequences in NCBI (v2.10.0+) and performed a tetra correlation comparison search with the JSpecies webserver against its own database (<http://jspecies.ribohost.com/jspeciesws/>).

The genome of *D. thermomarina* was compared by subtractive comparative genomics to the genomes of the hydrothermal bacteria *Thermosulfurimonas marina* (ASM1231758v1), *Thermosulfuriphilus ammonigenes* (ASM1120745v1), *Dissulfuribacter thermophilus* (ASM168733v1), and *Thermosulfurimonas dismutans* (ASM165258v1) to identify potential genetic markers of DNRA, and of thiosulfate disproportionation, two physiological properties absent in *D. thermomarina*, explored by excluding *D. thermomarina*'s genome. These genomes were compared by using the MaGE platform Pan-genome Analysis tool (<https://mage.genoscope.cns.fr/microscope/home/index.php>), based on the clustering algorithm SiLiX (<http://lbe.univ-lyon1.fr/-SiLiX-.html>) which clustered genomic CDSs by 50% amino acid identity and 80% amino acid alignment coverage, with permissive parameters. Resulting CDSs were blasted on the UniprotKB database and hypothetical protein CDSs were analyzed with InterProScan webserver (<https://www.ebi.ac.uk/interpro/>) for functional predictions.

Finally, to evaluate the hypothesis of Ward et al. (2020) [21] suggesting that the tail truncation of the AprB protein could be a molecular marker of the disproportionation capacity of sulfur, we extracted the CDS encoding the AprB protein (based on Prokka annotation) from the genomes of characterized sulfur disproportioners or sulfate reducers: *Thermosulfurimonas marina*, *Thermosulfuriphilus ammonigenes*, *Thermosulfurimonas dismutans*, *Dissulfuribacter thermophilus*, *Thermodesulfatator atlanticus*, *Thermodesulfatator autotrophicus* and *Thermodesulfatator indicus*, in addition to that of *D. thermomarina* [4–8,33–35]. The AprB putative protein sequences were then aligned and their length were calculated.

## 3. Results and Discussions

### 3.1. General Genome Properties and Genomic Islands

The complete genome sequence of *Dissulfurirhabdus thermomarina* strain SH388T was deposited in GenBank databases under the accession number JAATWC000000000. The strain is available in the DSMZ culture collection under the accession number DSM 100025T and in All-Russian Collection

of Microorganisms (VKM) under the accession number VKM B-2960T. The *D. thermomarina* SH388<sup>T</sup> genome sequence consisted of 36 contigs including two contigs of less than 200 bp with an overall size of 2,461,642 bp and a G + C content of 71.1 mol% (Figure 1). It is interesting to note that we found a higher G + C content than in Slobodkina et al. (2016) [7]. In this previous study, the DNA G + C content value was determined from the melting point with DNA of *Escherichia coli* K-12 as a reference. This method is more biased than determining the percentage of G + C directly from the genomic sequence. We therefore proposed to amend the description of the species *Dissulfurirhabdus thermomarina* in that respect.

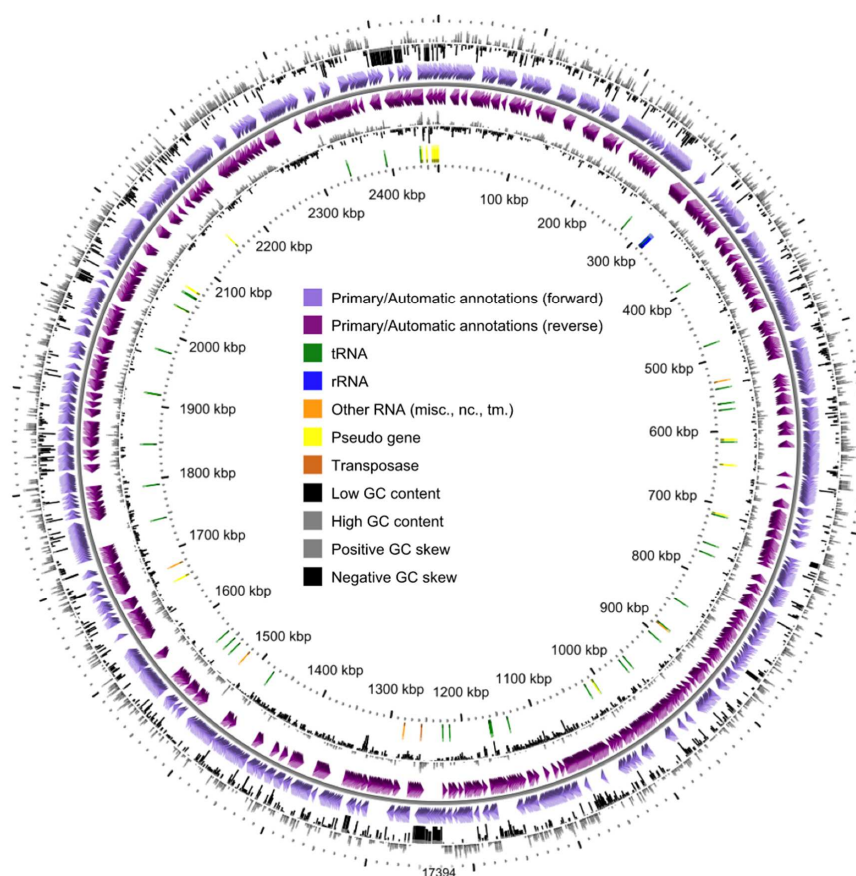


**Figure 1.** Circular mapping of the genome of *Dissulfurirhabdus thermomarina* SH388<sup>T</sup> from the circular genome viewer of the MaGe platform. GC content: guanine-cytosine content (mol%).

The longest contig was 713,503 bp, the  $N_{50}$  was 240,491 bp and the  $L_{50}$  was 3. The quality of this assembly was superior to that deposited previously in databases under the accession number ASM1049943v1 (Illumina HiSeq sequencing; draft genome of 2,569,312 bp in length, for 386 contigs with a  $N_{50}$  of 14,884 bp and a  $L_{50}$  of 54). The genome could be made up of one circular chromosome; indeed, no plasmids were detected when the genome was plotted with Bandage and by applying the plasmidVerify script to all contigs. CheckM estimated the genome to be 98.1922% complete based on the presence of default single-copy marker genes (four markers were missing) and without any hypothetical contamination. The average genome coverage was extremely high, around 1384.362 $\times$  according to raw pair read sequences extracted from MiSeq sequencing data (Table 1).

**Table 1.** General features and genome sequencing information for *Dissulfurirhabdus thermomarina* SH388T according to MICS recommendations.

Item	Description
<b>Investigation</b>	
Strain	<i>Dissulfurirhabdus thermomarina</i> strain SH388 <sup>T</sup>
Submitted to INSDC	GenBank
Investigation type	Bacteria
Project name	JAATWC000000000
Geographic location (latitude and longitude)	44°29.469' N, 146°06.247' E
Geographic location (country and/or sea, region)	Sea of Okhotsk, 250 m from the Kunashir Island shore (Sakhalin oblast, Russia)
Collection date	June 2013
Environment (biome)	marine hydrothermal vent biome ENVO:01000030
Environment (feature)	marine hydrothermal vent ENVO:01000122
Environment (material)	marine hydrothermal vent chimney ENVO:01000129
Depth	−12 m
<b>General features</b>	
Classification	Domain <i>Bacteria</i>
	Phylum <i>Proteobacteria</i>
	Class <i>Deltaproteobacteria</i>
	Not assigned to an Order
	Not assigned to a Family
	Genus <i>Dissulfurirhabdus</i>
	Species <i>Dissulfurirhabdus thermomarina</i>
Gram stain	Negative
Cell shape	short rods
Motility	Motile
Growth temperature	Thermophilic, optimum at 50 °C
Relationship to oxygen	Anaerobic
Trophic level	Chemolithoautotrophic
Biotic relationship	free-living
Isolation and growth conditions	DOI 10.1099/ijsem.0.001083
<b>Sequencing</b>	
Sequencing technology	Illumina MiSeq 2 × 150 bp
Sequencing platform	Molecular Research, MrDNA (Shallowater, TX, USA)
Assembler	Unicycler (version: 0.4.8-beta)
Contig number	36
N50	240,491
Genome coverage	1384.362x
Genome assembly NCBI	ASM1297923v1
Assembly level	Contigs
<b>Genomic features:</b>	
Genome size (bp)	2,461,642
GC content (mol%)	71.1
Protein coding genes	2267
Number of RNAs	50
tRNAs	47
16S-23S-5S rRNAs	1-1-1

Annotation with PGAP resulted in the prediction of 2321 genomic objects, among which 2267 were protein-coding sequences. The strain had a relatively streamlined genome with coding sequences covering approximately 90.8% of the entire genome. However, slightly different results were obtained with other annotation software: 2407 CDSs were found with RAST (1898/2407 were not integrated to subsystem categories), 2221 CDSs with Prokka, 2250 CDSs with Dfast and 2280 CDSs with MaGe annotation. The genome also contained one operon of 5S-16S-23S rRNA genes. We detected 47 tRNA with MaGe and PGAP which use the tRNA scan-SE RNA finder (<http://lowelab.ucsc.edu/tRNAscan-SE/index.html>), while 58 tRNA were detected with Prokka and Dfast based on ARAGORN RNA finder (<http://130.235.244.92/ARAGORN/>). However, the tRNA found in all cases corresponded to the 20 standard amino acids and selenocysteine. These results differ somewhat from those of Ward et al. (2020) [21] whom reported 2791 coding sequences and 53 RNAs, on a lower quality assembly of the genome.

Most of the CDSs obtained from the MaGe annotation pipeline (81.80%, 1865/2280 CDSs) could be assigned to at least one cluster of orthologous groups (COGs). The major predicted COG categories (encompassing more than 2% of the CDSs) were related to energy production and conversion (C) (8.2%), signal transduction mechanisms (T) (7.6%), translation-ribosomal structure-biogenesis (J) (7.1%), cell wall/membrane/envelope biogenesis (M) (6.9%), amino acid transport and metabolism (E) (6.3%), inorganic ion transport and metabolism (P) (5.2%), posttranslational modification-protein turnover-chaperones (O) (4.9%), coenzyme transport and metabolism (H) (4.6%), cell motility (N) (4.3%), replication-recombination-repair (L) (4.2%), carbohydrate transport and metabolism (G) (3.9%), transcription (K) (3.8%), intracellular trafficking-secretion-vesicular transport (U) (3.4%), lipid transport and metabolism (I) (2.4%), nucleotide transport and metabolism (F) (2.3%) and secondary metabolites biosynthesis, transport and catabolism (Q) (2.1%).

The gene locus tags associated to the genome assembly annotation given in GenBank and RefSeq (ASM1297923v1) are reported in the Table S.1.1.

Furthermore, four potential CRISPR loci were found using the CRISPRCasFinder server. These loci consisted of three putative CRISPR systems containing one spacer and a fourth one confirmed as a CRISPR locus, which was 466 bp long and included six spacers and repeats of 35 bp (GAAGGAATTGACCTGATTACTGAAGGGATTACGAC), but without cas genes.

Two regions of genomic plasticity were identified with the IslandViewer4 webserver, by using the genome of the closest database relative *Desulfuromonas* sp. DDH964 as a reference genome. These two genomic islands (GI) had a total length of 41.8 kb. The first GI was composed of genes involved in carbohydrate biosynthesis, degradation and transport-related CDSs (mostly mannose), as opposed to the second GI, composed mostly of hypothetical proteins CDSs (Table S.1.2.).

Interestingly, *D. thermomarina* seems to be quite unique among all the cultivated representatives of the *Bacteria* domain; based on 16S rRNA gene sequence identity, Average Nucleotide Identity (ANI) and phylogenetic placement based on concatenated references proteins (GTDB-Tk), we did not find any close relatives except *Dissulfuribacter thermophilus* strain S69<sup>T</sup> and *Dissulfurimicrobium hydrothermale* strain Sh68<sup>T</sup>, two *Deltaproteobacteria*, as already demonstrated by Slobodkina et al. (2016) [7]. *Dissulfurirhabdus thermomarina* SH388<sup>T</sup> was distantly related to these two closest cultured species, with its 16S rRNA gene sequence displaying only 91.6% and 90.4% gene sequence similarity with the 16S rRNA gene sequences of the *Dissulfuribacter thermophilus* strain S69<sup>T</sup> and *Dissulfurimicrobium hydrothermale* strain Sh68<sup>T</sup>, respectively. GTDB-Tk classified *D. thermomarina* within the *Dissulfuribacteriales* order, but has not associated it with any family or genus. The tetranucleotide signatures search showed strong similarities with species belonging to the *Gammaproteobacteria*, the *Actinobacteria* and the *Firmicutes* (Z-score > 0.9). On the basis of all these results, the proposal by Ward et al. (2020) [21] to assign *D. thermomarina* to a new family appears justified.



### 3.2. Central Carbon Metabolism

*D. thermomarina* SH388<sup>T</sup> is capable of growing autotrophically from CO<sub>2</sub>/HCO<sub>3</sub><sup>-</sup> [7]. We found a complete Wood–Ljungdahl pathway (reductive acetyl-CoA pathway) for carbon dioxide fixation and the generation of acetyl-CoA by integrating the annotations of PGAP, Biocyc, KEGG and Prokka (Table S.1.1). Based on the enzymes detected with MicroCyc, the strain appears also to have a complete glycolysis (Embden–Meyerhof), gluconeogenesis and pentose phosphate pathways. *D. thermomarina* seems also to possess some CDSs associated to the formate dehydrogenase. However, the capacity of *D. thermomarina* to oxidize formate into CO<sub>2</sub> has not been demonstrated experimentally, and Slobodkina et al. (2016) [7] demonstrated that formate does not stimulate the growth of *D. thermomarina*. Based on the KEGG and Biocyc databases, the tricarboxylic acid (TCA) cycle appears incomplete. Most probably, it serves for the formation of the necessary biosynthetic intermediates, in particular oxaloacetate, succinyl-CoA and 2-oxoglutarate. A key enzyme for the reverse TCA pathway, ATP-citrate lyase, is missing. According to KEGG and MicroCyc, *D. thermomarina* also appears to have a complete glycogen degradation pathway allowing the degradation of glycogen to G6P, or the reverse reaction. We also found a pyruvate fermentation pathway, oxidizing pyruvate to acetyl-CoA but Slobodkina et al. (2016) [7] showed experimentally that *D. thermomarina* does not ferment pyruvate. The addition of pyruvate in the medium could prevent the conversion of acetyl-CoA to pyruvate by the pyruvate synthase, and pyruvate could theoretically serve as a direct carbon substrate for gluconeogenesis. Nevertheless, according to MicroCyc, no other fermentative pathways were found, which is congruent with the autotrophic nature of the strain. In its natural habitat, this strain therefore probably develops from the CO<sub>2</sub> emitted in the hydrothermal fluid, and in other ecosystems, from the CO<sub>2</sub> produced by the microbial metabolism or abiotically.

### 3.3. Hydrogen Metabolism

*D. thermomarina* is capable of using hydrogen as an energy source [7]. Prokka, PGAP and MaGe annotations detected several hydrogenase-related proteins: maturation factors, hydrogenase formation chaperone, hydrogenases subunits and hydrogenase expression proteins (Table S.1.1). *D. thermomarina* appears to have a complete gene cluster encoding a membrane-bound [NiFe]-hydrogenase, belonging to the Group 1c [NiFe]-hydrogenase according to the HydDB classifier. Small and large subunit CDSs, as well as maturation factors, were found, but we were not able to clearly distinguish the four hydrogenase subunits HybO, HybA, HybB and HybC. This hydrogenase is likely to be involved in the anaerobic H<sub>2</sub>-uptake, for the hydrogenotrophic respiration with sulfite or SO<sub>2</sub> gas as terminal electron acceptors. As hydrothermal fluids are generally charged with dihydrogen (with particularly high concentrations at ultramafic sites), this highly energetic source feeds the autotrophic microorganisms inhabiting these unique habitats, such as *D. thermomarina*. In other anoxic habitats, microbial fermentations produce H<sub>2</sub>, as well as a number of abiotic reactions.

### 3.4. Nitrogen Metabolism

Species isolated from hydrothermal vents such as *Thermosulfurimonas dismutans*, *Thermosulfurimonas marina*, *Thermosulfuriphilus ammonigenes* and *Dissulfuribacter thermophilus* demonstrated the ability to use nitrate as an electron acceptor by performing DNRA metabolism [36]. We did not find any strong evidence for an energetic metabolism based on nitrogen compounds in *D. thermomarina*, which is congruent with the culture/physiology results [7]. Nevertheless, the genome contains a hydroxylamine oxidoreductase (EC: 1.7.2.6) and a hydroxylamine reductase (EC: 1.7.99.1) as evidenced by PGAP and Prokka annotations. An ammonia transporter and two P-II family nitrogen regulator CDSs were also found with Prokka. Nitrogen uptake pathways may not be canonical as no complete pathways were found, with the exception of one glutamine synthetase (EC: 6.3.1.2). From these results, *D. thermomarina* seems unlikely to participate to the global environmental nitrogen cycle.

### 3.5. Sulfur Metabolism

As has been shown for many bacteria, listed in the review by Slobodkin and Slobodkina (2019) [12], a complete sulfate reduction pathway was found in the genome of *D. thermomarina*, despite the fact that physiological experiments conducted in vitro showed that this strain does not grow from sulfate reduction [7]. Based on Prokka, Dfast and PGAP annotations, a complete dissimilatory sulfate reduction pathway was found, but no assimilatory sulfate reduction path (Table S.1.1). We found two CDSs associated to sulfate adenylyltransferases (*sat*) (EC: 2.7.7.4) displaying 29.25% identity with each other, both subunits alpha and beta of adenylyl-sulfate reductase (*aprA*, *aprB*) (EC: 1.8.99.2), a manganese-dependent inorganic pyrophosphatase, and subunits alpha, beta and gamma of dissimilatory sulfite reductase (*DsrA*, *DsrB*, and *DsrC*) (EC 1.8.99.5). A dissimilatory sulfite reductase D (*DsrD*) CDS was also found, but only with Prokka. CDSs corresponding to a complete *DsrMKJOP* complex were only found with RAST annotation, and they were confirmed to be related to menaquinol oxidoreductases by comparison to the UniProtKB database. A complete APS reductase-associated electron transfer complex (*QmoABC*) was found with PGAP and UniprotKB, if we refer to their homology with the *QmoABC* CDSs of *D. thermophilus*. Based on the complete pathways present in its genome, *D. thermomarina* would have the genetic potential to couple H<sub>2</sub> oxidation to sulfate reduction and should be able to grow through this metabolism; however, physiological results did not validate this hypothesis. Since *D. thermomarina* can reduce sulfite, the enzymes involved in the first step of the dissimilatory reduction of sulfate to sulfite, that are present in the genome, could have been good candidates for catalyzing the oxidation of sulfite to sulfate. However, these enzymes are not known to catalyze the reverse reaction of sulfate reduction to sulfite. In order to search for the genes involved in the disproportionation of sulfur, the genes known to be involved in the oxidation or reduction of inorganic sulfur compounds were searched for. None of the marker genes related to sulfur oxidation based on the genes cited in the recent review by Wasmund et al. (2017) [16] (e.g., sulfide:quinone oxidoreductase, Sox associated proteins, etc.) were found with any of the annotation software used. Genes encoding for sulfur oxygenase reductases (*SOR*), an enzyme performing elemental sulfur disproportionation under aerobic to microaerophilic conditions that had been found in the genome of the geothermal bacterium *Aquifex aeolicus* [37], was also searched for, but was not detected in *D. thermomarina*'s genome. As suggested previously, one can assume that all these CDSs attributed to dissimilatory sulfate reduction might be involved in inorganic sulfur disproportionation, through a currently undescribed process, with very likely an involvement of the adenylylsulfate reductase and the sulfate adenylyltransferase [11,12]. In addition, we found several CDSs without a clear determined function related to thiosulfate, tetrathionate and polysulfide molecules with PGAP and Prokka (polysulfide, tetrathionate and thiosulfate sulfurtransferase, reductase and dehydrogenase). These enigmatic CDSs might be as well be somehow related to sulfur compound disproportionation. Moreover, a *TorD*-like chaperon protein, four molybdopterin oxidoreductases and two rhodanese-like domain-containing proteins were found, as found in the genome of the alkaliphilic deltaproteobacterium *Desulfurivibrio alkaliphilus*, and hypothetically correlated to the oxidation of sulfides to sulfur by Thorup et al. (2017) [19]. Furthermore, thiosulfate cannot be disproportionated by *D. thermomarina* but one putative thiosulfate sulfurtransferase was identified in the genome by Prokka which shares 35% amino acids sequence identity with unreviewed proteins on UniprotKB database. However, considering the fact that the strain is phylogenetically distant from any cultivated representatives and relatively isolated within the bacterial domain, it is difficult to compare its CDSs to pertinent references.

These results highlight then the involvement of *D. thermomarina* into the sulfur cycle, (i) in particular in the reduction of sulfites, and (ii) somehow, still not well understood, in the disproportionation of sulfur, and (iii) finally in the sulfite disproportionation, possibly through the reverse dissimilatory sulfate reduction pathway.



### 3.6. Comparative Genomics

*D. thermomarina* was compared by subtractive comparative genomics to other genomes of hydrothermal bacteria with slightly different metabolic properties to identify in particular the potential genetic markers of DNRA and thiosulfate disproportionation. With this approach, 47 genes present in the genome of the four bacteria performing DNRA and thiosulfate dismutation and absent in the genome of *D. thermomarina* were identified (Figure S.1.3.). These CDSs are linked to the reactions of the nitrogen cycle including a periplasmic Nap-type nitrate reductase and a [FeMo]-nitrogenase (NifDKH). With regard to the disproportionation of thiosulfate, no CDS candidates were identified using this approach, with the exception of tetrathionate reductase subunit A for which the functional assignment is uncertain. A large number of hypothetical proteins were present in the subtracted gene pool, but without clear involvement in DNRA or thiosulfate dismutation reactions by InterProScan search. The thiosulfate disproportionation pathway and the DNRA route will therefore need to be studied using functional approaches in order to be deciphered.

In addition, CDS coding for AprB proteins was also analyzed for all these bacteria and we found, as in the results of Ward et al. (2020) [21], truncated proteins only in *Desulfovibrionales* and *Thermodesulfobacteriales*. However, by studying the length of CDS coding for AprB from different members of *Thermodesulfobacteriales* and comparing them to the metabolic properties of these strains, we were unable to correlate the length of these sequences with the ability or inability to disproportionate inorganic sulfur compounds. Indeed, the CDS coding for the AprB of the sulfur compounds disproportionating bacteria *Thermosulfurimonas dismutans*, *Thermosulfurimonas marina*, *Thermosulfuriphilus ammonigenes* are composed of 154 amino acids. On the other hand, the CDS coding for the AprB proteins of the sulfate-reducing bacteria *Thermodesulfatator atlanticus*, *Thermodesulfatator autotrophicus* and *Thermodesulfatator indicus* are composed of 150, 151 and 150 amino acids, respectively. Finally, the CDS coding for the AprB proteins of the sulfur disproportionators *Dissulfurirhabdus thermomarina* and *Dissulfuribacter thermophilus* are 148 amino acids long. More models are required to evaluate the hypothesis that an AprB gene truncation is associated to sulfur disproportionation, but seems unlikely to be, at least at the *Bacteria* domain scale.

### 3.7. Geographical and Environmental Distribution

The GBIF application (<https://www.gbif.org/species/>) enabled us to find the occurrences of the 16S rRNA gene sequences of the thermophilic sulfur disproportionators in gene libraries and metagenome datasets obtained from samples collected worldwide. While these data do not provide a comprehensive quantitative assessment, they allow to evaluate the geographical distribution of these bacteria. The analysis showed that among thermophilic sulfur-disproportionating bacteria, representatives of *Deltaproteobacteria* are more widespread than the representatives of *Thermodesulfobacteria* (Table 2).

**Table 2.** Occurrence of the thermophilic sulfur-disproportionating bacteria based on the GBIF (Global Biodiversity Information Facility) database.

Genus	Class	Occurrence		Georeferenced Records	
		Genus	Species	Genus	Species
<i>Dissulfurirhabdus</i>	<i>Deltaproteobacteria</i>	200	35 <sup>a</sup>	114	25 <sup>a</sup>
<i>Dissulfuribacter</i>	<i>Deltaproteobacteria</i>	230	27 <sup>b</sup>	130	14 <sup>b</sup>
<i>Caldimicrobium</i>	<i>Thermodesulfobacteria</i>	85	2 <sup>c</sup>	39	1 <sup>c</sup>
<i>Thermosulfurimonas</i>	<i>Thermodesulfobacteria</i>	27	17 <sup>d</sup>	5	3 <sup>d</sup>
<i>Thermosulfuriphilus</i>	<i>Thermodesulfobacteria</i>	0	NA	0	NA

The most abundant species of the genus are presented: <sup>a</sup> *Dissulfurirhabdus thermomarina*, <sup>b</sup> *Dissulfuribacter thermophilus*, <sup>c</sup> *Caldimicrobium thiodismutans*, <sup>d</sup> *Thermosulfurimonas dismutans* (Abbreviation: NA, not applicable).

The survey also revealed that the habitats of *D. thermomarina* are not limited to shallow sea hydrothermal vents, but also include marine coastal sediments, marine benthic sediments, ocean water column, pond soils, salt marshes or lagoon sediments contaminated with PAHs (<https://www.gbif.org/species/9334679>) (Figure 2A). In addition, 200 occurrences of the genus *Dissulfurirhabdus* of which 114 georeferenced were found primarily in different parts of the world ocean (<https://www.gbif.org/species/9334679>) (Figure 2B). Since no studied thermophilic sulfur disproportionators are known to form endospores or dormant cells, we can assume that they are in active metabolic state.



**Figure 2.** (A) Location of the 25 georeferenced records (among the total 35 occurrences) for the genus *Dissulfurirhabdus* in June 2020 based on the metagenomic 16S ribosomal RNA gene sequences from the GBIF database; (B) Location of the 114 georeferenced records (among the total 200 occurrences) for the genus *Dissulfurirhabdus* in June 2020 based on the metagenomic and metabarcoding 16S rRNA sequences from the GBIF database.

These results suggest that the diversity of the genus *Dissulfurirhabdus* is far from being explored, that this genus is distributed worldwide and could be involved in the global sulfur cycle in specific anoxic niches.

#### 4. Conclusions

*D. thermomarina* belongs to a little studied deeply branched phylogenetic group. The whole-genome annotation indicates its involvement in the sulfur cycle in shallow sea hydrothermal vents. The results found were generally supporting the main metabolic features demonstrated experimentally [7] and strengthen and complement the annotation performed by Ward et al. (2020) [21]. One interesting feature is that this species could reduce sulfite but not sulfate, even if the potential genomic resources are present. This genome analysis will potentially lead to a better understanding of inorganic sulfur compound disproportionation and sulfite reduction processes. In the future, functional approaches will have to be used to decipher the pathways of inorganic sulfur compounds disproportionation, and validate the functional hypotheses derived from genomic data. It is important to know the taxa that carry

out the dismutation of inorganic sulfur compounds in natural habitats as this process is not generally considered as such in global geochemical budgets. Indeed, it is crucial to determine what is the share of sulfur dismutation in the fluxes of sulfur species in habitats compared to those of sulfur-oxidation and sulfate-reduction, as dismutation is confused with these pathways in global budgets, since it leads to the production of sulfates and sulfides. Sulfur-disproportionating taxa do not necessarily have the same ecophysiological properties as sulfur-oxidizers and sulfate-reducers, and this could have a significant impact on our understanding of the biotic cycle of sulfur in natural environments.

**Supplementary Materials:** The following are available online at <http://www.mdpi.com/2076-2607/8/8/1132/s1>, Table S1.1: Correspondences between the loci of the annotations by Prokka, Dfast, RAST, PGAP (2020-03-30, build4489) and UniProtKB with the CDSs of the NCBI's online automated prokaryotic genome annotation pipeline, Table S1.2: Gene annotations within the genomic islands (GI) of *Dissulfurirhabdus thermomarina* SH388T, based on the IslandViewer 4 webserver, Figure S1.3: Homologous CDSs found by comparative genomics with the MaGE platform among the genomes of the hydrothermal bacteria *Thermosulfurimonas marina*, *Thermosulfuriphilus ammonigenes*, *Dissulfuribacter thermophilus*, and *Thermosulfurimonas dismutans*, excluding homologous CDSs from the genome of *D. thermomarina*.

**Author Contributions:** Conceptualization, M.A. and K.A.; Formal analysis, M.A., S.Y., G.S., A.S. and K.A.; Funding acquisition, G.S., A.S., Z.S., M.J. and K.A.; Investigation, M.A., S.Y., G.S., A.S. and K.A.; Methodology, M.A.; Supervision, M.A., Z.S., M.J. and K.A.; Validation, G.S., A.S., M.J. and K.A.; Writing—original draft, M.A., S.Y. and K.A.; Writing—review & editing, M.A., G.S., A.S. and K.A. All authors have read and agreed to the published version of the manuscript.

**Funding:** This research was funded by the French–Russian collaborative Project (CNRS/RFBR) Neptune (PRC Russie 2017 n°281295), by the Sino-French LIA/PRC 1211 MicrobSea, by the Russian Foundation for Basic Research, grant number 18-54-15008, and by the Ministry of Science and Higher Education of the Russian Federation. The study was supported by a grant from the French Ministry of Higher Education and Research, and from the Region Bretagne, to MA.

**Acknowledgments:** We are thankful to the LABGeM (CEA/Genoscope CNRS UMR8030), the France Génomique and French Bioinformatics Institute national infrastructures (funded as part of Investissement d'Avenir program managed by Agence Nationale pour la Recherche, contracts ANR-10-INBS-09 and ANR-11-INBS-0013), acknowledged for support within the MicroScope annotation platform.

**Conflicts of Interest:** The authors declare no conflict of interest.

## Abbreviations

ANI	Average nucleotide identity
CDS	Coding DNA sequences
COGs	Clusters of orthologous groups
CRISPR	Clustered regularly interspaced short palindromic repeats
DNRA	Dissimilatory nitrate reduction to ammonium
ENA	European Nucleotide Archive
G6P	Glucose-6-phosphate
INSDC	International Nucleotide Sequence Database Collaboration
KEGG	Kyoto Encyclopedia of Genes and Genomes
MIGS	Minimum information about a genome sequence
NCBI	National Center for Biotechnology Information
PAHs	Polycyclic aromatic hydrocarbons
PGAP	Prokaryotic genome annotation pipeline
bp	Base pair
SOR	Sulfur oxygenase reductase
TCA	Tricarboxylic acid cycle

## References

1. Tarasov, V.G.; Gebruk, A.V.; Mironov, A.N.; Moskalev, L.I. Deep-sea and shallow-water hydrothermal vent communities: Two different phenomena? *Chem. Geol.* **2005**, *224*, 5–39. [[CrossRef](#)]
2. Dick, G.J. The microbiomes of deep-sea hydrothermal vents: Distributed globally, shaped locally. *Nat. Rev. Microbiol.* **2019**, *17*, 271–283. [[CrossRef](#)] [[PubMed](#)]

3. Godfroy, A.; François, D.; Hartunians, J.; Moalic, Y.; Alain, K. Physiology, metabolism and ecology of thermophiles from deep-sea vents. In *The Microbiology of Deep-Sea*; Vetriani, C., Giovannelli, D., Eds.; Springer International: New York, NY, USA, in press.
4. Slobodkin, A.I.; Reysenbach, A.L.; Slobodkina, G.B.; Baslerov, R.V.; Kostrikin, N.A.; Wagner, I.D.; Bonch-Osmolovskaya, E.A. *Thermosulfurimonas dismutans* gen. nov.; sp. nov.; an extremely thermophilic sulfur-disproportionating bacterium from a deep-sea hydrothermal vent. *Int. J. Syst. Evol. Microbiol.* **2012**, *62*, 2565–2571. [[CrossRef](#)] [[PubMed](#)]
5. Slobodkin, A.I.; Reysenbach, A.L.; Slobodkina, G.B.; Kolganova, T.V.; Kostrikin, N.A.; Bonch-Osmolovskaya, E.A. *Dissulfuribacter thermophilus* gen. nov., sp. nov.; a thermophilic, autotrophic, sulfur disproportionating, deeply branching deltaproteobacterium from a deep-sea hydrothermal vent. *Int. J. Syst. Evol. Microbiol.* **2013**, *63*, 1967–1971. [[CrossRef](#)]
6. Slobodkina, G.B.; Reysenbach, A.L.; Kolganova, T.V.; Novikov, A.A.; Bonch-Osmolovskaya, E.A.; Slobodkin, A.I. *Thermosulfuriphilus ammonigenes* gen. nov.; sp. nov.; a thermophilic, chemolithoautotrophic bacterium capable of respiratory ammonification of nitrate with elemental sulfur. *Int. J. Syst. Evol. Microbiol.* **2017**, *67*, 3474–3479. [[CrossRef](#)]
7. Slobodkina, G.B.; Kolganova, T.V.; Kopitsyn, D.S.; Viryasov, M.B.; Bonch-Osmolovskaya, E.A.; Slobodkin, A.I. *Dissulfurirhabdus thermomarina* gen. nov.; sp. nov.; a thermophilic, autotrophic, sulfite-reducing and disproportionating deltaproteobacterium isolated from a shallow-sea hydrothermal vent. *Int. J. Syst. Evol. Microbiol.* **2016**, *66*, 2515–2519. [[CrossRef](#)]
8. Frolova, A.A.; Slobodkina, G.B.; Baslerov, R.V.; Novikov, A.A.; Slobodkin, A.I. *Thermosulfurimonas marina* sp. nov., an Autotrophic Sulfur-Disproportionating and Nitrate-Reducing Bacterium Isolated from a Shallow-Sea Hydrothermal Vent. *Microbiology* **2018**, *87*, 502–507. [[CrossRef](#)]
9. Bak, F.; Pfennig, N. Chemolithotrophic growth of *Desulfovibrio sulfodismutans* sp. nov. by disproportionation of inorganic sulfur compounds. *Arch. Microbiol.* **1987**, *147*, 184–189. [[CrossRef](#)]
10. Bak, F.; Cypionka, H. A novel type of energy metabolism involving fermentation of inorganic sulphur compounds. *Nature* **1987**, *326*, 891–892. [[CrossRef](#)]
11. Finster, K. Microbiological disproportionation of inorganic sulfur compounds. *J. Sulfur Chem.* **2008**, *29*, 281–292. [[CrossRef](#)]
12. Slobodkin, A.I.; Slobodkina, G.B. Diversity of Sulfur-Disproportionating Microorganisms. *Microbiology* **2019**, *88*, 509–522. [[CrossRef](#)]
13. Philippot, P.; Van Zuilen, M.; Lepot, K.; Thomazo, C.; Farquhar, J.; Van Kranendonk, M.J. Early Archaeon microorganisms preferred elemental sulfur, not sulfate. *Science* **2007**, *317*, 1534–1537. [[CrossRef](#)] [[PubMed](#)]
14. Wacey, D.; Kilburn, M.R.; Saunders, M.; Cliff, J.; Brasier, M.D. Microfossils of sulphur-metabolizing cells in 3.4-billion-year-old rocks of Western Australia. *Nat. Geosci.* **2011**, *4*, 698–702. [[CrossRef](#)]
15. Ollivier, B.; Zeyen, N.; Gales, G.; Hickman-Lewis, K.; Gaboyer, F.; Benzerara, K.; Westall, F. Importance of Prokaryotes in the Functioning and Evolution of the Present and Past Geosphere and Biosphere. In *Prokaryotes and Evolution*; Bertrand, J.C., Normand, P., Ollivier, B., Sime-Ngando, T., Eds.; Springer: Cham, Switzerland, 2018. [[CrossRef](#)]
16. Wasmund, K.; Mußmann, M.; Loy, A. The life sulfuric: Microbial ecology of sulfur cycling in marine sediments. *Environ. Microbiol. Rep.* **2017**, *9*, 323–344. [[CrossRef](#)]
17. Jørgensen, B.B.; Findlay, A.J.; Pellerin, A. The Biogeochemical Sulfur Cycle of Marine Sediments. *Front. Microbiol.* **2019**, *10*, 849. [[CrossRef](#)]
18. Mardanov, A.V.; Beletsky, A.V.; Kadnikov, V.V.; Slobodkin, A.I.; Ravin, N.V. Genome analysis of *Thermosulfurimonas dismutans*, the first thermophilic sulfur-disproportionating bacterium of the phylum *Thermodesulfobacteria*. *Front. Microbiol.* **2016**, *7*, 950. [[CrossRef](#)]
19. Thorup, C.; Schramm, A.; Findlay, A.J.; Finster, K.W.; Schreiber, L. Disguised as a sulfate reducer: Growth of the deltaproteobacterium *Desulfurivibrio alkaliphilus* by sulfide oxidation with nitrate. *mBio* **2017**, *8*, e00671-17. [[CrossRef](#)]
20. Florentino, A.P.; Pereira, I.A.C.; Boeren, S.; van den Born, M.; Stams, A.J.M.; Sánchez-Andrea, I. Insight into the sulfur metabolism of *Desulfurella amilsii* by differential proteomics. *Environ. Microbiol.* **2019**, *21*, 209–225. [[CrossRef](#)]
21. Ward, L.M.; Bertran, E.; Johnston, D.T. Genomic sequence analysis of *Dissulfurirhabdus thermomarina* SH388 and proposed reassignment to *Dissulfurirhabdaceae* fam. nov. *Microb. Genom.* **2020**. [[CrossRef](#)]

22. Wick, R.R.; Judd, L.M.; Gorrie, C.L.; Holt, K.E. Unicycler: Resolving bacterial genome assemblies from short and long sequencing reads. *PLoS Comput. Biol.* **2017**, *13*, e1005595. [[CrossRef](#)]
23. Wick, R.R.; Schultz, M.B.; Zobel, J.; Holt, K.E. Bandage: Interactive visualization of de novo genome assemblies. *Bioinformatics* **2015**, *31*, 3350–3352. [[CrossRef](#)] [[PubMed](#)]
24. Antipov, D.; Raiko, M.; Lapidus, A.; Pevzner, P.A. Plasmid detection and assembly in genomic and metagenomic data sets. *Genome Res.* **2019**, *29*, 961–968. [[CrossRef](#)] [[PubMed](#)]
25. Seemann, T. Prokka: Rapid prokaryotic genome annotation. *Bioinformatics* **2014**, *30*, 2068–2069. [[CrossRef](#)] [[PubMed](#)]
26. Brettin, T.; Davis, J.J.; Disz, T.; Edwards, R.A.; Gerdes, S.; Olsen, G.J.; Olson, R.; Overbeek, R.; Parrello, B.; Pusch, G.D.; et al. RASTtk: A modular and extensible implementation of the RAST algorithm for building custom annotation pipelines and annotating batches of genomes. *Sci. Rep.* **2015**, *5*, 8365. [[CrossRef](#)]
27. Tatusova, T.; DiCuccio, M.; Badretdin, A.; Chetvernin, V.; Nawrocki, E.P.; Zaslavsky, L.; Lomsadze, A.; Pruitt, K.D.; Borodovsky, M.; Ostell, J. NCBI prokaryotic genome annotation pipeline. *Nucleic Acids Res.* **2016**, *44*, 6614–6624. [[CrossRef](#)]
28. Vallenet, D.; Calteau, A.; Cruveiller, S.; Gachet, M.; Lajus, A.; Josso, A.; Médigue, C. MicroScope in 2017: An expanding and evolving integrated resource for community expertise of microbial genomes. *Nucleic Acids Res.* **2017**, *45*, D517–D528. [[CrossRef](#)]
29. Tanizawa, Y.; Fujisawa, T.; Nakamura, Y. DFAST: A flexible prokaryotic genome annotation pipeline for faster genome publication. *Bioinformatics* **2018**, *34*, 1037–1039. [[CrossRef](#)]
30. Søndergaard, D.; Pedersen, C.N.S.; Greening, C. HydDB: A web tool for hydrogenase classification and analysis. *Sci. Rep.* **2016**, *6*, 1–8. [[CrossRef](#)]
31. Couvin, D.; Bernheim, A.; Toffano-Nioche, C.; Touchon, M.; Michalik, J.; Néron, B.; Rocha, E.; Vergnaud, G.; Gautheret, D.; Pourcel, C. CRISPRCasFinder, an update of CRISPRFinder, includes a portable version, enhanced performance and integrates search for Cas proteins. *Nucleic Acids Res.* **2018**, *46*, W246–W251. [[CrossRef](#)]
32. Bertelli, C.; Laird, M.R.; Williams, K.P.; Simon Fraser University Research Computing Group; Lau, B.Y.; Hoad, G.; Winsor, G.L.; Brinkman, F. IslandViewer 4: Expanded prediction of genomic islands for larger-scale datasets. *Nucleic Acids Res.* **2017**, *45*, W30–W35. [[CrossRef](#)]
33. Moussard, H.; L'Haridon, S.; Tindall, B.J.; Banta, A.; Schumann, P.; Stackebrandt, E.; Reysenbach, A.L.; Jeanthon, C. *Thermodesulfator indicus* gen. nov.; sp. nov.; a novel thermophilic chemolithoautotrophic sulfate-reducing bacterium isolated from the Central Indian Ridge. *Int. J. Syst. Evol. Microbiol.* **2004**, *54*, 227–233. [[CrossRef](#)] [[PubMed](#)]
34. Alain, K.; Postec, A.; Grinsard, E.; Lesongeur, F.; Prieur, D.; Godfroy, A. *Thermodesulfator atlanticus* sp. nov., a thermophilic, chemolithoautotrophic, sulfate-reducing bacterium isolated from a Mid-Atlantic Ridge hydrothermal vent. *Int. J. Syst. Evol. Microbiol.* **2010**, *60*, 33–38. [[CrossRef](#)] [[PubMed](#)]
35. Lai, Q.; Cao, J.; Dupont, S.; Shao, Z.; Jebbar, M.; Alain, K. *Thermodesulfator autotrophicus* sp. nov.; a thermophilic sulfate-reducing bacterium from the Indian Ocean. *Int. J. Syst. Evol. Microbiol.* **2016**, *66*, 3978–3982. [[CrossRef](#)]
36. Slobodkina, G.B.; Mardanov, A.V.; Ravin, N.V.; Frolova, A.A.; Chernyh, N.A.; Bonch-Osmolovskaya, E.A.; Slobodkin, A.I. Respiratory Ammonification of Nitrate Coupled to Anaerobic Oxidation of Elemental Sulfur in Deep-Sea Autotrophic Thermophilic Bacteria. *Front. Microbiol.* **2017**, *8*, 87. [[CrossRef](#)] [[PubMed](#)]
37. Pelletier, N.; Leroy, G.; Guiral, M.; Giudici-Orticoni, M.T.; Aubert, C. First characterization of the active oligomer form of sulfur oxygenase reductase from the bacterium *Aquifex aeolicus*. *Extremophiles* **2008**, *12*, 205–215. [[CrossRef](#)]



© 2020 by the authors. Licensee MDPI, Basel, Switzerland. This article is an open access article distributed under the terms and conditions of the Creative Commons Attribution (CC BY) license (<http://creativecommons.org/licenses/by/4.0/>).



Supplementary material

**Genomic characterization and environmental distribution of a thermophilic anaerobe *Dissulfurirhabdus thermomarina* SH388<sup>T</sup> involved in disproportionation of sulfur compounds in shallow-sea hydrothermal vents**

Maxime Allieux<sup>1</sup>, Stéven Yvenou<sup>1</sup>, Galina Slobodkina<sup>2</sup>, Alexander Slobodkin<sup>2</sup>, Zongze Shao<sup>3</sup>, Mohamed Jebbar<sup>1</sup> and Karine Alain<sup>1,\*</sup>

<sup>1</sup> Univ Brest, CNRS, IFREMER, LIA1211, Laboratoire de Microbiologie des Environnements Extrêmes LM2E, IUEM, Rue Dumont d'Urville, F-29280 Plouzané, France; Maxime.Allieux@univ-brest.fr (M.A.); steven.yvenou@gmail.com (S.Y.); Mohamed.Jebbar@univ-brest.fr (M.J.); Karine.Alain@univ-brest.fr (K.A.)

<sup>2</sup> Winogradsky Institute of Microbiology, Research Center of Biotechnology of the Russian Academy of Sciences, 117312 Moscow, Russia; gslobodkina@mail.ru (G.S.); aslobodkin@hotmail.com (A.S.)

<sup>3</sup> Key Laboratory of Marine Genetic Resources, Third Institute of Oceanography, Ministry of Natural Resources, Xiamen 361005, China; shaozongze@tio.org.cn (Z.S.)

\* Correspondence: Karine.Alain@univ-brest.fr

**Supplementary Material S1: *Dissulfurirhabdus thermomarina* SH388<sup>T</sup> genome locus tags, genomic islands composition, and results of comparative genomics.**

### S1.1. Synthesis of the gene loci

**Table S1.1.** Correspondences between the loci of the annotations by Prokka, Dfast, RAST, PGAP (2020-03-30.build4489) and UniProtKB with the CDSs of the NCBI's online automated prokaryotic genome annotation pipeline. CDSs found with their associated loci, based on the assembly repository ASM1297923v1 (Abbreviation: NR, not retrieved).

Gene name	Gene associated Locus (NCBI PGAP)
<b>Gene related to carbon metabolism:</b>	
<b>Wood-Ljundhal</b>	
Formate dehydrogenase	HCU62_RS06340
formate--tetrahydrofolate ligase	HCU62_RS06190
FolD bifunctional 5,10-methylene-tetrahydrofolate dehydrogenase/cyclohydrolase	HCU62_RS06185
5-methyltetrahydrofolate:corrinoid/iron-sulfur protein co-methyltransferase	HCU62_RS06135
5,10-methylenetetrahydrofolate reductase	HCU62_RS06150
carbon monoxide dehydrogenase	HCU62_RS06180
Acetyl-CoA decarboxylase/synthase	HCU62_RS06140 ; HCU62_RS06145
<b>Glycolysis</b>	
glucose-6-phosphate isomerase	HCU62_RS09635
fructose-1,6-bisphosphatase	HCU62_RS01815
ATP-dependent 6-phosphofructokinase	HCU62_RS01170
fructose-bisphosphate aldolase	HCU62_RS04890
triose-phosphate isomerase	HCU62_RS06960
glyceraldehyde-3-phosphate dehydrogenase	HCU62_RS06940
phosphoglycerate kinase	HCU62_RS06955
2,3-bisphosphoglycerate-independent phosphoglycerate mutase	HCU62_RS01330 ; HCU62_RS03440
phosphopyruvate hydratase	HCU62_RS01970
phosphoenolpyruvate synthase	HCU62_RS09245
pyruvate kinase	HCU62_RS10405
<b>Glycogen degradation</b>	
glycogen phosphorylase	HCU62_RS04055
alpha-D-glucose phosphate-specific phosphoglucomutase	HCU62_RS05730
<b>Pyruvate fermentation to acetate</b>	
acetate--CoA ligase	HCU62_RS09440
pyruvate synthase	HCU62_RS00790 ; HCU62_RS00785 ; HCU62_RS00800
<b>Pentose phosphate pathway</b>	
glucose-6-phosphate dehydrogenase	HCU62_RS08000
6-phosphogluconolactonase	HCU62_RS07995
6-phosphogluconate dehydrogenase	HCU62_RS08005
ribose-5-phosphate isomerase	HCU62_RS01010
ribulose-phosphate 3-epimerase	HCU62_RS08705
transketolase (glycolaldehydetransferase)	HCU62_RS03690
transaldolase (dihydroxyacetone transferase)	HCU62_RS08675
<b>Formate associated enzymes</b>	
formate dehydrogenase	HCU62_RS01485 ; HCU62_RS06125 ; HCU62_RS06340
formate--tetrahydrofolate ligase	HCU62_RS06190



Gene name	Gene associated Locus (NCBI PGAP)
<b>Genes related to hydrogen metabolism:</b>	
methyl-viologen-reducing hydrogenase delta subunit/coenzyme F420-reducing hydrogenase delta subunit	HCU62_RS00680 ; HCU62_RS03360 ; HCU62_RS06160 ; HCU62_RS06170 ; HCU62_RS06335
HypC/HybG/HupF family hydrogenase formation chaperone	HCU62_RS01665
hydrogenase formation protein HypD	HCU62_RS01670
hydrogenase expression/formation protein HypE	HCU62_RS01675
hydrogenase maturation protease	HCU62_RS01680
hydrogenase maturation nickel metallochaperone HypA	HCU62_RS01685
hydrogenase nickel incorporation protein HypB	HCU62_RS01690
hydrogenase-2 small chain	HCU62_RS02130
nickel-dependent hydrogenase large subunit	HCU62_RS02135
Ni/Fe-hydrogenase, b-type cytochrome subunit	HCU62_RS02140
<b>Genes related to nitrogen metabolism:</b>	
hydroxylamine oxidase	HCU62_RS03110
hydroxylamine reductase	HCU62_RS07985
ammonia transporter	HCU62_02830
P-II family nitrogen regulator	HCU62_RS02830 ; HCU62_RS02845
<b>Genes related to sulfur metabolism:</b>	
sulfate adenyltransferase	HCU62_RS05615 ; HCU62_RS05700
adenyl-sulfate reductase subunit A	HCU62_RS05605
adenyl-sulfate reductase subunit B	HCU62_RS05610
manganese-dependent inorganic pyrophosphatase	HCU62_RS08685
dissimilatory sulfite reductase subunits alpha	HCU62_RS08555
dissimilatory sulfite reductase subunits beta	HCU62_RS08560
dissimilatory sulfite reductase subunits gamma	HCU62_RS09615
dissimilatory sulfite reductase D	HCU62_RS08565
DsrM	HCU62_RS08595
DsrK	HCU62_RS08600
DsrJ	HCU62_RS08605
DsrO	HCU62_RS08610
DsrP	HCU62_RS08615
QmoA	HCU62_RS05600
QmoB	HCU62_RS05595
QmoC	HCU62_RS05590
sulfurtransferase TusA family protein	HCU62_RS03365 ; HCU62_RS06620
sulfurtransferase	HCU62_RS06555 ; HCU62_RS06560
polysulfide reductase NrfD	HCU62_RS00235 ; HCU62_RS11490 ; HCU62_RS11500
polysulfide/tetrathionate/thiosulfate reductase associated proteins	HCU62_RS07540 ; NR
TorD-like chaperon protein	HCU62_RS07530
molybdopterin oxidoreductase	HCU62_RS06125 ; HCU62_RS07535 ; HCU62_RS07580 ; HCU62_RS10115
rhodanese-like domain-containing protein	HCU62_RS02325 ; HCU62_07590
putative thiosulfate sulfurtransferase	HCU62_RS06560

## S1.2. Annotation of Genes of Genomic Islands

**Table S1.2.** Gene annotations within the genomic islands (GI) of *Dissulfurirhabdus thermomarina* SH388<sup>T</sup>, based on the IslandViewer 4 webserver.

Genomic island	Gene start	Gene end	Strand	Product
GI 1	1793219	1795750	1	sugar ABC transporter substrate-binding protein
GI 1	1795761	1796717	1	LPS biosynthesis protein
GI 1	1796736	1797908	1	hypothetical protein
GI 1	1797905	1799242	1	polysaccharide biosynthesis related protein
GI 1	1799525	1800247	1	hypothetical protein
GI 1	1800508	1801404	1	sulfotransferase family protein
GI 1	1802691	1803914	1	glycosyl transferase family 1
GI 1	1803904	1804683	1	acetyl-mannosamine transferase
GI 1	1804791	1805603	1	hypothetical protein
GI 1	1805600	1806730	1	GDP-mannose 4,6-dehydratase
GI 1	1806768	1807709	1	GDP-L-fucose synthase
GI 1	1807723	1809150	1	mannose-6-phosphate isomerase
GI 1	1809117	1810670	-1	Phosphomannomutase
GI 2	1867701	1869266	1	hypothetical protein
GI 2	1870044	1870256	-1	hypothetical protein
GI 2	1870376	1870660	1	hypothetical protein
GI 2	1870586	1871059	-1	hypothetical protein
GI 2	1871214	1872170	1	IS30 family transposase
GI 2	1872355	1872564	-1	hypothetical protein
GI 2	1872561	1873196	-1	hypothetical protein
GI 2	1875044	1875547	-1	hypothetical protein
GI 2	1875917	1876378	-1	hypothetical protein
GI 2	1876378	1876983	-1	hypothetical protein
GI 2	1877128	1877793	-1	hypothetical protein
GI 2	1878138	1878791	-1	hypothetical protein
GI 2	1878926	1879153	-1	hypothetical protein
GI 2	1881275	1882240	1	hypothetical protein
GI 2	1882711	1884291	-1	RNA polymerase sigma factor RpoD

S1.3. Comparative genomics

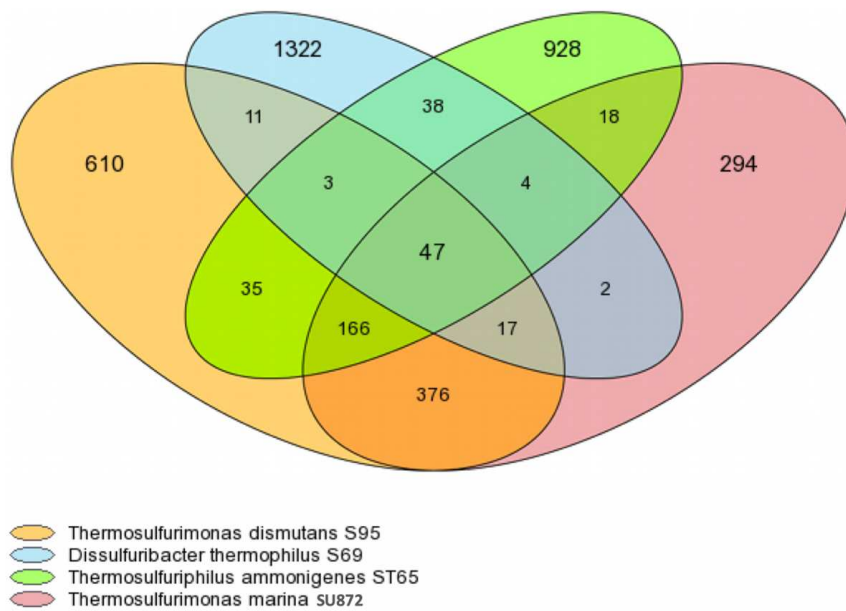


**Figure S1.3.** Homologous CDSs found by comparative genomics with the MaGE platform among the genomes of the hydrothermal bacteria *Thermosulfurimonas marina*, *Thermosulfuriphilus ammonigenes*, *Dissulfuribacter thermophilus*, and *Thermosulfurimonas dismutans*, excluding homologous CDSs from the genome of *D. thermomarina*.

### Genome analyses of strains isolated in this work

The genome of *Thermosulfurimonas* strain F29 that has been isolated at the middle of my PhD, was also sequenced, assembled, and analyzed. The draft article about this work can be found below. This article will be submitted to the journal *Microbial Genomics*.

1 **Genome analysis of a new sulfur disproportionating species**  
2 ***Thermosulfurimonas* strain F29 and comparative genomics of**  
3 **sulfur-disproportionating bacteria from marine hydrothermal**  
4 **vents**

5 **Maxime Allioux<sup>1</sup>, Stéven Yvenou<sup>1</sup>, Galina Slobodkina<sup>2</sup>, Alexander Slobodkin<sup>2</sup>, Anne**  
6 **Godfroy<sup>1</sup>, Zongze Shao<sup>3</sup>, Mohamed Jebbar<sup>1</sup> and Karine Alain<sup>1\*</sup>**

7

8 <sup>1</sup>Univ Brest, CNRS, IFREMER, IRP 1211 MicrobSea, Laboratoire de Microbiologie des  
9 Environnements Extrêmes LM2E, IUEM, Rue Dumont d'Urville, F-29280 Plouzané, France

10 <sup>2</sup>Winogradsky Institute of Microbiology, Research Center of Biotechnology of the Russian  
11 Academy of Sciences, Moscow, Russia

12 <sup>3</sup>Key Laboratory of Marine Genetic Resources, Third Institute of Oceanography, Ministry of  
13 Natural Resources, Xiamen 361005, China

14 **\* Correspondence:** Karine Alain

15 [Karine.Alain@univ-brest.fr](mailto:Karine.Alain@univ-brest.fr)

16

17

18 **Keywords:** *Thermosulfurimonas*, sulfur disproportionation, hydrothermal vents, thermophile,  
19 comparative genomics

20

21 **Abbreviations:** AAI, average amino-acid identity; ANI, average nucleotide identity; Cas,  
22 CRISPR associated protein; DDH, DNA-DNA hybridization; CDS, coding DNA sequence; CRISPR,  
23 clustered regularly interspaced short palindromic repeats; GI: genomic islands;  
24 DNRA, dissimilatory nitrate reduction to ammonium; PGAP, prokaryotic genome annotation  
25 pipeline.

26 **Abstract**

27 This paper reports on the genome analysis of strain F29 representing a new species of the  
28 genus *Thermosulfurimonas*. This strain, isolated from the Lucky Strike hydrothermal field on  
29 the Mid-Atlantic Ridge, is able to grow by disproportionation of  $S^0$  with  $CO_2$  as a carbon  
30 source. Strain F29 possesses a genome of 2,345,565 bp, with a G+C content of 58.09%, and at  
31 least one plasmid. The genome analysis revealed complete set of genes for  $CO_2$  fixation *via*  
32 the Wood–Ljungdahl pathway, for sulfate-reduction and for hydrogen oxidation, suggesting  
33 the involvement of the strain into carbon, sulfur, and hydrogen cycles of deep-sea  
34 hydrothermal vents. Strain F29 genome encodes also several CRISPR sequences, suggesting  
35 that the strain may be subjected to viral attacks. Comparative genomics was carried out to  
36 decipher sulfur disproportionation pathways and have been investigated by comparing the  
37 genomes of sulfur-disproportionating bacteria from marine hydrothermal vents, to the ones  
38 of non-sulfur-disproportionating bacteria. This analysis revealed the ubiquitous presence in  
39 these genomes of a molybdopterin protein consisting of a large and a small subunit, and an  
40 associated chaperone. We hypothesize that these proteins may be involved in the process of  
41 elemental sulfur disproportionation.

42

43 **Impact statement**

44

45 The disproportionation of inorganic sulfur compounds is poorly documented in the  
46 hydrothermal ecosystem and in natural environments in general. Its comprehensive  
47 apprehension might change our understanding of the hydrothermal sulfur cycle. Currently,  
48 the metabolic pathways and enzymatic mechanisms of this process are only partially resolved.  
49 In order to study the distribution and abundance of sulfur-disproportionators in natural  
50 environments, it might be helpful to find molecular signatures of this metabolism, if they  
51 exist. Here, we have performed a genome study of a new species disproportionating  
52 elemental sulfur, *Thermosulfurimonas* strain F29 sp. nov., and have performed comparative  
53 genomics within the genus *Thermosulfurimonas* and other sulfur-disproportionating genera  
54 of marine hydrothermal origin. This work has revealed a molybdopterin protein that may be  
55 involved in sulfur dismutation. However, its role will have to be confirmed by functional

56 approaches. The implementation of comparative genomics, followed by or combined with  
57 functional approaches should lead to a comprehensive understanding of microbial inorganic  
58 sulfur disproportionation in natural environments.

## 59 **1. Data summary**

60 The datasets generated and analyzed during the current study are available in the National  
61 Center for Biotechnology Information repository under BioProject number PRJNA753696. The  
62 assembled genome is available in the NCBI WGS database under accession numbers JAIFYA01  
63 and ASM1968873v1.

## 64 **INTRODUCTION**

65 Disproportionation or dismutation of inorganic sulfur compounds is a relatively  
66 undocumented metabolism and is not systematically studied in environmental studies of the  
67 microbial sulfur cycle. After having been the subject of several studies in the late 1980s,  
68 particularly focused on sedimentary ecosystems, it was then relatively poorly studied. In  
69 recent years, the study of this process has been revived, with the isolation of several new  
70 taxa, notably thermophilic ones, and with ecological and genomic studies in order to try to  
71 decipher it [1-5]. Since the discovery of this metabolism in 1987, its pathways have not been  
72 fully described, although it appears to proceed in part through a reverse pathway of the  
73 sulfate reduction path in some species [1,3,6,7]. The molecular markers of these pathways  
74 remain either putative, or they are enzymes common to the dissimilatory sulfate reduction  
75 pathway. A recent study inferred that a YDT gene cluster composed by yeddE, dsrE and Tusa  
76 related genes followed by hypothetical genes could be genomic markers of sulfur  
77 disproportionation [5]. However, the first steps of the elemental sulfur dismutation, in  
78 particular, is still completely unknown. In the current state of knowledge, it seems that it  
79 might exist several disproportionation pathways of sulfur inorganic compounds  
80 disproportionation [3]. To date, the share of sulfur dismutation in total sulfur geochemical  
81 cycle in various habitats compared to sulfur oxidation and sulfate reduction is not known  
82 because dismutation is confounded with these pathways in global budgets, since it leads to  
83 the production of sulfates and sulfides [1]. The geographical distribution of the niches where  
84 this process takes place and the abundance of sulfur-disproportionating taxa in natural

85 habitats is not known either, notably because of the lack of molecular markers to study it. Yet,  
86 it would be important to address all these issues. The genus *Thermosulfurimonas* was  
87 described relatively recently and was the first thermophilic microbial genus whose ability to  
88 disproportionate inorganic sulfur compounds has been reported [8]. The first species,  
89 *Thermosulfurimonas dismutans* S95<sup>T</sup> (NCBI:txid999894) was isolated from a deep-sea  
90 hydrothermal vent. It originates from a hydrothermal chimney from the Mariner  
91 hydrothermal field located on the Eastern Lau Spreading Center, in the Pacific Ocean, at a  
92 depth of 1910 m [8]. It grows at the optimum temperature of 74°C and a pH of 7.0. A second  
93 species was subsequently isolated from a shallow hydrothermal vent Sea of Okhotsk, located  
94 at 12 m water depth, and named *Thermosulfurimonas marina* SU872<sup>T</sup> (NCBI:txid2047767) [9].  
95 *T. marina* grows at an optimal temperature of 74°C and a pH of 6.7-7.0. These two types of  
96 environments where the genus *Thermosulfurimonas* is present, are characterized by  
97 physicochemical conditions that have similarities and differences. Both deep and shallow  
98 hydrothermal vents exhibit strong gradients in temperature, pH and chemical species in the  
99 mixing zones between the hot, reduced hydrothermal fluid and the cold, oxygenated sea  
100 water. Being located at low depth, in the photic zone, shallow hydrothermal vents allow both  
101 chemotrophic and phototroph primary producer to grow [10,11]. While being located at  
102 greater depth, deep sea hydrothermal vents are characterized by darkness, high pressures  
103 and so primary production is performed by only chemolithoautotrophic microorganisms [12].  
104 The physiology and genomic potential of these two *Thermosulfurimonas* species have been  
105 studied previously [8,9,13,14]. Both have small genomes and are able to grow by  
106 disproportionation of inorganic sulfur compounds and by dissimilatory nitrate reduction to  
107 ammonium (DNRA) [9,15]. *T. dismutans* draft genome was assembled from 61 contigs  
108 (ASM165258v1), it is 2,119,932 bp in size, with a GC content of 50.12%, 2,201 CDS and 48  
109 tRNAs genes. *T. marina* complete genome is 1,763,258 bp, with a GC content of 58.90%, 1,827  
110 CDS and 47 tRNAs genes and consist in of one circular chromosome (ASM1231758v1).  
111 Currently, genomic studies are powerful methods for studying sulfur-disproportionating  
112 microorganisms that are particularly difficult to grow. Here, we report the isolation,  
113 sequencing, assembly, taxonomic classification, and annotation of the genome of a new  
114 species of *Thermosulfurimonas* genus *Thermosulfurimonas* strain F29. Its genome was  
115 compared then to those of *T. dismutans*, *T. marina* and various members of the class



116 *Thermodesulfobacteriaceae* and other marine sulfur-disproportionators. These investigations  
117 were performed in order (i) to explore the genetic potential of a new species of  
118 *Thermosulfurimonas*, , its phylotaxonomic position and its putative metabolism, (ii) to  
119 contribute to a better knowledge of the genus *Thermosulfurimonas*, which is one of a  
120 relatively undocumented branches of life because it was recently discovered, and (iii) to  
121 improve understanding of the gens and enzymes involved in of sulfur compound dismutation  
122 pathways in order to be able to identify genomic markers that can be deployed in subsequent  
123 ecological studies.

124

## 125 **METHODS**

126

### 127 **Sampling**

128

129 A hydrothermal sulfide chimney sample, from which strain F29 was derived, was collected,  
130 during the MoMARSAT 2019 oceanographic cruise (June-July 2019) [16] from the Capelinhos  
131 site (37.289167 N 32.263889 W), located 1.5 km east of the Lucky Strike lava lake at a depth  
132 of 1672 m [17]. It was collected with the clamp of the *Nautilie* submersible, sample was  
133 brought to the surface into a decontaminated insulated box as described elsewhere [18], and  
134 referenced as M19Cap2 (PL1945-7). Once onboard, the sample was ground in a sterile mortar  
135 inside an anaerobic chamber under a N<sub>2</sub>/H<sub>2</sub> (90/10%) gas atmosphere to homogenize it, and  
136 then stored into Schott flasks under anaerobic conditions. Samples were stored at 4°C until  
137 subsequent use for enrichment culture.

138

### 139 **Culture conditions, strain isolation and physiological experiments**

140

141 Cultures were carried out in a sulfur disproportionation medium and according to the  
142 procedure described elsewhere [19]. Incubations were carried out in the mineral medium  
143 containing 90 mM ferrihydrite, at pH 6.5-7.0, at 60°C, with 5 g L<sup>-1</sup> of elemental sulfur and  
144 under a gas phase 100% CO<sub>2</sub> (1 bar relative pressure). The initial enrichment culture was  
145 performed by inoculating the medium with 10% (v/v) of chimney fragments suspended in  
146 artificial seawater. Then, three sub-cultures were performed, followed by serial dilutions to

147 1/10. The isolate was then cultivated at 70°C as growth was observed to be better than at  
148 60°C. In addition, to confirm that the isolate was able to grow by S<sup>0</sup> disproportionation, sulfate  
149 production was investigated and measured by ion chromatography using a Dionex ICS-900  
150 Ion Chromatography System (Dionex, Camberley, UK) equipped with an IonPac CS16 column  
151 maintained at 60°C in an UltiMate™3000 Thermostated Column Compartment (Thermo  
152 Scientific, Waltham, MA, USA), as described elsewhere [20]. In addition, three successive  
153 cultures of the isolate were performed in the absence of ferrihydrite, on which the production  
154 of both sulfate and H<sub>2</sub>S has been measured by a colorimetric test described elsewhere [21],  
155 and which were characterized by lower growth and biomass [1,3]. For genomic DNA  
156 extraction, the strain was cultivated anaerobically at 70°C, with elemental sulfur as an  
157 electron donor and acceptor and CO<sub>2</sub> as sole carbon source in gaseous phase.

158 The ability of the isolate to grow by sulfate reduction was investigated at 70°C, in triplicate,  
159 on the same medium but prepared with 20 mM of sodium sulfate, in the absence of sulfur  
160 and ferrihydrite, and reduced with 1 mM Na<sub>2</sub>S. 9H<sub>2</sub>O. These cultures were incubated with H<sub>2</sub>  
161 as an electron donor, and CO<sub>2</sub> as a carbon source (H<sub>2</sub>/CO<sub>2</sub>; 80/20%; 1 bar relative pressure  
162 gas phase).

163

#### 164 **Genome sequencing and assembly**

165

166 Cells were harvested in the late exponential phase of growth. Genomic DNA was extracted  
167 using a standard PCI DNA extraction protocol, coupled to dithionite addition to fully reduce  
168 the ferrihydrite which can affect the DNA extraction [22]. In order to identify and test the  
169 purity of the strain, the 16S rRNA genes were amplified from genomic DNA by PCR using  
170 BAC8F and 1492Runi 16S rRNA gene universal bacterial primers (1492Runi: 5'-  
171 CGGTTACCTTGTTACGACTT-3'; Bac8F: 5'-AGAGTTTGATCATGGCTCAG-3'). Sanger sequencing  
172 was then performed on the amplified sequences, and sequences were compared to the NCBI  
173 nucleotide collection. In addition, the 16S rRNA gene sequence was also extracted from the  
174 total genome assembly using the barnap module of Prokka (v1.14.6 -  
175 <https://github.com/tseemann/prokka>), for a better accuracy and to get full length 16 rRNA  
176 gene sequence [23]. Short read DNA sequencing was performed by Fasteris SA (Plan-les-  
177 Ouates, Switzerland) using the Illumina nanoMiSeq technology (2 × 150 bp paired-reads, Nano

178 V2 chemistry). Post-quality controls were performed by sequencing facilities and checked also  
179 with FastQC (v0.11.8 - <https://www.bioinformatics.babraham.ac.uk/projects/fastqc/>). Short  
180 reads were filtered with fastp (v0.20.1 - <https://github.com/OpenGene/fastp>) [24]. A long  
181 read additional DNA sequencing was performed with a MinIon (Oxford Nanopore) with the  
182 rapid sequencing kit (SQK-RAD004) and a R9.4.1 Flow Cell. Genome was assembled into  
183 contigs by using the Unicycler pipeline for *de novo* assembly (version: 0.4.9 -  
184 <https://github.com/rrwick/Unicycler>), and its dependencies (spades.py v3.13.0 ; makeblastdb  
185 v2.12.0+ ; tblastn v2.12.0+ ; bowtie2-build v2.4.4 ; bowtie2 v2.4.4 ; samtools v1.13 ; java  
186 v15.0.1 ; pilon v1.23) with “bold” parameter [25]. Genome assembly statistics were obtained  
187 with Quast (v5.0.2; <https://github.com/ablab/quast>) and used to compare different  
188 assemblies. Genome assembly visualization was plotted with Bandage (v0.8.1 -  
189 <http://rrwick.github.io/Bandage/>) in order to detect potential plasmids from obtained contigs  
190 and afterwards checked with viralVerify python script which predict plasmid and virus  
191 sequences (<https://github.com/ablab/viralVerify>) based on HMMs [26,27]. Genome  
192 completeness and potential contamination were controlled with CheckM (v1.1.2 -  
193 <https://ecogenomics.github.io/CheckM/>), and whole genome average coverage was  
194 calculated using BMap (v38.87 - BMap – Bushnell B. – [sourceforge.net/projects/bbmap/](https://sourceforge.net/projects/bbmap/))  
195 against total short reads sequences.

#### 196 **Genomic and taxonomic features**

197 Identification and classification of the CRISPR-Cas systems were performed by using the  
198 CRISPRCas Finder webserver, with default parameters (<https://crisprcas.i2bc.paris-saclay.fr/>)  
199 [28]. The prediction of laterally transferred gene clusters (genomic islands) was performed  
200 with the IslandViewer4 webserver (<http://www.pathogenomics.sfu.ca/islandviewer/>) based  
201 on a GenBank file generated by Prokka against *Thermosulfurimonas marina* genome  
202 reference, and IslandPath-DIMOB and SIGI-HMM predictions were taken in account [29]. To  
203 study the taxonomic position of the strain, 16S rRNA gene sequence was first compared to  
204 the NCBI nucleotide collection. Pairwise 16S rRNA gene sequence similarity was then  
205 determined using the EzTaxon-e server (<https://www.ezbiocloud.net/>) [30]. Estimated *in*  
206 *silico* DNA–DNA hybridization (DDH) values with the genomes of *T. dismutans* and *T. marina*  
207 were also determined using the Genome-to-Genome Distance Calculator (GGDC 2.1) using

208 formula 2 (<http://ggdc.dsmz.de/home.php>) [31]. For a more accurate classification, average  
209 nucleotide identity (ANI) and average amino acid identity (AAI) scores were also calculated,  
210 using default parameters of the software. OrthoANlu scores were calculated against the  
211 genomes of *Thermosulfurimonas dismutans* (ASM165258v1) and *Thermosulfurimonas marina*  
212 (ASM1231758v1), using the ANI calculator tool provided by the EzBioCloud web server  
213 (<https://www.ezbiocloud.net/tools/ani>) [32,33]. Average amino acid identity was calculated  
214 using the AAI calculator of the Enveomics collection (<http://enve-omics.ce.gatech.edu/>) with  
215 Prokka output [34]. We considered the following thresholds for classification: for 16S rRNA  
216 sequences, identity <98.7% for a new species and <94.5% for a new genus [35,36]. For digital  
217 DDH, score <70% for a new species [37]. For ANI, score <94–96% for a new species [38], and  
218 <70.85–76.56% for a new genus with alignment fraction [39]. For AAI, scores comprised 95  
219 and 100% for a same species, and between 65 and 95% for a same genus [40].

#### 220 **Genome annotation**

221 Genome was analyzed and annotated with the fast annotation software Prokka, the  
222 MicroScope Microbial Genome Annotation, Analysis Platform (MaGe)  
223 (<https://mage.genoscope.cns.fr/microscope/home/index.php>), using KEGG and BioCyc  
224 databases, the NCBI integrated PGAP pipeline, and RAST server (v2.0 -  
225 <https://rast.nmpdr.org/>), with default parameters and databases for all of the four  
226 software/pipelines [23,41-43]. Functional annotation of predicted CDSs was further blasted  
227 with UniProtKB + Swiss-Prot database (release 2021\_09). Hydrogenase classification has been  
228 checked using the HydDB webtool (<https://services.birc.au.dk/hyddb/>). All dsr genes were  
229 extracted and analyzed with the DiSCo perl script (v.1.0.0, [https://github.com/Genome-](https://github.com/Genome-Evolution-and-Ecology-Group-GEEG/DiSCo)  
230 [Evolution-and-Ecology-Group-GEEG/DiSCo](https://github.com/Genome-Evolution-and-Ecology-Group-GEEG/DiSCo)) from Prokka protein output sequences [44].

#### 231 **Comparative genomics**

232 The genome of the novel isolate was compared by subtractive comparative genomics, first  
233 with the genomes of *Thermosulfurimonas marina* SU872<sup>T</sup> (ASM1231758v1) and  
234 *Thermosulfurimonas dismutans* S95<sup>T</sup> (ASM165258v1), and second, to various genomes of  
235 sulfur-disproportionating taxa, and representatives of the *Thermodesulfobacteriaceae* family,  
236 as described a little below. The MaGe platform Pan-genome Analysis tool

237 (<https://mage.genoscope.cns.fr/microscope/home/index.php>) was used for comparative  
238 genomics, based on the clustering algorithm SiLiX (<http://lbbe.univ-lyon1.fr/-SiLiX-.html>).  
239 Genomic CDSs were clustered by 80% amino-acid identity and 80% amino-acid alignment  
240 coverage, with permissive parameters, for comparative genomic analyses performed  
241 between *Thermosulfurimonas* species and *Thermodesulfobacteriaceae* taxa and clustered by  
242 50% amino-acid identity and 80% amino-acid alignment coverage for the analyses aiming to  
243 decipher sulfur disproportionation pathways, because compared genomes belong to more  
244 phylogenetically distant taxa. In order to identify genes unique to *Thermosulfurimonas*  
245 species within the *Thermodesulfobacteriaceae* family, genomes of strain F29, *T. dismutans*  
246 and *T. marina* were compared with the exclusion of the available genomes of 10 other  
247 *Thermodesulfobacteriaceae*: *Caldimicrobium thiodismutans* TF1<sup>T</sup> (ASM154827v1),  
248 *Thermodesulfatator atlanticus* DSM 21156<sup>T</sup> (ASM42158v1), *Thermodesulfatator*  
249 *autotrophicus* S606<sup>T</sup> (ASM164232v1), *Thermodesulfatator indicus* DSM 15286<sup>T</sup>  
250 (ASM21779v1), *Thermodesulfobacterium geofontis* OPF15<sup>T</sup> (ASM21597v1),  
251 *Thermodesulfobacterium thermophilum* DSM 1276<sup>T</sup> (ASM42160v1), *Thermodesulfobacterium*  
252 *commune* DSM 2178<sup>T</sup> (ASM73401v1), *Thermodesulfobacterium hydrogeniphilum* DSM 14290<sup>T</sup>  
253 (ASM74625v1), *Thermodesulfobacterium hveragerdense* DSM 12571<sup>T</sup> (ASM42384v1), and  
254 *Thermosulfuriphilus ammonigenes* ST65<sup>T</sup> (ASM1120745v1). Afterwards, to identify putative  
255 genes associated to the sulfur disproportionation ability, the following genomes of marine  
256 hydrothermal sulfur-disproportionators were compared: strain F29, *T. dismutans*, *T. marina*,  
257 *T. ammonigenes*, *Dissulfuribacter thermophilus* S69<sup>T</sup> (ASM168733v1), and *Dissulfurirhabdus*  
258 *thermomarina* SH388<sup>T</sup> (ASM1297923v1). This analysis was performed by excluding the  
259 genomes of the following hydrothermal bacteria that are unable to disproportionate  
260 inorganic sulfur compounds: *Caminicella sporogenes* DSM 14501<sup>T</sup> (GCA\_900142285.1), an  
261 anaerobic, strictly chemoorganoheterotrophic bacterium, and *Thermodesulfatator indicus*  
262 DSM 15286<sup>T</sup>, able to grow by sulfate reduction but unable to grow by sulfur  
263 disproportionation nor by sulfur, thiosulfate and sulfite reduction, confirmed by culture. Two  
264 of the CDSs were subjected to subcellular localization prediction with the BUSCA server  
265 (<http://busca.biocomp.unibo.it/>) [45]. CDSs were then compared to the UniprotKB database,  
266 and all CDSs coding for hypothetical proteins were analyzed with the InterProScan webserver  
267 (<https://www.ebi.ac.uk/interpro/>) to perform functional predictions. Molybdopterin subunits

268 and chaperon sequences microsynteny was then analyzed and plotted with SimpleSynteny  
269 (<https://www.dveltri.com/simplesynteny/>) from the genomes of strain 29, *T. dismutans*, *T.*  
270 *marina*, *T. ammonigenes*, *D. thermophilus*, and *D. thermomarina* against the three following  
271 predicted protein sequences of strain 29 [46]. Protein sequences homologies between strains  
272 were calculated with Clustal Omega (<https://www.ebi.ac.uk/Tools/msa/clustalo/>).

## 273 RESULTS AND DISCUSSION

### 274 General genomic properties, genomic plasticity and taxonomy

275

276 Although hybrid sequencing was performed, only a draft genome could be reconstructed. The  
277 assembled genome of strain F29 consisted of 9 contigs, including 4 contigs of less than 5000  
278 bp, with an overall size of 2,345,565 bp and a G+C content of 58.09%. The longest contig was  
279 889,860 bp, the N50 was 737,680 bp and the L50 was 2. CheckM estimated the genome to be  
280 99.18% complete based on the presence of default single-copy marker genes (2 markers were  
281 missing), with 1.85% contamination (5 markers were duplicated) and a coding density of  
282 about 93.3%. The average genome coverage was around 76.4× according to raw pair read  
283 sequences from MiSeq sequencing data. In addition, hybrid sequencing allowed the detection  
284 of two or more putative plasmidic contigs, including one circular, observed with Bandage and  
285 confirmed by applying the viralVerify script to all contigs. The first putative plasmid (p1) was  
286 145,269 bp (contig 4) in size; the second one was a non-putative circularized plasmid (p2) of  
287 69,636 bp in size (contig 5). In addition, contigs 6 (1,354 bp), 7 (1,341 bp), 8 (1,177 bp) and 9  
288 (788 bp) were smaller and then uncertain to be chromosomal or plasmidic. Contig 4, named  
289 p1, was relatively long and could not be circularized and it is therefore not possible to state  
290 with certainty that it is a plasmid. The median size of known prokaryotic plasmids is 53,212  
291 bp according to the PLSDB database (<https://ccb-microbe.cs.uni-saarland.de/plsdb/>) but  
292 unknown within the class *Thermodesulfobacteria*, as no plasmids have been reported so far  
293 in any bacteria of this class. p2, and possibly p1, are thus the first reported plasmids in the  
294 genus *Thermosulfurimonas* and possibly in the *Thermodesulfobacteria* class. Contigs 6, 7, 8,  
295 and 9 were treated as chromosomal for analysis although their small size did not indicate  
296 whether they correspond to chromosomal or plasmid sequences. No viral sequences were  
297 detected in the genome. As not reported in previous studies, we also searched for plasmids

298 in *T. dismutans* genome and found two putative plasmid contigs (NZ\_LWLG01000026.1;  
299 NZ\_LWLG01000030.1) and other uncertain contigs. *Thermosulfurimonas* species from deep-  
300 sea hydrothermal vents thus appear to possess a plasmid diversity not revealed so far and  
301 carrying functions not studied to date. Annotation of the genome with Prokka resulted in the  
302 prediction of 2,348 CDSs in total, comprising 148 CDSs on p1 and 57 CDSs on p2. From MaGe,  
303 a total of 2,557 genomic objects including 2,463 CDS were found, and with PGAP, 2,400 genes  
304 including 2,345 CDSs were found. p1 carried few genes associated with DNA replication and  
305 a majority of sequences coding for hypothetical proteins (127/148 CDS), while p2 carried  
306 genes associated with type II secretion system, some carbohydrate-associated enzyme  
307 sequences, and a large majority of hypothetical protein sequences. The genome also  
308 contained one operon of 5S-16S-23S rRNA genes. We detected 48 tRNA with MaGe, and 49  
309 with PGAP which use the tRNA scan-SE RNA finder ([http://lowelab.ucsc.edu/tRNAscan-](http://lowelab.ucsc.edu/tRNAscan-SE/index.html)  
310 [SE/index.html](http://lowelab.ucsc.edu/tRNAscan-SE/index.html)), while 51 tRNA were detected with Prokka based on ARAGORN RNA finder  
311 (<http://130.235.244.92/ARAGORN/>). The 20 tRNAs associated with the essential amino acids  
312 were each encoded by at least one sequence. Furthermore, 8 potential CRISPR and 2 potential  
313 Cas cluster loci were found using the CRISPRCasFinder server. The CRISPR sequences  
314 consisted of four low evidence CRISPR loci containing 1 or 2 spacers and four high evidence  
315 CRISPR loci, with 8 spacers for 5'-GTTTGTAGTCCCTATAAGGGTTGAGAAG-3' sequence, 12  
316 spacers for 5'-GTCGCAATCCCTTATTCGTGAGGGAAAGTTTTCTCAC-3' sequence, 17 spacers for  
317 5'-GTTTGTAGTCCCTATAAGGGTTGAGAAG-3' sequence, and 38 spacers for 5'-  
318 GTTCCATTCCTCATAGGTAGGCTCGAAAC-3' sequence. Moreover, two Cas cluster loci were  
319 found, one Cas Type IIIB cluster of 9 genes and one Cas Type IB cluster of 8 genes. The  
320 presence of this large number of CRISPRs could indicate that the new isolate is undergoing  
321 various genomic transfers and is setting up defense mechanisms against invasions by  
322 bacteriophages and plasmids from its environment [47]. Several regions of genomic plasticity  
323 were identified with the IslandViewer4 webserver, by using the genome of *T. marina* as a  
324 reference genome. These 16 putative genomic islands (GI), 2 of which were present on  
325 plasmids, exhibited different lengths. There were two big GI of about 85 and 120 kbp, and 14  
326 GI of less than 22 kbp. GI were mainly composed of hypothetical proteins, transposases and  
327 several DNA replication related genes. Regarding taxonomy, strain F29 has the highest 16S  
328 rRNA gene sequence identity of 97.97% to *T. marina*, followed by *T. dismutans* with 97.85%.

329 The genome of strain F29 showed an OrthoANlu score of 75.18% (893,612 bp average aligned  
330 length) with the genome of *T. marina* and of 73.20% (789,715 average aligned length) with  
331 the genome of *T. dismutans*, and were far below the standard threshold level of 94-96% for  
332 the delineation of a new genomic species [38]. The digital DDH (dDDH) scores between the  
333 genome of strain F29 and those of *T. marina* and *T. dismutans* were respectively, 18.90% and  
334 19.30%, well below the threshold level (70%) for a new species delineation [37]. Finally, the  
335 AAI scores between the genome of the novel isolate and the ones of *T. marina* and *T.*  
336 *dismutans* were respectively 75.16% (from 1626 proteins; SD: 13.74%) and 73.62% (from 1675  
337 proteins; SD: 14.70%). Overall, all these genomic relatedness indices indicate that strain F29  
338 represents a new genomic species of the genus *Thermosulfurimonas*.

339

#### 340 **Central metabolism and energy production pathways**

341

342 The gene locus tags associated to the genome assembly annotation given in GenBank and  
343 RefSeq (ASM1968873v1) are reported in supplementary material S1.1. From a general  
344 metabolic point of view, strain F29 showed very similar metabolic profiles to other members  
345 of the genus *Thermosulfurimonas*, *T. dismutans* and *T. marina*, on the MaGe platform.

346

#### 347 *Carbon metabolism*

348

349 Consistent with the autotrophic growth ability of strain F29, the genome encodes a complete  
350 Wood–Ljungdahl (acetyl-CoA-reductive) pathway for CO<sub>2</sub> fixation, including a formate-  
351 tetrahydrofolate ligase, a methylenetetrahydrofolate dehydrogenase/cyclohydrolase, a  
352 methylenetetrahydrofolate reductase, a methyltetrahydrofolate:corrinoid iron–sulfur  
353 protein methyltransferase, and a CO dehydrogenase/acetyl CoA synthase complex. As in *T.*  
354 *dismutans* and *T. marina*, all these genes are arranged in one gene cluster. Key enzymes from  
355 other known autotrophic carbon fixation pathways, such as the reverse tricarboxylic acid  
356 cycle and the Calvin–Benson pathways have not been identified. Conversion of acetyl-CoA  
357 formed during CO<sub>2</sub> fixation to pyruvate can be performed by the pyruvate:ferredoxin  
358 oxidoreductase encoded by the *porABDG* genes. The genome of strain F29 encodes the  
359 complete Embden-Meyerhof pathway of glucose catabolism, which apparently operates in



360 reverse direction, towards gluconeogenesis. Consistently, the genome of strain F29 does not  
361 code for the pyruvate kinase, the enzyme that catalyzes the irreversible reactions of  
362 glycolysis. In contrast, this gene is present in the genomes of *T. dismutans* and *T. marina*.  
363 Strain F29 also has genes encoding enzymes that specifically catalyze reverse glycolysis  
364 reactions: phosphoenolpyruvate synthase and fructose-1,6-bisphosphatase. In addition,  
365 strain F29 possesses the genes for ribulose-5-phosphate 4-epimerase, ribose-5-phosphate  
366 isomerase and ribose-phosphate pyrophosphokinase that may also be involved in glucose  
367 synthesis. Strain F29 may not be able to utilize organic substrates because its genome  
368 encodes an incomplete tricarboxylic acid cycle (TCA), as evidenced by the absence of genes  
369 coding for the key enzyme of this pathway, citrate synthase, as well as genes for succinyl-CoA  
370 synthetase and succinate dehydrogenase.

371

#### 372 *Nitrogen metabolism*

373

374 Such as *T. dismutans* and *T. marina*, strain F29 possesses a gene cluster encoding proteins  
375 involved in nitrogen fixation. These include the nitrogenase (molybdenum-iron type; EC:  
376 1.18.6.1), proteins related to nitrogenase cofactors, nitrogen regulatory proteins and  
377 ammonium transporter. Genome of *Thermosulfurimonas* F29 hold genes *nap* *MADGH*  
378 encoding a periplasmic Nap-type nitrate reductase. Phylogenetic analysis of the catalytic  
379 subunit NapA of strain F29 placed it, together with two other species of the genus  
380 *Thermosulfurimonas*, in a clade formed mainly by NapA proteins of representatives of the class  
381 *Thermodesulfobacteria*, phylum *Desulfobacterota* (Figure 1). This clade also includes nitrate  
382 reductases of the closest neighbor, *Dissulfuribacter thermophilus*, and distantly related  
383 *Thermosulfidibacter takaii*. *D. thermophilus* belongs to class *Dissulfuribacteria* of the same  
384 phylum (*Desulfobacterota*). *T. takaii* belongs to another phylum, *Aquificae* (NCBI taxonomy)  
385 or *Thermosulfidibacterota* (GTDB taxonomy). Denitrification enzyme genes were absent in the  
386 genome of *Thermosulfurimonas* F29. The genome encoded NrfCD and NrfH proteins of the  
387 Nrf system of nitrite reduction to ammonia. However, the catalytic subunit NrfA (pentaheme  
388 cytochrome c nitrite reductase) was missing, indicating that the nitrite reduction to ammonia  
389 could not proceed *via* canonic Nrf system. The genomes of *T. dismutans* and *D. thermophilus*  
390 have been shown to have an 11 gene cluster consisting of nitrate reductase subunit genes

391 and other genes relevant to energy metabolism. It has been suggested that this  
392 oxidoreductase complex may be coupled to nitrite reduction [15,17]. We have found very  
393 similar gene clusters in *T. marina* and strain F29. In strain F29, the nitrate reductase genes  
394 (*nap MADGH*) are followed by the genes encoding two multiheme c-type cytochromes, the  
395 periplasmic iron–sulfur protein similar to subunit B of tetrathionate reductases and the  
396 membrane anchor protein of the NrfD family. In genomes of *T. takaii*, *Thermosulfuriphilus*  
397 *ammonigenes* and species of the genus *Thermodesulfatator*, *nap* genes are not part of such a  
398 cluster. It has been demonstrated *in vitro* for *Nautilia profundicola* that the conversion of  
399 nitrite to ammonium may proceed *via* a non-canonical mode, potentially through the  
400 production of hydroxylamine [48]. This pathway is not completely encoded in the strain F29  
401 as well as in *T. dismutans* and *T. marina*, although some genes of this pathway are present,  
402 namely hydroxylamine reductase and hydroxylamine oxidoreductase. Finally, three  
403 ammonium transporters were found in the genome of the strain F29. It indicates that it is  
404 probable that strain F29 participate to nitrogen cycle by reducing available nitrate and then  
405 perform DNRA metabolism, associated to a higher energy yield than sulfur  
406 disproportionation.

407

#### 408 *Sulfur metabolism*

409

410 For sulfur metabolism, we found all the key enzymes associated to the sulfate reduction  
411 pathway, sulfate adenylyltransferase, adenylylsulfate reductase subunit alpha and beta,  
412 sulfite reductase dissimilatory type subunit alpha, beta, gamma and DsrD. Moreover,  
413 complete APS reductase-associated electron transfer complex (QmoABC) and DsrMKJOP  
414 complex were found. A DsrT associated sequence was found, but no DsrL. Strain F29 was  
415 tested for sulfate reduction with dihydrogen as an electron donor but it was not able to grow.  
416 This is another case of bacterium that possesses the entire sulfate reduction pathway but is  
417 not able to grow by sulfate reduction, at least with hydrogen as an energy source, but can  
418 nevertheless grow by sulfur disproportionation, as reported previously [3,14,49,50]. One A  
419 subunit of tetrathionate reductase was found and three B subunits, however distant from the  
420 A subunit in the genome. A YDT gene cluster was found, as described with a YedE family  
421 protein, a sulfurtransferase TusA, a putative DrsE domain-containing protein and two

422 hypothetical proteins [5]. However, this YDT gene cluster seems unlikely to be a genomic  
423 marker of sulfur disproportionation, as this gene cluster is also present in the genome of  
424 *Thermodesulfatator indicus*, a strain that we have not been able to grow in the laboratory by  
425 disproportionation of thiosulfate, sulfite or  $S^0$ . Nevertheless, this gene cluster could be  
426 somehow indirectly linked, to the dismutation of inorganic sulfur compounds. Furthermore,  
427 three CDSs with no clear functional predictions but annotated as thiosulfate/tetrathionate  
428 reductase molybdopterin A and B subunits and, a TorD/DmsD chaperone, which could be  
429 related to sulfide oxidation according to previous studies, were also found [49,51]. These  
430 proteins could be associated with the sulfur disproportionation pathway. In addition, no  
431 rhodanese-like sulfurtransferases sequences were found in the genome of strain F29. From  
432 these results and the cultivation results, we can propose that strain F29 participates in the  
433 sulfur cycle of hydrothermal vents through its ability to disproportionate elemental sulfur,  
434 possibly sulfite but unlikely thiosulfate due to the absence of associated genes.

435

#### 436 *Hydrogen metabolism*

437

438 Two large hydrogenases subunits in the genome of strain F29 were confirmed with HydDB;  
439 one [NiFe] Group 1a and one [NiFe] Group 1c. For Group 1a [NiFe] hydrogenase, both large  
440 and small subunits were found. For Group 1c [NiFe] hydrogenase, both large and small  
441 subunits were identified as well as an iron/sulfur subunit associated with the catalytic site,  
442 and four hydrogenase factors (HypA, HypB, HypC, and HypD). This structure differs from what  
443 is reported about Group 1c (HupD, HybE, HypA, HypC) which was mainly described on the  
444 basis of *Gammaproteobacteria* hydrogenases but no transmembrane protein was found  
445 (HybB). All these results indicate that strain F29 has the genetic potential to grow by hydrogen  
446 oxidation, but no growth with  $H_2$  as an electron donor and sulfate as an electron acceptor was  
447 observed. Several hypotheses can be stated to explain this: (i) the strain may be able to oxidize  
448 hydrogen using another electron acceptor than sulfate; (ii) the optimal growth conditions in  
449 terms of temperature might be significantly different between sulfur disproportionation and  
450 hydrogen oxidation coupled with sulfate reduction, as demonstrated for the hydrothermal  
451 strain *Persephonella atlantica*, which preferably uses different redox couples depending on  
452 the temperature [52]. (iii) Both hydrogenases, predicted to be periplasmic or cytosolic and to

453 have FeS clusters, might act as electron bifurcators, coupling exergonic and endergonic  
454 oxidation-reduction reactions to balance electron flow in metabolism and minimize free  
455 energy loss, as already described elsewhere in other metabolic pathways [53-55]. Considering  
456 the lack of knowledge of the dismutation pathways of inorganic sulfur compounds, it cannot  
457 be excluded that the identified hydrogenase-like proteins may be involved in the bifurcation  
458 of electrons. Based on this hypothesis, hydrogenases were searched for and found in the  
459 genome of *Thermosulfuriphilus ammonigenes* and *Thermosulfurimonas marina*, two  
460 phylogenetically related bacteria capable of disproportionating sulfur but unable to use  
461 dihydrogen as an electron donor. Hydrogenases had not been previously searched for in these  
462 genomes because of the inability of these strains to grow by hydrogen oxidation [14,50]. Both  
463 genomes contain operons coding for hydrogenases. The genome of *T. marina* encodes a  
464 group 1c [NiFe] hydrogenase and a group 3c [NiFe] hydrogenase which are closely located on  
465 the genome (WP\_168719511 to WP\_168719521). The genome of *T. ammonigenes*, like that  
466 of strain F29, has a group 1a [NiFe] hydrogenase (WP\_166031792 to WP\_166031793) and a  
467 group 1c [NiFe] hydrogenase (WP\_166031912 to WP\_166031919). In addition, other  
468 thermophilic sulfur-disproportionators from hydrothermal vents, *Thermosulfurimonas*  
469 *dismutans* and *Dissulfurirhabdus thermomarina* have group 1c [NiFe] hydrogenases, but are  
470 able to use H<sub>2</sub> as an electron donor [13,49]. Therefore, the role of hydrogenases in strain F29  
471 is not elucidated and may be subject to functional analysis in the future to determine whether  
472 these proteins are involved in hydrogen oxidation or in electron transfer and bifurcation.

473

#### 474 **Comparative genomics**

475

476 Comparison of the genomes of the three species of the genus *Thermosulfurimonas*, showed  
477 that a very high number of CDSs are shared. Thus, 368 CDSs are shared (Figure 2) between  
478 the genomes of *T. dismutans*, *T. marina* and strain F29 (XXX). These numerous shared genes  
479 were associated with several metabolisms: energy, carbon, sulfur, nitrogen, cell mobility,  
480 stress resistance, membrane and transport proteins, nucleic acids, amino acids, proteins,  
481 vitamins and cofactors associated metabolisms, and conserved proteins with unknown  
482 functions. These three strains have the genetic potential to perform reduction or oxidation of  
483 inorganic sulfur compounds, potential reduction of nitrate, hydrogen oxidation, reduction of

484 carbon monoxide, reduction of tetrathionate and carbon fixation by the Wood-Ljungdahl  
485 pathway. Most of these properties have been experimentally confirmed for *T. marina* and *T.*  
486 *dismutans* by physiological experiments [8,9]. However, comparative genomic approaches  
487 provide only predictions of functional potentials. Thus, although *T. dismutans* and *T. marina*  
488 possess the complete sulfate reduction pathway, this property has not been demonstrated  
489 experimentally by testing several culture conditions [8,9]. Within *Thermodesulfobacteraceae*,  
490 no complete metabolic pathway is present solely within the genus *Thermosulfurimonas*. In  
491 conclusion, this shows that *Thermosulfurimonas* genes are relatively conserved, associated  
492 with a variety of pathways, regardless of the natural habitat of the bacteria, whether deep or  
493 shallow hydrothermal vents.

494

495 When comparing the six genomes of sulfur-disproportionating strains of marine  
496 hydrothermal origin, we find that they share 8 CDSs (XXX). These 8 CDSs code for: a cation  
497 efflux system protein, a MOSC domain protein (putative molybdenum cofactor sulfurase), a  
498 metallo-beta-lactamase family protein, an uncharacterized DUF1566 domain-containing  
499 protein, a molybdopterin oxidoreductase iron-sulfur subunit B, a molybdopterin  
500 oxidoreductase catalytic subunit A, a formate dehydrogenase subunit alpha and a putative  
501 phosphate-selective porin. The uncharacterized DUF1566 domain-containing protein and the  
502 putative phosphate-selective porin were not associated with any known function by  
503 InterProScan search. Molybdopterin, which contain two different subunits, have a 4Fe-4S di-  
504 cluster domain in the smaller subunit and an oxidoreductase activity in the larger subunit. The  
505 function of the MOSC domain protein may be associated with molybdopterin and was  
506 predicted to be a sulfur-carrier domain that receives sulfur extracted by pyridoxal phosphate-  
507 dependent NifS-like enzymes on its conserved cysteine, and delivers it for formation of  
508 diverse sulfur-metal clusters. Furthermore, by studying the microsynteny of molybdopterin,  
509 it appears that in these 6 genomes, a TorD/DmsD chaperone protein is also present, as  
510 identified in the genome of strain F29 and mentioned above, which could be related to the  
511 assembly of the molybdopterin protein (figure 3). The protein sequences homologies were  
512 higher for respective molybdopterin subunits than chaperone proteins (supplementary  
513 material S1.2.). The cluster of three CDSs, two molybdopterin and a chaperone protein was  
514 probably first stated in the study of Thorup et al. 2017 [51]. In this previous study, it was

515 observed that this gene cluster was more expressed in the sulfur disproportionation condition  
516 than in the DNRA condition. The authors hypothesized that it was related to the oxidation of  
517 sulfide to form elemental sulfur. By hypothesis, the reaction could occur in the opposite  
518 direction and then reduce the elemental sulfur to sulfide. Putative homologs of small and  
519 large subunits of molybdopterins were found among known bacteria capable of  
520 disproportionating sulfur from other environments with prokka, such as *Desulfurella amilsii*,  
521 *Caldimicrobium thiodismutans*, *Desulfocapsa sulfexigens* and *Dissulfurispira thermophila* [56-  
522 59]. However, there is a lack of negative microbial models to support this hypothesis and  
523 improve the comparison, i.e. sulfate reducers tested and confirmed to be unable to grow by  
524 sulfur dismutation.

525 Both subunits of molybdopterin from strain F29 were predicted by BUSCA as non-membrane  
526 and potentially extracellular proteins. The large subunit was predicted to be extracellular  
527 (score: 0.87), with a signal peptide at the beginning of the sequence, and the small subunit  
528 was estimated to be cytosolic (score: 0.7). This localization seems consistent with the  
529 hypotheses of Mardanov et al. 2016 and Florentino et al. 2019 who demonstrated that *T.*  
530 *dismutans* and *D. amilsii*, respectively, can perform elemental sulfur disproportionation  
531 without a direct cell-sulfur contact [13,58]. We can hypothesize in conclusion that this novel  
532 molybdopterin represented by at least one large and one small subunit and a chaperone  
533 protein might be related to the elemental sulfur disproportionation process. These genes are  
534 good candidate genes for sulfur disproportionation but in order to determine the role of the  
535 proteins they code for, it will be necessary to confirm their function and this hypothesis by  
536 functional analyses, with comparative proteomics for example.

537

538 In conclusion, the genome analysis of a new species of the genus *Thermosulfurimonas*, strain  
539 F29, was performed and showed that this strain is almost equidistant from *T. dismutans* and  
540 *T. marina*. This strain has at least one plasmid, which is one of the first plasmid identified  
541 within the class *Thermodesulfobacteria*. This work demonstrates that genomic annotation is  
542 a very interesting approach to predict the putative metabolism of difficult to grow  
543 microorganisms, particularly sulfur disproportionating bacteria, but does not replace  
544 physiological/cultural studies. The new strain F29 grows by sulfur disproportionation and has  
545 the genetic potential to grow by sulfite disproportionation, possible nitrate reduction, sulfate

546 reduction and hydrogen oxidation. A comparative genomics study demonstrated that the  
547 genes were highly conserved within the genus *Thermosulfurimonas* and associated with a  
548 wide range of metabolic pathways. It appears that the enzymes associated with the YDT gene  
549 cluster and especially the rhodanese-like proteins are probably not involved in sulfur  
550 dismutation in the known sulfur-disproportionating taxa of hydrothermal origin that have  
551 been studied here. In contrast, specific molybdopterin-like proteins, consisting of two  
552 subunits and associated with a chaperone protein, may play a role in the disproportionation  
553 reaction, in the bacterial models studied here. Furthermore, we found proteins annotated as  
554 hydrogenases in the genome of strain F29, *T. ammonigenes* and *T. marina* for which the ability  
555 to oxidize hydrogen has not been reported until now. We wonder about the role of these  
556 proteins and whether they might play an indirect role such as energy conservation in the  
557 disproportionation of sulfur. However, it is important to emphasize that these results remain  
558 hypothetical, predictive and are based only on marine hydrothermal genomic models. In  
559 addition, the dismutation of sulfur compounds could proceed through various pathways. In  
560 the future, it will be important to focus the effort to understand sulfur dismutation, based on  
561 more functional methods such as proteomics, enzymology or by employing genetic tools, in  
562 order to understand the whole process and the genes and proteins associated with it.

563

## 564 **Author statements**

### 565 **1.1 Authors and contributors**

566 Conceptualization (M.A, K.A.), Data curation (M.A.), Formal Analysis (M.A., S.Y., K.A., G.S.,  
567 A.S.), Funding acquisition (K.A., M.J., A.S.), Supervision (K.A), Validation (K.A.), Writing –  
568 original draft (M.A, K.A., G.S., A.S.), Review & editing (all co-authors)

569

### 570 **1.2 Conflicts of interest**

571 The author(s) declare that there are no conflicts of interest

572

573

574 **1.3 Funding information**

575 This work was supported by the French-Russian collaborative Project (CNRS/RFBR) Neptune  
576 (PRC Russie 2017 n°281295) to A.S. and M.J., by the Sino-French IRP 1211 MicrobSea to K.A.,  
577 by the ISblue project, Interdisciplinary graduate school for the blue planet(ANR-17-EURE-  
578 0015) and co-funded by a grant from the French government under the program  
579 "Investissements d'Avenir" (Theme 2, project DISMUT) to K.A., and by the Ministry of  
580 Science and Higher Education of the Russian Federation to A.S. and G.S. The study was  
581 supported by a grant from the French Ministry of Higher Education and Research, and from  
582 the Region Bretagne, to MA.

583

584 **1.4 Acknowledgements**

585 We thank the captains and crews of the R/V *Pourquoi pas?* and the Nautilie submersible team  
586 for their efficiency, as well as the chief scientists and scientific parties of the MoMARSAT 2019  
587 [16]. We acknowledge especially Françoise Lesongeur for the sampling and conditioning of  
588 samples, and Erwan Roussel and Xavier Phillippon for gas and ionic chromatography analyses.  
589 The LABGeM (CEA/Genoscope CNRS UMR8030), the France Génomique and French  
590 Bioinformatics Institute national infrastructures (funded as part of Investissement d'Avenir  
591 program managed by Agence Nationale pour la Recherche, contracts ANR-10-INBS-09 and  
592 ANR-11-INBS-0013) are acknowledged for support within the MicroScope annotation  
593 platform.

594

595 **References**

596

597 1. Finster, K. Microbiological disproportionation of inorganic sulfur compounds. *Journal of*  
598 *Sulfur Chemistry* 2008 29, 281–292. <https://doi.org/10.1080/17415990802105770>

599

600 2. Wasmund K, Mußmann M, Loy A. The life sulfuric: microbial ecology of sulfur cycling in  
601 marine sediments. *Environ Microbiol Rep.* 2017 Aug;9(4):323-344. doi: 10.1111/1758-  
602 2229.12538.



- 603 3. Slobodkin, A. I., & Slobodkina, G. B. Diversity of Sulfur-Disproportionating Microorganisms.  
604 *Microbiology*. 2019 88(5), 509-522. <https://doi.org/10.1134/S0026261719050138>  
605
- 606 4. Wu B, Liu F, Fang W, Yang T, Chen GH, He Z, Wang S. Microbial sulfur metabolism and  
607 environmental implications. *Sci Total Environ*. 2021 Jul 15;778:146085. doi:  
608 10.1016/j.scitotenv.2021.146085.
- 609 5. Umezawa K, Kojima H, Kato Y, Fukui M. Disproportionation of inorganic sulfur compounds  
610 by a novel autotrophic bacterium belonging to *Nitrospirota*. *Syst Appl Microbiol*. 2020  
611 Sep;43(5):126110. doi: 10.1016/j.syapm.2020.126110.  
612
- 613 6. Bak F, Cypionka H. A novel type of energy metabolism involving fermentation of inorganic  
614 sulphur compounds. *Nature*. 1987 Apr 30-May 6;326(6116):891-2. doi: 10.1038/326891a0.  
615
- 616 7. Bak, F., Pfennig, N. Chemolithotrophic growth of *Desulfovibrio sulfodismutans* sp. nov. by  
617 disproportionation of inorganic sulfur compounds. *Arch. Microbiol*. 147, 184–189 (1987).  
618 <https://doi.org/10.1007/BF00415282>  
619
- 620 8. Slobodkin AI, Reysenbach AL, Slobodkina GB, Baslerov RV, Kostrikina NA, Wagner ID, Bonch-  
621 Osmolovskaya EA. *Thermosulfurimonas dismutans* gen. nov., sp. nov., an extremely  
622 thermophilic sulfur-disproportionating bacterium from a deep-sea hydrothermal vent. *Int J*  
623 *Syst Evol Microbiol*. 2012 Nov;62(Pt 11):2565-2571. doi: 10.1099/ijs.0.034397-0.  
624
- 625 9. Frolova, AA, Slobodkina, GB, Baslerov, R. V, Novikov, AA, Bonch-Osmolovskaya, EA, &  
626 Slobodkin, AI. *Thermosulfurimonas marina* sp. nov., an Autotrophic Sulfur-Disproportionating  
627 and Nitrate-Reducing Bacterium Isolated from a Shallow-Sea Hydrothermal Vent.  
628 *Microbiology* 2018 Jul 87(4), 502–507. doi:10.1134/S0026261718040082  
629
- 630 10. Tarasov, V. G., Gebruk, A. V, Mironov, A. N., & Moskalev, L. I. Deep-sea and shallow-water  
631 hydrothermal vent communities: Two different phenomena? *Chemical Geology*. 2005 224(1),  
632 5–39. <https://doi.org/10.1016/j.chemgeo.2005.07.021>

- 633 11. Price, R. E., & Giovannelli, D. A Review of the Geochemistry and Microbiology of Marine  
634 Shallow-Water Hydrothermal Vents. *Reference Module in Earth Systems and Environmental*  
635 *Sciences*. 2017. <https://doi.org/10.1016/B978-0-12-409548-9.09523-3>  
636
- 637 12. Dick GJ. The microbiomes of deep-sea hydrothermal vents: distributed globally, shaped  
638 locally. *Nat Rev Microbiol*. 2019 May;17(5):271-283. doi: 10.1038/s41579-019-0160-2.  
639
- 640 13. Mardanov AV, Beletsky AV, Kadnikov VV, Slobodkin AI, Ravin NV. Genome Analysis of  
641 *Thermosulfurimonas dismutans*, the First Thermophilic Sulfur-Disproportionating Bacterium  
642 of the Phylum *Thermodesulfobacteria*. *Front Microbiol*. 2016 Jun 17;7:950. doi:  
643 10.3389/fmicb.2016.00950.  
644
- 645 14. Allieux M, Jebbar M, Slobodkina G, Slobodkin A, Moalic Y, Frolova A, Shao Z, Alain K.  
646 Complete genome sequence of *Thermosulfurimonas marina* SU872T, an anaerobic  
647 thermophilic chemolithoautotrophic bacterium isolated from a shallow marine hydrothermal  
648 vent. *Mar Genomics*. 2021 Feb;55:100800. doi:10.1016/j.margen.2020.100800.  
649
- 650 15. Slobodkina GB, Mardanov AV, Ravin NV, Frolova AA, Chernyh NA, Bonch-Osmolovskaya  
651 EA, Slobodkin AI. Respiratory Ammonification of Nitrate Coupled to Anaerobic Oxidation of  
652 Elemental Sulfur in Deep-Sea Autotrophic Thermophilic Bacteria. *Front Microbiol*. 2017 Jan  
653 30;8:87. doi: 10.3389/fmicb.2017.00087.  
654
- 655 16. Sarradin P.M., Legrand J. (2019) MOMARSAT2019 cruise, RV Pourquoi pas  
656 ?, <https://doi.org/10.17600/18001110>.  
657
- 658 17. Chavagnac, V., Leleu, T., Fontaine, F., Cannat, M., Ceuleneer, G., & Castillo, A. (2018).  
659 Spatial Variations in Vent Chemistry at the Lucky Strike Hydrothermal Field, Mid-Atlantic  
660 Ridge (37°N): Updates for Subseafloor Flow Geometry From the Newly Discovered Capelinhos  
661 Vent. In *Geochemistry, Geophysics, Geosystems* (Vol. 19, Issue 11, pp. 4444–4458). American  
662 Geophysical Union (AGU). <https://doi.org/10.1029/2018gc007765>  
663

- 664 18. Francois D. Dynamique spatiale et temporelle des communautés microbiennes dans les  
665 édifices hydrothermaux actifs / Spatial and temporal dynamics of microbial communities in  
666 active hydrothermal vents. 2021. PhD Thesis, Université de Bretagne Occidentale.  
667 <https://archimer.ifremer.fr/doc/00690/80209/>  
668
- 669 19. Slobodkin AI, Tourova TP, Kuznetsov BB, Kostrikina NA, Chernyh NA, Bonch-Osmolovskaya  
670 EA. *Thermoanaerobacter siderophilus* sp. nov., a novel dissimilatory Fe(III)-reducing,  
671 anaerobic, thermophilic bacterium. *Int J Syst Bacteriol*. 1999 Oct;49 Pt 4:1471-8. doi:  
672 10.1099/00207713-49-4-1471.  
673
- 674 20. Webster G, Rinna J, Roussel EG, Fry JC, Weightman AJ, Parkes RJ. Prokaryotic functional  
675 diversity in different biogeochemical depth zones in tidal sediments of the Severn Estuary,  
676 UK, revealed by stable-isotope probing. *FEMS Microbiol Ecol*. 2010 May;72(2):179-97. doi:  
677 10.1111/j.1574-6941.2010.00848.x.  
678
- 679 21. Cord-Ruwisch R. A quick method for the determination of dissolved and precipitated  
680 sulfides in cultures of sulfate-reducing bacteria. *Journal of Microbiological Methods*. 1985,  
681 Volume 4, Issue 1, [https://doi.org/10.1016/0167-7012\(85\)90005-3](https://doi.org/10.1016/0167-7012(85)90005-3)  
682
- 683 22. Thamdrup B, Finster K, Hansen JW, Bak F. Bacterial disproportionation of elemental sulfur  
684 coupled to chemical reduction of iron or manganese. *Appl Environ Microbiol*. 1993  
685 Jan;59(1):101-8. doi: 10.1128/aem.59.1.101-108.1993.  
686
- 687 23. Seemann T. Prokka: rapid prokaryotic genome annotation. *Bioinformatics*. 2014 Jul  
688 15;30(14):2068-9. doi: 10.1093/bioinformatics/btu153.  
689
- 690 24. Chen S, Zhou Y, Chen Y, Gu J. fastp: an ultra-fast all-in-one FASTQ preprocessor.  
691 *Bioinformatics*. 2018 Sep 1;34(17):i884-i890. doi: 10.1093/bioinformatics/bty560.  
692

693 25. Wick RR, Judd LM, Gorrie CL, Holt KE. Unicycler: Resolving bacterial genome assemblies  
694 from short and long sequencing reads. *PLoS Comput Biol*. 2017 Jun 8;13(6):e1005595. doi:  
695 10.1371/journal.pcbi.1005595.  
696

697 26. Wick RR, Schultz MB, Zobel J, Holt KE. Bandage: interactive visualization of de novo  
698 genome assemblies. *Bioinformatics*. 2015 Oct 15;31(20):3350-2. doi:  
699 10.1093/bioinformatics/btv383.  
700

701 27. Antipov D, Raiko M, Lapidus A, Pevzner PA. Plasmid detection and assembly in genomic  
702 and metagenomic data sets. *Genome Res*. 2019 Jun;29(6):961-968. doi:  
703 10.1101/gr.241299.118.  
704

705 28. Couvin D, Bernheim A, Toffano-Nioche C, Touchon M, Michalik J, Néron B, Rocha EPC,  
706 Vergnaud G, Gautheret D, Pourcel C. CRISPRCasFinder, an update of CRISRFinder, includes a  
707 portable version, enhanced performance and integrates search for Cas proteins. *Nucleic Acids*  
708 *Res*. 2018 Jul 2;46(W1):W246-W251. doi: 10.1093/nar/gky425.  
709

710 29. Bertelli C, Laird MR, Williams KP; Simon Fraser University Research Computing Group, Lau  
711 BY, Hoad G, Winsor GL, Brinkman FSL. IslandViewer 4: expanded prediction of genomic islands  
712 for larger-scale datasets. *Nucleic Acids Res*. 2017 Jul 3;45(W1):W30-W35. doi:  
713 10.1093/nar/gkx343.  
714

715 30. Kim OS, Cho YJ, Lee K, Yoon SH, Kim M, Na H, Park SC, Jeon YS, Lee JH, Yi H, Won S, Chun  
716 J. Introducing EzTaxon-e: a prokaryotic 16S rRNA gene sequence database with phylotypes  
717 that represent uncultured species. *Int J Syst Evol Microbiol*. 2012 Mar;62(Pt 3):716-721. doi:  
718 10.1099/ijs.0.038075-0.  
719

720 31. Meier-Kolthoff JP, Auch AF, Klenk HP, Göker M. Genome sequence-based species  
721 delimitation with confidence intervals and improved distance functions. *BMC Bioinformatics*.  
722 2013 Feb 21;14:60. doi: 10.1186/1471-2105-14-60.  
723

- 724 32. Lee I, Ouk Kim Y, Park SC, Chun J. OrthoANI: An improved algorithm and software for  
725 calculating average nucleotide identity. *Int J Syst Evol Microbiol*. 2016 Feb;66(2):1100-1103.  
726 doi: 10.1099/ijsem.0.000760.  
727
- 728 33. Yoon SH, Ha SM, Lim J, Kwon S, Chun J. A large-scale evaluation of algorithms to calculate  
729 average nucleotide identity. *Antonie Van Leeuwenhoek*. 2017 Oct;110(10):1281-1286. doi:  
730 10.1007/s10482-017-0844-4.  
731
- 732 34. Rodriguez-R LM, Konstantinidis KT. 2016. The enveomics collection : a toolbox for  
733 specialized analyses of microbial genomes and metagenomes. *PeerJ Preprints*. 2016  
734 4:e1900v1 <https://doi.org/10.7287/peerj.preprints.1900v1>  
735
- 736 35. Stackebrandt E, Ebers J. Taxonomic parameters revisited: tarnished gold standards.  
737 *Microbiology Today* 2006;33:152.  
738
- 739 36. Yarza P, Yilmaz P, Pruesse E, Glöckner FO, Ludwig W, Schleifer KH, Whitman WB, Euzéby  
740 J, Amann R, Rosselló-Móra R. Uniting the classification of cultured and uncultured bacteria  
741 and archaea using 16S rRNA gene sequences. *Nat Rev Microbiol*. 2014 Sep;12(9):635-45. doi:  
742 10.1038/nrmicro3330.  
743
- 744 37. Wayne, L.G., Brenner, D.J., Colwell, R.R., Grimont, P.A.D., Kandler, O., Krichevsky,  
745 M.I., Moore, L.H., Moore, W.E.C., Murray, R.g.e., Stackebrandt, E., M. P. Starr and H. G.  
746 Truper. Report of the ad hoc committee on reconciliation of approaches to bacterial  
747 systematics. *Int. J. Syst. Evol. Microbiol*. 1987 37 (4), 463–464. doi:10.1099/00207713-37-4-  
748 463  
749
- 750 38. Richter M, Rosselló-Móra R. Shifting the genomic gold standard for the prokaryotic species  
751 definition. *Proc Natl Acad Sci U S A*. 2009 Nov 10;106(45):19126-31. doi:  
752 10.1073/pnas.0906412106.  
753

754 39. Barco RA, Garrity GM, Scott JJ, Amend JP, Nealson KH, Emerson D. A Genus Definition for  
755 Bacteria and Archaea Based on a Standard Genome Relatedness Index. *mBio*. 2020 Jan  
756 14;11(1):e02475-19. doi: 10.1128/mBio.02475-19.  
757  
758 40. Konstantinidis KT, Rosselló-Móra R, Amann R. Uncultivated microbes in need of their own  
759 taxonomy. *ISME J*. 2017 Nov;11(11):2399-2406. doi: 10.1038/ismej.2017.113.  
760  
761 41. Brettin T, Davis JJ, Disz T, Edwards RA, Gerdes S, Olsen GJ, Olson R, Overbeek R, Parrello  
762 B, Pusch GD, Shukla M, Thomason JA 3rd, Stevens R, Vonstein V, Wattam AR, Xia F. RASTtk: a  
763 modular and extensible implementation of the RAST algorithm for building custom  
764 annotation pipelines and annotating batches of genomes. *Sci Rep*. 2015 Feb 10;5:8365. doi:  
765 10.1038/srep08365.  
766  
767 42. Tatusova T, DiCuccio M, Badretdin A, Chetvernin V, Nawrocki EP, Zaslavsky L, Lomsadze A,  
768 Pruitt KD, Borodovsky M, Ostell J. NCBI prokaryotic genome annotation pipeline. *Nucleic Acids*  
769 *Res*. 2016 Aug 19;44(14):6614-24. doi: 10.1093/nar/gkw569.  
770  
771 43. Vallenet D, Calteau A, Cruveiller S, Gachet M, Lajus A, Josso A, Mercier J, Renaux A, Rollin  
772 J, Rouy Z, Roche D, Scarpelli C, Médigue C. MicroScope in 2017: an expanding and evolving  
773 integrated resource for community expertise of microbial genomes. *Nucleic Acids Res*. 2017  
774 Jan 4;45(D1):D517-D528. doi: 10.1093/nar/gkw1101.  
775  
776 44. Neukirchen S, Sousa FL. DiSCo: a sequence-based type-specific predictor of Dsr-dependent  
777 dissimilatory sulphur metabolism in microbial data. *Microb Genom*. 2021 Jul;7(7). doi:  
778 10.1099/mgen.0.000603.  
779  
780 45. Savojardo C, Martelli PL, Fariselli P, Profiti G, Casadio R. BUSCA: an integrative web server  
781 to predict subcellular localization of proteins. *Nucleic Acids Res*. 2018 Jul 2;46(W1):W459-  
782 W466. doi: 10.1093/nar/gky320.  
783

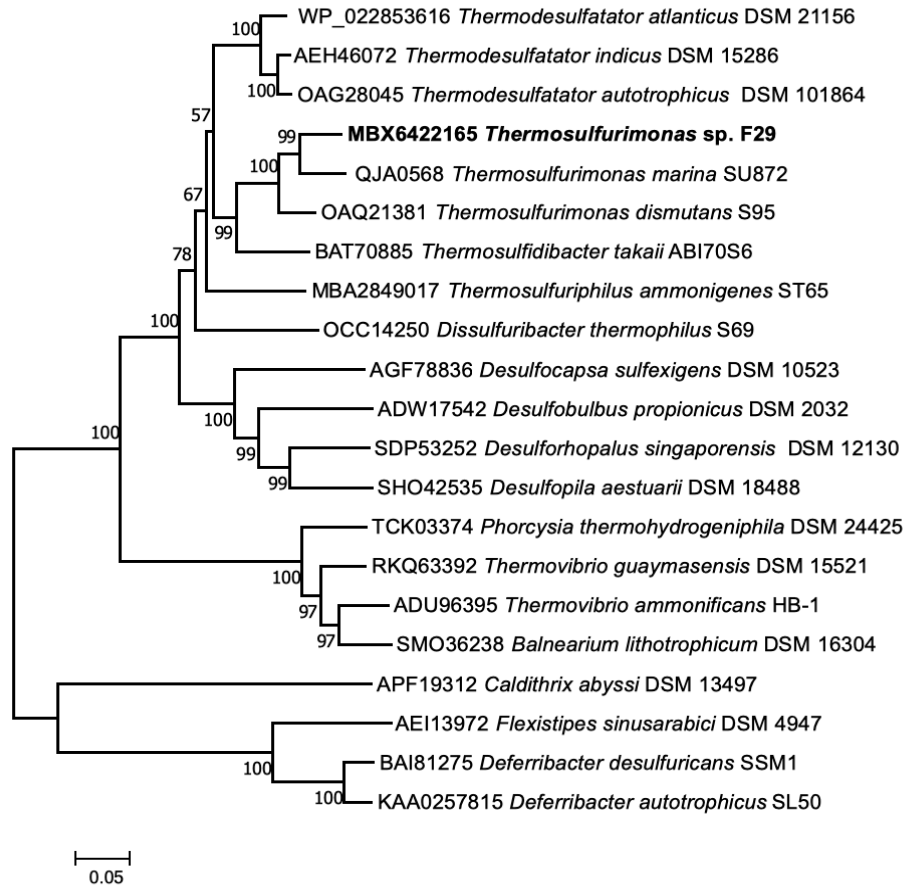
- 784 46. Veltri D, Wight MM, Crouch JA. SimpleSynteny: a web-based tool for visualization of  
785 microsynteny across multiple species. *Nucleic Acids Res.* 2016 Jul 8;44(W1):W41-5. doi:  
786 10.1093/nar/gkw330.  
787
- 788 47. Castelán-Sánchez HG, Lopéz-Rosas I, García-Suastegui WA, Peralta R, Dobson ADW,  
789 Batista-García RA, Dávila-Ramos S. Extremophile deep-sea viral communities from  
790 hydrothermal vents: Structural and functional analysis. *Mar Genomics.* 2019 Aug;46:16-28.  
791 doi: 10.1016/j.margen.2019.03.001.
- 792 48. Hanson TE, Campbell BJ, Kalis KM, Campbell MA, Klotz MG. Nitrate ammonification by  
793 *Nautilia profundicola* AmH: experimental evidence consistent with a free hydroxylamine  
794 intermediate. *Front Microbiol.* 2013 Jul 4;4:180. doi: 10.3389/fmicb.2013.00180.  
795
- 796 49. Allieux M, Yvenou S, Slobodkina G, Slobodkin A, Shao Z, Jebbar M, Alain K. Genomic  
797 Characterization and Environmental Distribution of a Thermophilic Anaerobe  
798 *Dissulfurirhabdus thermomarina* SH388T Involved in Disproportionation of Sulfur Compounds  
799 in Shallow Sea Hydrothermal Vents. *Microorganisms.* 2020 Jul 27;8(8):1132. doi:  
800 10.3390/microorganisms8081132.  
801
- 802 50. Slobodkina G, Allieux M, Merkel A, Alain K, Jebbar M, Slobodkin A. Genome analysis of  
803 *Thermosulfuriphilus ammonigenes* ST65T, an anaerobic thermophilic chemolithoautotrophic  
804 bacterium isolated from a deep-sea hydrothermal vent. *Mar Genomics.* 2020 Dec;54:100786.  
805 doi: 10.1016/j.margen.2020.100786.  
806
- 807 51. Thorup, C.; Schramm, A.; Findlay, A.J.; Finster, K.W.; Schreiber, L. Disguised as a sulfate  
808 reducer: Growth of the deltaproteobacterium *Desulfurivibrio alkaliphilus* by sulfide oxidation  
809 with nitrate. *mBio* 2017, 8, e00671-17.  
810
- 811 52. François DX, Godfroy A, Mathien C, Aubé J, Cathalot C, Lesongeur F, L'Haridon S, Philippon  
812 X, Roussel EG. *Persephonella atlantica* sp. nov.: How to adapt to physico-chemical gradients  
813 in high temperature hydrothermal habitats. *Syst Appl Microbiol.* 2021 Jan;44(1):126176. doi:  
814 10.1016/j.syapm.2020.126176.

815 53. Peters JW, Miller AF, Jones AK, King PW, Adams MW. Electron bifurcation. *Curr Opin Chem*  
816 *Biol.* 2016 Apr;31:146-52. doi: 10.1016/j.cbpa.2016.03.007.  
817  
818 54. Baffert C, Kpebe A, Avilan L, Brugna M. Hydrogenases and H<sub>2</sub> metabolism in sulfate-  
819 reducing bacteria of the *Desulfovibrio* genus. *Advances in Microbial Physiology*, 74, pp.143-  
820 189, 2019. hal-02180360  
821  
822 55. Furlan, C., Chongdar, N., Gupta, P., Lubitz, W., Ogata, H., Blaza, J., & Birrell, J. (2021).  
823 Structural insight on the mechanism of an electron-bifurcating [FeFe] hydrogenase.  
824 Cambridge University Press (CUP). <https://doi.org/10.33774/chemrxiv-2021-m2jgl>  
825  
826 56. Finster KW, Kjeldsen KU, Kube M, Reinhardt R, Mussmann M, Amann R, Schreiber L.  
827 Complete genome sequence of *Desulfocapsa sulfexigens*, a marine deltaproteobacterium  
828 specialized in disproportionating inorganic sulfur compounds. *Stand Genomic Sci.* 2013 Apr  
829 15;8(1):58-68. doi: 10.4056/sigs.3777412.  
830  
831 57. Kojima H, Umezawa K, Fukui M. *Caldimicrobium thiodismutans* sp. nov., a sulfur-  
832 disproportionating bacterium isolated from a hot spring, and emended description of the  
833 genus *Caldimicrobium*. *Int J Syst Evol Microbiol.* 2016 Apr;66(4):1828-1831. doi:  
834 10.1099/ijsem.0.000947.  
835  
836 58. Florentino AP, Pereira IAC, Boeren S, van den Born M, Stams AJM, Sánchez-Andrea I.  
837 Insight into the sulfur metabolism of *Desulfurella amilsii* by differential proteomics. *Environ*  
838 *Microbiol.* 2019 Jan;21(1):209-225. doi: 10.1111/1462-2920.14442.  
839  
840 59. Umezawa K, Kojima H, Kato Y, Fukui M. *Dissulfurispira thermophila* gen. nov., sp. nov., a  
841 thermophilic chemolithoautotroph growing by sulfur disproportionation, and proposal of  
842 novel taxa in the phylum *Nitrospirota* to reclassify the genus *Thermodesulfovibrio*. *Syst Appl*  
843 *Microbiol.* 2021 Apr;44(2):126184. doi: 10.1016/j.syapm.2021.126184.  
844  
845



846 **2. Figures and tables**

847



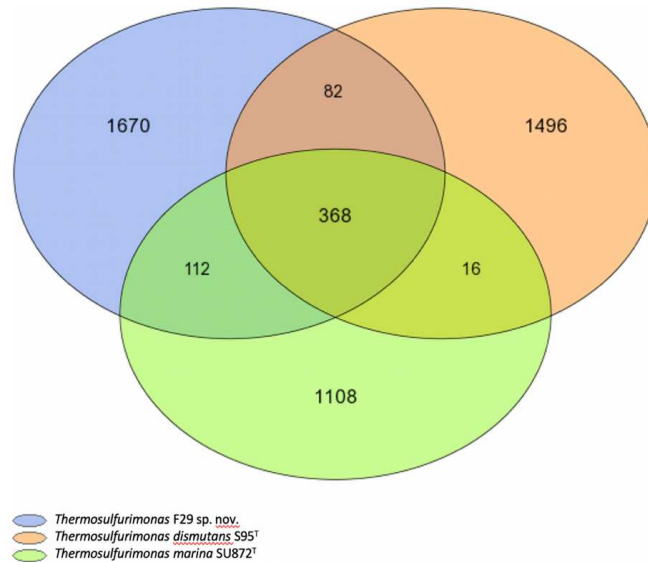
848

849 Figure 1. Neighbor joining phylogenetic tree showing the position of the gene NapA of strain  
 850 F29 within the closest bacterial sequences annotated as NapA, the periplasmic nitrate  
 851 reductases, or molybdopterin-containing oxidoreductases genes. Bootstrap values based on  
 852 1000 replications are shown at branch nodes. Bar, 5% estimated substitutions.

853

854

855



856

857 Figure 2. Venn diagram of the CDSs shared among *Thermosulfurimonas* F29 sp. nov.,  
 858 *Thermosulfurimonas dismutans* S95<sup>T</sup>, and *Thermosulfurimonas marina* SU872<sup>T</sup> against the  
 859 genome of 10 other members of the *Thermodesulfobacteriaceae* family (*Caldimicrobium*  
 860 *thiodismutans* TF1<sup>T</sup>, *Thermodesulfatator atlanticus* DSM 21156<sup>T</sup>, *Thermodesulfatator*  
 861 *autotrophicus* S606<sup>T</sup>, *Thermodesulfatator indicus* DSM 15286<sup>T</sup>, *Thermodesulfobacterium*  
 862 *geofontis* OPF15<sup>T</sup>, *Thermodesulfobacterium thermophilum* DSM 1276<sup>T</sup>,  
 863 *Thermodesulfobacterium commune* DSM 2178<sup>T</sup>, *Thermodesulfobacterium hydrogeniphilum*  
 864 DSM 14290<sup>T</sup>, *Thermodesulfobacterium hveragerdense* DSM 12571<sup>T</sup>, and *Thermosulfuriphilus*  
 865 *ammonigenes* ST65<sup>T</sup>).

866

867

868

869

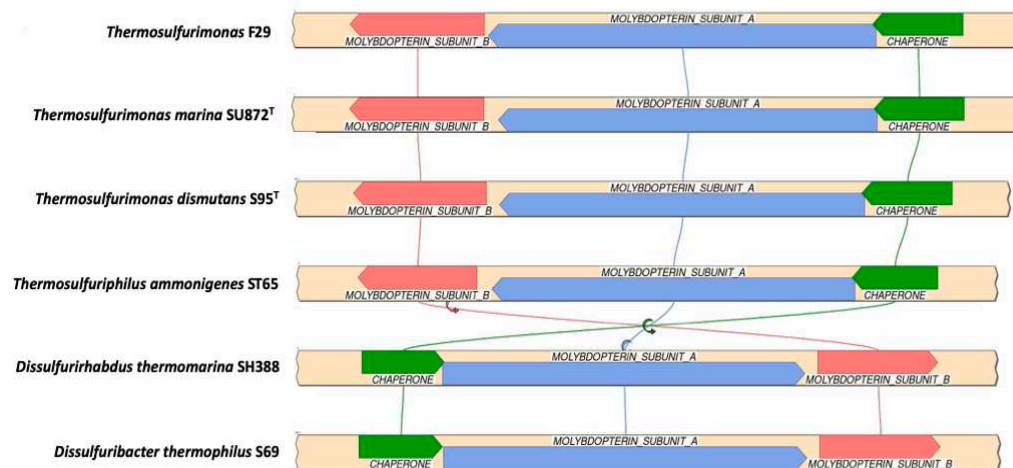
870

871

872

873

874



875

876 Figure 3. Microsyntenic ordering of the three putative CDSs associated with sulfur  
 877 disproportionation, found by comparative genomics, showing gene locus tags, molybdopterin  
 878 subunits A and B, and the associated chaperone protein, within the genomes of strain F29  
 879 (K3767\_RS01060 to K3767\_RS01070), *T. marina* (FVE67\_RS02285 to FVE67\_RS02295), *T.*  
 880 *dismutans* (TDIS\_RS03055 to TDIS\_RS03065), *T. ammonigenes* (G4V39\_RS07125 to  
 881 G4V39\_RS07135), *D. thermomarina* (HCU62\_RS07530 to HCU62\_RS07540), and *D.*  
 882 *thermophilus* (DBT\_RS08130 to DBT\_RS08140).

883

*Supplementary material*

**Genome analysis of a new sulfur disproportionating species  
*Thermosulfurimonas* strain F29 and comparative genomics of  
sulfur-disproportionating bacteria from marine hydrothermal  
vents**

**Maxime Allieux<sup>1</sup>, Stéven Yvenou<sup>1</sup>, Galina Slobodkina<sup>2</sup>, Alexander Slobodkin<sup>2</sup>, Anne Godfroy<sup>1</sup>, Zongze Shao<sup>3</sup>, Mohamed Jebbar<sup>1</sup> and Karine Alain<sup>1\*</sup>**

<sup>1</sup>Univ Brest, CNRS, IFREMER, IRP 1211 MicrobSea, Laboratoire de Microbiologie des Environnements Extrêmes LM2E, IUEM, Rue Dumont d'Urville, F-29280 Plouzané, France

<sup>2</sup>Winogradsky Institute of Microbiology, Research Center of Biotechnology of the Russian Academy of Sciences, Moscow, Russia

<sup>3</sup>Key Laboratory of Marine Genetic Resources, Third Institute of Oceanography, Ministry of Natural Resources, Xiamen 361005, China

\* **Correspondence:** Karine Alain  
[Karine.Alain@univ-brest.fr](mailto:Karine.Alain@univ-brest.fr)

**Supplementary Material S1:**

Table S1.1. References of the CDSs annotated by Prokka, RAST, MaGe and UniProtKB with the available protein sequences data on the NCBI's online automated prokaryotic genome annotation pipeline. CDSs were found with their associated loci, based on the assembly repository ASM1968873v1.

Gene name	Protein sequence accession number
<b>Genes related to carbon metabolism:</b>	
Formate dehydrogenase [EC 1.2.2.43]	WP_221172701 ; WP_221172702
5-methyltetrahydrofolate:corrinoid/iron-sulfur protein Co-methyltransferase (ascE) [EC 2.1.1.258]	WP_221172703
Acetyl-CoA synthase corrinoid iron-sulfur protein, large subunit acsC [EC:2.1.1.245]	WP_221172704
CO dehydrogenase/acetyl-CoA synthase, acetyl-CoA synthase subunit [EC 2.3.1.169]	WP_221172705
5,10-methylenetetrahydrofolate reductase [EC 1.5.1.20]	WP_221172706
5,10-methylenetetrahydrofolate reductase, small subunit [EC 1.5.1.20]	WP_221172707
CO dehydrogenase /acetyl-CoA synthase, CO dehydrogenase subunit cooS, acsA [EC 1.2.7.4],	WP_221172712
Methylenetetrahydrofolate cyclohydrolase [EC 3.5.4.9] / Methylenetetrahydrofolate dehydrogenase (NADP+) [EC 1.5.1.5]	WP_221172713
Formate-tetrahydrofolate ligase [EC 6.3.4.3]	WP_221172714
Pyruvate: ferredoxin oxidoreductase [EC:1.2.7.1]	WP_221172159 ; WP_221172156
Glucokinase	WP_221173395
Glucose-6-phosphate isomerase [EC 5.3.1.9]	WP_221171986
Fructose 1,6-bisphosphatase [EC 4.1.2.13]	WP_221172601
ATP-dependent 6-phosphofructokinase [EC 2.7.1.11]	WP_221173515
Transketolase [EC 2.2.1.1]	WP_221173097
Transaldolase [EC 2.2.1.2]	WP_221171757
Triosephosphate isomerase [EC 5.3.1.1]	WP_221172452
NAD-dependent glyceraldehyde-3-phosphate dehydrogenase [EC 1.2.1.12]	WP_221172665
Phosphoglycerate kinase [EC 2.7.2.3]	WP_221172669
2,3-bisphosphoglycerate-independent phosphoglycerate mutase	WP_221172388
Phosphopyruvate hydratase	WP_221173282
Pyruvate phosphate dikinase	WP_221172666
Phosphoenolpyruvate synthase [EC 2.7.9.2]	WP_221172720
Ribulose-5-phosphate 4-epimerase	WP_221172245
Ribose-5-phosphate isomerase B [EC 5.3.1.6]	WP_221173605
Ribose-phosphate pyrophosphokinase [EC 2.7.6.1]	WP_221172369
Aconitate hydratase [EC 4.2.1.3]	WP_221172563
Isocitrate dehydrogenase [NADP] [EC 1.1.1.42]	WP_221173063
2-oxoglutarate oxidoreductase	WP_221172104 ; WP_221172105 ; WP_221172386 ; WP_221172385
Fumarate hydratase	WP_221171610 ; WP_221173249
Malate dehydrogenase [EC 1.1.1.37]	WP_221173530
<b>Genes related to hydrogen metabolism:</b>	
[NiFe] Group 1a hydrogenase large subunit	WP_221172697
[NiFe] Group 1a hydrogenase small subunit	WP_221172699
[NiFe] Group 1c hydrogenase large subunit	WP_221173559
[NiFe] Group 1c hydrogenase small subunit	WP_221173558
[NiFe] Group 1c hydrogenase cytochrome subunit	WP_221173560
[NiFe] Group 1c hydrogenase putative iron-sulfur subunit	WP_221173557
[NiFe] Group 1c hydrogenase F420-non-reducing hydrogenase subunit G	WP_221173556
[NiFe] Group 1c hydrogenase maturation factor HypA	WP_221173563
[NiFe] Group 1c hydrogenase maturation factor HypB	WP_221173564
[NiFe] Group 1c hydrogenase maturation factor HypC	WP_221173562
[NiFe] Group 1c hydrogenase maturation factor HupD	WP_221173561

Gene name	Protein sequence accession number
<b>Genes related to nitrogen metabolism:</b>	
P-II family nitrogen regulator	WP_221172613 ; WP_221172620 ; WP_221172621
Ammonium transporter	WP_221172614
Nitrogenase FeMo-cofactor scaffold and assembly protein NifE	WP_221172615
Nitrogenase (molybdenum-iron) beta chain (EC 1.18.6.1)	WP_221172616
Nitrogenase (molybdenum-iron) alpha chain (EC 1.18.6.1) MBX6423085	WP_221172617
Nitrogenase FeMo-cofactor synthesis FeS core scaffold and assembly protein NifB	WP_221172618
Nitrogenase iron protein	WP_221172619
Ferredoxin-type protein NapH	WP_221171699
Ferredoxin-type protein NapG	WP_221171700
Periplasmic nitrate reductase chaperone NapD	WP_221171701
Periplasmic nitrate reductase NapA [EC:1.7.99.4]	WP_221171702
Periplasmic nitrate reductase subunit NapM	WP_221171703
Multiheme cytochrome c family protein, hydroxylamine oxidoreductase	WP_221171706
Polysulfide reductase NrfD	WP_221171707
Tetrathionate reductase subunit B	WP_221171708
Cytochrome c3 family protein	WP_221171709
Hydroxylamine reductase	WP_221173055
Ammonium transporter	WP_221171880 ; WP_221171881
4Fe-4S dicluster domain-containing protein NrfC	WP_221172692
Polysulfide reductase NrfD	WP_221172693
Cytochrome c family protein NrfH	WP_221172694
<b>Genes related to sulfur metabolism:</b>	
Sulfate adenyltransferase	WP_221173271
Adenylyl-sulfate reductase subunit A	WP_221173268
Adenylyl-sulfate reductase subunit B	WP_221173269
Manganese-dependent inorganic pyrophosphatase	WP_221172681
DsrA	WP_221171921
DsrB	WP_221171920
DsrC	WP_221173469
DsrM	WP_221173160
DsrK	WP_221173159
DsrJ	WP_221173158
DsrO	WP_221173157
DsrP	WP_221173156
QmoA	WP_221173267
QmoB	WP_221173266
QmoC	WP_221173265
DsrD	WP_221172373
DsrT	WP_221173161
TorD/DmsD chaperon protein	WP_221171715
Molybdopterin oxidoreductase large subunit	WP_221171714
Molybdopterin oxidoreductase small subunit	WP_221171713
Tetrathionate reductase subunit A	WP_221172121
Tetrathionate reductase subunit B	WP_221172692 ; WP_221171708 ; WP_221171713
YeeE/YedE family protein	WP_221172062
Sulfurtransferase TusA	WP_221172063
putative DrsE domain-containing protein	WP_221172064
YDT cluster hp1	WP_221172065
YDT cluster hp2	WP_221172066

Table S1.2. Identity matrix of protein sequence homologies of the three CDSs found by comparative genomics, namely the molybdopterin A subunits (**A**), the molybdopterin B subunits (**B**) and the chaperone protein (**C**), between the genomes of strain F29, *T. marina*, *T. dismutans*, *T. ammonigenes*, *D. thermomarina* and *D. thermophilus*.

<b>A</b>	Thermosulfurimonas_dismutans_Molybdopterin_subunit_A	100.00	83.72	84.24	70.73	69.88	69.65
	Thermosulfurimonas_F29_Molybdopterin_subunit_A	83.72	100.00	86.38	70.21	68.56	68.20
	Thermosulfurimonas_marina_Molybdopterin_subunit_A	84.24	86.38	100.00	70.60	68.16	67.81
	Thermosulfuriphilus_ammonigenes_Molybdopterin_subunit_A	70.73	70.21	70.60	100.00	70.98	70.60
	Dissulfurirhabdus_thermomarina_Molybdopterin_subunit_A	69.88	68.56	68.16	70.98	100.00	72.24
	Dissulfuribacter_thermophilus_Molybdopterin_subunit_A	69.65	68.20	67.81	70.60	72.24	100.00
<b>B</b>	Thermosulfuriphilus_ammonigenes_Molybdopterin_subunit_B	100.00	68.02	67.61	68.42	71.84	69.80
	Thermosulfurimonas_dismutans_Molybdopterin_subunit_B	68.02	100.00	86.13	85.77	70.04	72.29
	Thermosulfurimonas_F29_Molybdopterin_subunit_B	67.61	86.13	100.00	89.45	71.66	68.67
	Thermosulfurimonas_marina_Molybdopterin_subunit_B	68.42	85.77	89.45	100.00	72.06	69.48
	Dissulfurirhabdus_thermomarina_Molybdopterin_subunit_B	71.84	70.04	71.66	72.06	100.00	77.33
	Dissulfuribacter_thermophilus_Molybdopterin_subunit_B	69.80	72.29	68.67	69.48	77.33	100.00
<b>C</b>	Dissulfuribacter_thermophilus_Chaperone	100.00	36.46	45.14	33.33	34.97	37.16
	Thermosulfuriphilus_ammonigenes_Chaperone	36.46	100.00	49.72	45.60	45.05	45.60
	Dissulfurirhabdus_thermomarina_Chaperone	45.14	49.72	100.00	48.59	50.85	50.85
	Thermosulfurimonas_F29_Chaperone	33.33	45.60	48.59	100.00	78.38	77.30
	Thermosulfurimonas_marina_Chaperone	34.97	45.05	50.85	78.38	100.00	77.30
	Thermosulfurimonas_dismutans_Chaperone	37.16	45.60	50.85	77.30	77.30	100.00

In addition, the genomes of the three new sulfur disproportionators representing new genera of *Deltaproteobacteria* isolated from deep-sea hydrothermal vent were also sequenced. However, due to a lack of time and the low quality of assemblies, genomes have still not been analyzed. It will be planned to analyze these genomes after the PhD defense.

Thus, only the assembly quality is reported below:

- The genome of strain M19, representing a new genus of the *Desulfobulbaceae* family was assembled by hybrid sequencing (MiSeq and MinIon) into 90 contigs. This draft genome has a total length of 3,101,069 bp, a GC% of 49.39, a N50 of 261,071 and a L50 of 5.
- The genome of strain M45, representing a new genus of the family *Dissulfuribacteraceae* was assembled by short read sequencing into 94 contigs, for a total length of 5,437,415 bp, a GC% of 48.67, a N50 of 158,333 and a L50 of 11. However, the sequencing of the genome revealed that this strain was not pure, and should be purified before further physiological analyses.
- The genome of strain B35 representing a new genus of the family *Desulfobulbaceae* was assembled by short read sequencing into 127 contigs, for a total length of 4,130,618 bp, with a GC% of 60.73, a N50 of 179,123 and a L50 of 8.

In conclusion, we were able to sequence, assemble and analyze four genomes of thermophilic ISC-disproportionators of hydrothermal origin. In addition, two other strains of ISC-disproportionators representing novel genera have been isolated and another one is highly enriched. These strains/genomes can be studied in the future. Analyses of new genomes of *Deltaproteobacteria* and *Thermodesulfobacteria* could be important to consider according to the recent changes into their taxonomic classification (Wait et al., 2020; Ward et al., 2021).

### 3.2 Search for genomic markers of ISC disproportionation

Part of my work was aimed at searching for genomic markers of ISC-dismutation by comparative genomics. First investigations were performed with large dataset of genomes focusing on most known ISC-disproportionators. These analyses did not allow for the extraction of genetic markers of dismutation. Results of interest had been obtained by working solely with marine hydrothermal originating bacteria.



We compared the genomes of *Dissulfuribacter thermophilus* S69<sup>T</sup> (ASM168733v1), *Thermodesulfator atlanticus* DSM 21156<sup>T</sup> (ASM42158v1), *Thermosulfurimonas dismutans* S95<sup>T</sup> (ASM165258v1), *Thermosulfuriphilus ammonigenes* ST65<sup>T</sup> (ASM1120745v1), *Thermosulfurimonas marina* SU872<sup>T</sup> (ASM1231758v1), and *Dissulfurirhabdus thermomarina* SH388<sup>T</sup> (ASM1297923v1). To focus on relevant CDSs (*coding DNA sequences*) and remove core genes, we subtracted whole CDSs present in the genomes of species, *Caminicella sporogenes* DSM 14501<sup>T</sup> (GCA\_900142285.1) an anaerobic, strictly chemoorganoheterotrophic bacterium, *Thermodesulfator autotrophicus* S606<sup>T</sup> (ASM164232v1), and *Thermodesulfator indicus* DSM 15286<sup>T</sup> (ASM21779v1), *Thermodesulfator* able to grow by sulfate reduction but unable to grow by ISC disproportionation. As said before, *T. atlanticus* disproportionates elemental sulfur (demonstrated *in vivo*) but not sulfite and thiosulfate. *T. atlanticus* was compared to *T. autotrophicus* and *T. indicus*, which are species of the same genus unable to disproportionate ISC. Therefore, CDSs found by this approach, might be related solely to the S<sup>0</sup>-disproportionation, and not to thiosulfate and sulfite disproportionation.

A total of two CDSs were shared among the six genomes of ISC-disproportionators from marine hydrothermal vents. These CDSs are associated to two subunits of a sulfur metabolism enzyme. An analysis of the genomic environment of these CDSs showed that these two CDS were micro-syntenic and formed a gene cluster of 3 CDSs, with a third CDS less homolog but still similar (Fig. 22). The identified gene cluster was composed of one short sequence of about 189 amino acids in length (36 to 77 % amino acid identity between each strain), a long central sequence of about 768 amino acids in length (62 to 84 % identity between each strain) and a last short sequence of about 255 amino acids in length (68 to 86 % identity between each strain). One of these CDS encoded for a molybdopterin already proposed to be involved in sulfur disproportionation in the species *Thermosulfurimonas dismutans*, in the article by Mardanov et al. (2016) (TDIS\_0614 locus).



Figure 22: Comparison of the synteny of the three candidate CDSs discovered by comparative genomics. The genomic environment of *Dissulfurirhabdus thermomarina* SH388<sup>T</sup> as a reference was compared (from the top to the bottom), to the ones of *Thermosulfuriphilus ammonigenes* ST65<sup>T</sup>, *Thermodesulfatator atlanticus* DSM 21156<sup>T</sup>, *Thermosulfurimonas dismutans* S95<sup>T</sup>, *Thermosulfurimonas marina* SU872<sup>T</sup> and *Dissulfuribacter thermophilus* S69<sup>T</sup>.

The putative functions of these CDSs based on MaGe, UniprotKb, PGAP and InterProScan annotations are given in Table 5.

*Table 5: Results of the genomic annotation of the three candidate CDSs of sulfur disproportionation obtained with various software (MaGe platform, blast against NCBI and UniprotKB database and functional prediction by InterProScan) for the 6 species: Dissulfuribacter thermophilus, Thermodesulfatator atlanticus, Thermosulfurimonas dismutans, Thermosulfurimonas marina, Thermosulfuriphilus ammonigenes and Dissulfurirhabdus thermomarina. Legend: nr: no results. The annotation by MaGe corresponds to an automatic annotation as opposed to the annotations of NCBI and UniprotKB which correspond to the manually reported most homologous associated CDSs. Functional prediction by InterProScan was made on the basis of protein family membership and gene ontology.*

	MaGe annotation	UniprotKb	NCBI pgap	Interproscan
<b>Dissulfuribacter thermophilus</b>				
Short CDS 1 END	Chaperone protein TorD	Chaperone protein TorD	chaperone protein TorD	DMSO/Nitrate reductase chaperone (IPRO20945)
Long CDS Middle	Molybdopter in oxydoreductase (Polysulfide/thiosulfate), catalytic subunit A	Molybdopter in oxydoreductase (Polysulfide/thiosulfate), catalytic subunit A	molybdopter in-dependent oxydoreductase / twin-arginine translocation pathway signal protein	oxidation-reduction process (GO:0055114) oxydoreductase activity (GO:0016491) molybdopter in cofactor binding (GO:0043546)
Short CDS 2 END	Molybdopter in oxydoreductase, iron-sulfur subunit B	Molybdopter in oxydoreductase, iron-sulfur subunit B	4Fe-4S dicluster domain-containing protein	nr
<b>Thermodesulfatator atlanticus</b>				
Short CDS 1 END	Chaperone protein TorD	Chaperone protein TorD	molecular chaperone TorD family protein	DMSO/Nitrate reductase chaperone (IPRO20945)
Long CDS Middle	Molybdopter in oxydoreductase, catalytic subunit A	Molybdopter in oxydoreductase, catalytic subunit A	molybdopter in-dependent oxydoreductase	oxidation-reduction process (GO:0055114) oxydoreductase activity (GO:0016491) molybdopter in cofactor binding (GO:0043546)
Short CDS 2 END	Molybdopter in oxydoreductase, iron-sulfur subunit B	Molybdopter in oxydoreductase, iron-sulfur subunit B	4Fe-4S dicluster domain-containing protein	nr
<b>Thermosulfurimonas dismutans</b>				
Short CDS 1 END	Chaperone protein TorD	Chaperone protein TorD	Chaperone protein TorD / hypothetical protein	DMSO/Nitrate reductase chaperone (IPRO20945)
Long CDS Middle	Anaerobic dehydrogenases, typically selenocysteine-containing	Molybdopter in oxydoreductase, catalytic subunit A	molybdopter in-dependent oxydoreductase / twin-arginine translocation pathway signal protein	oxidation-reduction process (GO:0055114) oxydoreductase activity (GO:0016491) molybdopter in cofactor binding (GO:0043546)
Short CDS 2 END	Molybdopter in oxydoreductase, iron-sulfur subunit B	Molybdopter in oxydoreductase, iron-sulfur subunit B	4Fe-4S dicluster domain-containing protein	nr
<b>Thermosulfurimonas marina</b>				
Short CDS 1 END	Putative oxydoreductase component of anaerobic dehydrogenases; Functional role page for Chaperone protein TorD	Chaperone protein TorD	hypothetical protein FVE67_02280	DMSO/Nitrate reductase chaperone (IPRO20945)
Long CDS Middle	Anaerobic dehydrogenases, typically selenocysteine-containing	Molybdopter in oxydoreductase, catalytic subunit A	molybdopter in-dependent oxydoreductase	oxidation-reduction process (GO:0055114) oxydoreductase activity (GO:0016491) molybdopter in cofactor binding (GO:0043546)
Short CDS 2 END	4Fe-4S dicluster domain-containing protein	Molybdopter in oxydoreductase, iron-sulfur subunit B	4Fe-4S dicluster domain-containing protein	nr
<b>Thermosulfuriphilus ammonigenes</b>				
Short CDS 1 END	Putative oxydoreductase component of anaerobic dehydrogenases; Functional role page for Chaperone protein TorD	Chaperone protein TorD	hypothetical protein	DMSO/Nitrate reductase chaperone (IPRO20945)
Long CDS Middle	Anaerobic dehydrogenases, typically selenocysteine-containing	Molybdopter in oxydoreductase (Polysulfide/thiosulfate), catalytic subunit A	molybdopter in-dependent oxydoreductase	oxidation-reduction process (GO:0055114) oxydoreductase activity (GO:0016491) molybdopter in cofactor binding (GO:0043546)
Short CDS 2 END	4Fe-4S dicluster domain-containing protein	Molybdopter in oxydoreductase, iron-sulfur subunit B	4Fe-4S dicluster domain-containing protein	nr
<b>Dissulfurirhabdus thermomarina</b>				
Short CDS 1 END	Chaperone protein TorD	Chaperone protein TorD	molecular chaperone TorD family protein	DMSO/Nitrate reductase chaperone (IPRO20945)
Long CDS Middle	Molybdopter in oxydoreductase (Polysulfide/thiosulfate), catalytic subunit A	Molybdopter in oxydoreductase (Polysulfide/thiosulfate), catalytic subunit A	molybdopter in-dependent oxydoreductase	oxidation-reduction process (GO:0055114) oxydoreductase activity (GO:0016491) molybdopter in cofactor binding (GO:0043546)
Short CDS 2 END	Molybdopter in oxydoreductase, iron-sulfur subunit B	Molybdopter in oxydoreductase, iron-sulfur subunit B (Dissulfuribacter thermophilus)	4Fe-4S dicluster domain-containing protei	nr

These results are poorly informative, but may suggest some reductive or oxidative capacity for the encoded proteins. This gene cluster contains three potential proteins, which are, respectively predicted as a putative chaperone protein, and two subunits of a molybdopterin oxidoreductase with possibly interactions with polysulfides/thiosulfate. However, similarities with homologous proteins are in some cases weak, especially with respect to the putative chaperone protein. The latter shows only about 35% similarity with chaperone protein sequences certified according to UniprotKb, and automatic annotation biases are present. The first associated chaperone protein sequence could, as with trimethylamine N-oxide (TMAO) reductase, allow a higher expression of the two other CDSs (Ilbert et al., 2003; Pommier et al., 2008). In contrast, macro-synteny was not observed among the six genomes, and other syntenic genes found around the cluster of interest were involved in different processes than sulfur disproportionation (3-oxoacyl-[acyl-carrier-protein] synthase II, Methylenetetrahydrofolate--tRNA-(uracil-5-)-methyltransferase, threonyl-tRNA synthetase, Phenylalanine--tRNA ligase beta subunit, Acriflavin resistance protein or Efflux transporter, RND family genes and an unknown permease).

The prediction of the secondary structures of these proteins indicate that they are probably not located on the membrane but are more likely extracellular, cytoplasmic, or periplasmic. TmHMM predicted that the proteins of *Dissulfurirhabdus thermomarina*, *Dissulfuribacter thermophilus*, and *Thermodesulfatator atlanticus* may be extracellular proteins. *Thermosulfurimonas marina*, *Thermosulfurimonas dismutans* and *Thermosulfuriphilus ammonigenes* proteins contain only a transmembrane helix alpha but are likely not membrane proteins as they have less than 3  $\alpha$ -helices. Nevertheless, they might have few transmembrane structures and be partially embedded in the membrane with the middle longest protein with respectively two transmembrane structures of a probability of 0.4 and 0.5 for *T. marina*, of 0.2 and 0.3 for *T. dismutans* and of 0.7 and 0.8 for *T. ammonigenes* (Fig. 23 left). Phyre2 analyses predicted that all long central proteins have a unique transmembrane helix, except the one of *T. atlanticus* (Fig. 23 right), suggesting a potential attachment to the membrane.

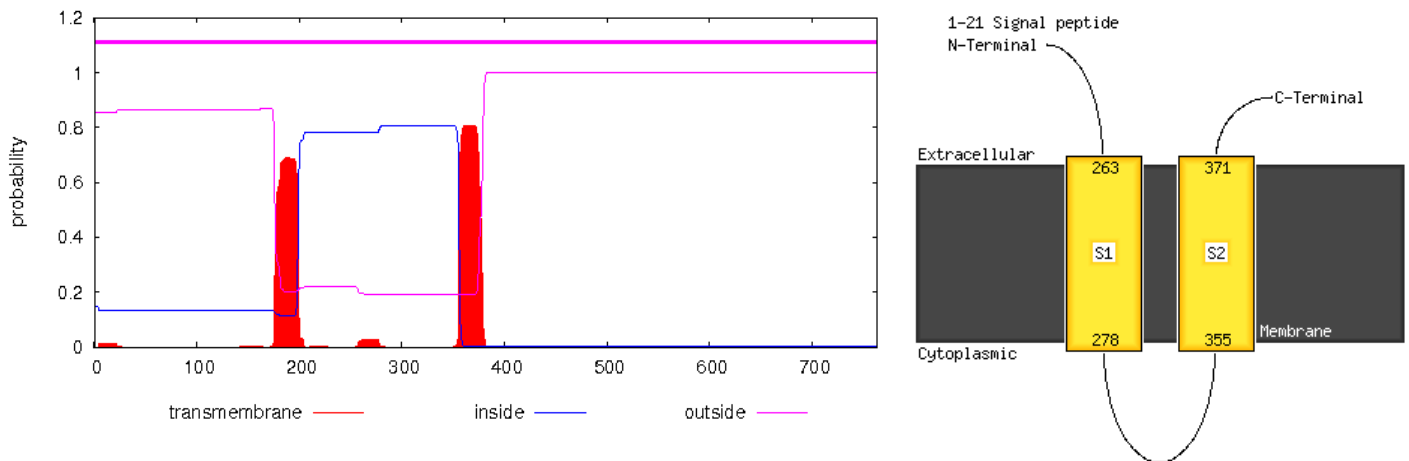


Figure 23: TmHMM statistics (left) and Phyre2 predictions diagrams (right) for *Thermosulfuriphilus ammonigenes* longest central protein obtained by comparative genomics.

With BUSCA, some subunits A of molybdopterin were found to have a putative signal peptide, namely the ones of *T. atlanticus*, *T. marina* and *T. ammonigenes* (Table 6). Chaperone subunits of *D. thermophilus*, *D. thermomarina* and *T. ammonigenes* showed putative transmembrane helix alpha (one or two). In summary, proteins are probably cytosolic or extracellular as they have less than 3  $\alpha$ -helices.

Table 6: BUSCA prediction of GO-terms and protein features for each of the 3 CDSs of *Dissulfuribacter thermophilus*, *Thermodesulfatator atlanticus*, *Thermosulfurimonas dismutans*, *Thermosulfurimonas marina*, *Thermosulfuriphilus ammonigenes* and *Dissulfurirhabdus thermomarina*.

▲ Protein Accession/ID	◆ GO-id	◆ GO-term	◆ Score	◆ Alternative Localization	◆ Features
◆ Dissulfuribacter_thermophilus_Chaperone	GO:0005886	C:plasma membrane	0.47	-	Transmembrane Alpha Helix
◆ Dissulfuribacter_thermophilus_Molybdopterin_subunit_A	GO:0005737	C:cytoplasm	0.7	-	
◆ Dissulfuribacter_thermophilus_Molybdopterin_subunit_B	GO:0005737	C:cytoplasm	0.7	-	
◆ Dissulfurirhabdus_thermomarina_Chaperone	GO:0005886	C:plasma membrane	0.68	-	Transmembrane Alpha Helix
◆ Dissulfurirhabdus_thermomarina_Molybdopterin_subunit_A	GO:0005737	C:cytoplasm	0.7	-	
◆ Dissulfurirhabdus_thermomarina_Molybdopterin_subunit_B	GO:0005737	C:cytoplasm	0.7	-	
◆ Thermodesulfatator_atlanticus_Chaperone	GO:0005737	C:cytoplasm	0.7	-	
◆ Thermodesulfatator_atlanticus_Molybdopterin_subunit_A	GO:0005615	C:extracellular space	0.87	-	Signal Peptide
◆ Thermodesulfatator_atlanticus_Molybdopterin_subunit_B	GO:0005737	C:cytoplasm	0.7	-	
◆ Thermosulfurimonas_dismutans_Chaperone	GO:0005737	C:cytoplasm	0.7	-	
◆ Thermosulfurimonas_dismutans_Molybdopterin_subunit_A	GO:0005737	C:cytoplasm	0.7	-	
◆ Thermosulfurimonas_dismutans_Molybdopterin_subunit_B	GO:0005737	C:cytoplasm	0.7	-	
◆ Thermosulfurimonas_marina_Chaperone	GO:0005737	C:cytoplasm	0.7	-	
◆ Thermosulfurimonas_marina_Molybdopterin_subunit_A	GO:0005615	C:extracellular space	0.85	-	Signal Peptide
◆ Thermosulfurimonas_marina_Molybdopterin_subunit_B	GO:0005737	C:cytoplasm	0.7	-	
◆ Thermosulfuriphilus_ammonigenes_Chaperone	GO:0005886	C:plasma membrane	0.57	-	Transmembrane Alpha Helix
◆ Thermosulfuriphilus_ammonigenes_Molybdopterin_subunit_A	GO:0005615	C:extracellular space	0.8	-	Signal Peptide
◆ Thermosulfuriphilus_ammonigenes_Molybdopterin_subunit_B	GO:0005737	C:cytoplasm	0.7	-	

Finally, results given by TmHMM, Phyre2 and BUSCA were slightly different, but all converge to the conclusion that proteins are obviously cytosolic, extracellular or periplasmic. Moreover, it can be thought that an attachment to the membrane is possible, in periplasmic or extracellular side. Molybdopterin A or chaperone subunit proteins could be attached to the membrane, as suggested previously elsewhere for some different proteins (Mardanov et al., 2016). For example, polysulfide reductase of *Wolinella succinogenes* is extracellular but attached to an anchor membrane protein (Klimmek et al., 2004). However, it is difficult to assess potential interactions between the three proteins, but it is likely that subunit A and B of molybdopterins oxidoreductase are linked.

The long central proteins of the 6 studied bacteria had a significant homology with the polysulfide reductase with bound quinone inhibitor, pentachlorophenol (PCP) of *Thermus thermophilus* HB27 (<https://www.rcsb.org/structure/2vpy>), sharing about 40% sequence identity, and with the ethylbenzene dehydrogenase of *Aromatoleum aromaticum* (<https://www.rcsb.org/structure/2ivf>) and the perchlorate reductase PcrAB from *Azospira suillum* PS (<https://www.rcsb.org/structure/4ydd>) with around 30% sequence identity for those two proteins. These findings are interesting as the polysulfide reductase, as well as the ethylbenzene dehydrogenase, are composed of three protein subunits, that we can correlate to our three CDS. Regarding to this polysulfide reductase which has some homology to our protein, it is composed of three proteins present twice, namely two small units of 195 and 253 amino acids (Fig. 24C and 24D) and one big unit of 765 amino acids, that are very close in size to the subunits of our three proteins (Fig. 24B). In addition, the second short CDS retrieved in the 6 sulfur disproportionating bacteria had an important homology with the NRFC protein molecule of the polysulfide reductase (Fig. 24C). In the polysulfide reductase described in the literature, a protein present in the membrane allows binding of the whole protein (Fig. 28D). The latter does not seem to be present in our bacteria and binding could be achieved by the central core protein. In conclusion the protein conformation (and obviously its function) is likely to be a little different from the one of the polysulfide reductase of *Thermus thermophilus*.

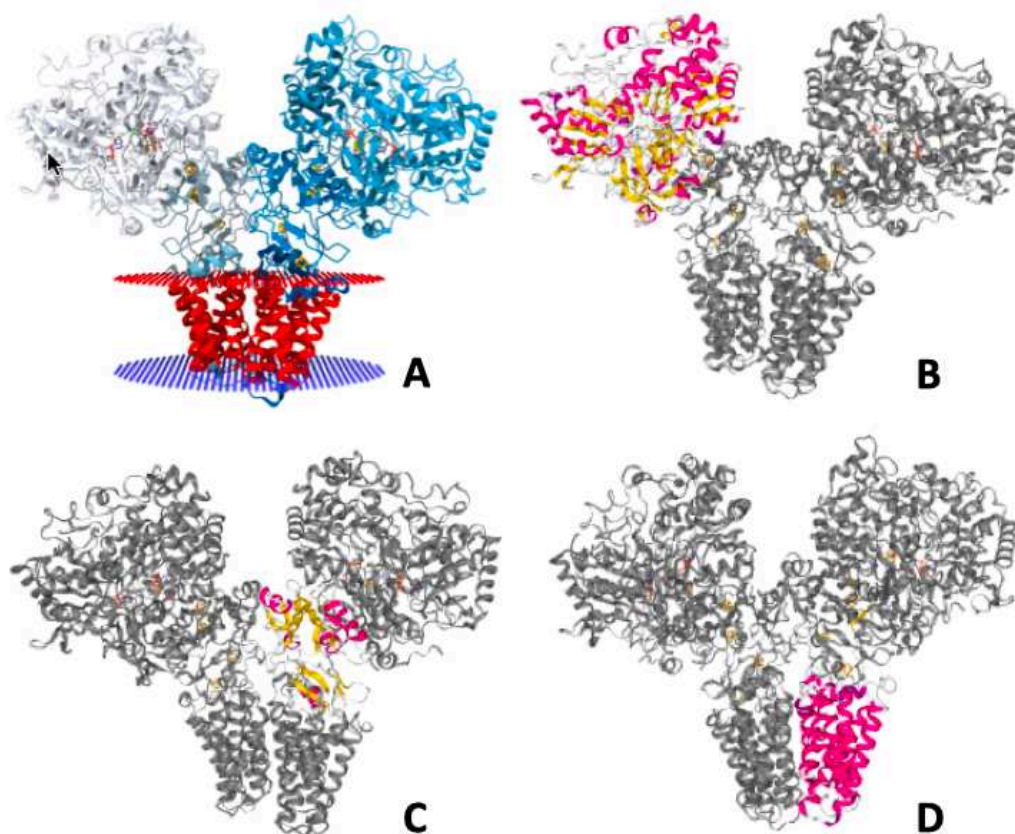


Figure 24: Structural representation of the polysulfide reductase with bound quinone inhibitor, pentachlorophenol (PCP) of *Thermus thermophilus* HB27 from RCSB PDB database (<https://www.rcsb.org/structure/2vpy>). A: Structural representation among the lipid membrane, with in red the extracellular side membrane and in blue the cytosolic side membrane. B: thiosulfate reductase big unit. C: NRFC protein small unit. D: membrane spanning protein unit.

However, with the Quick2D precision software, no sequences associated with the transmembrane were detected for any of the three CDSs of each of the six bacteria. In conclusion, based on the assumption that the three CDS found by comparative genomics are involved in the disproportionation of elemental sulfur, it is still very difficult to assert that the entire protein will be structured by the two or three proteins identified. This protein is likely periplasmic or attached to the membrane or maybe even extracellular.

The protein encoded by the first short CDS, which have homology to the chaperon protein TorD, could have an impact on the topology of the whole protein, such as TorD for the TMAO reductase (Fig. 25).



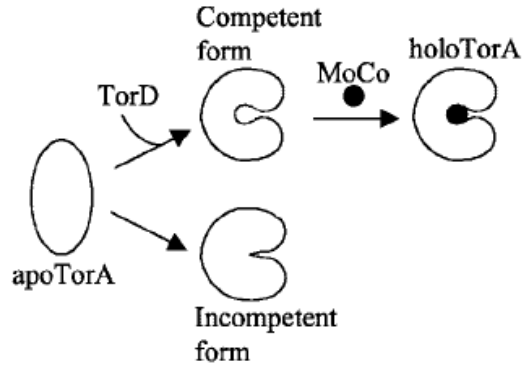


Figure 25: Model for the role of TorD in the TorA maturation pathway with bis(MGD)Mo cofactor (Ilbert et al., 2003).

As said before, this protein could be periplasmic and may have attachment to the membrane. It was suggested that, in *Thermosulfurimonas dismutans* (Mardanov et al., 2016) and in *Desulfurella amilsii* (Florentino et al., 2019), a direct cellular contact with elemental sulfur is not strictly required for the disproportionation reaction.

Additionally, putative homologs of small and large subunits of molybdopterin were found with Prokka within other known  $S^0$ -disproportionating bacteria, such as *Desulfurella amilsii*, *Caldimicrobium thiodismutans*, *Desulfocapsa sulfexigens* and *Dissulfurispira thermophila*, but sharing less amino acid identity. However, homologs of putative chaperone protein were not always found. This suggests that the first CDS candidate for sulfur-disproportionation could not be mandatory for the reaction, but it is purely hypothetical.

Complementary comparative genomic analyses were also performed in the article draft about the genome of *Thermosulfurimonas* strain F29.

Analyses of gene expression in other bacterial models published by other teams revealed interesting features about these CDSs that we identified and which could be putative genomic markers of sulfur disproportionation. It was observed in *Desulfurivibrio alkaliphilus* that genes associated to molybdopterin and TorD-like were more expressed under  $S^0$  disproportionation conditions than under DNRA growth conditions (Thorup et al., 2017). Moreover, in *Sulfurimonas* sp. NW10, the same genes encoding molybdopterin and TorD-like proteins were more expressed under sulfur reduction conditions than under nitrate reduction growth conditions (Wang et al., 2021). From those results, we can infer that these three genes are likely associated to elemental sulfur and maybe to elemental sulfur reduction, and possibly associated



to the reduction path of the disproportionation reaction. In any case, functional approaches require to be performed in order to elucidate the function of these three CDSs.

### 3.3 Monitoring of the $S^0$ -dismutation reaction by proteomics and chemical analysis: a preliminary study

#### Protein extraction

First trial of protein extraction provided protein in sufficient quantity and quality to send the cellular soluble extracts for proteomic analyses by LC-MS/MS analyses for the strains *Thermodesulfatator atlanticus* and *Dissulfuribacter thermophilus*, under both  $S^0$ -dismutation and sulfate-reduction, and for *Thermosulfurimonas dismutans* grown by  $S^0$ -dismutation. *T. dismutans* grown by sulfate reduction did not provide a lot of biomass and then enough protein. Thus, we sent 10  $\mu\text{g}$  of proteins to the sequencing platform for all conditions, as recommended, and only 1.3  $\mu\text{g}$  of proteins for *T. dismutans* under sulfate reduction growth conditions. Protein extraction didn't show any clear specific pattern according to the medium or the species but greatest protein concentrations were found for *T. atlanticus* and *D. thermophilus* grown under sulfate reduction conditions.

A second experiment was performed only with *T. atlanticus* and *D. thermophilus* also in  $S^0$  disproportionation and sulfate conditions, but in four replicates for each condition. This second experiment targeted cellular soluble (cytosolic and non-membrane periplasmic proteins) and insoluble (membrane proteins) proteins, and extracellular proteins. Unfortunately, the protein extraction of this second experiment did not work for many conditions, so we did not sequence the proteomes.

In order to understand where most of the proteins were lost in this second experiment, Solenne Giardi (Master student) performed a cell quantification on filters, after staining with acridine range after the removal of ferrihydrite by slow centrifugation (Table 7).

Table 7: Mean cell concentration between the four replicates of cultures carried out under  $S^0$  dismutation and sulfate reduction, in *T. atlanticus* and *D. thermophilus* cultures, before and after a short centrifugation to remove the ferrihydrite.

Strain / Condition (4 replicates)	Mean cellular density (cells/ml)	Mean cellular density after centrifugation at 500g for 1min (cells/ml)	Final number of cells
<i>T. atlanticus</i> / $S^0$	4,37E+07 ( $\pm$ 1,16E+07)	1,55E+07 ( $\pm$ 4,85E+06)	1,39E+09
<i>T. atlanticus</i> / $SO_4^{2-}$	1,12E+08 ( $\pm$ 4,34E+07)		1,01E+10
<i>D. thermophilus</i> / $S^0$	4,50E+07( $\pm$ 1,01E+07)	1,62E+07 ( $\pm$ 4,82E+06)	1,46E+09
<i>D. thermophilus</i> / $SO_4^{2-}$	7,48E+07 ( $\pm$ 1,31E+07)		6,73E+09

Cell counting indicated that few cells were removed with the ferrihydrite, but showed there were still enough cells after centrifugation to perform protein extraction. So, the failure of the experiment was not due to this step.

Proteins were then extracted for each culture condition and each strain, and protein extracts were quantified except for extracellular protein extracts from  $S^0$  disproportionation medium because due to the precipitation of iron species, Amicon filtration units were blocked and no protein concentrates could be obtained at the end. Protein concentrations are given in Table 8.

Table 8: Protein concentrations for each culture condition, and each protein fraction.

Growth condition	Concentration ( $\mu\text{g}\cdot\mu\text{l}$ )	<i>T. atlanticus</i>		<i>D. thermophilus</i>	
		Mean	Standard deviation	Mean	Standard deviation
$S^0$	Cytosolic	0.008	$\pm$ 0.021	0.004	$\pm$ 0.044
	Membrane	1.575	$\pm$ 0.516	0.382	$\pm$ 0.214
$SO_4^{2-}$	Cytosolic	14.818	$\pm$ 1.353	5.520	$\pm$ 2.070
	Membrane	3.139	$\pm$ 0.937	2.512	$\pm$ 1.870
	Extracellular	0.239	$\pm$ 0.013	-0.051	$\pm$ 0.008

These quantifications showed that we got enough proteins for LC-MS/MS analyses only for few conditions: (i) for *T. atlanticus* membrane extracts got under  $S^0$  disproportionation; (ii) for *T. atlanticus* for soluble and membrane protein extracts got under sulfate reduction conditions; (iii) for *D. thermophilus* soluble and membrane protein extracts obtained under sulfate

reduction conditions. We were not able to obtain enough proteins of other fractions and other conditions. These proteins extracts were migrated in an agarose gel electrophoresis which showed that no clear differences could be observed between  $S^0$  disproportionation versus sulfate reduction conditions.

The unsatisfactory results obtained in this second experiment may probably due to human error. Indeed, afterwards we noticed that sonication was performed at 20% amplitude as opposed to 40% in the trial. Whole experiment, from culture growth to protein extraction were repeated with same protocol but by adjusting the amplitude of sonication to 40%, but we still were not able to recover enough proteins. By hypothesis, we can postulate that the presence of ferrihydrite interfere with protein extraction and induced low yields. Several efforts were done in order to increase the protein yields, such as changing the sonication amplitude, using an ultrasound bath and a Covaris system but no good alternative was found.

Moreover, it is difficult to determine if in addition of low protein extraction yields, ferrihydrite could affect and interact with proteins and then change the final results. Indeed, ferrihydrite might interact with proteins.

In conclusion, protein extracts were not sent to the LC-MS/MS platform as our condition dataset was incomplete. In the future, it would be interesting to repeat this experiment of comparative proteomics under sulfate reduction and  $S^0$  disproportionation conditions without ferrihydrite, to facilitate all steps. This experiment could be carried in a gas-lift bioreactor under a continuous gas sweep, which would allow to continuously evacuate the  $H_2S$  produced and to obtain high cellular biomasses.

#### Chemical monitoring and growth kinetics

Because we were not able to get high protein yields in this experiment, aliquots taken throughout the growth of the strains for ion chromatography analysis were not analyzed. We however managed to see sulfate production over time among *T. atlanticus* cultures incubated under  $S^0$  disproportionation conditions (data not shown). Only gas chromatography and cell concentrations that were carried out in real time during the monitoring of the cultures are reported here.

Growth curves of both strains cultivated under conditions of sulfur dismutation and conditions of sulfate reduction are shown in Figure 26. Standard deviation is quite high at the beginning of growth kinetics, as cell abundances were very low.

Aliquots of these cultures were fixed with glutaraldehyde and stored at  $-20^{\circ}\text{C}$ . It would have been necessary to count again these aliquots to be sure to count  $>500$ -stained cells (instead of a given number of fields) to decrease the standard error. However, these cell counting won't be done as the whole experiment will be restarted from the beginning.

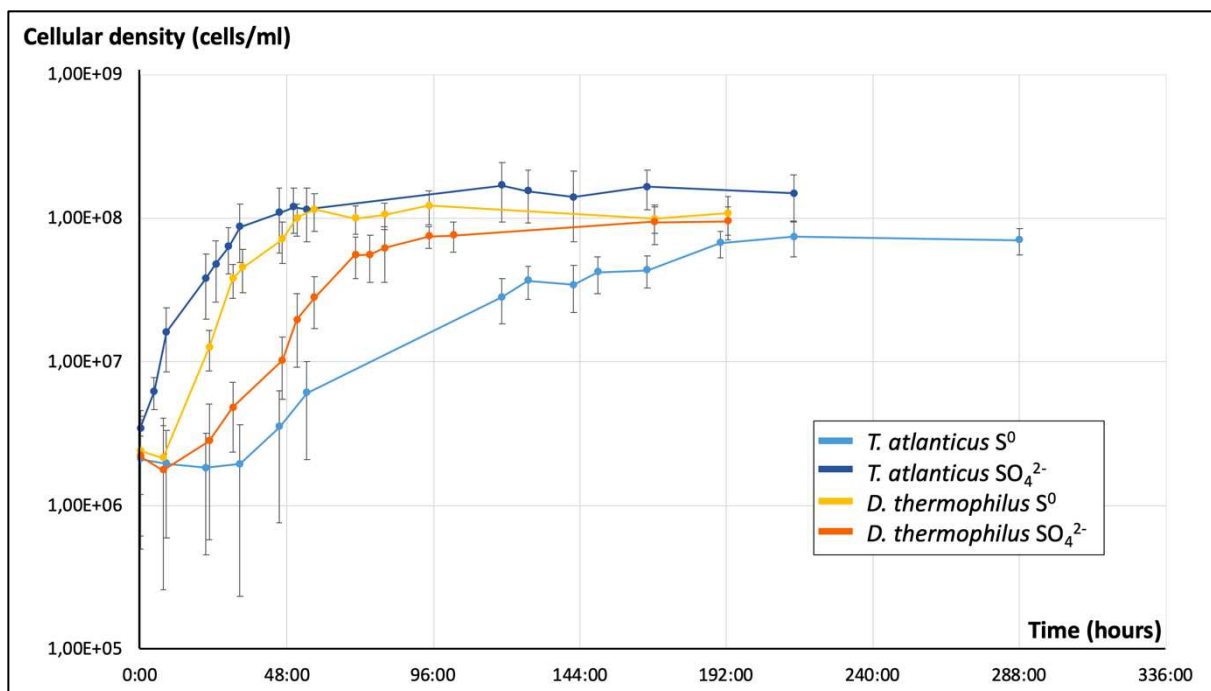


Figure 26: Growth curves of *T. atlanticus* and *D. thermophilus* under  $\text{S}^0$  disproportionation and dissimilatory sulfate reduction growth conditions based on three replicates. Cellular density is reported in  $\log_{10}$ .

Gas chromatography analyses of cultures carried out under sulfate reduction conditions revealed an  $\text{H}_2\text{S}$  production in all replicate cultures of both strains, as opposed to the negative controls (Fig. 27). We can then confirm that *D. thermophilus* can grow by dissimilatory sulfate reduction. To assert this, in the future, it would be nice to measure sulfate evolution by ionic chromatography, and  $\text{H}_2$  and  $\text{CO}_2$  evolution by gas chromatography.

It is important to note that  $\text{H}_2\text{S}$  is also present in the soluble phase, but it was not calculated for this experiment. Gas chromatography associated to  $\text{S}^0$  disproportionation cultures was also not reported because  $\text{H}_2\text{S}$  is scavenged by ferrihydrite, and its quantification implies the

acidification of the medium to release it. In conclusion, in the future, it would be preferable to carry out this experiment without ferrihydrite, both to get higher protein extraction yields and also to quantify sulfide production.

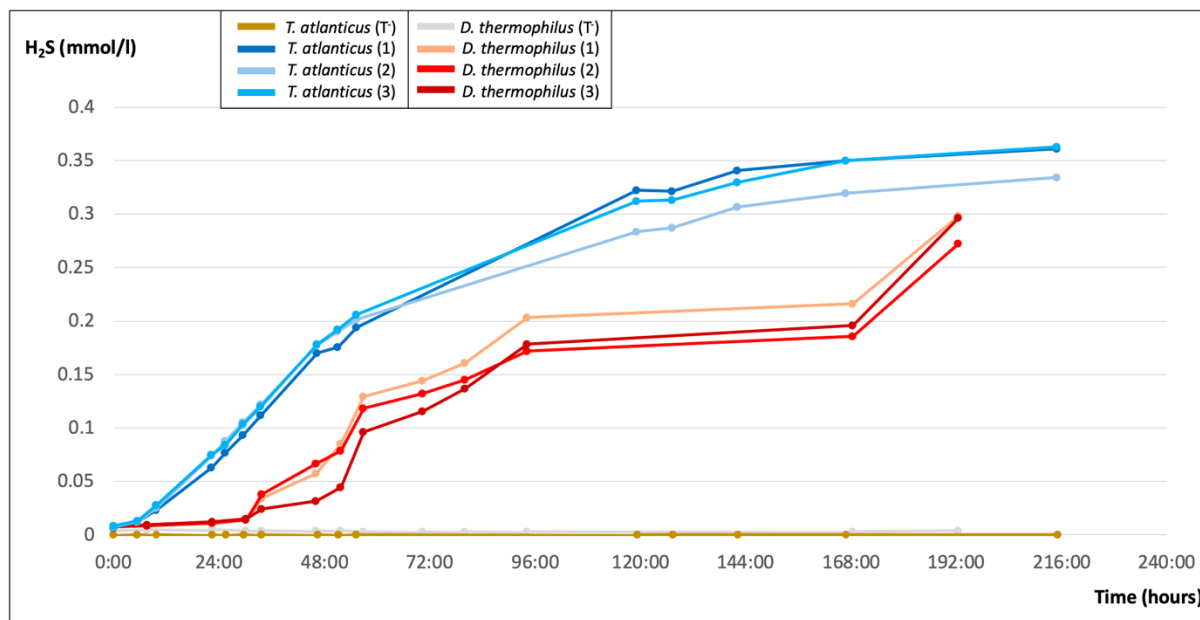


Figure 27: Hydrogen sulfide production over time for the three replicates of *T. atlanticus* and *D. thermophilus* and associated negative controls incubated under dissimilatory sulfate reduction conditions.

#### Proteome analysis on trial data

We decided to analyze proteomes of *T. atlanticus*, *D. thermophilus* and *T. dismutans* incubated under  $S^0$  disproportionation and sulfate reduction conditions (but without replicates) from the trial experiment; as there were no replicate in this experiment, their interpretation is very limited. Chromatograms are given in Figure 28.

As expected, the chromatogram of *T. dismutans* under sulfate reduction conditions was not of good quality. This confirms that 1.3  $\mu\text{g}$  of proteins is not enough for LC-MS/MS analysis, with the protocol of our collaborator. As spectra obtained with the different bacteria and under the two conditions shared resemblances and differences, we analyzed them thanks to available predicted proteomes obtained from genome annotations.

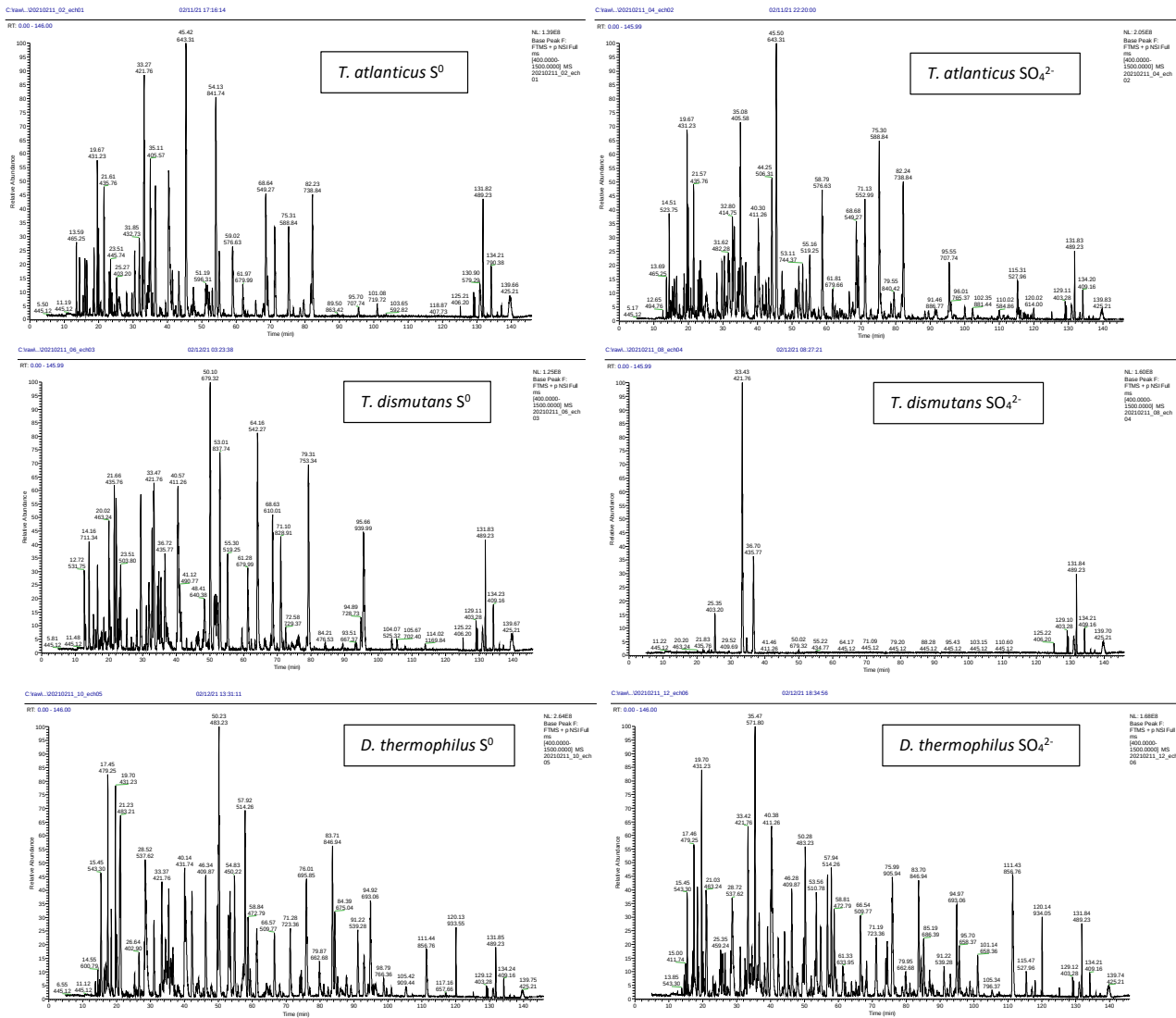


Figure 28: Chromatograms from LC-MS/MS analyses of cellular soluble protein extracts of *T. atlanticus*, *D. thermophilus* and *T. dismutans* under  $S^0$  disproportionation and sulfate reduction growth conditions.

The results transmitted by the platform were in the form of a number of spectra (or peptides) affiliated for each protein identified in a given sample. From these data, different indicators were calculated:

- The number of specific spectra: this index corresponds to the number of mass spectra from the MS/MS analysis that were assigned to a single identified protein.

- The PAI (Protein Abundance Index): this index corresponds to the number of spectra (or peptides) affiliated, divided by the theoretical number of tryptic peptides composing the protein of interest. This index is a good indicator of the relative amount of a protein in a sample.
- The NSAF (Normalized Spectral Abundance): this indicator is calculated as the number of spectra (or peptides) affiliated with a protein, normalized by its length (or mass), and divided by the sum of spectra affiliated with each identified protein, normalized by their respective length (or mass). An analysis based on counting the identified spectra, without considering the respective length of each protein, would tend to overestimate the abundance of long sequence proteins, and conversely for short sequence proteins.

Globally, based on spectra annotations, less proteins and peptides were identified under  $S^0$  disproportionation conditions than under sulfate reduction conditions (except for *T. dismutans* for which we had a low amount of proteins) (Table 9). Number of spectra from first step analyses (separation by hydrophobicity) was similar but it was at the second step analysis (separation by hydrophobicity) that we observed different amounts of spectra according to growth conditions; but without replicates, statistical analyses are excluded. Spectra assignment were between 24.62% and 35.80% but only based on cellular soluble proteins, putative cytosolic and non-membrane periplasmic proteins, and then discussion was difficult taking account also that protein extraction protocol may have an impact of the protein recovered especially when ferrihydrite is present.

Table 9: Results and associated statistics of LC-MS/MS analyses for cellular soluble protein extracts of *T. atlanticus*, *D. thermophilus* and *T. dismutans* under  $S^0$  disproportionation and sulfate reduction conditions based on PGAP annotations and predictions.

Protein extracts	Specters MS1	Specters MS2	Spectra assignation (%)	Total identified proteins	Total identified peptides
<i>T. dismutans</i> $S^0$	19418	10916	28.57	203	1819
<i>T. dismutans</i> $SO_4^{2-}$	19498	624	35.80	23	124
<i>T. atlanticus</i> $S^0$	19916	7887	25.47	138	1146
<i>T. atlanticus</i> $SO_4^{2-}$	16287	30644	32.15	703	6144
<i>D. thermophilus</i> $S^0$	18833	15562	24.62	168	1803
<i>D. thermophilus</i> $SO_4^{2-}$	17861	21478	28.36	376	3511

For each strain and condition, we then tried to identify which proteins were present and moreover, compare them between growth conditions in order to determine which proteins are associated to S<sup>0</sup> disproportionation and which ones are associated to sulfate reduction growth conditions (Tables 10, 11 and 12). For each table, we manually retrieved the proteins associated with the spectra when specific spectra, PAI, and NSAF had significant values and when the associated protein name correlated with the S<sup>0</sup> disproportionation or sulfate reduction pathways.

Results are given below:

*Table 10: Spectra annotation analyses and comparison of D. thermophilus grown under S<sup>0</sup> disproportionation and sulfate reduction conditions. Annotations were done according to a putative proteome reference based on Prokka predictions. Differential PAI is green when proteins are more abundant in S<sup>0</sup> disproportionation conditions and in red when protein are more abundant in sulfate reduction condition. In bold is referenced three genes found by comparative genomics.*

Accession (Prokka)	Annotations	% Specific Spectra		% PAI		% NSAF		Diff % PAI
		S <sup>0</sup>	SO <sub>4</sub> <sup>2-</sup>	S <sup>0</sup>	SO <sub>4</sub> <sup>2-</sup>	S <sup>0</sup>	SO <sub>4</sub> <sup>2-</sup>	
GBDBCHIF_01321	Adenylate kinase	2,8239	1,0771	3,5325	1,4004	4,3345	1,5837	2,0719
GBDBCHIF_00302	Sulfite reductase, dissimilatory-type subunit beta	6,9103	2,9944	4,0371	1,9171	5,7807	2,3995	2,0524
GBDBCHIF_01401	Adenylylsulfate reductase subunit alpha	<b>20,3987</b>	8,8970	3,6030	1,9034	10,3106	4,3079	1,6398
GBDBCHIF_00301	Sulfite reductase, dissimilatory-type subunit alpha	4,4186	2,3266	2,3404	1,1528	3,4384	1,7343	1,1484
GBDBCHIF_01108	Bifunctional purine biosynthesis protein PurH	1,4286	0,7324	1,5832	0,6810	1,1274	0,5537	0,8754
GBDBCHIF_00016	hypothetical protein	0,5648	0,3662	1,7494	0,8963	1,7180	1,0671	0,8240
GBDBCHIF_01400	Adenylylsulfate reductase subunit beta	2,7575	1,7665	2,3069	1,4938	6,2343	3,8258	1,7757
GBDBCHIF_01138	Chaperone protein DnaK	2,0930	1,0556	1,3457	0,5924	1,0825	0,5230	0,7306
GBDBCHIF_00017	hypothetical protein	0,4983	0,2585	1,4803	0,7469	1,4757	0,7333	0,7087
GBDBCHIF_01376	hypothetical protein	0,4983	0,1293	0,9719	0,2490	0,7478	0,1858	0,7060
GBDBCHIF_01403	hypothetical protein	3,5548	1,6372	1,3129	0,5921	1,5388	0,6789	0,6987
GBDBCHIF_01111	Coenzyme A disulfide reductase	1,4950	0,5816	1,0766	0,3735	0,8746	0,3259	0,6846
GBDBCHIF_01402	hypothetical protein	0,9635	0,5601	1,0573	0,5068	0,7768	0,4326	0,5328
GBDBCHIF_00015	Sulfur carrier protein TusA	0,9302	0,9048	2,2428	1,6805	3,6620	3,4119	0,5266
GBDBCHIF_02213	hypothetical protein	1,4950	1,0340	1,3083	0,7677	0,5426	0,3595	0,5192
GBDBCHIF_01988	Glyceraldehyde-3-phosphate dehydrogenase 2	1,0963	0,6894	1,1588	0,6224	0,8755	0,5274	0,5172
GBDBCHIF_01259	Glutamine synthetase	1,3953	0,9694	1,4899	0,9603	0,9934	0,6611	0,5054
GBDBCHIF_00261	Nucleoside diphosphate kinase	0,3654	0,1939	0,9252	0,4201	0,8926	0,4536	0,4895
GBDBCHIF_02233	hypothetical protein	0,2326	0,0862	0,6729	0,2134	0,6886	0,2444	0,4478
GBDBCHIF_00969	Manganese-dependent inorganic pyrophosphatase	1,2292	1,0125	1,3457	0,8869	1,3354	1,0537	0,4370
GBDBCHIF_00092	Single-stranded DNA-binding protein	0,0332	0,0215	0,6729	0,2490	0,7580	0,3139	0,4124
GBDBCHIF_01926	Nitroreductase NfnB	0,5316	0,3878	0,8281	0,4884	0,8085	0,5650	0,3262
GBDBCHIF_00610	Thioredoxin 1	0,3987	0,3447	1,0766	0,7469	1,2239	1,0136	0,3123
GBDBCHIF_00662	ATP synthase subunit alpha	1,0631	0,9048	0,8411	0,5913	0,7003	0,5709	0,2363
GBDBCHIF_00660	ATP synthase subunit beta	1,1628	1,0987	0,9933	0,7647	0,8296	0,7509	0,2128
GBDBCHIF_00831	Formate--tetrahydrofolate ligase	1,7608	1,9819	1,1962	0,9820	1,0037	1,0822	0,1954
GBDBCHIF_00227	10 kDa chaperonin	0,2326	0,2370	0,9420	0,8216	0,8106	0,7912	0,1058
GBDBCHIF_01538	Sulfite reductase, dissimilatory-type subunit gamma	0,4319	0,3662	0,5887	0,5135	1,3634	1,1074	0,0661
GBDBCHIF_00640	Sulfate adenylyltransferase	1,1960	1,8526	1,0253	0,9959	0,8854	1,3138	0,0138
GBDBCHIF_00602	D-3-phosphoglycerate dehydrogenase	0,6312	0,7971	0,4325	0,4668	0,4016	0,4857	-0,0407
GBDBCHIF_01835	Alkyl hydroperoxide reductase C	0,2990	0,3231	0,8971	0,9336	0,5053	0,5231	-0,0499
GBDBCHIF_01466	50S ribosomal protein L22	0,1661	0,1939	1,3457	1,4938	0,5053	0,5650	-0,1680
GBDBCHIF_01630	<b>Tetrathionate reductase subunit B</b>	<b>0,0000</b>	<b>0,2154</b>	<b>0,0000</b>	<b>0,2873</b>	<b>0,0000</b>	<b>0,2740</b>	<b>-0,2864</b>
GBDBCHIF_01629	<b>Polysulfide reductase chain A</b>	<b>0,0000</b>	<b>0,6894</b>	<b>0,0000</b>	<b>0,3405</b>	<b>0,0000</b>	<b>0,2892</b>	<b>-0,3394</b>
GBDBCHIF_00303	Protein DsvD	0,0000	0,1723	0,0000	0,5228	0,0000	0,6737	-0,5212
GBDBCHIF_01646	Molybdate-binding protein ModA	0,0000	0,3662	0,0000	0,5432	0,0000	0,4714	-0,5415
GBDBCHIF_00875	hypothetical protein	0,0000	0,1293	0,0000	0,5602	0,0000	0,4992	-0,5584
GBDBCHIF_01004	hypothetical protein	0,0332	0,1077	0,3364	0,9336	0,1463	0,4543	-0,6004
GBDBCHIF_00228	60 kDa chaperonin 1	1,3621	3,1452	0,9221	1,6045	0,8394	1,8566	-0,6942
GBDBCHIF_00554	Acetyl-coenzyme A synthetase	0,0000	1,1202	0,0000	0,7038	0,0000	0,5408	-0,7016
GBDBCHIF_01510	3-isopropylmalate dehydrogenase	0,0000	0,6894	0,0000	0,7202	0,0000	0,6224	-0,7180
GBDBCHIF_00595	Elongation factor G	0,0000	1,4433	0,0000	0,7349	0,0000	0,6784	-0,7326
GBDBCHIF_01409	Elongation factor Tu	0,2658	1,4218	0,2691	1,0083	0,2246	1,1508	-0,7409
GBDBCHIF_01834	Rubryerythrin	0,0000	0,4308	0,0000	0,7469	0,0000	0,7230	-0,7446
GBDBCHIF_00347	TRAP-T-associated universal stress protein TeaD	0,0000	0,2801	0,0000	0,8216	0,0000	0,5945	-0,8190
GBDBCHIF_01229	hypothetical protein	0,0332	0,5170	0,1682	1,3071	0,0889	1,3258	-1,1379
GBDBCHIF_01587	Carbon monoxide dehydrogenase	0,2326	3,2960	0,1884	1,5834	0,1245	1,6904	-1,3935



Table 11: Spectra annotation analyses and comparison of *T. atlanticus* grown under  $S^0$  disproportionation and sulfate reduction conditions. Annotations were done according to a putative proteome reference based on Prokka predictions. Differential PAI is green when proteins are more abundant in  $S^0$  disproportionation conditions and in red when protein are more abundant in sulfate reduction condition. In bold are referenced the three genes found by comparative genomics.

Accession (Prokka)	Annotations	% Specific Spectra		% PAI		% NSAF		Diff % PAI
		$S^0$	$SO_4^{2-}$	$S^0$	$SO_4^{2-}$	$S^0$	$SO_4^{2-}$	
LILJINEH_01845	Adenylylsulfate reductase subunit alpha	20,6897	9,2428	4,6589	1,8128	9,2404	4,1996	2,8461
LILJINEH_01846	Adenylylsulfate reductase subunit beta	3,6472	1,1554	4,5664	1,8841	7,2324	2,3308	2,6822
LILJINEH_00495	hypothetical protein	0,3316	0,0825	2,8540	0,5652	0,8885	0,2250	2,2887
LILJINEH_00494	Sulfur carrier protein TusA	1,1936	0,4126	3,0442	0,8793	4,1284	1,4519	2,1650
LILJINEH_00496	hypothetical protein	1,7905	0,3301	2,7724	0,8075	4,4014	0,8255	2,9650
LILJINEH_00497	hypothetical protein	0,4642	0,1032	1,9978	0,3768	2,3402	0,5291	2,6210
LILJINEH_01422	Manganese-dependent inorganic pyrophosphatase	3,4483	1,6092	2,5836	1,1106	3,3410	1,5862	2,4730
LILJINEH_00709	Sulfite reductase, dissimilatory-type subunit gamma	0,8621	0,1238	1,5221	0,2512	2,4191	0,3534	2,7709
LILJINEH_01367	Single-stranded DNA-binding protein	0,4642	0,1238	1,5982	0,4522	1,0005	0,2714	2,1460
LILJINEH_01844	hypothetical protein	2,0557	1,0316	1,9027	0,8583	1,4664	0,7486	2,1443
LILJINEH_01928	Sulfite reductase, dissimilatory-type subunit alpha	3,8462	2,5170	2,2832	1,2779	2,6668	1,7754	2,1053
LILJINEH_01683	hypothetical protein	0,5968	0,1651	1,1416	0,2931	0,7685	0,2162	2,0485
LILJINEH_01746	Formate-tetrahydrofolate ligase	2,3210	1,0522	1,3862	0,5922	1,1761	0,5424	2,0794
LILJINEH_00942	Fructose-1,6-bisphosphate aldolase/phosphatase	1,8568	1,0109	1,6823	0,8925	1,4496	0,8029	2,0789
LILJINEH_01843	hypothetical protein	3,1830	1,3410	1,3884	0,6009	1,2847	0,5506	2,0785
LILJINEH_02031	hypothetical protein	0,1989	0,0619	1,1416	0,3768	0,7586	0,2401	2,0768
LILJINEH_00458	Glyceraldehyde-3-phosphate dehydrogenase 1	1,3926	0,5983	1,2684	0,5443	0,9839	0,4300	2,0724
LILJINEH_00402	hypothetical protein	0,3979	0,1857	1,4270	0,7537	1,0381	0,4929	2,0673
LILJINEH_01759	5-methyltetrahydrofolate:corrinoid/iron-sulfur protein co-methyltransferase	0,6631	0,5777	1,3319	0,7222	0,9267	0,6913	2,0696
LILJINEH_01563	hypothetical protein	1,6578	1,3410	2,2832	1,6748	4,1790	3,4390	2,0684
LILJINEH_02088	Adenylate kinase	1,2599	1,0935	1,9718	1,3703	1,7513	1,5462	2,0616
LILJINEH_00460	Glyceraldehyde-3-phosphate dehydrogenase	1,1273	0,6396	1,1416	0,5985	1,0040	0,5794	2,0543
LILJINEH_00616	Bifunctional purine biosynthesis protein PurH	1,4589	0,8459	1,1960	0,6819	1,0068	0,5939	2,0541
LILJINEH_01927	Sulfite reductase, dissimilatory-type subunit beta	3,0504	2,8471	2,0817	1,5960	2,2130	2,1013	2,0485
LILJINEH_02007	Acetyl-coenzyme A synthetase	1,9894	1,3823	1,1416	0,6908	0,8925	0,6309	2,0450
LILJINEH_01288	hypothetical protein	0,8621	0,6808	1,0601	0,6998	0,5526	0,4440	2,0360
LILJINEH_02128	Ketol-acid reductoisomerase (NAD(+))	0,7294	0,5364	1,1416	0,7879	0,6575	0,4919	2,0357
LILJINEH_00577	Thioredoxin	0,5305	0,4333	1,1416	0,8075	1,4747	1,2253	2,0334
LILJINEH_00592	Chaperone protein DnaK	1,6578	1,4236	1,0503	0,8742	0,7622	0,6658	2,0170
LILJINEH_00443	60 kDa chaperonin 1	2,4536	3,0534	1,4678	1,4669	1,3540	1,7142	2,0008
LILJINEH_01915	Rubryerythrin	0,3979	0,4333	0,6227	0,6509	0,6229	0,6900	2,0028
LILJINEH_02109	50S ribosomal protein L3	0,3979	0,5570	0,6850	0,9044	0,5556	0,7914	2,0194
LILJINEH_00295	<b>Tetrathionate reductase subunit B</b>	<b>0,0000</b>	<b>0,1651</b>	<b>0,0000</b>	<b>0,2512</b>	<b>0,0000</b>	<b>0,2181</b>	<b>2,0251</b>
LILJINEH_02107	50S ribosomal protein L23	0,1989	0,2476	0,8562	1,1305	0,6164	0,7804	2,0243
LILJINEH_00619	Nucleoside diphosphate kinase	0,2653	0,3920	0,7611	1,0677	0,5596	0,8413	2,0306
LILJINEH_01849	Hydrogenase-2 large chain	0,0000	0,6189	0,0000	0,4845	0,0000	0,3309	2,0484
LILJINEH_00294	<b>Thiosulfate reductase molybdopterin-containing subunit PhsA</b>	<b>0,0000</b>	<b>0,7221</b>	<b>0,0000</b>	<b>0,4974</b>	<b>0,0000</b>	<b>0,2883</b>	<b>2,0497</b>
LILJINEH_00026	3-isopropylmalate dehydrogenase	0,1989	0,7427	0,2283	0,7788	0,1644	0,6243	2,0550
LILJINEH_02091	50S ribosomal protein L30	0,0663	0,1238	0,5708	1,1305	0,3234	0,6141	2,0559
LILJINEH_01696	Inositol-3-phosphate synthase	0,0000	0,6808	0,0000	0,6594	0,0000	0,5598	2,0659
LILJINEH_01269	hypothetical protein	0,0000	0,3920	0,0000	0,6594	0,0000	0,6857	2,0659
LILJINEH_01327	Periplasmic nitrate reductase	0,0000	1,3823	0,0000	0,6650	0,0000	0,5229	2,0660
LILJINEH_01667	ATP synthase subunit beta	0,1326	1,4236	0,1038	0,7708	0,0832	0,9088	2,0667
LILJINEH_00914	Selenocysteine-containing peroxiredoxin PrxU	0,0000	0,2063	0,0000	0,6783	0,0000	0,5574	2,0678
LILJINEH_00325	hypothetical protein	0,0000	0,4539	0,0000	0,6908	0,0000	0,5494	2,0698
LILJINEH_02046	30S ribosomal protein S7	0,0663	0,3301	0,1631	0,8613	0,1256	0,6362	2,0698
LILJINEH_00423	Pyruvate synthase subunit PorB	0,0000	0,5364	0,0000	0,7222	0,0000	0,5203	2,0722
LILJINEH_01926	Protein DsvD	0,2653	0,4745	1,1416	1,8841	0,9987	1,8176	2,0742
LILJINEH_01266	hypothetical protein	0,0000	0,1444	0,0000	0,8793	0,0000	0,9932	2,0879
LILJINEH_00090	hypothetical protein	0,0000	0,2063	0,0000	0,9421	0,0000	0,6121	2,0942
LILJINEH_00936	hypothetical protein	0,0000	0,5158	0,0000	0,9892	0,0000	0,5738	2,0989
LILJINEH_00741	hypothetical protein	0,0000	0,2063	0,0000	1,1305	0,0000	0,6861	2,1305
LILJINEH_01272	hypothetical protein	0,0663	0,8871	0,1142	1,4696	0,0540	0,7355	2,1355
LILJINEH_00553	50S ribosomal protein L33	0,0000	0,1651	0,0000	1,5073	0,0000	0,8919	2,1507
LILJINEH_01562	Sulfate adenylyltransferase	0,0663	3,5073	0,0457	1,5827	0,0436	2,3481	2,1537
LILJINEH_00240	DNA-binding protein HU	0,0000	0,5158	0,0000	2,7634	0,0000	1,7342	2,2634
LILJINEH_01158	hypothetical protein	0,0000	0,3714	0,0000	2,8262	0,0000	1,4407	2,8262

Table 12: Spectra annotation analyses and comparison of *T. dismutans* grown under  $S^0$  disproportionation and sulfate reduction conditions. Annotations were done according to a putative proteome reference based on Prokka predictions. Differential PAI is green when proteins are more abundant in  $S^0$  disproportionation conditions and in red when protein are more abundant in sulfate reduction condition.

Accession (Prokka)	Annotations	% Specific Spectra		% PAI		% NSAF		Diff % PAI
		$S^0$	$SO_4^{2-}$	$S^0$	$SO_4^{2-}$	$S^0$	$SO_4^{2-}$	
KACJOEPB_00885	hypothetical protein	0,5123	0,0000	2,2390	0,0000	1,4253	0,0000	2,2390
KACJOEPB_00998	protein co-methyltransferase	1,5370	0,0000	1,7641	0,0000	1,5783	0,0000	1,7641
KACJOEPB_00061	Bifunctional purine biosynthesis protein PurH	1,8631	0,0000	1,5341	0,0000	1,3228	0,0000	1,5341
KACJOEPB_00767	Nucleoside diphosphate kinase	0,5589	0,0000	1,4927	0,0000	1,2130	0,0000	1,4927
KACJOEPB_00416	Cold shock-like protein	0,2795	0,0000	1,4927	0,0000	1,2764	0,0000	1,4927
KACJOEPB_00708	50S ribosomal protein L29	0,2795	0,0000	1,4927	0,0000	1,3157	0,0000	1,4927
KACJOEPB_01510	hypothetical protein	1,0247	0,0000	1,4097	0,0000	2,6350	0,0000	1,4097
KACJOEPB_00504	50S ribosomal protein L20	0,2329	0,0000	1,2439	0,0000	0,6039	0,0000	1,2439
KACJOEPB_00707	50S ribosomal protein L16	0,3726	0,0000	1,1941	0,0000	0,8203	0,0000	1,1941
KACJOEPB_00719	50S ribosomal protein L15	0,3726	0,0000	1,1941	0,0000	0,7453	0,0000	1,1941
KACJOEPB_01700	3-isopropylmalate dehydrogenase	1,1178	0,0000	1,1728	0,0000	0,9502	0,0000	1,1728
KACJOEPB_00886	Sulfur carrier protein TusA	0,4192	0,0000	1,1195	0,0000	1,5091	0,0000	1,1195
KACJOEPB_00642	Thioredoxin 1	0,3726	0,0000	1,0449	0,0000	1,0558	0,0000	1,0449
KACJOEPB_00007	Chaperone protein DnaK	1,7233	0,0000	1,0047	0,0000	0,8163	0,0000	1,0047
KACJOEPB_00700	50S ribosomal protein L3	0,5589	0,0000	0,9951	0,0000	0,8106	0,0000	0,9951
KACJOEPB_01110	50S ribosomal protein L19	0,3726	0,0000	0,8530	0,0000	0,9915	0,0000	0,8530
KACJOEPB_01440	Rubryerythrin-2	0,4192	0,0000	0,8396	0,0000	0,7681	0,0000	0,8396
KACJOEPB_01282	LL-diaminopimelate aminotransferase	0,8384	0,0000	0,7902	0,0000	0,6629	0,0000	0,7902
KACJOEPB_01147	Manganese-dependent inorganic pyrophosphatase	2,0028	0,8403	1,6585	0,8756	1,9395	1,0875	0,7829
KACJOEPB_01689	Sulfite reductase, dissimilatory-type subunit alpha	2,4220	0,8403	1,3861	0,7505	1,7236	0,7992	0,6355
KACJOEPB_01611	Sulfite reductase, dissimilatory-type subunit gamma	0,3260	0,0000	0,6219	0,0000	0,9412	0,0000	0,6219
KACJOEPB_01477	NADH peroxidase	0,8850	0,0000	0,6106	0,0000	0,4759	0,0000	0,6106
KACJOEPB_00246	hypothetical protein	0,5123	0,0000	0,6106	0,0000	0,7918	0,0000	0,6106
KACJOEPB_01780	hypothetical protein	0,1863	0,0000	0,5971	0,0000	0,4287	0,0000	0,5971
KACJOEPB_01506	hypothetical protein	2,5151	2,5210	1,0086	1,2779	1,0514	1,4084	0,2694
KACJOEPB_00813	Bifunctional purine biosynthesis protein PurH	0,8384	0,8403	1,2688	1,5761	1,2828	1,7183	0,3074
KACJOEPB_00656	Transaldolase	0,6986	0,8403	0,8612	1,2124	0,9852	1,5836	0,3513
KACJOEPB_00985	Formate-tetrahydrofolate ligase	1,3041	1,6807	0,6949	1,0870	0,6799	1,1709	0,3921
KACJOEPB_00209	Acetyl-coenzyme A synthetase	1,2110	1,6807	0,6664	1,1258	0,5606	1,0398	0,4594
KACJOEPB_01511	Sulfate adenylyltransferase	0,1863	0,8403	0,1106	0,5838	0,1264	0,7620	0,4732
KACJOEPB_00472	Aspartate-semialdehyde dehydrogenase 2	0,4192	0,8403	0,3732	0,9851	0,3762	1,0078	0,6119
KACJOEPB_00485	Isocitrate dehydrogenase [NADP]	1,2110	1,6807	0,9122	1,7513	0,9105	1,6887	0,8391
KACJOEPB_00467	hypothetical protein	0,6055	0,8403	1,3861	2,2516	1,6397	3,0412	0,8656
KACJOEPB_02000	Glyceraldehyde-3-phosphate dehydrogenase 2	1,2110	1,6807	1,3327	2,2516	0,8995	1,6682	0,9189
KACJOEPB_02002	Glyceraldehyde-3-phosphate dehydrogenase	0,6055	1,6807	0,5390	1,7513	0,5548	2,0578	1,2122
KACJOEPB_00438	Rubryerythrin	0,1397	0,8403	0,2239	1,5761	0,2239	1,7992	1,3522
KACJOEPB_00016	4-hydroxy-tetrahydrodipicolinate reductase	0,6055	1,6807	0,6468	2,1015	0,6863	2,5456	1,4547
KACJOEPB_00222	Ketol-acid reductoisomerase (NAD(+))	1,1178	2,5210	0,9951	2,6269	1,0366	3,1241	1,6318
KACJOEPB_01199	S-adenosylmethionine synthase	0,5589	2,5210	0,4714	2,4886	0,4420	2,6640	2,0173
KACJOEPB_02056	hypothetical protein	0,1397	0,8403	0,4478	3,1523	0,3751	3,0145	2,7045
KACJOEPB_00884	hypothetical protein	0,8850	1,6807	1,2128	3,9403	2,2381	5,6802	2,7275
KACJOEPB_01507	hypothetical protein	1,8165	4,2017	1,4097	4,3781	1,3459	4,1604	2,9684
KACJOEPB_00685	Fructose-1,6-bisphosphate aldolase/phosphatase	2,0494	5,0420	1,8907	6,3045	1,6460	5,4118	4,4138
KACJOEPB_00764	Glutamine synthetase	0,9781	5,0420	0,9454	6,3045	0,6368	4,3870	5,3592
KACJOEPB_01690	Sulfite reductase, dissimilatory-type subunit beta	3,6330	6,7227	2,3323	7,8807	2,7115	6,7054	5,5484
KACJOEPB_00129	60 kDa chaperonin 1	2,1425	9,2437	1,3733	6,9350	1,2141	7,0003	5,5617
KACJOEPB_01367	Flagellin	0,9315	5,8824	0,9329	6,8956	0,5090	4,2956	5,9627
KACJOEPB_01509	Adenylylsulfate reductase subunit beta	3,2604	3,3613	2,6655	9,0065	6,4786	8,9260	6,3410
KACJOEPB_01508	Adenylylsulfate reductase subunit alpha	14,0196	27,7311	2,9627	14,3285	6,4417	17,0277	11,3657

From spectra analyses, we made a limited discussion because we did not have replicates for this experiment. We also elaborated few hypotheses:

Firstly, proteins associated to the sulfate reduction pathway (AprA, AprB, DsrA and DsrB) were present under  $S^0$  disproportionation and under sulfate reduction conditions, and were generally more expressed under  $S^0$  disproportionation conditions in this dataset without replicates. We can think that those enzymes are clearly associated to both processes in these bacterial taxa, as already shown in other bacterial model. Under  $S^0$ -disproportionation condition, the adenylyl sulfate reductase (AprAB) accounts for 2.3% (beta-subunit) to 3.6% (alpha-subunit), 4.6% to 4.7%, and 2.7% to 3.0% of the total cytosolic proteins identified in *D. thermophilus*, *T. atlanticus*, and *T. dismutans*, respectively (%PAI). These proteins are thus always overexpressed compared to the sulfate reduction condition for *D. thermophilus* and *T. atlanticus*. Nonetheless, this overexpression is not observed for the sulfate adenylyltransferase (SAT). These data suggest that the adenylyl sulfate reductase is a predominant functional enzyme in the elemental sulfur dismutation pathway(s) in the three strains studied. Furthermore, a manganese-dependent inorganic pyrophosphatase associated to sulfate reduction was overexpressed under  $S^0$  disproportionation condition. However, as discussed, ferrihydrite could have an impact on protein extraction but also directly on bacteria which can induce the production of associated protein, as stress induced protein. For example, in the iron-respiring archaea *Ferroglobus placidus*, AprA-like and *sat* genes showed increased mRNA transcripts when grown on insoluble Fe(III) oxide (Smith et al., 2015).

Additionally, the adenylate kinase protein was overexpressed under  $S^0$  disproportionation condition. This protein is generally involved in phosphate transfer, cellular energy homeostasis and may potentially be involved in oxidative process of disproportionation, relative to ATP production. It might indicate that more phosphate groups are transferred during this disproportionation process.

We also found that the sulfur carrier protein TusA was overexpressed under  $S^0$  disproportionation condition. This seems logical because elemental sulfur was totally absent in sulfate reduction cultures, already studied elsewhere (Slobodkin and Slobodkina, 2019; Umezawa et al.; 2020). Sulfur carrier protein may act as a cytoplasmic sulfur donor protein to proteins such as DsrC or rhodanese proteins (Stockdreher et al., 2014). The TusA protein, which belongs to the YTD genomic cluster, has been proposed to be a genomic marker of sulfur disproportionation in a recent study by Umezawa et al. (2020). However, TusA and the whole

YTD gene cluster were found in the genome of *T. autotrophicus* and *T. indicus*, which are unable to disproportionate sulfur compounds, indicating that this genomic cluster is not specific to ISC-disproportionators. It cannot then be considered as a genomic marker but it is very likely that at least TusA from the YTD gene cluster is involved in S<sup>0</sup> disproportionation pathway. Some hypothetical proteins and proteins involved in other metabolic reactions were also more present under S<sup>0</sup> disproportionation condition, notably in *D. thermophilus* and *T. atlanticus*. Those enzymes were associated to three uncharacterized proteins, thioredoxin, and putative adenylylsulfate reductase-associated electron transfer protein QmoA and QmoB. The QmoC subunit known to be on the membrane was not detected here. However, those proteins won't be discussed here due to the inherent biases of our approach. Finally, some proteins observed only under S<sup>0</sup> disproportionation condition were observed, namely 1 protein for *T. atlanticus* (catalase-peroxidase) and 9 proteins for *D. thermophilus* (fumarylacetoacetate hydrolase family, regulatory FmdB family, DUF3373 domain-containing, alginate export protein, uncharacterized, thioredoxin reductase, cytochrome c family, tetrathionate reductase subunit A and NUDIX hydrolase). These results won't be discussed for the same reasons.

In order to compare these results with those of comparative genomics, we searched for the three CDSs predicted to be involved in S<sup>0</sup> disproportionation (chaperone protein, and two subunits of molybdopterin oxidoreductase). Surprisingly, we observed that the large and small subunits of molybdopterin were only expressed under sulfate reduction conditions. Chaperone associated protein was not found in any condition which may indicate that this protein is extracellular or membrane associated. We can conclude that the three CDS we found by comparative genomics seem unlikely involved in the reaction of S<sup>0</sup> disproportionation condition.

In conclusion, the results are difficult to interpret because these analyses are only based on two bacterial models for which we have all the results, *D. thermophilus* and *T. atlanticus*, grown only under two conditions and without replicates. In addition, this experiment considered only the cellular soluble protein fractions (proteins from the cytosol and the periplasm), and did not take into account the potential effects of ferrihydrite on final protein extract composition.

We can nevertheless speculate that *T. dismutans*, *D. thermophilus* and *T. atlanticus* use dissimilatory sulfite reductase and adenylylsulfate reductase in reverse direction, and adenylate kinase proteins to produce energy, in opposite direction of dissimilatory sulfate reduction pathway, which had been already hypothesized several times or confirmed in some bacterial

models (Krämer and Cypionka, 1989; Cypionka et al., 1998; Frederiksen and Finster, 2003; Finster, 2008; Mardanov et al., 2016; Slobodkin and Slobodkina, 2019; Allieux et al., 2020). Nonetheless, as proposed by Slobodkin and Slobodkina (2019), our results suggest also that the *sat* gene might not be important for the sulfur disproportionation process but some other genes could, such as the gene coding for the sulfur carrier TusA. Furthermore, one might think that pathways are different for each strain studied, and that most strains, depending on their genomic resources, will use a specific and adapted pathway to perform the dismutation of sulfur compounds. However, these hypotheses need to be substantiated and these data may be interesting to compare with the results of experiments that will be conducted in the future in our laboratory on this subject.

### **3. Discussion, conclusions and perspectives**

Various approaches were implemented in this work in order to better understand the ecophysiology of  $S^0$  disproportionators from marine hydrothermal vents, their genomic potential and their catabolic pathways.

In summary, we obtained several new enrichment cultures under sulfur disproportionation conditions and we were able to isolate three new  $S^0$ -disproportionating taxa from deep-sea hydrothermal vents at the Lucky Strike vent field (Mid-Atlantic Ridge):

- (i) One new species of the genus *Thermosulfurimonas* in the phylum *Thermodesulfobacteria*, recently proposed to be reclassified in the new phylum *Desulfobacterota* (Waite et al., 2020), *Thermosulfurimonas* strain F29.
- (ii) Two new strains of the family *Desulfobulbaceae*, strains M19 and B35, in the phylum *Deltaproteobacteria* recently proposed to be reclassified in the new phylum *Desulfobacterota* (Waite et al., 2020). Because they are predicted to represent new genera, it would be interesting to characterize the physiology of strains M19 and B35 and to analyze their genome content.

The physiological characterizations of the new *Desulfobulbaceae* isolates, namely strain M19 and *Thermosulfurimonas* strain F29 are currently in progress in the lab (work of Erwann Vince and Stéven Yvenou).

From those results, we can observe that we were able to isolate relatively easily several S<sup>0</sup>-disproportionators from various hydrothermal samples. S<sup>0</sup> disproportionation is endergonic under standard conditions. This suggests that ISC-disproportionators are probably not rare in deep-sea hydrothermal vent ecosystems and that deep-sea hydrothermal vent conditions are thermodynamically favorable for this reaction.

Some efforts have been done in order to find some ISC-disproportionating archaea (anaerobic, *sor*-independent ones), but without success. From an evolutionary perspective, it might be interesting to pursue these investigations in order to try to discover archaea carrying out this reaction.

In the current state of the art, we can observe that ISC-disproportionators are present in a large range of natural environments and belong to various phyla. After many advances made in the 80's and 90's, then very few studies at the beginning of the 2000's, this process is experiencing a renewed interest. We can reasonably think that we will probably discover new taxa carrying out this reaction (for their growth or their maintenance) in the near future.

This metabolic capacity is rarely sought during physiological characterizations of new taxa. In this work, we demonstrated that the species *Thermodesulfatator atlanticus* is able to disproportionate elemental sulfur, while *Thermodesulfatator autotrophicus* and *Thermodesulfatator indicus* are not. This metabolic property had not been tested during the first works carried out on these strains. It is possible that other prokaryotic taxa have the ability to disproportionate ISC but have not been tested for. Models tested and confirmed to be able to disproportionate sulfur compounds or not, are very valuable for downstream applications. For example, *T. autotrophicus* and *T. indicus* are taxa unable to perform S<sup>0</sup> disproportionation but are very similar to *T. atlanticus*, *T. dismutans*, *T. marina*, *Thermosulfurimonas* strain F29, and *T. ammonigenes*, and are relevant models for comparative genomics and proteomics purposes. Alternatively, finding other or new microorganisms involved in the sulfur cycle with genes associated with sulfate reduction or sulfide oxidation and confirming their inability to perform ISC-dismutation could significantly help us downstream by incorporating them into comparative omics analyses.

Finally, we believe that some improvements should be made to our culture media to promote the disproportionation process of sulfur compounds, by adjusting some elements such as sulfate and sulfide scavengers. For example, we have seen that ferrihydrite can have an impact on downstream applications, but we will discuss that point later.

In this work, we also optimized a procedure to study the genomic capital of  $S^0$ -disproportionating microbial models. Genomic annotation showed especially to be of great use to analyze microorganisms difficult to grow in the laboratory. Genomic analyses were carried out from genomes of 4 strains (*Dissulfurirhabdus thermomarina*, *Thermosulfuriphilus ammonigenes*, *Thermosulfurimonas marina* and *Thermosulfurimonas* strain F29) and two additional genomes of new  $S^0$ -disproportionators (*Desulfobulbaceae* strains M19 and B35) were also assembled. Three articles have already been published, and one will be submitted soon. Genomes of the *Desulfobulbaceae*'s strains M19 and B35 will be valorized as draft genome assemblies (maybe with additional long reads sequences) and analyses, after the PhD defense. Those results allowed us to better understand the genomic capital of bacteria isolated from deep-sea or shallow-sea hydrothermal vents and to build new hypothesis regarding them. We could observe that the genomes of those four bacteria were relatively small but with a high coding sequences density. Genes of the sulfate reduction pathway were present in all of the 4 genomes analyzed, which can indicate that the reducing branch of the microbial sulfur dismutation pathway could proceed *via* the sulfate reduction pathway in reverse direction, in these bacterial strains. As a perspective, it would be interesting to analyze and annotate new genomes of sulfur disproportionators. It would be particularly interesting to analyze the genome of *Dissulfurimicrobium hydrothermale* as this strain only grows *via* ISC disproportionation (Slobodkina et al., 2016). This project already started in the framework of another PhD project. In addition, it would be of interest to perform additional genome analyses of species in the genus *Caldimicrobium* and comparative genomics on this group. Finally, it would also be of great interest to annotate and compare the genome of an ISC-dismutating *Archaea*, if one can be found in culture.

Gathering all genomic data, we performed comparative genomic analyses focused on the genomes of all ISC-disproportionators but we were unable to identify gene sequences shared among all of them. We then compared genomes based on their phylogenetic position, diversity of disproportionation sulfur species abilities, and bacteria's isolation sources. We finally retrieved three CDS, two subunits of molybdopterins oxidoreductases and an associated

chaperon protein, similar to thiosulfate and polysulfide reductases proteins, from genomes of  $S^0$  disproportionators isolated from marine hydrothermal vents. This reinforces the hypothesis that there are several dismutation proteins and pathways involved in ISC disproportionation. In addition, we were able to find those three CDSs in the genome of *Thermosulfurimonas* strain F29 and also in the genomes of *Desulfurella amilii*, *Caldimicrobium thiodismutans*, *Desulfocapsa sulfexigens* and *Dissulfurispira thermophila* but with less protein identity and sometimes with the chaperone protein missing at the micro-synteny scale. Those proteins could be good candidates of proteins involved in ISC disproportionation. However, our preliminary proteomic analyses are not congruent with this hypothesis. Nevertheless, it has to be kept in mind that our proteomic analyses were biased as they did not include biological nor technical replicates and as these experiments were performed in the presence of ferrihydrite which might have impacted protein patterns. We observed that the two molybdopterins subunits were only detected in the subset data got under sulfate reduction condition in *D. thermophilus* and *T. atlanticus* and were not observed in *T. dismutans* in any conditions.

The same three CDSs were obtained furthermore in the comparative genomics study of *Thermosulfurimonas* strain F29, in addition to other genes (article draft). The finding that those three associated proteins were not found in the proteomes of trial experiment still doesn't strictly exclude their involvement or attribution as genomic markers of  $S^0$  disproportionation. These proteins could be extracellular or associated to the cell membrane or also affected by ferrihydrite in  $S^0$  disproportionation growth conditions. To definitely answer this question, it will be necessary to analyze full proteomes, with replicates, got from cultures preferably grown without ferrihydrite.

Hence, from all our data, it is then impossible to conclude if our three-candidate genes found in  $S^0$ -disproportionators' genomes can be used as genomic markers specific of  $S^0$  disproportionation.

In the comparative genomic analyses described in the article draft about *Thermosulfurimonas* F29 genome, we report about the enigmatic presence of hydrogenases in the genome of strain F29, and in *T. marina* and *T. ammonigenes* genomes, while these strains were described to be unable to use  $H_2$  as an electron donor (strain F29 only tested with sulfate as a terminal electron acceptor). We speculated that those hydrogenases might be involved in other metabolic pathways and possibly in ISC disproportionation. Hydrogenases may act as electron bifurcators, coupling exergonic and endergonic oxidation-reduction reactions to balance



electron flow in metabolism and minimize free energy loss, as described elsewhere in other metabolic pathways (Peters et al., 2016; Greene et al., 2017; Baffert et al., 2019).

Furthermore, as underlined by Bell et al. (2020), dissimilatory sulfate reduction cannot be determined definitively from genomic features alone, and this is also the case for ISC disproportionation. For example, the dissimilatory sulfite reductase D (*dsrD*), which has a hypothetical role in regulation, was considered as a feature of sulfate reducers as this gene is absent in some microorganisms that use the reverse dissimilatory sulfite reductase for sulfur oxidation. It was reported exceptions to this rule which are *Desulfurivibrio alkaliphilus* reported to oxidize sulfide, despite having the complete dissimilatory sulfate reduction pathway and *Desulfocapsa sulfexigens*, unable to reduce sulfate despite having the complete set of genes known to be involved in dissimilatory sulfate reduction (Bell et al., 2020). We can complete their list with our published results: *T. marina*, *T. ammonigenes* and *D. thermomarina*, which are known to be unable to perform sulfate reduction but are able to disproportionate sulfur, possess all *dsrD* homologs (Allioux et al., 2020; Slobodkina et al., 2020; Allioux et al., 2021).

We analyzed also other hypotheses recently proposed by other researchers regarding genomic markers of dismutation pathways, such as shorter AprB gene sequences (Ward et al., 2020), or an associated rhodanese-like protein (Florentino et al., 2019), or the presence of a YTD gene cluster (Umezawa et al., 2020). Not all of these hypotheses are supported in our microbial models of marine hydrothermal origin, and these genomic markers of dismutation are likely not universal. In conclusion, it is still very unclear if it exists specific markers of ISC disproportionation pathways.

Our proteomic experiments unfortunately failed, very likely due to the presence of ferrihydrite in the medium. We only obtained sufficient protein concentrations for few conditions, and did not send them for LC-MS/MS analyses as our dataset was incomplete.

We then decided to integrate the results of our trial LC-MS/MS analyses, but this experiment only considered cellular soluble protein extracts. Thus, the interpretation of these data is quite limited. Interestingly, we observed that some enzymes of the sulfate reduction pathway were probably more abundant under S<sup>0</sup> disproportionation condition such as AprA, AprB, DsrA, DsrB, QmoA and QmoB than under sulfate reduction condition. Conversely, the SAT protein might not be involved in the S<sup>0</sup> disproportionation process, in the tested bacteria. Moreover, we also found that TusA protein (but not the whole proteins encoded by the YTD gene cluster),

adenylate kinase and few uncharacterized proteins were overexpressed under  $S^0$  disproportionation condition. It could be interesting to explore their function in more details.

In these experiments, we had also several issues with ferrihydrite. Ferrihydrite very likely impacted protein extraction and reduced significantly protein extraction yields. Ferrihydrite also prevented measuring the concentration of dissolved  $H_2S$ . In the framework of this experiment, by following certain substrates and products of the metabolism and by following the evolution of the cell density during growth, we also confirmed that *T. atlanticus* is able to grow by  $S^0$  disproportionation. Preliminary and aborted ionic chromatography analyses on *T. atlanticus* suggested that sulfate was produced over time under  $S^0$  disproportionation conditions (data not shown). Gas chromatography analyses showed a  $H_2S$  production over time in the culture of *D. thermophilus* incubated under sulfate reduction growth conditions. The main point of this experiment is that the genes that we found by comparative genomics were not found in sulfur disproportionation growth condition, but only in sulfate reduction condition. In conclusion, we were not able to observe a specific protein pattern for  $S^0$  disproportionation. We can speculate that the disproportionation process is even more complex and that pathways for disproportionation are different for each strain, and that strains, depending on their genomic resources, will use a specific and adapted pathway to perform ISC disproportionation. The specific pathways could be shared between species, genera, families, or phyla, for example. But if this hypothesis holds true, it means that it is unlikely that a single universal marker for sulfur disproportionation can be found. Finally, these results are very limited as indicated above and further experiments should be performed to confirm or refute these hypotheses. In any case, our proteomic results cannot be considered as valid.

The problems encountered during this thesis encourage us to consider repeating these experiments in the future without adding ferrihydrite to the  $S^0$  dismutation medium. Nevertheless, this could result in a very low biomass if cultures are performed in batch. It should also be important to limit the amount of elemental sulfur added to the medium, due to other potential interferences. A good alternative would be to repeat this experiment without ferrihydrite, in a gas lift bioreactor, to remove  $H_2S$  from the medium and reach high biomass. This will be done in the framework of the following PhD thesis of Stéven Yvenou.

We further believe that polysulfides should be interesting to follow in this experiment, as the first steps of  $S^0$  disproportionation are not known. Polysulfides could be analyzed during the disproportionation process by chemical analyses under specific conditions as detailed elsewhere (Manan et al., 2011). Studying the disproportionation of other inorganic sulfur

species such as tetrathionate could also be also very interesting, and notably the ones which are not well studied.

In addition, other approaches could be helpful to decipher ISC disproportionation pathways. Analyses of gene expression based on RT-qPCR could be very helpful, for example (Thorup et al., 2017; Wang et al., 2019). Analyses with stable or radiolabelled sulfur isotopes could also be planned, to identify the chemical intermediates of the reaction, very valuable data, and then elaborate new hypotheses. Approaches with radiolabelled substrates are more sensitive than ion chromatography and were already carried out for investigating ISC disproportionation (Jørgensen et al., 1990; Jørgensen and Bak, 1991; Cypionka et al., 1998; Böttcher and Thamdrup, 2001; Böttcher et al., 2001; Böttcher et al., 2005).

Moreover, it would be interesting to consider a theoretical thermodynamic study *in silico* on the ISC disproportionation, *via* a similar approach used elsewhere (Amend et al., 2020). The disproportionation reaction occurs as a function of temperature, pH, redox potential, and additionally the concentration of sulfur species and other chemical species, particularly sulfates and sulfides. High temperature, high pH, and low sulfide and sulfate concentrations have been shown to promote disproportionation. As these are quite general rules, we decided to investigate in greater details the thermodynamics of  $S^0$  disproportionation. This reaction is endergonic under standard conditions, but several species of hydrothermal origin are able to disproportionate  $S^0$ . In the framework of a collaboration with the Amend lab of University of Southern California (Jan Amend and Heidi Aronson), we predicted the Gibbs energy of the reaction of  $S^0$  dismutation by varying the main physico-chemical parameters of the reaction (temperature, pressure, salinity, pH, sulfate, sulfides) in pairs. We then calculated the free energy values of  $S^0$  dismutation from environmental data at four hydrothermal sites located in different geological settings and characterized by contrasted fluid compositions. I will be associated to this publication as a co-author. The analyses are just finished and showed that  $S^0$  disproportionation reaction is exergonic in the vicinity of hydrothermal vents, independently of the tectonic or geological context. One of the main objectives of this study was to test our hypothesis that the disproportionation catabolism may be more widespread than previously thought.

The global study of the distribution and abundance of ISC-disproportionating species is still limited, due to the lack of specific markers of the reaction. This PhD project didn't answer to this question but supports the idea that more effort should be done towards a comprehensive understanding of this metabolism. The discovery of genomic markers of this process, if they exist, could modify our understanding of the microbial sulfur cycle and allow evaluating its importance, not only in hydrothermal vents but in all ecosystem on Earth driven by the sulfur cycle. Indeed, genomic markers can be looked for by metabarcoding and metagenomic approaches, which are culture independent methods.

In conclusion, much about microbial sulfur disproportionation remains to be discovered. The comprehensive understanding of this process might have a significant impact on our insight of the global sulfur cycle, with implications on ecology, evolution of metabolisms and ocean biogeochemistry.

# Chapter 4: Investigation of sulfur comproportionation in hydrothermal and geothermal samples, and with pure strains

## 1. Preamble

Inorganic sulfur compound comproportionation was described in the manuscript introduction as a hypothetical metabolism. This subject was approached as a side project because this metabolism corresponds to the reverse reaction of the ISC-dismutation and was predicted at the beginning of the PhD. Cultures were carried out with samples from deep-sea hydrothermal vents and acidic geothermal hot springs, and with pure strains. First tests were performed with the help of the intern Stéven Yvenou. As in Chapter two on organic sulfur compounds, this project did not yield conclusive results, but the purpose of this chapter is to report on what was done.

## 2. Materials and Methods

### Natural samples and strains used as inocula

The starting material used for these experiments consisted in natural samples from three acidic hot springs from the Kerguelen Islands in the Southern and Antarctic regions, chimney samples from three hydrothermal vents at the Lucky Strike vent field (Mid-Atlantic Ridge), and two pure strains:

- Geothermal hot spring samples from the Kerguelens Islands have been collected in 2016 in the Ralier du Baty peninsula, and were referenced as: **hot spring 35** (S 49° 37' 33.168" E 68° 47' 55.392"), **hot spring 39** (S 49° 37' 30.864" E 68° 47' 53.664") and **hot spring 107** (S 49° 37' 30.864" E 68° 47' 53.664").

- Hydrothermal samples were collected in 2019 during the MoMARSAT 2019 oceanographic cruise at the Lucky strike vent field, and were referenced as: **1939** (sample MOM19 Aisics 2 PL1939-1-PBT3; Aisics chimney; N 37° 17' 20.34" W 32° 16' 33.899"; 1690 m depth), **1945** (sample MOM19 Cap2 PL1945-7; Capelinhos vent; N 37° 17' 20.34" W 32° 16' 33.899"; 1663 m depth), and **1947** (sample MOM19 PL1947-PBT2-DEAFS; Montségur vent; N 37° 17' 20.34" W 32° 16' 33.899"; 1699 m depth).
- *Desulfurella amilsii* strain TR1<sup>T</sup> (DSM 29984<sup>T</sup>) pure culture was chosen because it is able to perform sulfur disproportionation and moreover, it can grow by sulfur reduction at acidic pH (Florentino et al., 2016).
- The strain M19, representing a new species of the family *Desulfobulbaceae*, was isolated during the PhD from the Capelinhos vent field. This Strain M19 was chosen because of it grows by sulfur disproportionation and because its genome codes for the *sqr* enzyme, involved in sulfide oxidation.

#### Medium targeting ISC-comproportionation

This medium was composed of a mineral basis, and contained sulfate as an electron acceptor, sulfide as an electron donor, and an atmosphere of 100% CO<sub>2</sub> as a carbon source. The medium composition was adjusted for each type of inoculum, as described below (table 4).

Table 13: Composition of sulfur comproportionation media and incubation conditions, for each inoculum type.

Composition (masse (g) or volume (mL) per 1 liter of medium)	Geothermal hot spring Kerguelen samples	Momarsat 2019 hydrothermal samples	<i>Desulfurella amilsii</i>	<i>Desulfobulbaceae</i> nov sp. strain M19
NaCl	0.5 g	25 g	5 g	25 g
MgCl <sub>2</sub> .6H <sub>2</sub> O	0.5 g	0.5 g	0.5 g	4.4 g
CaCl <sub>2</sub> .2H <sub>2</sub> O	0.1 g	0.1 g	0.1 g	0.3 g
NH <sub>4</sub> Cl	0.3 g	0.3 g	0.3 g	0.3 g
KH <sub>2</sub> PO <sub>4</sub>	0.3 g	0.3 g	0.3 g	0.3 g
KCl	0.5 g	0.5 g	0.5 g	0.5 g
Resazurin	2 drops	2 drops	2 drops	2 drops
Trace element solution SL-10	1.0 ml	1.0 ml	1.0 ml	1.0 ml
Vitamin solution	1.0 ml	1.0 ml	1.0 ml	1.0 ml
Se-W solution	1.0 ml	0 ml	1.0 ml	1.0 ml
Yeast Extract	0.1 g	0 g	0.1 g	0 g
Sodium sulfate	50 mM	50 mM	50 mM	20 mM
Na <sub>2</sub> S.9H <sub>2</sub> O	5 mM	5 mM	5 mM	5 mM
pH	3.0, 4.5 and 6.0	3.0	3.0, 4.5 and 6.0	3.0 and 5.0
Gaseous phase	CO <sub>2</sub> 100%	CO <sub>2</sub> 100%	CO <sub>2</sub> 100%	CO <sub>2</sub> 100%
T°C	30°C, 45°C and 65°C	19°C and 30°C	30°C, 45°C and 65°C	4°C and 19°C

Initial enrichment culture and subsequent subcultures were inoculated to 1/10<sup>th</sup>.

### Chemical analyses

Chemical analyses of gases phases and dissolved anions were performed in *D. amilsii* subcultures. Sulfate and thiosulfate concentrations were measured by ionic chromatography using a Dionex ICS-900 Ion Chromatography System (Dionex, Camberley, UK) equipped with an IonPac CS16 column maintained at 60°C in an UltiMate™3000 Thermostated Column Compartment (Thermo Scientific, Waltham, MA, USA). H<sub>2</sub>S and CO<sub>2</sub> concentrations were measured with a Micro GC FUSION Gas Analyser (INFICON, Bâle, Switzerland) with a pressure analyser (CTE80005AY0, Sensortech GmbH).

### **3. Results and Discussion**

Enrichment cultures carried out with the three Kerguelen samples provided growth in all initial enrichment cultures but only the culture from the hot spring 35 could be maintained over two subcultures at 30°C. However, the third subculture did not provide any growth (after more than one month of incubation). In conclusion, sulfur comproportionating microorganisms could not be isolated from these hot spring samples under our experimental culture conditions.

Enrichment cultures carried out with three hydrothermal samples did not give any growth, which suggests that sulfur comproportionators are unlikely to be present in the deep-sea hydrothermal samples tested.

Cultures carried out with *D. amilsii* were still positive with poor growth after five subcultures under our experimental conditions favoring theoretically sulfur comproportionation. These cultures were incubated at 30°C and pH 3.0. However, *D. amilsii* requires yeast extract to grow, which can also be used as an energy source. In order to study the composition of the gas and liquid phase, we analyzed two subcultures, one after 13 days of incubation, and another one after 41 days of incubation. Ionic chromatography was used to measure sulfate and thiosulfate concentrations in the liquid phase, and gas chromatography was used to measure hydrogen sulfide and carbon dioxide in the atmosphere of the vials. Low amounts of H<sub>2</sub>S were measured and carbon dioxide concentration did not change. These analyses did not provide any evidence that ISC-comproportionation was at work in these cultures. It is more likely that *D. amilsii* grew by sulfate reduction by using the yeast extract or the vitamins as electron donors.

Cultures with *Desulfobulbaceae* strain M19 were incubated at two temperatures (4°C and 19°C) and two pH (3.0 and 5.0). After two subcultures in our experimental conditions targeting ISC-comproportionation, no growth could be obtained.



#### **4. Conclusions and Perspectives**

As a conclusion, these few tests of culture from the samples we had at our disposal did not allow to grow microorganisms under sulfur comproportionation conditions. To try to isolate microorganisms growing via these reactions, it would be necessary to try to find ecosystems perfectly suited to the most favorable thermodynamic conditions for this reaction.

Because sulfur comproportionation is considered as the opposite reaction of sulfur disproportionation, we could speculate that common pathway may be shared between sulfur disproportionation and comproportionation such as for sulfate reduction and sulfide oxidation. However, it stays very hypothetical and the discovery of a microorganism able to grow by sulfur comproportionation and the analysis of its genome could help us to understand the process and open lots of perspectives.

From an ecological point, if this metabolism exists in nature, it could be used as a survival strategy in environments with high gradients of temperature and pH such as hydrothermal vents. It could be beneficial for microorganisms living in and around hydrothermal vents to be able to simply maintain themselves in certain conditions by reaching more favorable conditions for their growth. However, this remains totally speculative as to date no microorganism developing by this process has been isolated.

# Chapter 5: Investigation of the microbial sulfur cycle in geothermal springs

## 1. Preamble

The initial goal of this part was to integrate the knowledge about the sulfur cycle into an ecological context by studying the microbial actors of the sulfur cycle in a hydrothermal sediment core. We planned to combine chemical and mineral characterization of sedimentary horizons to descriptions of the microbial diversity, based on 16S rRNA gene sequences and gene markers of sulfur/sulfide oxidation, sulfate/sulfur reduction and ISC disproportionation, and abundance of microbial actors of the sulfur cycle, throughout a sediment core.

Unfortunately, as the oceanographic mission in which I was supposed to participate was cancelled (Covid-19 pandemia), this study was carried out from 4 samples of terrestrial hot springs of the Kerguelens Islands (in the Southern and Antarctic regions) which were available in the laboratory and which were particularly interesting because the microbial communities that they host are very little documented. These samples from geothermal sources of the Kerguelen Islands were particularly interesting because the microbial communities from these hot springs had never been studied before through metagenomics, nor even through metabarcoding approaches. Only few cultural investigations and few 16S rRNA gene libraries have been done before. The Kerguelen Islands are located in the southern part of the Indian Ocean and are very isolated geographically and poorly anthropized. The goal of our analysis was not to present a deeply and fully characterization of microbial diversity of Kerguelen hot springs but more to introduce some of the diversity present. The article planned should be considered as a preliminary study of the microbial diversity of these hot springs found in these insulated islands.

## 2. Article section

Hereafter is presented a manuscript in preparation that we will submit to *Scientific Reports* under the title: “Insulated geothermal springs in the Kerguelen Islands host a large fraction of new genomic microbial taxa”. The draft manuscript should be reworked before submission.

1 **Insulated geothermal springs in the Kerguelen**  
2 **Islands host a large fraction of new genomic microbial**  
3 **taxa**

4  
5 Maxime Allieux<sup>1</sup>, Stéven Yvenou<sup>1</sup>, Alexander Merkel<sup>2</sup>, Marc Cozannet<sup>1</sup>, Johanne Aube<sup>1</sup>, Marc  
6 Le Romancer<sup>3</sup>, Damien Guillaume<sup>4</sup>, Alexander Slobodkin<sup>2</sup>, Galina Slobdokina<sup>2</sup>, Guillaume  
7 Lannuzel<sup>1</sup> & Karine Alain<sup>1\*</sup>

8  
9 <sup>1</sup>Univ Brest, CNRS, IFREMER, IRP 1211 MicrobSea, Laboratoire de Microbiologie des Environnements  
10 Extrêmes LM2E, IUEM, Rue Dumont d'Urville, F-29280 Plouzané, France

11 <sup>2</sup>Winogradsky Institute of Microbiology, Research Center of Biotechnology of the Russian Academy of Sciences,  
12 Moscow, Russia

13 <sup>3</sup> missing

14 <sup>4</sup> missing

15  
16 \*Karine.Alain@univ-brest.fr

17  
18 **Abstract**

19  
20 The Kerguelen Islands, located in the southern part of the Indian Ocean, are very isolated  
21 geographically and poorly anthropized. They have been the subject of very few microbiological  
22 investigations. In particular, their microbial diversity has never been analyzed with high-  
23 throughput sequencing methods and no sequencing studies of the genomes of the microbial  
24 communities have been performed. In this article we analyzed for the first time the  
25 microorganisms present in the Kerguelen hot springs by metagenomics. From four different hot  
26 springs, we assembled metagenomes and recovered 42 metagenome-assembled genomes,  
27 mostly associated with new taxa. Bacterial and archaeal MAGs were studied in details and  
28 showed affiliations to new species, genera, families and orders. Metabolic predictions from  
29 MAGs suggest the presence of primary producers involved in the sulfur cycle and the abundant  
30 presence of heterotrophs. This paper, which focuses on only four of the dozens of hot springs  
31 in the Kerguelen Islands, is a preliminary study of the microorganisms, particularly  
32 thermophiles, inhabiting the hot springs of these insulated islands. These results show that more  
33 efforts should be made to better understand these ecosystems as they represent a reservoir of  
34 unknown microbial lineages and potential new metabolic pathways.

35  
36 Key words: Kerguelen islands, hot springs, metagenomics, microorganism, metabolism

37  
38 **Introduction**

39  
40 Terrestrial hot springs are found all over the world, on all continents, and are abundant in areas  
41 of volcanic activity such as Iceland, Japan, Russia, Chile, Algeria or New Zealand (Mehtad and  
42 Satyanarayana, 2013; Des Marais and Walter, 2019). With possible exception in the  
43 polyextreme Dallol area (Belilla et al., 2019), all studied geothermal environments harbor

44 microbial cohorts. Microbial cohorts in terrestrial hot springs are often composed of *Bacteria*  
45 belonging to *Aquificae*, *Chloroflexi*, *Deinococcus-Thermus* and *Thermotogae*, and *Archaea*  
46 belonging to *Desulfurococcaceae*, *Thermoproteaceae* and *Thermococcaceae* (Urbieta et al.,  
47 2015; Power et al., 2018; Lezcano et al., 2019). The microbial communities of hot springs in  
48 the polar regions are partly different in their composition. For example, the fumaroles of  
49 Deception Island (Antarctica) contain prokaryotic taxa belonging to *Verrucomicrobia*,  
50 *Proteobacteria*, *Planctomycetes*, *Patescibacteria*, *Firmicutes*, *Chloroflexi*, *Calditrichaeota*,  
51 *Bacteroidetes*, *Thaumarchaeota*, *Nanoarchaeota*, *Euryarchaeota* and *Crenarchaeota* (Muñoz  
52 et al., 2011; Amenabar et al., 2013; Bendia et al., 2018).

53 Most of terrestrial hot springs, like those of Yellowstone (USA) or Kamchatka (Russia) areas,  
54 have been the subject of extensive microbiological investigations, including the study of the  
55 microbial community composition, the isolation and physiological characterization of  
56 microorganisms, the investigation of the adaptive mechanisms of indigenous taxa, and the  
57 mining of extremophilic species for potential enzymes, activities or molecules of  
58 biotechnological interest (e.g. Brock et al., 1972; Meyer-Dombard et al., 2005; Kublanov et al.,  
59 2009; Reigstad et al., 2010; Wemheuer et al., 2013; Wilkins et al., 2019). Studies of bacteria  
60 and archaea living in geothermal systems are essential for our knowledge of the history of life,  
61 as these environments are early Earth analogs and one of the possible cradles of life (Deamer  
62 and Georgiou, 2015; Van Kranendonk et al., 2017; Des Marais and Walter, 2019; Lezcano et  
63 al., 2019).

64 The volcanic Kerguelen Archipelago, which is part to the French Southern and Antarctic Lands,  
65 is located in the southern part of the Indian Ocean (49°S, 69°E). It is located at 3300 km from  
66 the first inhabited areas, it is a natural reserve and it is thus very little anthropized. It forms the  
67 only emerged part, together with the active volcanic Heard and MacDonal Islands, of the vast  
68 Kerguelen oceanic Plateau. Kerguelen Archipelago is the third largest volcanic island complex  
69 in the world, after Iceland and Hawaii (Giret et al. 1997). The last volcanic activity, dated  $26 \pm$   
70  $3$  Ka, took place on the Rallier du Baty (RB) Peninsula in the south-western part of the  
71 Kerguelen Islands (Gagnevin et al. 2003). Current volcanic activity, due to the Kerguelen  
72 hotspot, is evidenced by fumaroles, mud pots, hydrothermal discharges and small hot springs  
73 that rise from sea level to at least 500 m altitude (Charvis et al. 1995). Those biotopes are  
74 charged with minerals, and their pH range from acidic to alkaline (pH 3–11), under a wide  
75 range of temperature conditions from 35 to over 100°C. The geochemical properties of the most  
76 accessible parts of this system have been monitored more or less regularly over the last decades  
77 (Parikka et al., 2018; Renac et al., 2020). These geothermal habitats represent unique  
78 biodiversity sanctuaries in very insulated polar environments. Preliminary investigations based  
79 on 16S rRNA gene amplicon cloning and sequencing revealed a diverse collection of microbial  
80 community lineages composed of *Proteobacteria*, *Deinococcus-Thermus*, *Chloroflexi*,  
81 *Firmicutes*, *Actinobacteria*, *Aquificae* *Euryarchaeota*, *Crenarchaeota* (*Thermoproteales*,  
82 *Desulfurococcales*, *Acidilobales*, *Sulfolobales*) and *Thaumarchaeota* (Postec et al., 2009,  
83 Gramain et al., 2011). Those lineages are more or less distantly related to known taxa, that were  
84 partly different from those described in Antarctic geothermal sites but also from those usually  
85 observed in similar habitats. A small number of new species have also been isolated from these

86 regions, and a study targeting specifically a methanogenic lineage also integrated geothermal  
87 samples from the Kerguelen (Postec *et al.*, 2010; Cozannet *et al.*, 2021). Apart from these few  
88 studies, this area has not been subjected to any comprehensive microbiological investigation to  
89 date. The microbial diversity hosted in these hot springs remain largely unknown, as well as its  
90 functional (metabolism, physiology, adaptations) potential. Microbial communities might be  
91 shaped by the biogeographic position and the physicochemical parameters of the hot springs  
92 (temperature, pH, *in situ* chemistry) which probably exert a strong selective pressure on  
93 indigenous communities (Bendia *et al.*, 2018). Yet, these geothermal springs represent  
94 undoubtedly unique diversity, and reservoirs of new functions and innovation.

95  
96 In this study, we focused on four small geothermal hot springs from the Kerguelen Islands  
97 whose microbial communities have never been studied before. We analyzed the metagenomes  
98 of the hot springs RB10, RB13 and RB32, located on the "plateau des Fumeroles" at about 450  
99 m altitude on the west coast of the Rallier du Baty Peninsula, and of the ephemeral spring  
100 RB108 which flows slightly above sea level into the riverbed of the Infernet glacier (located at  
101 the base of the plateau des Fumerolles), in order to study the taxonomic diversity and to predict  
102 its functions (Figure 1).

## 103 104 **Results and Discussion**

### 105 106 **MAG binning and general features**

107  
108 From the four hot springs, we assembled four associated metagenomes and then binned a total  
109 of 42 MAGs. We recovered 12 MAGs from the RB10 hot spring, 13 from RB13, 14 from RB32  
110 and 3 from RB108. Out of these 42 MAGs, 7 were of high-quality, 25 of nearly-high quality, 9  
111 of medium quality and 1 of low quality (Table 1) from metagenomics standards (Bowers *et al.*,  
112 2017). The GC% was quite variable, ranging from 25.76% to 70.35% among all MAGs and  
113 between 32.15% and 69.21% only among the high- and near high-quality MAGs. At least  
114 twenty-three of these 42 MAGs were unique. With the exception of RB108 from which we only  
115 recovered bacterial MAGs, we retrieved both bacterial and archaeal MAGs in the other hot  
116 springs. Two thirds of the MAGs (26/42) were assigned to the domain *Bacteria* and the rest to  
117 the domain *Archaea* (Table 2).

### 118 119 **Taxonomic and phylogenomic analyses of MAGs**

120  
121 The taxonomic affiliation of the MAGs was investigated in details through GTDB-Tk (release  
122 95) (Table 2) and through phylogenomic analyses (Fig. S1 A-I).

123  
124 For *Bacteria*, GTDB-Tk analyses allowed us to place the MAGs in the following clades: six in  
125 the phylum *Aquificota* from the four different springs, comprising four MAGs belonging to the  
126 genus *Hydrogenivirga* (family *Aquificaceae*) (RB10-MAG07, RB13-MAG10, RB32-MAG07,  
127 RB108-MAG02), and two belonging to the family *Hydrogenobaculaceae* (RB10-MAG12,  
128 RB32-MAG11) (Table 2, Fig. S1A). Their closest cultured relatives originated either from hot  
129 springs or from deep-sea hydrothermal vents. Three MAGs from three geothermal sources

130 belonged to the phylum *Armatimonadota* (RB10-MAG03, RB13-MAG04, RB32-MAG03) and  
131 had no cultured relatives. They were most closely related to MAGs reconstructed from hot  
132 springs from USA. Seven MAGs have been classified into the phylum *Chloroflexota*,  
133 comprising three MAGs belonging to the genus *Thermoflexus* from three different springs  
134 (RB10-MAG04, RB13-MAG05, RB32-MAG02), one affiliating with the genus  
135 *Thermomicrobium* (RB32-MAG08), one falling into the family *Ktedonobacteraceae* (RB108-  
136 MAG03) and one belonging to the class *Dehalococcoidia* (RB32-MAG04). Six MAGs from  
137 four various hot springs belonged to the phylum *Deinococcota*, and to the genera *Thermus*  
138 (RB10-MAG08, RB10-MAG11, RB13-MAG09, RB32-MAG10, RB108-MAG01) and  
139 *Meiothermus* (RB13-MAG13). One MAG belonged to the family *Sulfurifustaceae* (RB13-  
140 MAG01), in the phylum *Proteobacteria* (in the *Gamma*- class). The MAG referenced as RB32-  
141 MAG13 was classified into the phylum *Patescibacteria*, in the class *Paceibacteria*, and was  
142 distantly related to MAGs originating from groundwater and from hot springs. Finally, two  
143 MAGs from two different springs belonged to the phylum WOR-3, in the genus *Caldipriscus*  
144 (RB32-MAG12, RB10-MAG09).

145

146 For *Archaea*, almost all the MAGs reconstructed in this study, i.e. 15 of the 16 archaeal MAGs,  
147 belonged to the phylum *Thermoproteota*. Among them, four belonged to the genus *Ignisphaera*  
148 (RB10-MAG05, RB13-MAG08, RB13-MAG11, RB32-MAG05), three to the genus  
149 *Thermofilum* (RB10-MAG06, RB13-MAG03), two to the genus *Zestosphaera* (RB10-MAG02,  
150 RB13-MAG06), two to the family *Acidilobaceae* (RB13-MAG02, RB32-MAG01) and two to  
151 the class *Thermoproteia* (RB10-MAG10, RB32-MAG06). The MAG belonging to another  
152 phylum was affiliated with the *Aenigmataarchaeota*, class *Aenigmataarchaeia*, and was distantly  
153 related to MAGs from hot springs and from deep-sea hydrothermal vent sediments.

154

155 Out of these 42 MAGs, 23 corresponded to different taxa at the taxonomic rank of species or  
156 higher. Eighteen of them belonged to lineages with several cultivated representatives and were  
157 distributed respectively, into 1 known species called *Thermus thermophilus*, 10 new genomic  
158 species within the genera *Zestosphaera*, *Thermoflexus*, *Ignisphaera* ( $\times 2$ ), *Thermofilum*,  
159 *Hydrogenivirga*, *Thermus*, *Meiothermus*, *Caldipriscus* and *Thermomicrobium*, 5 putative new  
160 genera belonging to the families *Acidilobaceae*, *Thermocladiaceae*, *Sulfurifustaceae*,  
161 *Hydrogenobaculaceae* and *Ktedonobacteraceae*, and 3 putative new orders within the classes  
162 *Dehalococcoidia* and *Thermoproteia* ( $\times 2$ ). In addition, five MAGs belonged to lineages that  
163 are predominantly or exclusively known through environmental DNA sequences. They were  
164 classified as 1 new genomic species in the phylum *Armatimonadota*, 2 putative new genera in  
165 the classes *Aenigmataarchaeia* et *Paceibacteria*, and 1 putative new family in the phylum  
166 *Chloroflexota*.

167

168 Thus, these 42 MAGs comprised a broad phylogenetic range of *Bacteria* and *Archaea* at  
169 different levels of taxonomic organization, of which a large majority were new.

170

171 The approaches implemented here were not intended to describe the microbial diversity present  
172 in these sources in an exhaustive way and to compare them in a fine way, and do not allow it.  
173 However, they do provide an overview of the microbial diversity effectively present. If we

174 compare the phylogenetic diversity of the MAGs found in the 4 hot springs, we can observe  
175 that 3 phyla (*Deinococcota*, *Aquificota* and *Chloroflexota*: phyla names according to GTDB)  
176 were found in the 4 sources, 2 families (*Thermaceae* and *Aquificaceae*) were shared, but no  
177 common genus was found (Figure 3). In addition, hot springs RB10, RB13 and RB32, that are  
178 geographically close, also share 2 other phyla (*Thermoproteota* and *Armatimonadota*) and 4  
179 other common families (*Acidilobaceae*, *Ignisphaeraceae*, *Thermofilaceae* and  
180 *Thermoflexaceae*) (Figure 3). These phyla and families that are shared between sources are very  
181 common lineages of terrestrial geothermal habitats (e.g. Urbietta et al., 2015; Power et al., 2018;  
182 Lezcano et al., 2019; Wilkins et al., 2019). Phyla and families detected in the hot environments  
183 of Antarctica are also found here, such as *Patescibacteria* for example (Muñoz et al., 2011).

184

185 In summary, this metagenomic analysis highlighted the presence of bacterial and archaeal  
186 lineages commonly found in hot springs, and lineages found in hot habitats from polar areas  
187 (e.g. Muñoz et al., 2011; Urbietta et al., 2015; Power et al., 2018; Kochetkova et al., 2019;  
188 Lezcano et al., 2019). The microbial communities in these Kerguelen Island hot springs were  
189 diverse, particularly in RB10, RB13, and RB32 hot springs. However, within these lineages  
190 that have been previously reported to occur in geothermal environments, a majority of the  
191 genomic species detected here were new, sometimes at a high taxonomic rank.

192

193

#### 194 **Metabolic potential of MAGs**

195

196 An extensive genomic characterization has been performed on the 42 MAGs to explore the  
197 pathways and the possible adaptations of the microorganisms from which these MAG originate.  
198 The annotations of the KEGG Decoder obtained by Anvi'o highlighted various pathways  
199 associated with carbohydrate degradation, sulfur, nitrogen, oxidative phosphorylation and  
200 amino-acid metabolisms, among others (Figure 3).

201 Based on these results, a deeper annotation was performed by combining data generated by  
202 Prokka with the MetaCyc database, in order to confirm the first results concerning energetic  
203 metabolisms. Efforts have been directed at studying energetic metabolisms, particularly  
204 inorganic nutrient metabolisms. These results are not representative of the metabolic diversity  
205 of all the hot spring ecosystems studied, but reflect some of the microbial metabolisms likely  
206 to be used *in situ* to produce energy and by hypothesis the most abundant. Metabolic predictions  
207 are presented hereafter at the level of the different taxonomic ranks.

208

209 MAGs affiliated with the genus *Thermoflexus* (RB10-MAG04, RB13-MAG05, RB32-  
210 MAG02) encode pathways for carbon monoxide oxidation, hydrogen oxidation and nitrate  
211 respiration, but the only cultivated known representative of this genus is a heterotrophic  
212 bacterium (Dodsworth et al., 2014). The *Dehalococcoidia*'s MAG (RB32-MAG04) codes for  
213 carbon monoxide oxidation pathway only, but the genus consists of hydrogenotrophic,  
214 organohalide-respiring metabolism and strict anaerobic bacteria (Löffler et al., 2013). In the  
215 MAG associated with the genus *Thermomicrobium* (RB32-MAG08), we predicted pathways  
216 for dimethyl sulfide degradation, thiosulfate disproportionation and carbon monoxide  
217 oxidation; moreover, carbon monoxide oxidation has been confirmed in this genus by culture

218 (King and King, 2014). In the *Chloroflexota*'s RB32-MAG14, carbon monoxide oxidation and,  
219 thiosulfate disproportionation pathways are present; however, this phylum is known as  
220 filamentous anoxygenic phototrophs, but no phototrophy associated CDSs were found (Hanada,  
221 2014). The *Ktedonobacteraceae*'s MAG RB108-MAG03 encode enzymes for four pathways  
222 of hydrogen oxidation (aerobic), for carbon monoxide oxidation, dimethyl sulfide degradation,  
223 selenate reduction, thiosulfate oxidation and disproportionation and finally tetrathionate  
224 oxidation; nevertheless, this family contains heterotrophic bacterium but likely without any  
225 thermophilic representatives (Yabe et al., 2017). Within *Hydrogenobaculaceae* MAGs (RB10-  
226 MAG12, RB32-MAG11), we retrieved a thiosulfate disproportionation pathway; probably  
227 chemotrophs because most of the species within this family are capable of chemolithotrophic  
228 micro and aerophilic growth (Gupta, 2014). MAGs belonging to the genus *Hydrogenivirga*  
229 (RB10-MAG07, RB13-MAG10, RB32-MAG07, RB108-MAG02) possess genes coding for  
230 enzymes of aerobic respiration, thiosulfate oxidation, thiosulfate disproportionation,  
231 tetrathionate reduction, and hydrogen oxidation (aerobic and anaerobic); in agreement with  
232 what is known about the genus (nitrate and molecular oxygen to oxidize hydrogen, sulfur, or  
233 thiosulfate) (Gupta, 2014). In MAGs associated with the genus *Thermus* (RB10-MAG08,  
234 RB10-MAG11, RB13-MAG09, RB32-MAG10, RB108-MAG01), pathways for aerobic  
235 respiration, assimilatory sulfate reduction, hydrogen oxidation, selenate reduction, thiosulfate  
236 oxidation and thiosulfate disproportionation were found; the genus is well described and  
237 possesses diverse chemolithotrophy and aerobic respiration (Ming et al., 2020). The MAG  
238 belonging to the genus *Meiothermus* MAG (RB13-MAG13) possesses carbon monoxide  
239 oxidation, hydrogen oxidation, thiosulfate oxidation and thiosulfate disproportionation  
240 pathways, however, it is known that growth of *Meiothermus* is chemoorganotrophic, and  
241 aerobic with a respiratory type of metabolism, but some species grow with nitrate as the  
242 terminal electron acceptor but neither putative genes were found (Albuquerque and da Costa,  
243 2014). For the RB13-MAG01 belonging to the *Sulfurifustaceae*, we predicted the genetic  
244 potential for aerobic respiration, ammonia oxidation, dissimilatory sulfate reduction, sulfite  
245 oxidation, sulfide oxidation (to sulfur globules), tetrathionate reduction, thiosulfate oxidation  
246 and thiosulfate disproportionation; *Sulfurifustaceae* (referenced as *Acidiferrobacteraceae* in the  
247 LPSN taxonomy) are known to be able to oxidize sulfur and iron, and the founded MAG  
248 representative may possess a larger panel of chemolithotrophic metabolic pathways (Issotta et  
249 al., 2018). For *Armatimonadota*'s members (RB10-MAG03, RB13-MAG04, RB32-MAG03),  
250 we predicted pathways for assimilatory sulfate reduction, carbon monoxide oxidation, selenate  
251 reduction and thiosulfate disproportionation; the members of the phylum are known as  
252 heterotrophs, able to perform aerobic respiration (Lee and al., 2014). In *Zestosphaera*'s and  
253 *Ignisphaera*'s MAGs (RB10-MAG02, RB13-MAG06) (RB10-MAG05, RB13-MAG08,  
254 RB13-MAG11, RB32-MAG05), we retrieved sulfur reduction (sulfur and polysulfides)  
255 pathway; those MAGs classified in the *Desulfurococcaceae* in the LPSN taxonomy, are known  
256 as heterotrophs, using sulfur compounds as electron acceptors (Niederberger et al., 2006; St.  
257 John et al., 2018). In MAGs associated with the class *Thermoproteia* (RB10-MAG10, RB13-  
258 MAG07, RB32-MAG06), dissimilatory sulfate reduction pathway was predicted; this class  
259 encompasses various energetical metabolic pathways (Itoh, 2014). In MAGs related to the  
260 genus *Caldipriscus* (RB10-MAG09, RB32-MAG12), phylum *Patescibacteria* (RB32-  
261 MAG13), family *Acidilobaceae* (RB10-MAG01, RB13-MAG02, RB32-MAG01), family



262 *Thermofilaceae* (RB10-MAG06, RB13-MAG03, RB32-MAG09) and class *Aenigmataarchaea*  
263 (RB13-MAG12), we did not find any inorganic nutrient energetical pathways implemented in  
264 the MetaCyc database. This could be explained by the low completion of the MAGs and/or the  
265 fact that only well-known pathways are described in this database. However, all these MAGs  
266 have pathways associated with carbohydrate and protein degradation. This may indicate that  
267 these taxa are chemoheterotrophs, which are already been reported in geothermal environments  
268 and already described for relatives of some of these taxa (Belkova et al., 2007; Sahn et al.,  
269 2013).

270  
271 Sulfide oxidation may be a possible energy production pathway for some of these MAGs based  
272 on the KEGG Decoder (Figure 3), since they code for a sulfide:quinone oxidoreductase  
273 (K17218) and a flavoprotein chain of sulfide dehydrogenase (K17229), but this hypothesis was  
274 not confirmed by MetaCyc. Due to the high representations of sulfur metabolisms, the genes of  
275 the MAGs were evaluated with DiSCo, which gave similar results to those obtained when  
276 analyzed with the Pathway tools. Clear patterns were observed for two MAGs that possess the  
277 essential sulfate reduction enzymes, for usual reduction processes (RB13-MAG07) but also, for  
278 oxidation processes (RB13-MAG01), for likely potential sulfide oxidation by reverse sulfate  
279 reduction pathway. The assimilatory sulfate reduction pathway was more represented in the  
280 whole MAG dataset than the dissimilatory pathway, which is likely related to the low sulfate  
281 concentration measured within the four hot springs, ranging from 123.2  $\mu\text{M}$  to 231.2  $\mu\text{M}$  of  
282 sulfate (Table S1). The thiosulfate disproportionation pathway detected by MetaCyc in many  
283 MAGs simply refers to the detection of an enzyme, the rhodanese-type thiosulfate  
284 sulfurtransferase. However, in the current state of knowledge on the dismutation pathways of  
285 inorganic sulfur compounds (Slobodkin and Slobodkina, 2019; Allieux et al., 2020), this  
286 enzyme alone does not allow the implementation of this energy production pathway. If we  
287 consider all the genes present in these MAGs, nothing indicates that the disproportionation of  
288 inorganic sulfur compounds can be achieved by the microorganisms from which these MAGs  
289 originate.

290  
291 No enzymes clearly associated with photosystems I and II were found, and only a few isolated  
292 putative photosystem assembly proteins were detected. Nevertheless, it cannot be ruled out that  
293 these energy production pathways are absent in microorganisms indigenous to these sources.  
294 On the other hand, our results show that these sources host chemolithoautotrophic taxa involved  
295 in the carbon and sulfur cycle, and to a lesser extent in the hydrogen and nitrogen cycles. Several  
296 taxa are likely to be involved in the primary production of these sources, but additionally,  
297 heterotrophs seem to be highly present and diverse in the collected samples. However,  
298 additional studies are needed to better understand the food webs of these hot springs and their  
299 microbial actors, and to better understand the functioning of the microbial communities of the  
300 Kerguelen hot springs and their interactions with their biotic and abiotic environment.

301  
302 In conclusion, this study allowed the assembly of 42 MAGs, from 4 hot springs, many of which  
303 represented new taxa, namely 11 new genomic species, 7 new putative genera, 1 new putative  
304 family and 3 new putative orders. This is the first metagenomic overview of the microbial  
305 diversity of Kerguelen hot springs. Based on their genetic potential, these taxa are

306 chemolithoautotrophs and chemorganoheterotrophs involved in the carbon, sulfur, hydrogen  
307 and nitrogen cycle. As geographically isolated sites, the Kerguelen Islands are reservoirs of  
308 diversity and taxa of novel microorganisms that should be interesting to study the evolution of  
309 microbial life and speciation processes. It has been difficult to fully assess the microbial  
310 metabolic diversity of these sources due to the inherent limitations of MAG reconstruction and  
311 the state of knowledge of microbial pathways that remains limited. However, ecosystems could  
312 be reservoirs of novel metabolic pathways with new microbial interactions and should be  
313 examined in detail through further and broader metagenomic studies and cultural approaches.

314

## 315 **Methods**

316

### 317 **Sample collection**

318 Water samples, mixed with surficial sediments were collected from four hot springs, during the  
319 austral summer 2016-2017 (1<sup>st</sup> of December – 11<sup>th</sup> of February). These samples were collected  
320 during the TALISKER sampling mission organized by the French Polar Institute Paul Emile  
321 Victor (<https://www.institut-polaire.fr>). These water and sediment samples were collected  
322 aseptically in sterile 50 mL Becton, Dickinson and Company-syringes, then stored  
323 (anaerobically) in sterile glass bottles at 4°C. Field measurements of fluid parameters consisted  
324 of pH, temperature (°C), alkalinity (mg/l), and electrical conductivity measurements (mS/cm)  
325 (Table S1).

### 326 **DNA extraction and sequencing**

327

328 Hot spring's samples analyzed here were originally collected to grow thermophilic taxa. They  
329 were stored at 4°C before DNA was extracted. This long storage has probably led to changes  
330 in microbial communities and to the selective loss or enrichment of some taxa. As a result, no  
331 analysis of abundance or absence of taxa can be conducted from these metagenomes and the  
332 results are discussed taking this bias into account.

333 For each hot spring sample, three replicates of DNA extraction were conducted individually,  
334 and combined as a composition sample, before the sequencing. DNA was extracted with a  
335 standard PCI (Phenol: Chloroform: Isoamyl Alcohol (25:24:1)) protocol, as described  
336 elsewhere, from 10 g environmental matrix (Charbonnier et al., 1995). One negative control  
337 was included and contained 10 mL of DNA-free sterile water. Elution of total DNA extracts  
338 was performed in 30 to 50 µL EB buffer (10 mM Tris-Cl, pH 8.5). Nucleic acid solution quality  
339 was determined using the NanoDrop™ 8000 (Thermo Scientific, Waltham, MA, USA)  
340 spectrophotometer. Double-strand DNA concentration was measured using the kit  
341 Quantifluor™ dsDNA system. DNA samples were sequenced by NovaSeq 6000 (2 × 150 bp,  
342 paired-end reads) technology by the Duke Center for Genomic and Computational Biology  
343 (GCB) (<https://genome.duke.edu/>).

344

345

346

347

## 348 **Sequence processing, metagenomic assembly and binning**

349

350 Metagenome sequences' quality were controlled by FastQC (v0.11.9 - [https://github.com/s-](https://github.com/s-andrews/FastQC)  
351 [andrews/FastQC](https://github.com/s-andrews/FastQC)) and MultiQC (v1.9 - <https://github.com/ewels/MultiQC>). Sequences were  
352 then processed with the snakemake of Anvi'o (Köster and Rahmann, 2012 ; Shaiber et al., 2020  
353 ; Eren et al., 2021) (v7 - <https://github.com/merenlab/anvio>), filtered by integrated minoche  
354 script (v2.8 - <https://github.com/merenlab/illumina-utils>). Next, we used MetaSpades (Nurk et  
355 al., 2017) (v3.14.1 - <https://github.com/ablab/spades>) as genome assembler and Concoct  
356 (Alneberg et al., 2014) (v1.1.0 - <https://github.com/BinPro/CONCOCT>) as genome binner with  
357 `anvi_cluster_contigs` function with "all against all" mode. Furthermore, MAGs were manually  
358 refined with `anvi-refine` function. Genome mapping was performed with bowtie2 (v2.4.2 -  
359 <https://sourceforge.net/projects/bowtie-bio/files/bowtie2/2.4.2/>) and samtools (v1.7 -  
360 <https://samtools.github.io/>), MAGs' quality were estimated by Anvi'o and furthermore by  
361 CheckM (v1.1.3 - <https://ecogenomics.github.io/CheckM/>), all with default parameters. Total  
362 length, number of contigs, N50, GC% content were extracted with `anvi-summarize` function  
363 but no dereplication was performed.

364

## 365 **Taxonomic and phylogenetic inference of metagenomic assemblies and MAGs**

366

367 According to the standards proposed elsewhere (Bowers et al., 2017), bins were defined as  
368 high-quality MAGs (>90% completion, <5% contamination, presence of the 23S, 16S and 5S  
369 rRNA genes and at least 18 tRNAs), nearly high-quality MAGs (>90% completion, <5%  
370 contamination, other criteria partially covered), medium-quality MAGs (≥50% completion,  
371 <10% contamination) and poor-quality MAGs (<50% completion, <10% contamination). The  
372 taxonomic affiliation of the MAGs was first investigated by placing the MAGs in a  
373 phylogenomic context. The taxonomy of the MAGs was assessed with GTDB-Tk (v1.4.1 -  
374 <https://github.com/ECogenomics/GTDBTk>) and GTDB associated database R95 release. As the  
375 taxonomy proposed by GTDB-Tk is new and does not correspond exactly to the one recognized  
376 by the International Code of Nomenclature of prokaryotes (ICNP), we also analyzed the data  
377 according to the rules of the Code and its nomenclature. For this purpose, we implemented a  
378 combination of genomic indices classically used for the delineation of the different taxonomic  
379 ranks, namely: 16S rRNA gene sequence similarity, average nucleotide identity score (ANI)  
380 and average amino-acid identity value (AAI). The approach followed and the results are given  
381 in supplementary material.

382

## 383 **Metabolic profiling**

384

385 MAGs were processed with KEGG Decoder script  
386 (<https://github.com/bjtully/BioData/tree/master/KEGGDecoder>) from Anvi'o gene calls tables  
387 generated with `kegg_kofams` and then plotted with R packages (ComplexHeatmap, circize,  
388 RColorBrewer, and dplyr) to get a general annotation with R version 3.6.3 (Gu, 2014, 2016).  
389 A more accurate annotation was performed with Prokka (Seeman, 2016) (v1.14.6 -  
390 <https://github.com/tseemann/prokka>) and its outputs were analyzed by using the Pathway Tools  
391 software (v.24.5) (Karp et al., 2019) with the MetaCyc database (v.24.5) (Caspi et al., 2019) to

392 explore in details the putative metabolisms encoded in MAGs. Regarding sulfur metabolisms,  
393 for dsr genes, the perl script DiSCo (v.1.0.0, [https://github.com/Genome-Evolution-and-](https://github.com/Genome-Evolution-and-Ecology-Group-GEEG/DiSCo)  
394 [Ecology-Group-GEEG/DiSCo](https://github.com/Genome-Evolution-and-Ecology-Group-GEEG/DiSCo)) was used on the Prokka protein sequences outputs of each MAG  
395 to highlight the specific genes (Neukirchen and Sousa, 2021).

396  
397

## 398 **References**

399

400 Albuquerque L., da Costa M.S. (2014) The Family *Thermaceae*. In: Rosenberg E., DeLong  
401 E.F., Lory S., Stackebrandt E., Thompson F. (eds) *The Prokaryotes*. Springer, Berlin,  
402 Heidelberg. [https://doi.org/10.1007/978-3-642-38954-2\\_128](https://doi.org/10.1007/978-3-642-38954-2_128)

403

404 Allieux, M., Yvenou, S., Slobodkina, G., Slobodkin, A., Shao, Z., Jebbar, M., & Alain, K.  
405 (2020). Genomic Characterization and Environmental Distribution of a Thermophilic Anaerobe  
406 *Dissulfurirhabdus thermomarina* SH388<sup>T</sup> Involved in Disproportionation of Sulfur  
407 Compounds in Shallow Sea Hydrothermal Vents. *Microorganisms*, 8(8), 1132.  
408 <https://doi.org/10.3390/microorganisms8081132>

409

410 Alneberg, J., Bjarnason, B. S., de Bruijn, I., Schirmer, M., Quick, J., Ijaz, U. Z., Lahti, L.,  
411 Loman, N. J., Andersson, A. F., & Quince, C. (2014). Binning metagenomic contigs by  
412 coverage and composition. *Nature methods*, 11(11), 1144–1146.  
413 <https://doi.org/10.1038/nmeth.3103>

414

415 Amenabar, M.J., Flores, P.A., Pugin, B., Blamey, J.M. (2013). Archaeal diversity from  
416 hydrothermal systems of Deception Island, Antarctica. *Polar Biology*, 36, 373–80.  
417 <https://doi.org/10.1007/s00300-012-1267-3>

418

419 Belilla, J., Moreira, D., Jardillier, L., Reboul, G., Benzerara, K., López-García, J. M., Bertolino,  
420 P., López-Archilla, A. I., & López-García, P. (2019). Hyperdiverse archaea near life limits at  
421 the polyextreme geothermal Dallol area. *Nature Ecology & Evolution*, 3(11), 1552–1561.  
422 <https://doi.org/10.1038/s41559-019-1005-0>

423

424 Belkova, N. L., Tazaki, K., Zakharova, J. R., & Parfenova, V. V. (2007). Activity of bacteria  
425 in water of hot springs from Southern and Central Kamchatskaya geothermal provinces,  
426 Kamchatka Peninsula, Russia. *Microbiological Research*, 162(2), 99–107.  
427 <https://doi.org/10.1016/j.micres.2006.01.006>

428

429 Bendia A.G., Signori C. N., Franco D. C., Duarte R.T. D., Bohannon B.J. M., Pellizari V. H.  
430 (2018). A Mosaic of Geothermal and Marine Features Shapes Microbial Community Structure  
431 on Deception Island Volcano, Antarctica. *Frontiers in Microbiology*, 9, 899.  
432 <https://doi.org/10.3389/fmicb.2018.00899>

433

434 Bowers, R. M., Kyrpides, N. C., Stepanauskas, R., Harmon-Smith, M., Doud, D., Reddy, T.,  
435 Schulz, F., Jarett, J., Rivers, A. R., Eloie-Fadrosch, E. A., Tringe, S. G., Ivanova, N. N., Copeland,

436 A., Clum, A., Becraft, E. D., Malmstrom, R. R., Birren, B., Podar, M., Bork, P., Weinstock, G.  
437 M., ... Woyke, T. (2017). Minimum information about a single amplified genome (MISAG)  
438 and a metagenome-assembled genome (MIMAG) of bacteria and archaea. *Nature*  
439 *Biotechnology*, 35(8), 725–731. <https://doi.org/10.1038/nbt.3893>  
440  
441 Brock, T. D., Brock, K. M., Belly, R. T., & Weiss, R. L. (1972). Sulfolobus: a new genus of  
442 sulfur-oxidizing bacteria living at low pH and high temperature. *Archiv fur Mikrobiologie*,  
443 84(1), 54–68. <https://doi.org/10.1007/BF00408082>  
444  
445 Caspi, R., Billington, R., Keseler, I. M., Kothari, A., Krummenacker, M., Midford, P. E., Ong,  
446 W. K., Paley, S., Subhraveti, P., & Karp, P. D. (2020). The MetaCyc database of metabolic  
447 pathways and enzymes - a 2019 update. *Nucleic acids research*, 48(D1), D445–D453.  
448 <https://doi.org/10.1093/nar/gkz862>  
449  
450 Chaumeil, P. A., Mussig, A. J., Hugenholtz, P., & Parks, D. H. (2019). GTDB-Tk: a toolkit to  
451 classify genomes with the Genome Taxonomy Database. *Bioinformatics* (Oxford, England),  
452 36(6), 1925–1927. Advance online publication. <https://doi.org/10.1093/bioinformatics/btz848>  
453  
454 Charbonnier, F., Forterre, P., Erauso, G., Prieur, D., (1995). Purification of plasmids from  
455 thermophilic and hyperthermophilic archaeobacteria. In: Robb, F. T. (Editor in Chief), Place,  
456 A.R., DasSarma, S., Schreier, H.J., Fleischmann, E.M. (Eds.), *Archaea: A Laboratory Manual*.  
457 *Cold Spring Harbor Laboratory Press*, NY. *Thermophiles*, pp. 87–90 1995.  
458  
459 Charvis P, Recq M, Operto S, Brefort D (1995). Deep structure of the northern Kerguelen  
460 Plateau and hotspot-related activity. *Geophys J Int* 122:899–924.  
461 <https://doi.org/10.1111/j.1365-246X.1995.tb06845.x>  
462  
463 Deamer, D., Damer, B., & Kompanichenko, V. (2019). Hydrothermal Chemistry and the Origin  
464 of Cellular Life. *Astrobiology*, 19(12), 1523–1537. <https://doi.org/10.1089/ast.2018.1979>  
465  
466 Des Marais, D. J., & Walter, M. R. (2019). Terrestrial Hot Spring Systems: Introduction.  
467 *Astrobiology*, 19(12), 1419–1432. <https://doi.org/10.1089/ast.2018.1976>  
468  
469 Dodsworth, J. A., Gevorkian, J., Despujos, F., Cole, J. K., Murugapiran, S. K., Ming, H., Li,  
470 W. J., Zhang, G., Dohnalkova, A., & Hedlund, B. P. (2014). *Thermoflexus hugenholtzii* gen.  
471 nov., sp. nov., a thermophilic, microaerophilic, filamentous bacterium representing a novel  
472 class in the *Chloroflexi*, *Thermoflexia* classis nov., and description of *Thermoflexaceae* fam.  
473 nov. and *Thermoflexales* ord. nov. *International journal of systematic and evolutionary*  
474 *microbiology*, 64(Pt 6), 2119–2127. <https://doi.org/10.1099/ijs.0.055855-0>  
475  
476  
477  
478

479 Eren, A. M., Kiefl, E., Shaiber, A., Veseli, I., Miller, S. E., Schechter, M. S., Fink, I., Pan, J.  
480 N., Yousef, M., Fogarty, E. C., Trigodet, F., Watson, A. R., Esen, Ö. C., Moore, R. M.,  
481 Clayssen, Q., Lee, M. D., Kivenson, V., Graham, E. D., Merrill, B. D., Karkman, A., ... Willis,  
482 A. D. (2021). Community-led, integrated, reproducible multi-omics with anvio. *Nature*  
483 *microbiology*, 6(1), 3–6. <https://doi.org/10.1038/s41564-020-00834-3>  
484

485 Gagnevin D, Ethien R, Bonin B, Giret A (2003) Open-system processes in the genesis of silica-  
486 oversaturated alkaline series of the Rallier du Baty peninsula, Kerguelen archipelago (Indian  
487 Ocean). *J Volc Geotherm Res* 123:267–300. [https://doi.org/10.1016/S0377-0273\(02\)00509-7](https://doi.org/10.1016/S0377-0273(02)00509-7)  
488

489 Giret, A., Grégoire, M., Cottin, J.Y., Michon, G., (1997). Kerguelen, a third type of oceanic  
490 island? In: “The Antarctic Region: Geological Evolution and Processes”, C.A. Ricci ed., Terra  
491 Antarctica Publication, Siena, 735-741. [https://doi.org/10.1016/0012-821X\(79\)90154-7](https://doi.org/10.1016/0012-821X(79)90154-7)  
492

493 Gramain, A., Brillet, F., Birrien, J.L., Le Romancer, M. (2011). Novel hyperthermophilic  
494 archaea flying over the Kerguelen islands: a dissemination study: in “Thermophiles 2011”  
495 conference, Big Sky, Montana USA, September 11-16.  
496

497 Gu, Z., Gu, L., Eils, R., Schlesner, M., & Brors, B. (2014). circlize Implements and enhances  
498 circular visualization in R. *Bioinformatics* (Oxford, England), 30(19), 2811–2812.  
499 <https://doi.org/10.1093/bioinformatics/btu393>  
500

501 Gu, Z., Eils, R., & Schlesner, M. (2016). Complex heatmaps reveal patterns and correlations in  
502 multidimensional genomic data. *Bioinformatics* (Oxford, England), 32(18), 2847–2849.  
503 <https://doi.org/10.1093/bioinformatics/btw313>  
504

505 Gupta R.S. (2014) The Phylum Aquificae. In: Rosenberg E., DeLong E.F., Lory S.,  
506 Stackebrandt E., Thompson F. (eds) *The Prokaryotes*. Springer, Berlin, Heidelberg.  
507 [https://doi.org/10.1007/978-3-642-38954-2\\_119](https://doi.org/10.1007/978-3-642-38954-2_119)  
508

509 Hanada S. (2014) The Phylum *Chloroflexi*, the Family *Chloroflexaceae*, and the Related  
510 Phototrophic Families *Oscillochloridaceae* and *Roseiflexaceae*. In: Rosenberg E., DeLong  
511 E.F., Lory S., Stackebrandt E., Thompson F. (eds) *The Prokaryotes*. Springer, Berlin,  
512 Heidelberg. [https://doi.org/10.1007/978-3-642-38954-2\\_165](https://doi.org/10.1007/978-3-642-38954-2_165)  
513

514 Issotta, F., Moya-Beltrán, A., Mena, C., Covarrubias, P. C., Thyssen, C., Bellenberg, S., Sand,  
515 W., Quatrini, R., & Vera, M. (2018). Insights into the biology of acidophilic members of the  
516 Acidiferrobacteraceae family derived from comparative genomic analyses. *Research in*  
517 *microbiology*, 169(10), 608–617. <https://doi.org/10.1016/j.resmic.2018.08.001>  
518

519 Itoh T. (2014) The Family *Thermoproteaceae*. In: Rosenberg E., DeLong E.F., Lory S.,  
520 Stackebrandt E., Thompson F. (eds) *The Prokaryotes*. Springer, Berlin, Heidelberg.  
521 [https://doi.org/10.1007/978-3-642-38954-2\\_330](https://doi.org/10.1007/978-3-642-38954-2_330)  
522

523 Karp, P. D., Midford, P. E., Billington, R., Kothari, A., Krummenacker, M., Latendresse, M.,  
524 Ong, W. K., Subhraveti, P., Caspi, R., Fulcher, C., Keseler, I. M., & Paley, S. M. (2021).  
525 Pathway Tools version 23.0 update: software for pathway/genome informatics and systems  
526 biology. *Briefings in bioinformatics*, 22(1), 109–126. <https://doi.org/10.1093/bib/bbz104>  
527

528 King, C. E., & King, G. M. (2014). *Thermomicrobium carboxidum* sp. nov., and *Thermorudis*  
529 *peleae* gen. nov., sp. nov., carbon monoxide-oxidizing bacteria isolated from geothermally  
530 heated biofilms. *International journal of systematic and evolutionary microbiology*, 64(Pt 8),  
531 2586–2592. <https://doi.org/10.1099/ijms.0.060327-0>  
532

533 Kochetkova, T. V., Toshchakov, S. V., Zayulina, K. S., Elcheninov, A. G., Zavarzina, D. G.,  
534 Lavrushin, V. Y., Bonch-Osmolovskaya, E. A., & Kublanov, I. V. (2020). Hot in Cold:  
535 Microbial Life in the Hottest Springs in Permafrost. *Microorganisms*, 8(9), 1308.  
536 <https://doi.org/10.3390/microorganisms8091308>  
537

538 Köster, J., & Rahmann, S. (2012). Snakemake--a scalable bioinformatics workflow engine.  
539 *Bioinformatics* (Oxford, England), 28(19), 2520–2522.  
540 <https://doi.org/10.1093/bioinformatics/bts480>  
541

542 Kublanov, I. V., Perevalova, A. A., Slobodkina, G. B., Lebedinsky, A. V., Bidzhieva, S. K.,  
543 Kolganova, T. V., Kaliberda, E. N., Rumsh, L. D., Haertlé, T., & Bonch-Osmolovskaya, E. A.  
544 (2009). Biodiversity of thermophilic prokaryotes with hydrolytic activities in hot springs of  
545 Uzon Caldera, Kamchatka (Russia). *Applied and environmental microbiology*, 75(1), 286–291.  
546 <https://doi.org/10.1128/AEM.00607-08>  
547

548 Lee K.C.Y., Dunfield P.F., Stott M.B. (2014) The Phylum Armatimonadetes. In: Rosenberg  
549 E., DeLong E.F., Lory S., Stackebrandt E., Thompson F. (eds) *The Prokaryotes*. Springer,  
550 Berlin, Heidelberg. [https://doi.org/10.1007/978-3-642-38954-2\\_388](https://doi.org/10.1007/978-3-642-38954-2_388)  
551

552 Lezcano, M. Á., Moreno-Paz, M., Carrizo, D., Prieto-Ballesteros, O., Fernández-Martínez, M.  
553 Á., Sánchez-García, L., Blanco, Y., Puente-Sánchez, F., de Diego-Castilla, G., García-  
554 Villadangos, M., Fairén, A. G., & Parro, V. (2019). Biomarker Profiling of Microbial Mats in  
555 the Geothermal Band of Cerro Caliente, Deception Island (Antarctica): Life at the Edge of Heat  
556 and Cold. *Astrobiology*, 19(12), 1490–1504. <https://doi.org/10.1089/ast.2018.2004>  
557

558 Löffler, F. E., Yan, J., Ritalahti, K. M., Adrian, L., Edwards, E. A., Konstantinidis, K. T.,  
559 Müller, J. A., Fullerton, H., Zinder, S. H., & Spormann, A. M. (2013). *Dehalococcoides*  
560 *mccartyi* gen. nov., sp. nov., obligately organohalide-respiring anaerobic bacteria relevant to  
561 halogen cycling and bioremediation, belong to a novel bacterial class, *Dehalococcoidia*  
562 classis nov., order *Dehalococcoidales* ord. nov. and family *Dehalococcoidaceae* fam. nov.,  
563 within the phylum *Chloroflexi*. *International journal of systematic and evolutionary*  
564 *microbiology*, 63(Pt 2), 625–635. <https://doi.org/10.1099/ijms.0.034926-0>  
565



566 Mehtad D., Satyanarayana T. (2013) Diversity of Hot Environments and Thermophilic  
567 Microbes. In: Satyanarayana T., Littlechild J., Kawarabayasi Y. (eds) *Thermophilic Microbes*  
568 *in Environmental and Industrial Biotechnology*. Springer, Dordrecht.  
569 [https://doi.org/10.1007/978-94-007-5899-5\\_1](https://doi.org/10.1007/978-94-007-5899-5_1)  
570

571 Meyer-Dombard, D.R., Shock, E.L. and Amend, J.P. (2005), Archaeal and bacterial  
572 communities in geochemically diverse hot springs of Yellowstone National Park, USA.  
573 *Geobiology*, 3: 211-227. <https://doi.org/10.1111/j.1472-4669.2005.00052.x>  
574

575 Ming, H., Zhao, Z. L., Ji, W. L., Ding, C. L., Cheng, L. J., Niu, M. M., Li, M., Yi, B. F., Xia,  
576 T. T., & Nie, G. X. (2020). *Thermus thermamylovorans* sp. nov., isolated from a hot spring.  
577 *International journal of systematic and evolutionary microbiology*, 70(3), 1729–1737.  
578 <https://doi.org/10.1099/ijsem.0.003965>  
579

580 Muñoz, P.A., Flores, P.A, Boehmwald, F.A., Blamey, J.M. Thermophilic bacteria present in a  
581 sample from Fumarole Bay, Deception Island. *Antarctic Science*, 23, 549–55.  
582

583 Neukirchen, S., & Sousa, F. L. (2021). DiSCo: a sequence-based type-specific predictor of Dsr-  
584 dependent dissimilatory sulphur metabolism in microbial data. *Microbial genomics*, 7(7),  
585 10.1099/mgen.0.000603. <https://doi.org/10.1099/mgen.0.000603>  
586

587 Niederberger, T. D., Götz, D. K., McDonald, I. R., Ronimus, R. S., & Morgan, H. W. (2006).  
588 *Ignisphaera aggregans* gen. nov., sp. nov., a novel hyperthermophilic crenarchaeote isolated  
589 from hot springs in Rotorua and Tokaanu, New Zealand. *International journal of systematic*  
590 *and evolutionary microbiology*, 56(Pt 5), 965–971. <https://doi.org/10.1099/ijms.0.63899-0>  
591

592 Nurk, S., Meleshko, D., Korobeynikov, A., & Pevzner, P. A. (2017). metaSPAdes: a new  
593 versatile metagenomic assembler. *Genome research*, 27(5), 824–834.  
594 <https://doi.org/10.1101/gr.213959.116>  
595

596 Parikka, K.J., Jacquet, S., Colombet, J., Guillaume, D., & Le Romancer, M. (2018). Abundance  
597 and observations of thermophilic microbial and viral communities in submarine and terrestrial  
598 hot fluid systems of the French Southern and Antarctic Lands. *Polar Biol* **41**, 1335–1352.  
599 <https://doi.org/10.1007/s00300-018-2288-3>  
600

601 Postec, A., Ciobanu, M., Birrien, J.L., Prieur, D. & Le Romancer, M. (2009). Microbial  
602 biodiversity of thermophilic communities in remote geothermal springs of Saint-Paul and  
603 Kerguelen Islands. Proc. In “Thermophiles 2009” conference, Beijing, China, August, 16-21.  
604

605 Power, J. F., Carere, C. R., Lee, C. K., Wakerley, G., Evans, D. W., Button, M., White, D.,  
606 Climo, M. D., Hinze, A. M., Morgan, X. C., McDonald, I. R., Cary, S. C., & Stott, M. B. (2018).  
607 Microbial biogeography of 925 geothermal springs in New Zealand. *Nature communications*,  
608 9(1), 2876. <https://doi.org/10.1038/s41467-018-05020-y>  
609



610 Reigstad, L. J., Jorgensen, S. L., & Schleper, C. (2010). Diversity and abundance of  
611 Korarchaeota in terrestrial hot springs of Iceland and Kamchatka. *The ISME journal*, 4(3), 346–  
612 356. <https://doi.org/10.1038/ismej.2009.126>  
613  
614 Renac, C., Moine, B., Goudour, J.P., Le Romancer, M. & Perrache, C. (2020). Stable isotope  
615 study of rainfall, river drainage and hot springs of the Kerguelen Archipelago, SW Indian  
616 Ocean, *Geothermics*, 83, 101726. <https://doi.org/10.1016/j.geothermics.2019.101726>.  
617  
618 Shaiber, A., Willis, A.D., Delmont, T.O. et al. Functional and genetic markers of niche  
619 partitioning among enigmatic members of the human oral microbiome. *Genome Biol* 21, 292  
620 (2020). <https://doi.org/10.1186/s13059-020-02195-w>  
621  
622 Sahm, K., John, P., Nacke, H., Wemheuer, B., Grote, R., Daniel, R., & Antranikian, G. (2013).  
623 High abundance of heterotrophic prokaryotes in hydrothermal springs of the Azores as revealed  
624 by a network of 16S rRNA gene-based methods. *Extremophiles : life under extreme conditions*,  
625 17(4), 649–662. <https://doi.org/10.1007/s00792-013-0548-2>  
626  
627 Seemann T. Prokka: rapid prokaryotic genome annotation. *Bioinformatics*. 2014 Jul  
628 15;30(14):2068-9. doi: 10.1093/bioinformatics/btu153.  
629  
630 Slobodkin, A. I., & Slobodkina, G. B., (2019). Diversity of Sulfur-Disproportionating  
631 Microorganisms. *Microbiology*, 88(5), 509-522. <https://doi.org/10.1134/S0026261719050138>  
632  
633 St John, E., Liu, Y., Podar, M., Stott, M. B., Meneghin, J., Chen, Z., Lagutin, K., Mitchell, K.,  
634 & Reysenbach, A. L. (2019). A new symbiotic nanoarchaeote (*Candidatus Nanoclepta*  
635 *minutus*) and its host (*Zestosphaera tikiterensis* gen. nov., sp. nov.) from a New Zealand hot  
636 spring. *Systematic and applied microbiology*, 42(1), 94–106.  
637 <https://doi.org/10.1016/j.syapm.2018.08.005>  
638  
639 Urbietta, M. S., Porati, G. W., Segretin, A. B., González-Toril, E., Giaveno, M. A., & Donati,  
640 E. R. (2015). Copahue Geothermal System: A Volcanic Environment with Rich Extreme  
641 Prokaryotic Biodiversity. *Microorganisms*, 3(3), 344–363.  
642 <https://doi.org/10.3390/microorganisms3030344>  
643  
644 Van Kranendonk MJ, Deamer DW, Djokic T. Life Springs. *Sci Am*. 2017 Jul 16;317(2):28-35.  
645 doi: 10.1038/scientificamerican0817-28.  
646  
647 Wemheuer, B., Taube, R., Akyol, P., Wemheuer, F., & Daniel, R. (2013). Microbial diversity  
648 and biochemical potential encoded by thermal spring metagenomes derived from the  
649 Kamchatka Peninsula. *Archaea* (Vancouver, B.C.), 2013, 136714.  
650 <https://doi.org/10.1155/2013/136714>  
651

652 Wilkins, L., Ettinger, C. L., Jospin, G., & Eisen, J. A. (2019). Metagenome-assembled genomes  
653 provide new insight into the microbial diversity of two thermal pools in Kamchatka, Russia.  
654 *Scientific reports*, 9(1), 3059. <https://doi.org/10.1038/s41598-019-39576-6>

655

656 Yabe, S., Sakai, Y., Abe, K., Yokota, A., Také, A., Matsumoto, A., Sugiharto, A., Susilowati,  
657 D., Hamada, M., Nara, K., Made Sudiana, I., & Otsuka, S. (2017). *Dictyobacter aurantiacus*  
658 gen. nov., sp. nov., a member of the family *Ktedonobacteraceae*, isolated from soil, and  
659 emended description of the genus *Thermosporothrix*. *International journal of systematic and*  
660 *evolutionary microbiology*, 67(8), 2615–2621. <https://doi.org/10.1099/ijsem.0.001985>

661

662 Yarza, P., Yilmaz, P., Pruesse, E., Glöckner, F. O., Ludwig, W., Schleifer, K. H., Whitman, W.  
663 B., Euzéby, J., Amann, R., & Rosselló-Móra, R. (2014). Uniting the classification of cultured  
664 and uncultured bacteria and archaea using 16S rRNA gene sequences. *Nature reviews.*  
665 *Microbiology*, 12(9), 635–645. <https://doi.org/10.1038/nrmicro3330>

666

667

## 668 **Acknowledgements**

669

670 We are grateful to the Territoire des Terres Australes et Antarctiques Françaises (TAAF), the  
671 IPEV (Institut Paul-Emile Victor) and its logistical staff for logistic support for transit and  
672 fieldwork in the Kerguelen archipelago. We thank M. Jebbar and Z. Shao, co-supervisors of  
673 M.A., for letting him do this study which was not in the scope of his thesis. We acknowledge  
674 the LABGeM (CEA/Genoscope & CNRS UMR8030), the France Génomique and French  
675 Bioinformatics Institute national infrastructures (funded as part of Investissements d’Avenir  
676 program managed by Agence Nationale pour la Recherche, contracts ANR-10-INBS-09 and  
677 ANR-11-INBS-0013) are acknowledged for support within the MicroScope annotation  
678 platform.

679

680 We are grateful for the financial support of IPEV provided by the TALISKER program N°1077  
681 to D.G. and HOTVIR program N°408 to M.L.R. Metagenomic analyses were funded by the  
682 Sino-French IRP 1211 MicrobSea to K.A. and by the MERLIN “Abyss” program funded by  
683 Ifremer to K.A. The study was supported by a grant from the French Ministry of Higher  
684 Education and Research, and from the Région Bretagne, to MA.

685

## 686 **Author contributions**

687

688 Conceptualization, M.A. and K.A.; Formal analysis, M.A., S.Y., A.M., D.G., J.A., and K.A.;  
689 Funding acquisition, D.G., M.L.R. and K.A.; Investigation, M.A., S.Y., A.M., M.C., D.G., J.A.,  
690 G.S., A.S., G.L. and K.A.; Supervision, K.A.; Writing—original draft, M.A., S.Y. and K.A.;  
691 Review & editing, all coauthors. All authors have read and agreed to the published version of  
692 the manuscript.

693

694

695 **Competing interests**

696

697 The authors declare no conflict of interest.

698

699 **Data Availability**

700

701 The following metagenomes and MAGs were referenced in the Table 3, available on the  
702 European Nucleotide Archive (ENA) (<https://www.ebi.ac.uk/ena/browser/home>).

703

704 **Supplementary data**

705

706 **Text S1. Attempt to classify MAGs on the basis of genome relatedness indices**

707

708 **Table S1.** Physico-chemical conditions of the RB108, RB13, RB10 and RB32 geothermal  
709 springs. NR, Not Reported.

710

711 **Table S2.** Taxonomical diversity classification of the 42 MAGs according to LPSN taxonomy  
712 (<https://lpsn.dsmz.de/>) based on average relatedness indices.

713

714 **Figure S1.** Phylogenomic trees showing the positioning of the 42 MAGs based on GTDB-Tk  
715 classification and GTDB database (R95).

716

717 **Figure legends**

718

719 **Figure 1.** Sampling locations at the “plateau des Fumeroles” in the Rallier du Baty Peninsula,  
720 Kerguelen Islands, French Southern and Antarctic Lands and photographs of the 4 hot springs  
721 studied, and their temperature and pH conditions.

722

723 **Figure 2.** Venn diagrams showing the shared phyla, families and genera within the  
724 reconstructed MAGs from the hot springs RB10, RB13, RB32 and RB108.

725

726 **Figure 3:** Metabolic pathway diagram of the 42 MAGs based on KEGG Decoder annotations,  
727 showing MAG classification according to GTDB-Tk and estimated genome completion.

728

729 **Tables**

730

731 **Table 1.** General characteristics of the 42 MAGs obtained from RB10, RB13, RB32 and  
732 RB108 hot springs (HQ: high quality, NHQ: near- high quality, MQ: medium quality, PQ:  
733 poor quality, *rrn*: ribosomal RNA).

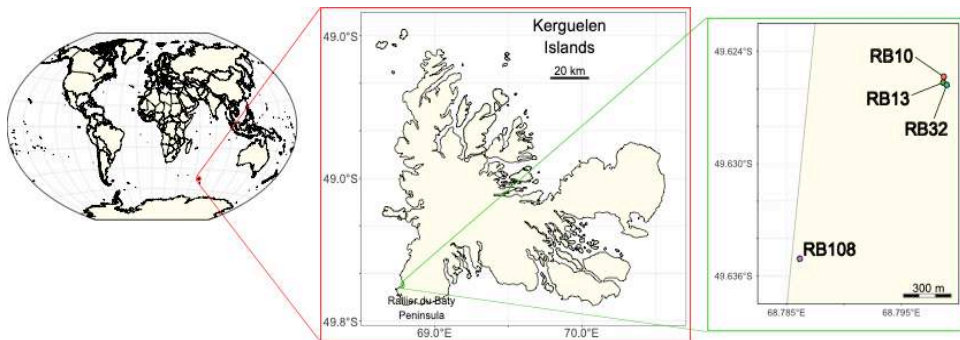
734

735 **Table 2.** Classification of the MAGs based on the taxonomic classification of GTDB-Tk.

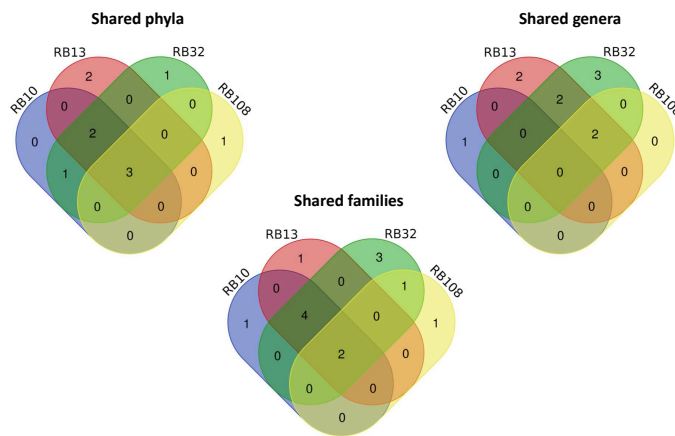
736

737 **Table 3.** Metagenomes and MAGs accessions numbers on ENA (Study ID: PRJEB46766).

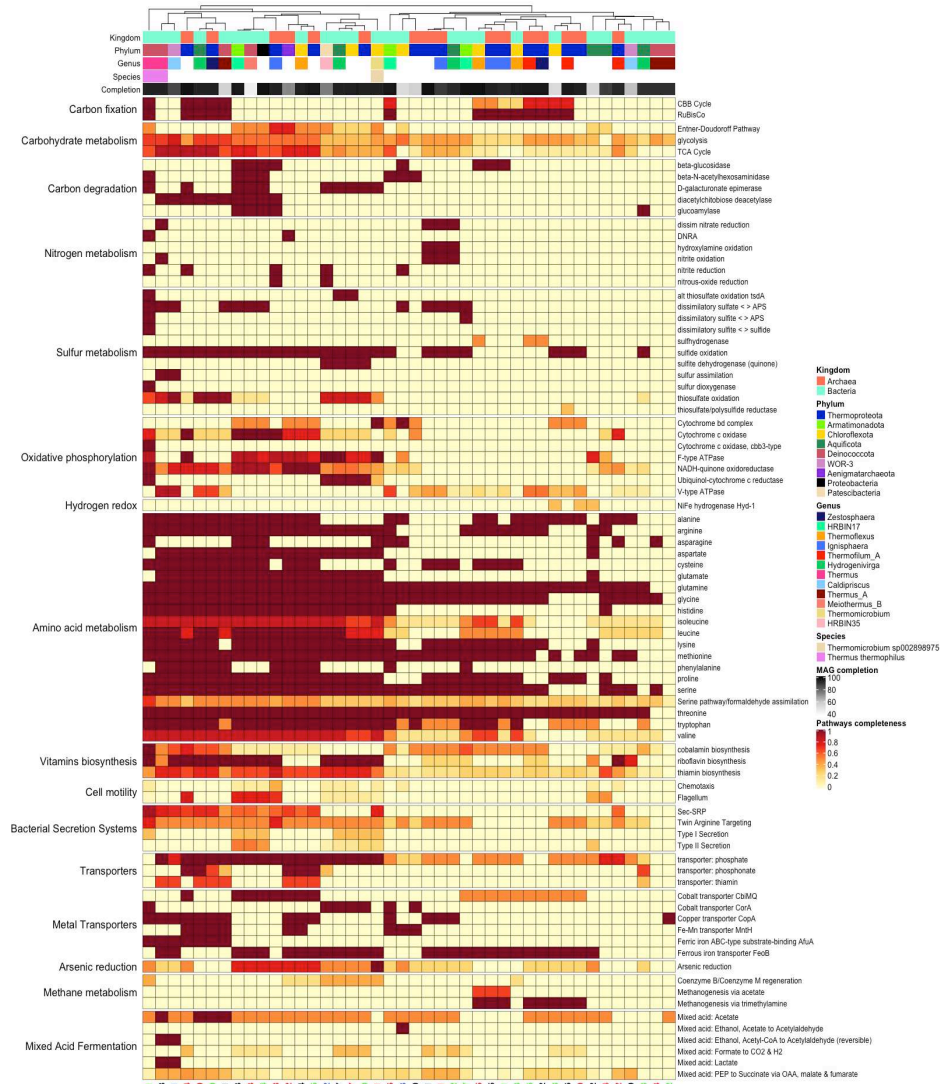
738



739  
740  
741  
742  
743  
744  
745  
746



747  
748



750  
751  
752  
753  
754  
755  
756  
757  
758

759

Sample	MAG quality	Percent complet.	Percent contam.	Mean Coverage	GC content	Size (Mbp)	Contig number	N50	tRNA	<i>rnr</i> sequences (5S-16S-23S)
RB10-MAG01	NHQ	96.84	0.95	61.98	57.01	1.78	59	78.449	35	1-0-0
RB10-MAG02	NHQ	98.00	0.63	40.11	38.88	1.49	212	15.625	33	1-0-0
RB10-MAG03	NHQ	92.59	0.19	38.28	56.24	2.65	72	76.979	47	1-1-0
RB10-MAG04	HQ	92.73	1.82	125.94	65.49	2.50	119	38.887	45	1-1-1
RB10-MAG05	NHQ	94.34	0.00	20.12	33.97	1.60	309	8.060	17	1-0-0
RB10-MAG06	HQ	97.79	0.74	74.51	53.43	1.72	322	11.699	19	1-1-1
RB10-MAG07	HQ	97.56	0.41	4822.70	53.78	1.44	153	17.997	43	1-1-1
RB10-MAG08	HQ	96.75	0.85	448.27	69.15	2.01	196	20.594	45	0-0-0
RB10-MAG09	MQ	54.88	0.00	12.64	42.63	0.75	417	1.860	16	0-0-0
RB10-MAG10	MQ	57.09	0.00	12.99	33.71	0.86	455	2.000	10	0-0-0
RB10-MAG11	NHQ	91.61	0.14	118.61	65.66	1.78	159	22.734	33	0-0-0
RB10-MAG12	MQ	54.21	0.81	13.87	31.69	0.75	413	1.839	12	1-0-0
RB13-MAG01	NHQ	93.29	1.22	50.58	67.39	2.20	188	24.091	35	1-0-1
RB13-MAG02	NHQ	96.52	0.63	1385.16	56.92	1.82	69	74.252	33	1-0-1
RB13-MAG03	NHQ	97.79	0.74	189.70	53.64	1.67	246	22.516	47	1-0-0
RB13-MAG04	NHQ	90.74	0.19	23.91	56.24	2.56	329	11.396	45	1-0-0
RB13-MAG05	NHQ	93.03	1.01	31.18	65.49	2.35	243	14.935	17	1-0-1
RB13-MAG06	NHQ	97.20	1.58	224.61	38.67	1.41	228	9.959	19	1-0-0
RB13-MAG07	NHQ	92.65	0.74	36.10	52.52	1.24	149	14.053	43	1-0-0
RB13-MAG08	NHQ	92.72	1.58	209.57	36.07	1.23	126	22.470	45	0-0-0
RB13-MAG09	NHQ	100.00	0.00	118.59	65.33	2.01	179	35.402	16	0-0-0
RB13-MAG10	HQ	97.43	0.41	118.59	53.62	1.41	147	14.581	10	1-1-1
RB13-MAG11	MQ	87.62	0.95	574.42	34.11	1.50	306	7.292	33	0-0-0
RB13-MAG12	MQ	72.90	3.27	125.85	25.76	0.74	154	8.912	12	1-0-0
RB13-MAG13	PQ	30.02	0.43	90.33	66.35	0.83	520	1.613	35	1-0-1
RB32-MAG01	NHQ	97.47	0.95	29.75	56.80	1.75	57	88.979	33	0-0-0
RB32-MAG02	HQ	94.55	1.82	421.42	65.38	2.54	148	29.008	47	1-1-2
RB32-MAG03	HQ	92.59	0.19	845.13	56.23	2.67	84	95.702	45	1-1-1
RB32-MAG04	NHQ	94.72	0.00	24.31	64.77	2.45	128	40.031	17	1-0-1
RB32-MAG05	NHQ	98.73	0.00	28.06	34.36	1.76	238	16.008	19	1-0-1
RB32-MAG06	NHQ	91.18	0.00	302.91	34.75	1.96	305	12.851	43	1-0-0
RB32-MAG07	NHQ	97.83	0.41	1025.50	53.50	1.45	157	17867.00	45	1-0-1
RB32-MAG08	NHQ	94.95	0.93	1025.50	65.25	2.55	629	5.755	16	0-0-0
RB32-MAG09	NHQ	94.85	1.47	94.92	53.78	1.57	334	8.549	10	1-0-0
RB32-MAG10	NHQ	100.00	1.27	184.55	65.39	1.99	128	41.211	33	1-0-1
RB32-MAG11	NHQ	94.70	2.28	20.34	32.15	1.30	295	6.491	12	0-0-0
RB32-MAG12	MQ	80.35	0.00	11.95	42.38	1.20	362	20.577	35	1-0-0
RB32-MAG13	MQ	70.82	0.00	129.49	27.82	0.55	176	19.960	33	0-0-1
RB32-MAG14	MQ	55.12	0.00	11.32	70.35	1.47	834	1.812	47	0-0-0
RB108-MAG01	NHQ	99.15	1.27	1120.09	69.21	2.04	126	30.509	45	0-0-0
RB108-MAG02	NHQ	96.75	0.00	579.13	53.28	1.45	75	29.169	17	1-0-0
RB108-MAG03	MQ	53.38	4.73	86.68	56.73	3.96	2105	1.944	19	0-0-0

760  
761  
762  
763  
764  
765  
766  
767  
768  
769  
770  
771  
772  
773  
774  
775  
776  
777  
778  
779  
780  
781

MAG ID	Domain	Phylum	Class	Order	Family	Genus	Species
RB10-MAG07	Bacteria	Aquificota	Aquificae	Aquificales	Aquificaceae	Hydrogenivirga	New
RB10-MAG12	Bacteria	Aquificota	Aquificae	Aquificales	Hydrogenobaculaceae	New	
RB13-MAG10	Bacteria	Aquificota	Aquificae	Aquificales	Aquificaceae	Hydrogenivirga	New
RB32-MAG07	Bacteria	Aquificota	Aquificae	Aquificales	Aquificaceae	Hydrogenivirga	New
RB32-MAG11	Bacteria	Aquificota	Aquificae	Aquificales	Hydrogenobaculaceae	New	
RB108-MAG02	Bacteria	Aquificota	Aquificae	Aquificales	Aquificaceae	Hydrogenivirga	New
RB10-MAG03	Bacteria	Armatimonadota	HRBIN17	HRBIN17	HRBIN17	HRBIN17	New
RB13-MAG04	Bacteria	Armatimonadota	HRBIN17	HRBIN17	HRBIN17	HRBIN17	New
RB32-MAG03	Bacteria	Armatimonadota	HRBIN17	HRBIN17	HRBIN17	HRBIN17	New
RB10-MAG04	Bacteria	Chloroflexota	Anaerolineae	Thermoflexales	Thermoflexaceae	Thermoflexus	New
RB13-MAG05	Bacteria	Chloroflexota	Anaerolineae	Thermoflexales	Thermoflexaceae	Thermoflexus	New
RB32-MAG02	Bacteria	Chloroflexota	Anaerolineae	Thermoflexales	Thermoflexaceae	Thermoflexus	New
RB32-MAG04	Bacteria	Chloroflexota	Dehalococcoidia	New			
RB32-MAG08	Bacteria	Chloroflexota	Chloroflexia	Thermomicrobiales	Thermomicrobiaceae	Thermomicrobium	New
RB32-MAG14	Bacteria	Chloroflexota	FW602-bin22	FW602-bin22	New		
RB108-MAG03	Bacteria	Chloroflexota	Kiedonobacteria	Kiedonobacterales	Kiedonobacteraceae	New	
RB10-MAG01	Archaea	Thermoproteota	Thermoproteia	Sulfolobales	Acidilobaceae	New	
RB10-MAG02	Archaea	Thermoproteota	Thermoproteia	Sulfolobales	NBVN01	Zestosphaera	New
RB10-MAG05	Archaea	Thermoproteota	Thermoproteia	Sulfolobales	Ignisphaeraceae	Ignisphaera	New
RB10-MAG06	Archaea	Thermoproteota	Thermoproteia	Thermofilales	Thermofilaceae	Thermofilum_A	New
RB10-MAG10	Archaea	Thermoproteota	Thermoproteia	New			
RB13-MAG02	Archaea	Thermoproteota	Thermoproteia	Sulfolobales	Acidilobaceae	New	
RB13-MAG03	Archaea	Thermoproteota	Thermoproteia	Thermofilales	Thermofilaceae	Thermofilum_A	New
RB13-MAG06	Archaea	Thermoproteota	Thermoproteia	Sulfolobales	NBVN01	Zestosphaera	New
RB13-MAG07	Archaea	Thermoproteota	Thermoproteia	Thermoproteales	Thermocladiaceae	New	
RB13-MAG08	Archaea	Thermoproteota	Thermoproteia	Sulfolobales	Ignisphaeraceae	Ignisphaera	New
RB13-MAG11	Archaea	Thermoproteota	Thermoproteia	Sulfolobales	Ignisphaeraceae	Ignisphaera	New
RB32-MAG01	Archaea	Thermoproteota	Thermoproteia	Sulfolobales	Acidilobaceae	New	
RB32-MAG05	Archaea	Thermoproteota	Thermoproteia	Sulfolobales	Ignisphaeraceae	Ignisphaera	New
RB32-MAG06	Archaea	Thermoproteota	Thermoproteia	New			
RB32-MAG09	Archaea	Thermoproteota	Thermoproteia	Thermofilales	Thermofilaceae	Thermofilum_A	New
RB10-MAG08	Bacteria	Deinococcota	Deinococci	Deinococcales	Thermaceae	Thermus	thermophilus
RB10-MAG11	Bacteria	Deinococcota	Deinococci	Deinococcales	Thermaceae	Thermus	New
RB13-MAG09	Bacteria	Deinococcota	Deinococci	Deinococcales	Thermaceae	Thermus	New
RB13-MAG13	Bacteria	Deinococcota	Deinococci	Deinococcales	Thermaceae	Meiothermus_B	New
RB32-MAG10	Bacteria	Deinococcota	Deinococci	Deinococcales	Thermaceae	Thermus	New
RB108-MAG01	Bacteria	Deinococcota	Deinococci	Deinococcales	Thermaceae	Thermus	thermophilus
RB13-MAG12	Archaea	Aenigmataarchaeota	Aenigmataarchaeia	CG10238-14	EX4484-224	New	
RB13-MAG01	Bacteria	Proteobacteria	Gammaaproteobacteria	Acidiferrobacterales	Sulfurifustaceae	New	
RB32-MAG13	Bacteria	Patescibacteria	Patecibacteria	UBA6257	HR35	New	
RB32-MAG12	Bacteria	WOR-3	Hydrothermia	LBFQ01	LBFQ01	Caldipriscus	New
RB10-MAG09	Bacteria	WOR-3	Hydrothermia	LBFQ01	LBFQ01	Caldipriscus	New

783  
784  
785  
786  
787  
788  
789



790

Assembly name	Assembly accession number	Sample accession number
<b>RB10</b>		
RB10-MAG01	GCA_916099525	ERS7299774
RB10-MAG02	GCA_916101595	ERS7299775
RB10-MAG03	GCA_916102575	ERS7299776
RB10-MAG04	GCA_916102815	ERS7299777
RB10-MAG05	GCA_916103375	ERS7299778
RB10-MAG06	GCA_916103935	ERS7299779
RB10-MAG07	GCA_916103025	ERS7299780
RB10-MAG08	GCA_916101605	ERS7299781
RB10-MAG09	GCA_916098365	ERS7299782
RB10-MAG10	GCA_916100445	ERS7299783
RB10-MAG11	GCA_916100255	ERS7299784
RB10-MAG12	GCA_916103405	ERS7299785
<b>RB13</b>		
RB13-MAG01	GCA_916101585	ERS7299786
RB13-MAG02	GCA_916101625	ERS7299787
RB13-MAG03	GCA_916101685	ERS7299788
RB13-MAG04	GCA_916101675	ERS7299789
RB13-MAG05	GCA_916104055	ERS7299790
RB13-MAG06	GCA_916104685	ERS7299791
RB13-MAG07	GCA_916099935	ERS7299792
RB13-MAG08	GCA_916104555	ERS7299793
RB13-MAG09	GCA_916098735	ERS7299794
RB13-MAG10	GCA_916103555	ERS7299795
RB13-MAG11	GCA_916103205	ERS7299796
RB13-MAG12	GCA_916101905	ERS7299797
RB13-MAG13	GCA_916101985	ERS7299798
<b>RB32</b>		
RB32-MAG01	GCA_916099235	ERS7299799
RB32-MAG02	GCA_916099675	ERS7299800
RB32-MAG03	GCA_916102075	ERS7299801
RB32-MAG04	GCA_916098805	ERS7299802
RB32-MAG05	GCA_916098685	ERS7299803
RB32-MAG06	GCA_916102535	ERS7299804
RB32-MAG07	GCA_916109635	ERS7299805
RB32-MAG08	GCA_916109905	ERS7299806
RB32-MAG09	GCA_916110065	ERS7299807
RB32-MAG10	GCA_916105685	ERS7299808
RB32-MAG11	GCA_916112325	ERS7299809
RB32-MAG12	GCA_916112475	ERS7299810
RB32-MAG13	GCA_916111365	ERS7299811
RB32-MAG14	GCA_916108235	ERS7299812
<b>RB108</b>		
RB108-MAG01	GCA_916116595	ERS7299813
RB108-MAG02	GCA_916109075	ERS7299814
RB108-MAG03	GCA_916109065	ERS7299815

791

792



## **Insulated geothermal springs in the Kerguelen Islands host a large fraction of new genomic microbial taxa**

Maxime Allieux<sup>1</sup>, Stéven Yvenou<sup>1</sup>, Alexander Merkel<sup>2</sup>, Marc Cozannet<sup>1</sup>, Johanne Aube<sup>1</sup>, Marc Le Romancer<sup>3</sup>, Damien Guillaume<sup>4</sup>, Alexander Slobodkin<sup>2</sup>, Galina Slobdokina<sup>2</sup>, Guillaume Lannuzel<sup>1</sup> & Karine Alain<sup>1\*</sup>

<sup>1</sup>Univ Brest, CNRS, IFREMER, IRP 1211 MicrobSea, Laboratoire de Microbiologie des Environnements Extrêmes LM2E, IUEM, Rue Dumont d'Urville, F-29280 Plouzané, France

<sup>2</sup>Winogradsky Institute of Microbiology, Research Center of Biotechnology of the Russian Academy of Sciences, Moscow, Russia

<sup>3</sup> missing

<sup>4</sup> missing

\*Karine.Alain@univ-brest.fr

**Text S1.** Attempt to classify MAGs on the basis of genome relatedness indices.

In attempt to go further than the classification made by GTDB-Tk, and as the taxonomy proposed by GTDB is new and does not correspond exactly to the one recognized by the International Code of Nomenclature of prokaryotes (ICNP), we also analyzed the data according to the rules of the Code and its nomenclature. For this purpose, we performed a tentative classification based on the LPSN taxonomy by using a combination of overall genomic indices classically used with isolates for the delineation of the different taxonomic ranks, namely: 16S rRNA gene sequence similarity, average nucleotide identity score (ANI) and average amino-acid identity value (AAI). We considered the following thresholds for the different taxonomic ranks and sequences/indices considered: i/ on the basis of 16S rRNA sequences, <98.7% for a new species, <94.5% for a new genus, <86.5% for a novel order (Yarza et al., 2014); ii/ on the basis of ANI, <94–96% for a new species (Richter & Rosselló-Móra, 2009), <70.85–76.56% for a new genus (Barco et al., 2020); on the basis of AAI, 95–100% for a same species, 65–95% for a same genus and 45–65% for a same family (Konstantinidis et al., 2017). When considering the value of the standard deviation calculated for the indices, the taxonomic affiliation could not be resolved, the two possible taxonomic affiliations were indicated in Table S2 with a superscript number. When these indices could not be considered due to the lack of cultivated close relatives, we considered GTDB-Tk classification.

For *Bacteria*, taxonomic, phylogenomic and phylogenetic analyses allowed us to place the MAGs in the following clades: three in the *Thermoflexus* genus from three different springs (RB10-MAG04, RB13-MAG05, RB32-MAG02), one in the *Dehalococcoidales* order (RB32-MAG04), one in the *Thermomicrobium* genus (RB32-MAG08), one in the *Chloroflexales* order (RB32-MAG14), one in the *Ktedonobacteraceae* family (RB108-MAG03), four in the *Hydrogenivirga* genus from the four different springs (RB10-MAG07, RB13-MAG10, RB32-MAG07, RB108-MAG02), two in the *Aquificaceae* family (RB10-MAG12, RB32-MAG11), five in the *Thermus* genus from the four geothermal sources (RB10-MAG08, RB10-MAG11, RB13-MAG09, RB32-MAG10, RB108-MAG01), one in the *Meiothermus* genus (RB13-MAG13), two in the ‘*Candidatus* Caldipriscus’ genus (RB10-MAG09, RB32-MAG12), one in the *Acidiferrobacteraceae* family (RB13-MAG01), three in the Armatimonadetes phylum (RB10-MAG03, RB13-MAG04, RB32-MAG03), and one in the ‘*Candidatus* Patescibacteria’ superphylum (RB32-MAG13).

For *Archaea*, assignments of the MAGs were as followed: three in the *Acidilobaceae* family (RB10-MAG01, RB13-MAG02, RB32-MAG01), two in the *Zestosphaera* genus (RB10-MAG02, RB13-MAG06), four in the *Ignisphaera* genus (RB10-MAG05, RB13-MAG08, RB13-MAG11, RB32-MAG05), three in the *Thermofilaceae* family (RB10-MAG06, RB13-MAG03, RB32-MAG09), three in the *Thermoproteales* order (RB10-MAG10, RB13-MAG07, RB32-MAG06), and one could not be classified (RB13-MAG12).

Out of these 42 MAGs, 23 corresponded to different taxa at the taxonomic rank of species or higher and were distributed respectively, into 1 known species called *Thermus thermophilus*, 11 new genomic species within the genera *Zestosphaera*, *Thermoflexus*, *Ignisphaera* (×2), *Thermofilum*, *Hydrogenivirga*, *Thermus*, *Meiothermus*, ‘*Candidatus* Caldipriscus’ and *Thermomicrobium*, 4 putative new genera belonging to the families *Acidilobaceae*, *Acidiferrobacteraceae*, *Aquificaceae* and *Ktedonobacteraceae*, 5 putative new families within the order *Armatimonadales* and *Thermoproteales* (×2), *Dehalococcoidales* and *Chloroflexales*, and 1 putative new class within the superphylum ‘*Candidatus* Patescibacteria’.

These analyses have made it possible to refine the classification of the taxa present in these sources but must be considered with care because a MAG is a consensus genome of a population, and not equivalent to a genome from an isolated strain, from a clone (Van Rossum et al., 2020).

**Table S1.** Physico-chemical conditions of the RB108, RB13, RB10 and RB32 geothermal springs. NR, Not Reported.

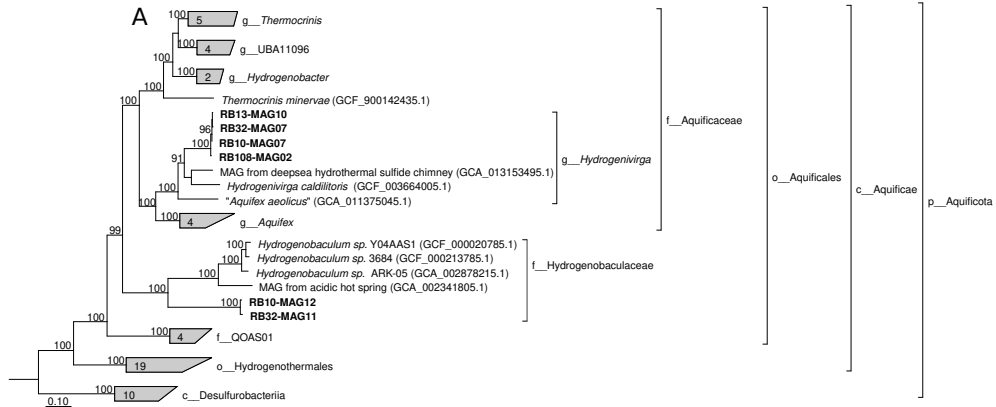
Samples	Field measurements					Laboratory measurements (mg/L)										
	T°C	pH	mV pH	mS/cm	alkalinity CaCO <sub>3</sub> (mg/L)	Cl <sup>-</sup>	HCO <sub>3</sub> <sup>-</sup>	F <sup>-</sup>	Cl <sup>-</sup>	Br <sup>-</sup>	SO <sub>4</sub> <sup>-</sup>	Na <sup>+</sup>	NH <sub>4</sub> <sup>+</sup>	K <sup>+</sup>	Mg <sup>++</sup>	Ca <sup>++</sup>
<b>RB108</b>	101.3	9.59	-111.9	3.45	83	3450	83	9.894	1039.8	2.763	22.209	1868,00	NR	107.9	NR	186.8
<b>RB13</b>	93	7.61	-67.7	0.149	25	166	29	0.376	14.321	NR	11.833	53.151	0.136	11.228	0.67	5.919
<b>RB10</b>	78.4	8.7	-10.9	0.166	29	149	25	0.547	13.516	NR	12.348	49.959	NR	8.658	0.317	4.41
<b>RB32</b>	97	5.79	95.1	0.086	3.2	86	3.2	NR	5.529	NR	14.361	16.41	1.07	4.062	0.279	0.742

**Table S2.** Taxonomical diversity classification of the 42 MAGs according to LPSN taxonomy (<https://lpsn.dsmz.de/>) based on average relatedness indices. AAI analysis was used to determine the taxonomy of some MAGs and for some of them the calculated standard deviations did not allow for an accurate and unique classification. In these cases, the possible alternative classifications, considering the standard deviations, are presented in Table 2 with an asterisk number, meaning: <sup>1</sup>Possibly a new family considering the standard deviation. <sup>2</sup>Possibly a new genus considering the standard deviation. <sup>3</sup>Possibly the family *Armatimonadaceae* considering the standard deviation. <sup>4</sup>Possibly the family *Thermoproteaceae* considering the standard deviation. <sup>5</sup>Possibly the family *Dehalococcoidaceae* considering the standard deviation. <sup>6</sup>Possibly the family *Chloroflexaceae* considering the standard deviation. \*: GTDB-Tk classification.

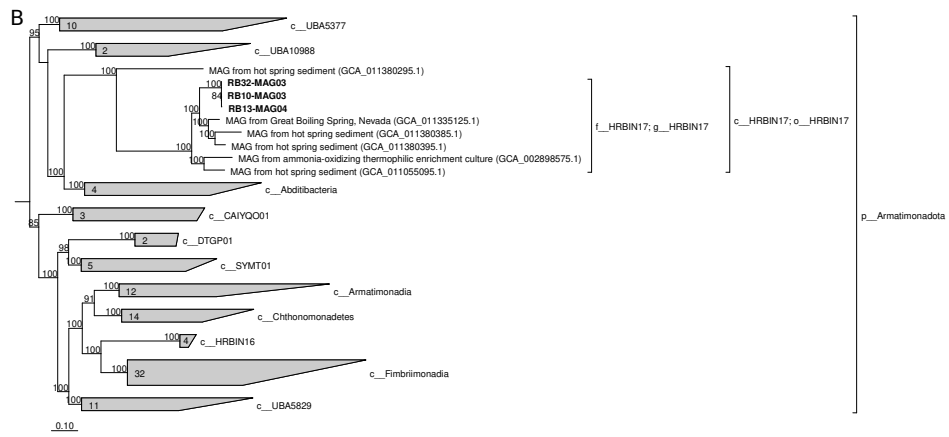
MAG ID	Domain	Phylum	Class	Order	Family	Genus	Species
RB10-MAG01	Archaea	Crenarchaeota	Thermoprotei	Acidilobales	Acidilobaceae <sup>2</sup>	New	
RB10-MAG02	Archaea	Crenarchaeota	Thermoprotei	Desulfurococcales	Desulfurococcaceae	Zestospaera <sup>3</sup>	New
RB10-MAG03	Bacteria	Armatimonadetes	Armatimonadia	Armatimonadales	New <sup>4</sup>		
RB10-MAG04	Bacteria	Chloroflexi	Thermoflexia	Thermoflexales	Thermoflexaceae	Thermoflexus	New
RB10-MAG05	Archaea	Crenarchaeota	Thermoprotei	Desulfurococcales	Desulfurococcaceae	Ignisphaera	New
RB10-MAG06	Archaea	Crenarchaeota	Thermoprotei	Thermoproteales	Thermoflaccae	Thermoflum	New
RB10-MAG07	Bacteria	Aquificae	Aquificae	Aquificales	Aquificaceae	Hydrogenivirga	New
RB10-MAG08	Bacteria	Deinococcus-Thermus	Deinococci	Thermales	Thermaceae	Thermus	thermophilus
RB10-MAG09	Bacteria	WOR-3*	Hydrothermia*	LBF001*	LBF001*	Caldipriscus*	New
RB10-MAG10	Archaea	Crenarchaeota	Thermoprotei	Thermoproteales	New <sup>4</sup>		
RB10-MAG11	Bacteria	Deinococcus-Thermus	Deinococci	Thermales	Thermaceae	Thermus	New
RB10-MAG12	Bacteria	Aquificae	Aquificae	Aquificales	Aquificaceae <sup>1</sup>	New	
RB13-MAG01	Bacteria	Proteobacteria	Gammaproteobacteria	Acidiferrobacterales	Acidiferrobacteraceae <sup>1</sup>	New	
RB13-MAG02	Archaea	Crenarchaeota	Thermoprotei	Acidilobales	Acidilobaceae <sup>2</sup>	New	
RB13-MAG03	Archaea	Crenarchaeota	Thermoprotei	Thermoproteales	Thermoflaccae <sup>1</sup>	New	
RB13-MAG04	Bacteria	Armatimonadetes	Armatimonadia	Armatimonadales	New <sup>4</sup>		
RB13-MAG05	Bacteria	Chloroflexi	Thermoflexia	Thermoflexales	Thermoflexaceae	Thermoflexus	New
RB13-MAG06	Archaea	Crenarchaeota	Thermoprotei	Desulfurococcales	Desulfurococcaceae	Zestospaera	New
RB13-MAG07	Archaea	Crenarchaeota	Thermoprotei	Thermoproteales	New <sup>4</sup>		
RB13-MAG08	Archaea	Crenarchaeota	Thermoprotei	Desulfurococcales	Desulfurococcaceae	Ignisphaera	New
RB13-MAG09	Bacteria	Deinococcus-Thermus	Deinococci	Thermales	Thermaceae	Thermus	New
RB13-MAG10	Bacteria	Aquificae	Aquificae	Aquificales	Aquificaceae	Hydrogenivirga	New
RB13-MAG11	Archaea	Crenarchaeota	Thermoprotei	Desulfurococcales	Desulfurococcaceae	Ignisphaera	New
RB13-MAG12	Archaea	Not defined					
RB13-MAG13	Bacteria	Deinococcus-Thermus	Deinococci	Thermales	Thermaceae	Mcirothermus <sup>2</sup>	New
RB32-MAG01	Archaea	Crenarchaeota	Thermoprotei	Acidilobales	Acidilobaceae <sup>2</sup>	New	
RB32-MAG02	Bacteria	Chloroflexi	Thermoflexia	Thermoflexales	Thermoflexaceae	Thermoflexus	New
RB32-MAG03	Bacteria	Armatimonadetes	Armatimonadia	Armatimonadales	New <sup>4</sup>		
RB32-MAG04	Bacteria	Chloroflexi	Dehalococcoidia	Dehalococcoidales	New <sup>4</sup>		
RB32-MAG05	Archaea	Crenarchaeota	Thermoprotei	Desulfurococcales	Desulfurococcaceae	Ignisphaera	New
RB32-MAG06	Archaea	Crenarchaeota	Thermoprotei	Thermoproteales	New <sup>4</sup>		
RB32-MAG07	Bacteria	Aquificae	Aquificae	Aquificales	Aquificaceae	Hydrogenivirga	New
RB32-MAG08	Bacteria	Chloroflexi	Thermomicrobia	Thermomicrobiales	Thermomicrobiaceae	Thermomicrobium	New
RB32-MAG09	Archaea	Crenarchaeota	Thermoprotei	Thermoproteales	Thermoflaccae <sup>1</sup>	New	
RB32-MAG10	Bacteria	Deinococcus-Thermus	Deinococci	Thermales	Thermaceae	Thermus	New
RB32-MAG11	Bacteria	Aquificae	Aquificae	Aquificales	Aquificaceae <sup>1</sup>	New	
RB32-MAG12	Bacteria	WOR-3*	Hydrothermia*	LBF001*	LBF001*	Caldipriscus*	New <sup>4</sup>
RB32-MAG13	Bacteria	Superphylum 'Candidatus Patescibacteria'*	Facetibacteria*	UBA6257*	HR35*	HRBN35*	
RB32-MAG14	Bacteria	Chloroflexi	Chloroflexia	Chloroflexales	New <sup>4</sup>		
RB108-MAG01	Bacteria	Deinococcus-Thermus	Deinococci	Thermales	Thermaceae	Thermus	thermophilus
RB108-MAG02	Bacteria	Aquificae	Aquificae	Aquificales	Aquificaceae	Hydrogenivirga	New
RB108-MAG03	Bacteria	Chloroflexi	Ktedonobacteria	Ktedonobacterales	Ktedonobacteraceae <sup>1</sup>	New	

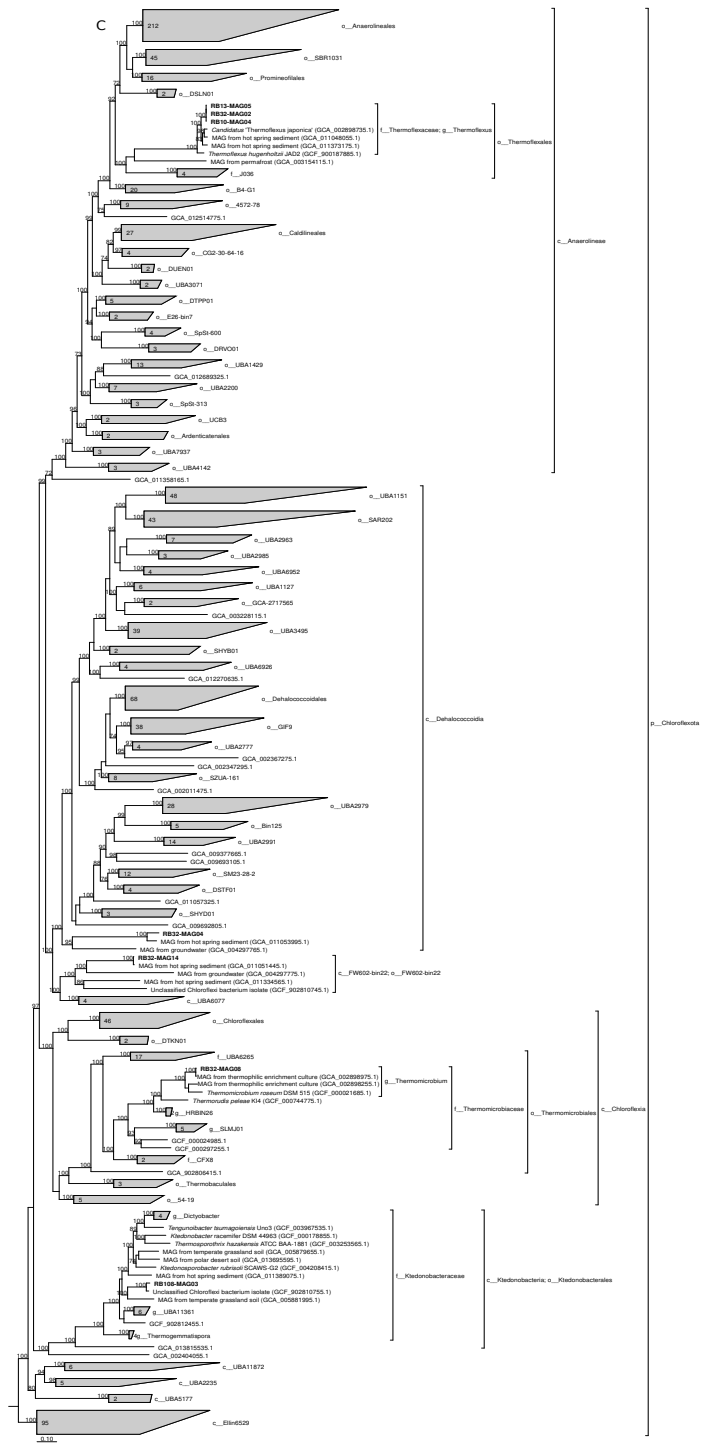
5

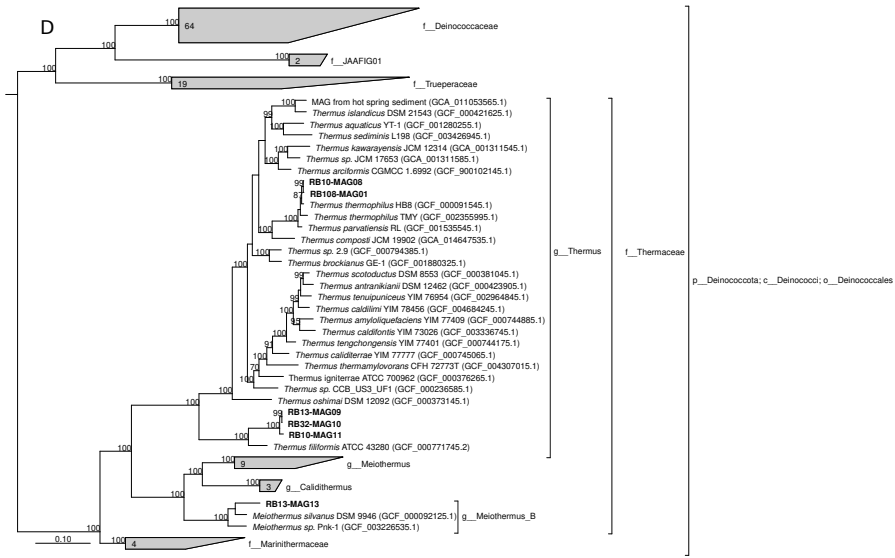
**Figure S1:** Phylogenetic trees showing the positioning of the 42 MAGs based on GTDB-Tk classification and GTDB database (R95). A, *Aquificota*; B, *Armatimonadota*; C, *Chloroflexota*; D, *Deinococcota*; E, *Proteobacteria*; F, *Patescibacteria*; G, *WOR-3*; H, *Thermoproteota*; and I, *Aenigmataarchaeota*.

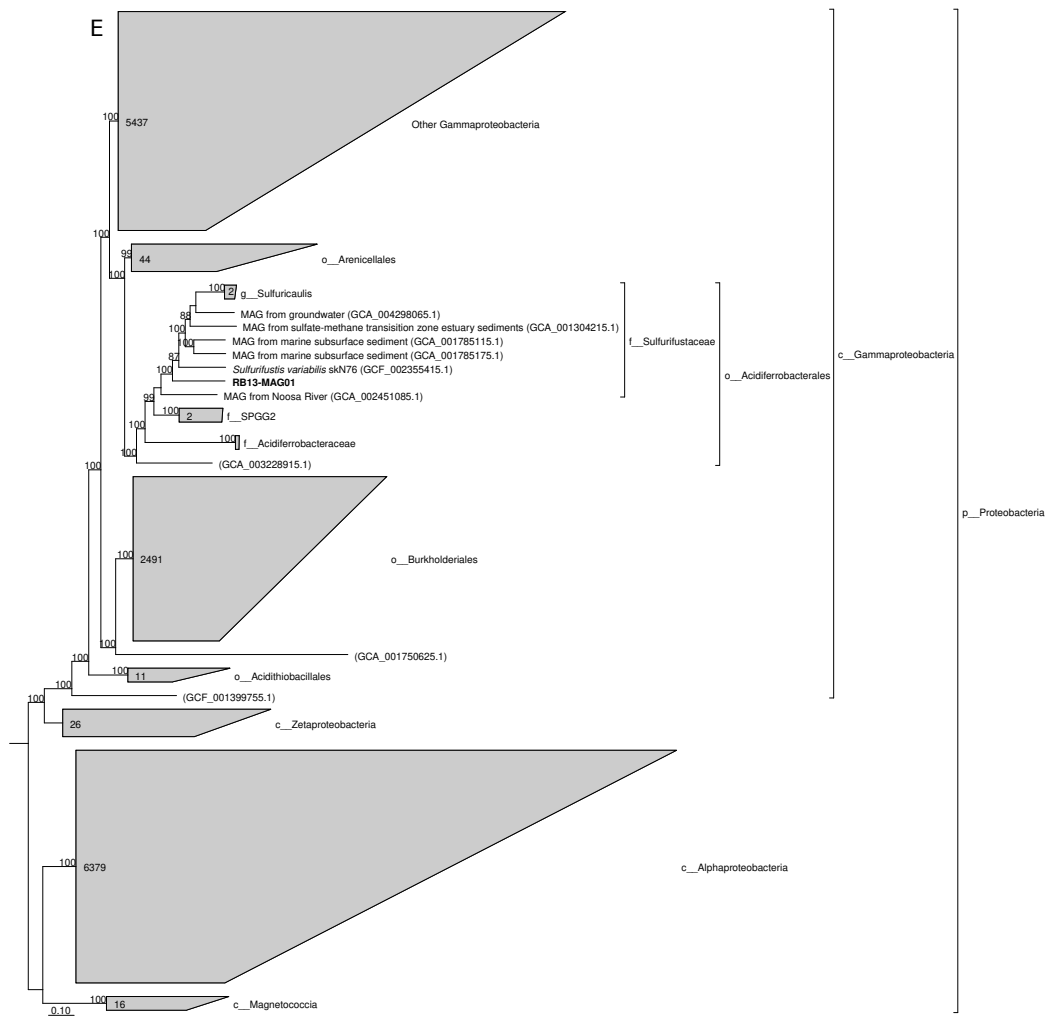


6

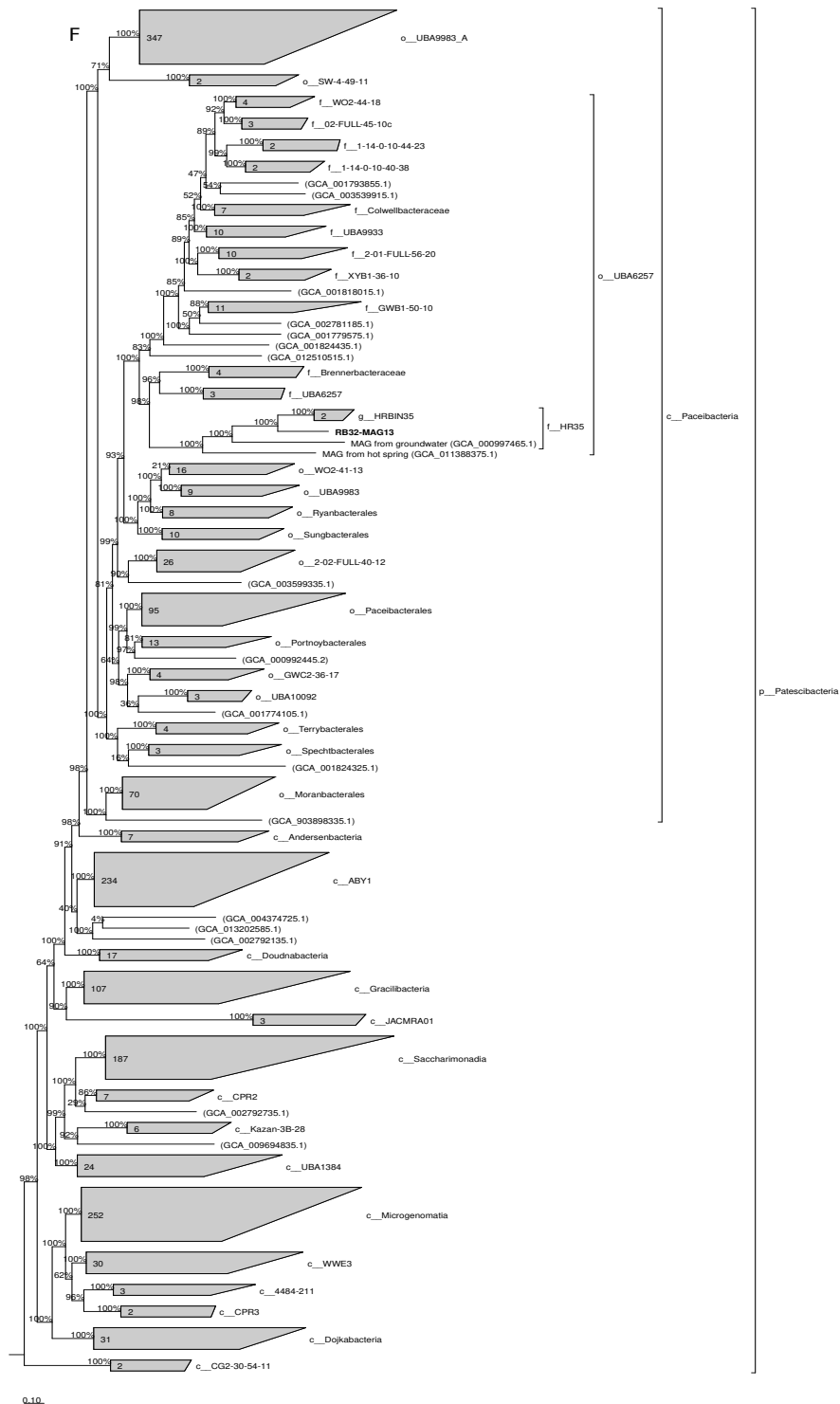


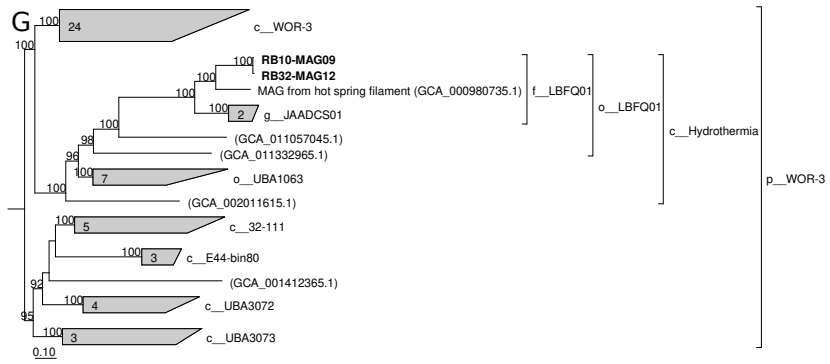


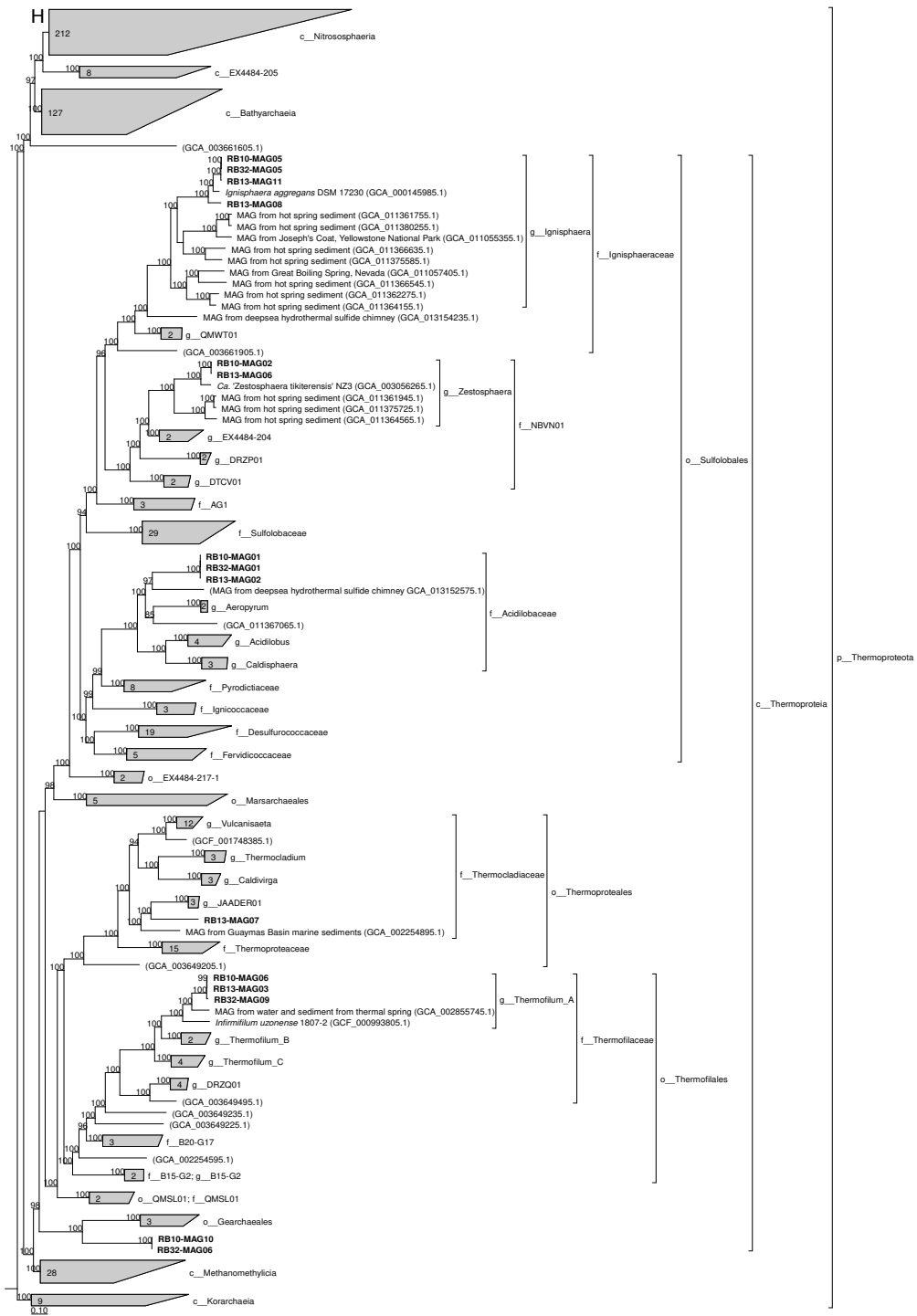














## References

- Barco, R. A., Garrity, G. M., Scott, J. J., Amend, J. P., Neelson, K. H., & Emerson, D. (2020). A Genus Definition for Bacteria and Archaea Based on a Standard Genome Relatedness Index. *mBio*, 11(1), e02475-19. <https://doi.org/10.1128/mBio.02475-19>
- Konstantinidis, K. T., Rosselló-Móra, R., & Amann, R. (2017). Uncultivated microbes in need of their own taxonomy. *The ISME journal*, 11(11), 2399–2406. <https://doi.org/10.1038/ismej.2017.113>
- Richter, M., & Rosselló-Móra, R. (2009). Shifting the genomic gold standard for the prokaryotic species definition. *Proceedings of the National Academy of Sciences of the United States of America*, 106(45), 19126–19131. <https://doi.org/10.1073/pnas.0906412106>
- Van Rossum, T., Ferretti, P., Maistrenko, O.M. and Bork, P. Diversity within species: interpreting strains in microbiomes. *Nat Rev Microbiol* **18**, 491–506 (2020). <https://doi.org/10.1038/s41579-020-0368-1>
- Yarza, P., Yilmaz, P., Pruesse, E., Glöckner, F. O., Ludwig, W., Schleifer, K. H., Whitman, W. B., Euzéby, J., Amann, R., & Rosselló-Móra, R. (2014). Uniting the classification of cultured and uncultured bacteria and archaea using 16S rRNA gene sequences. *Nature reviews. Microbiology*, 12(9), 635–645. <https://doi.org/10.1038/nrmicro3330>

### **3. Conclusions and Perspectives**

As this part of the work is very descriptive, it is difficult to discuss these results in greater details. As conclusion, we successfully analyzed these metagenomes from the Kerguelen Islands and wrote an article draft that we will be completed and submitted soon. Our results highlight that more efforts should be made in order to better document the microbial communities from these ecosystems, as they represent a reservoir of unknown microbial lineages with potentially novel activities and new metabolic pathways. As the Kerguelen Islands are very isolated geographically and located more than 3000 km from the first inhabited areas, new analyzes should be interesting to perform. In order to study the whole microbial diversity, microbial functions and adaptations encoded in microbial metagenomes and expressed in metatranscriptomes of the 80 terrestrial and submarine geothermal sources found in these areas. These microbial communities are also particularly interesting to study for evolution prospects. Finally, the microbial communities of these insulated areas also require special attention for their protection and conservation.

## General conclusion

In summary, all of the analyses performed during this PhD may seem rather scattered but this is partly due to various parameters and problems such as time, sanitary conditions, materials and sample availability, and also to my own scientific curiosity. We have successfully exploited almost all the data we were able to generate. But there is still a lot of work to be done on the different axes of the project. This is why we have reported most of the negative results to aid future analyses, to lead to a better overall understanding of the microbial sulfur cycle. If I could have changed anything in these three years of the thesis, I would have started earlier and focused more on the comparative proteomic study, which took a lot of effort and time, but would have yielded very valuable results for understanding elemental sulfur disproportionation process.

However, this work has allowed us to advance our knowledge of the sulfur cycle at different scales of organization of living organisms, from genomic to ecosystemic scale. Four new sulfur disproportionating taxa of hydrothermal origin were isolated, four genomes were annotated and progress was made in establishing a protocol for comparative proteomics with  $S^0$ -disproportionating microorganisms. Finally, a metagenomic study of microbial communities has allowed us to better understand the taxa present in hot springs that had not been studied before and that may have implications in the future for our understanding of the processes (deterministic *versus* stochastic) that govern microbial assemblages.

Regarding PhD valorization, we managed to publish the three following scientific articles:

- **Allioux, M.**, Jebbar, M., Slobodkina, G., Slobodkin, A., Moalic, Y., Frolova, A., Shao, Z. & Alain, K. (2021). Complete genome sequence of *Thermosulfurimonas marina* sp. nov., an anaerobic thermophilic chemolithoautotrophic bacterium isolated from a shallow hydrothermal vent. *Marine Genomics*, 55, 100800. <https://doi.org/10.1016/j.margen.2020.100800>.
- **Allioux, M.**, Yvenou, S., Slobodkina, G., Slobodkin, A., Shao, Z., Jebbar, M., & Alain, K. (2020). Genomic characterization and environmental distribution of a thermophilic anaerobe *Dissulfurirhabdus thermomarina* SH388<sup>T</sup> involved in disproportionation of sulfur compounds in shallow sea hydrothermal vents. *Microorganisms*, 8(1132), 1-14. <https://doi.org/10.3390/microorganisms8081132>.

- Slobodkina, G., **Allioux, M.**, Merkel, A., Alain, K. Jebbar, M. & Slobodkin, A. (2020). Genome analysis of *Thermosulfuriphilus ammonigenes* ST65<sup>T</sup>, an anaerobic thermophilic chemolithoautotrophic bacterium isolated from a shallow hydrothermal vent. *Marine Genomics*, 54: 100786. <https://doi.org/10.1016/j.margen.2020.100786>

Moreover, we wrote two following draft articles that will be submitted soon:

- **Allioux, M.**, Yvenou, S., Slobodkina, G., Slobodkin, A., Godfroy, A., Shao, Z., Jebbar, M. & Alain, K. (**in preparation**). Genome analysis of a new sulfur disproportionating species *Thermosulfurimonas* strain F29 and comparative genomics of sulfur-disproportionating bacteria from marine hydrothermal vents. *Microbial Genomics*.
- **Allioux, M.**, Yvenou, S., Merkel, A., Cozannet, M., Aube, J., Le Romancer, M., Guillaume, D., Slobodkin, A., Slobodkina, Lannuzel, G. & Alain, K. (**in preparation**). Insulated geothermal springs in the Kerguelen Islands host a large fraction of new genomic microbial taxa. *Scientific Reports*.

The microbial actors and the catabolic reactions of the sulfur cycle became better documented over the years, including in hydrothermal ecosystems. Nevertheless, some ecosystems in insulated regions are still understudied and will require further efforts. This is also the case for some metabolic reactions investigated in this work such as ISC disproportionation, use of organosulfur compounds as electron donors or electron acceptors, and sulfur comproportionation. First step of sulfur disproportionation and complete pathways of ISC disproportionation are still not totally understood. It is very likely that several pathways of ISC dismutation exist. Thus, despite efforts done during this PhD and investigations done by others labs, we still do not have genetic markers of this process and it is still not clear if they exist, (Chapter 3). Such genetic markers could open new perspectives for the understanding of the sulfur cycle of natural ecosystems. It is still not known if sulfur comproportionation exists in nature, but thermodynamics calculations predict its existence (Chapter 4). Sulfur organic compounds should be also of special interest in deep-sea hydrothermal sediments, and genomic markers have been already characterized (Chapter 2).

In conclusion, there are still many grey areas in our knowledge of microbial reactions of the sulfur cycle, at the molecular, cellular, individual, community and ecosystem scales. This work has brought elements of knowledge at each of these levels, but the road is still long to have a global vision of the hydrothermal sulfur cycle, and of its interconnections with other cycles, and with biotic and abiotic components of this environment.



## Additional works

Additional works and activities were performed during this PhD. However, due to the sanitary situation, some participation to congress, to an oceanographic cruise and to public outreach events were cancelled. Here is a summary of the activities in which I took part:

In the framework of the GDR Archaea, I participated to the writing of a book chapter, intended to students, about “Archaea”:

- Alain, K., Cozannet, M., **Allioux, M.**, Thiroux, S., Hartunians, J. (**Submitted**) Archées : habitats et physiologies associées. In Clouet d’Orval, B., Franzetti, B., Oger, P. (eds), Biologie des archées, Volume 3 : Les archées dans leur environnement. Editions ISTE.

I gave practical teaching of bacteriology at the university (TP L2 Bactériologie, UBO) during 2020 and 2021 academic years for a total of 48 hours.

I co-supervised several interns:

- Master student for 6 months, Stéven Yvenou, “Microbial culture and genomics approaches of inorganic sulfur compounds disproportionation and comproportionation in geothermal context” (2020).
- Bachelor student for 2 months, Mélanie Le Moigne, “Searching for archaea able to disproportionate inorganic sulfur compounds in anaerobic conditions” (2020-2021).
- Master student for 6 months, Solenne Giardi, “Physiology and proteomics of hydrothermal microorganisms able to disproportionate inorganic sulfur compounds” (2021).
- High school student for 1 week, Mila Dierre, research introduction (2021).

I participated to the 5<sup>th</sup> EBAME Workshop on Computational Microbial Ecogenomics in October and November 2019. It provided me a good formation and state of arts on bioinformatics applied to microbial ecology and ecogenomics.

I participated to the online edition of Sulfur in the Earth system: From microbes to global cycles through Earth history. I managed to have a 15 minutes short talk: “Microbial sulfur disproportionation at marine hydrothermal vents: a reconsideration of the global biological sulfur cycle?”

I was also involved in the consortium of the PRC CNRS-RFBR Neptune project, which focus on sulfur and nitrogen cycles at marine hydrothermal vents, with a collaboration with colleagues from the from the laboratory of Diversity and Ecology of Extremophilic Microorganisms in Moscow. The four genomic annotation publications fall within the scope of this project. In the framework of this project. I also participated to the analyses and the writing of other articles:

- Slobodkin, A., Slobodkina, G., **Allioux, M.**, Alain, K., Jebbar, M., Shadrin, V., Kublanov, I., Toshchakov, S., & Bonch-Osmolovskaya, E. (2019). Genomic Insights into the Carbon and Energy Metabolism of a Thermophilic Deep-Sea Bacterium *Deferribacter autotrophicus* Revealed New Metabolic Traits in the Phylum *Deferribacteres*. *Genes*, 10(11), 849. <https://doi.org/10.3390/genes10110849>
- Slobodkina, G., **Allioux, M.**, Merkel, A., Cambon-Bonavita, M. A., Alain, K., Jebbar, M., & Slobodkin, A. (2021). Physiological and Genomic Characterization of a Hyperthermophilic Archaeon *Archaeoglobus neptunius* sp. nov. Isolated From a Deep-Sea Hydrothermal Vent Warrants the Reclassification of the Genus *Archaeoglobus*. *Frontiers in Microbiology*, 12, 679245. <https://doi.org/10.3389/fmicb.2021.679245>

Finally, I also participated to the analyses and the writing of another article associated to the PhD project of Marc Cozannet:

- Cozannet, M., Borrel, G., Roussel, E., Moalic, Y., **Allioux, M.**, Sanvoisin, A., Toffin, L., & Alain, K. (2020). New Insights into the Ecology and Physiology of *Methanomassiliicoccales* from Terrestrial and Aquatic Environments. *Microorganisms*, 9(1), 30. <https://doi.org/10.3390/microorganisms9010030>

## References

### A

- Alain, K., Postec, A., Grinsard, E., Lesongeur, F., Prieur, D., & Godfroy, A. (2010). *Thermodesulfatator atlanticus* sp. nov., a thermophilic, chemolithoautotrophic, sulfate-reducing bacterium isolated from a Mid-Atlantic Ridge hydrothermal vent. In *International Journal of Systematic and Evolutionary Microbiology* (Vol. 60, Issue 1, pp. 33–38). Microbiology Society. <https://doi.org/10.1099/ijs.0.009449-0>
- Allioux, M., Yvenou, S., Slobodkina, G., Slobodkin, A., Shao, Z., Jebbar, M., & Alain, K. (2020). Genomic Characterization and Environmental Distribution of a Thermophilic Anaerobe *Dissulfurirhabdus thermomarina* SH388T Involved in Disproportionation of Sulfur Compounds in Shallow Sea Hydrothermal Vents. In *Microorganisms* (Vol. 8, Issue 8, p. 1132). MDPI AG. <https://doi.org/10.3390/microorganisms8081132>
- Allioux, M., Jebbar, M., Slobodkina, G., Slobodkin, A., Moalic, Y., Frolova, A., Shao, Z., & Alain, K. (2021). Complete genome sequence of *Thermosulfurimonas marina* SU872T, an anaerobic thermophilic chemolithoautotrophic bacterium isolated from a shallow marine hydrothermal vent. In *Marine Genomics* (Vol. 55, p. 100800). Elsevier BV. <https://doi.org/10.1016/j.margen.2020.100800>
- Amend, J. P., Rogers, K. L., & Meyer-Dombard, D. R. (2004). Microbially mediated sulfur-redox: Energetics in marine hydrothermal vent systems. In *Sulfur Biogeochemistry - Past and Present*. Geological Society of America. <https://doi.org/10.1130/0-8137-2379-5.17>
- Amend, J. P., & LaRowe, D. E. (2019). Minireview: demystifying microbial reaction energetics. *Environmental microbiology*, 21(10), 3539–3547. <https://doi.org/10.1111/1462-2920.14778>
- Amend, J. P., Aronson, H. S., Macalady, J., & LaRowe, D. E. (2020). Another chemolithotrophic metabolism missing in nature: sulfur comproportionation. *Environmental microbiology*, 22(6), 1971–1976. <https://doi.org/10.1111/1462-2920.14982>
- Anantharaman, K., Hausmann, B., Jungbluth, S. P., Kantor, R. S., Lavy, A., Warren, L. A., Rappé, M. S., Pester, M., Loy, A., Thomas, B. C., & Banfield, J. F. (2018). Expanded diversity of microbial groups that shape the dissimilatory sulfur cycle. *The ISME journal*, 12(7), 1715–1728. <https://doi.org/10.1038/s41396-018-0078-0>
- Antipov, D., Raiko, M., Lapidus, A., & Pevzner, P. A. (2019). Plasmid detection and assembly in genomic and metagenomic data sets. In *Genome Research* (Vol. 29, Issue 6, pp. 961–968). Cold Spring Harbor Laboratory. <https://doi.org/10.1101/gr.241299.118>
- Arney, G., Domagal-Goldman, S. D., & Meadows, V. S. (2018). Organic Haze as a Biosignature in Anoxic Earth-like Atmospheres. In *Astrobiology* (Vol. 18, Issue 3, pp. 311–329). Mary Ann Liebert Inc. <https://doi.org/10.1089/ast.2017.1666>
- Avetisyan, K., Eckert, W., Findlay, A.J. et al. Diurnal variations in sulfur transformations at the chemocline of a stratified freshwater lake. *Biogeochemistry* 146, 83–100 (2019). <https://doi.org/10.1007/s10533-019-00601-5>

Ayling, M., Clark, M. D., & Leggett, R. M. (2020). New approaches for metagenome assembly with short reads. *Briefings in bioinformatics*, 21(2), 584–594. <https://doi.org/10.1093/bib/bbz020>

## B

Baffert, C., Kpebe, A., Avilan, L., & Brugna, M. (2019). Hydrogenases and H<sub>2</sub> metabolism in sulfate-reducing bacteria of the *Desulfovibrio* genus. *Advances in microbial physiology*, 74, 143–189. <https://doi.org/10.1016/bs.ampbs.2019.03.001>

Bak, F., & Cypionka, H. (1987). A novel type of energy metabolism involving fermentation of inorganic sulphur compounds. In *Nature* (Vol. 326, Issue 6116, pp. 891–892). Springer Science and Business Media LLC. <https://doi.org/10.1038/326891a0>

Bak, F., & Pfennig, N. (1987). Chemolithotrophic growth of *Desulfovibrio sulfodismutans* sp. nov. by disproportionation of inorganic sulfur compounds. In *Archives of Microbiology* (Vol. 147, Issue 2, pp. 184–189). Springer Science and Business Media LLC. <https://doi.org/10.1007/bf00415282>

Barco, R. A., Garrity, G. M., Scott, J. J., Amend, J. P., Nealson, K. H., & Emerson, D. (2020). A Genus Definition for *Bacteria* and *Archaea* Based on a Standard Genome Relatedness Index. In S. J. Giovannoni (Ed.), *mBio* (Vol. 11, Issue 1). American Society for Microbiology. <https://doi.org/10.1128/mbio.02475-19>

Barnes, I., Hjorth, J., & Mihalopoulos, N. (2006). Dimethyl Sulfide and Dimethyl Sulfoxide and Their Oxidation in the Atmosphere. In *Chemical Reviews* (Vol. 106, Issue 3, pp. 940–975). American Chemical Society (ACS). <https://doi.org/10.1021/cr020529+>

Belilla, J., Moreira, D., Jardillier, L., Reboul, G., Benzerara, K., López-García, J. M., Bertolino, P., López-Archilla, A. I., & López-García, P. (2019). Hyperdiverse archaea near life limits at the polyextreme geothermal Dallol area. *Nature Ecology & Evolution*, 3(11), 1552–1561. <https://doi.org/10.1038/s41559-019-1005-0>

Belkin, S., Wirsén, C. O., & Jannasch, H. W. (1985). Biological and Abiological Sulfur Reduction at High Temperatures. In *Applied and Environmental Microbiology* (Vol. 49, Issue 5, pp. 1057–1061). American Society for Microbiology. <https://doi.org/10.1128/aem.49.5.1057-1061.1985>

Bell, E., Lamminmäki, T., Alneberg, J., Andersson, A. F., Qian, C., Xiong, W., Hettich, R. L., Frutschi, M., & Bernier-Latmani, R. (2020). Active sulfur cycling in the terrestrial deep subsurface. *The ISME journal*, 14(5), 1260–1272. <https://doi.org/10.1038/s41396-020-0602-x>

Bell, E., Lamminmäki, T., Alneberg, J., Qian, C., Xiong, W., Hettich, R. L., Frutschi, M., & Bernier-Latmani, R. (2021). Active anaerobic methane oxidation and sulfur disproportionation in the deep terrestrial subsurface. Cold Spring Harbor Laboratory. <https://doi.org/10.1101/2021.08.21.457207>

Benatti, C. T., Tavares, C. R. G., & Lenzi, E. (2009). Sulfate removal from waste chemicals by precipitation. In *Journal of Environmental Management* (Vol. 90, Issue 1, pp. 504–511). Elsevier BV. <https://doi.org/10.1016/j.jenvman.2007.12.006>

Berg, J. S., Schwedt, A., Kreutzmann, A. C., Kuypers, M. M., & Milucka, J. (2014). Polysulfides as intermediates in the oxidation of sulfide to sulfate by *Beggiatoa* spp. *Applied and environmental microbiology*, 80(2), 629–636. <https://doi.org/10.1128/AEM.02852-13>

Bertelli, C., Laird, M. R., Williams, K. P., Lau, B. Y., Hoad, G., Winsor, G. L., & Brinkman, F. S. (2017). IslandViewer 4: expanded prediction of genomic islands for larger-scale datasets. In *Nucleic Acids Research* (Vol. 45, Issue W1, pp. W30–W35). Oxford University Press (OUP). <https://doi.org/10.1093/nar/gkx343>

Bertran, E. 2019. Cellular and Intracellular Insights Into Microbial Sulfate Reduction and Sulfur Disproportionation. Doctoral dissertation, Harvard University, Graduate School of Arts & Sciences. <http://nrs.harvard.edu/urn-3:HUL.InstRepos:42013126>

Böttcher, M. E., & Thamdrup, B. (2001). Anaerobic sulfide oxidation and stable isotope fractionation associated with bacterial sulfur disproportionation in the presence of MnO<sub>2</sub>. In *Geochimica et Cosmochimica Acta* (Vol. 65, Issue 10, pp. 1573–1581). Elsevier BV. [https://doi.org/10.1016/s0016-7037\(00\)00622-0](https://doi.org/10.1016/s0016-7037(00)00622-0)

Böttcher, M. E., Thamdrup, B., & Vennemann, T. W. (2001). Oxygen and sulfur isotope fractionation during anaerobic bacterial disproportionation of elemental sulfur. In *Geochimica et Cosmochimica Acta* (Vol. 65, Issue 10, pp. 1601–1609). Elsevier BV. [https://doi.org/10.1016/s0016-7037\(00\)00628-1](https://doi.org/10.1016/s0016-7037(00)00628-1)

Böttcher, M. E., Thamdrup, B., Gehre, M., & Theune, A. (2005). 34S/32S and 18O/16O Fractionation During Sulfur Disproportionation by *Desulfobulbus propionicus*. In *Geomicrobiology Journal* (Vol. 22, Issue 5, pp. 219–226). Informa UK Limited. <https://doi.org/10.1080/01490450590947751>

Bowles, M. W., Mogollón, J. M., Kasten, S., Zabel, M., & Hinrichs, K. U. (2014). Global rates of marine sulfate reduction and implications for sub-sea-floor metabolic activities. *Science (New York, N.Y.)*, 344(6186), 889–891. <https://doi.org/10.1126/science.1249213>

Bradford, M. M. (1976). A rapid and sensitive method for the quantitation of microgram quantities of protein utilizing the principle of protein-dye binding. In *Analytical Biochemistry* (Vol. 72, Issues 1–2, pp. 248–254). Elsevier BV. [https://doi.org/10.1016/0003-2697\(76\)90527-3](https://doi.org/10.1016/0003-2697(76)90527-3)

Brettin, T., Davis, J. J., Disz, T., Edwards, R. A., Gerdes, S., Olsen, G. J., Olson, R., Overbeek, R., Parrello, B., Pusch, G. D., Shukla, M., Thomason, J. A., III, Stevens, R., Vonstein, V., Wattam, A. R., & Xia, F. (2015). RASTtk: A modular and extensible implementation of the RAST algorithm for building custom annotation pipelines and annotating batches of genomes. In *Scientific Reports* (Vol. 5, Issue 1). Springer Science and Business Media LLC. <https://doi.org/10.1038/srep08365>

Brock, T. D., Brock, K. M., Belly, R. T., & Weiss, R. L. (1972). *Sulfolobus*: a new genus of sulfur-oxidizing bacteria living at low pH and high temperature. *Archiv für Mikrobiologie*, 84(1), 54–68. <https://doi.org/10.1007/BF00408082>

## C

- Callac, N. (2013). Cycles biogéochimiques du Fer et du Soufre dans les systèmes hydrothermaux en contexte sédimentaire du Bassin de Guaymas : traçages isotopiques et interactions micro-organismes / minéraux. PhD Thesis, Université de Bretagne Occidentale.
- Callbeck, C.M., Canfield, D.E., Kuypers, M.M.M., Yilmaz, P., Lavik, G., Thamdrup, B., Schubert, C.J. and Bristow, L.A. (2021), Sulfur cycling in oceanic oxygen minimum zones. *Limnol Oceanogr*, 66: 2360-2392. <https://doi.org/10.1002/lno.11759>
- Camacho, D., Frazao, R., Fouillen, A., Nanci, A., Lang, B. F., Apte, S. C., Baron, C., & Warren, L. A. (2020). New Insights Into *Acidithiobacillus thiooxidans* Sulfur Metabolism Through Coupled Gene Expression, Solution Chemistry, Microscopy, and Spectroscopy Analyses. *Frontiers in microbiology*, 11, 411. <https://doi.org/10.3389/fmicb.2020.00411>
- Canfield, D. E., & Thamdrup, B. (1994). The Production of  $^{34}\text{S}$ -Depleted Sulfide During Bacterial Disproportionation of Elemental Sulfur. In *Science* (Vol. 266, Issue 5193, pp. 1973–1975). American Association for the Advancement of Science (AAAS). <https://doi.org/10.1126/science.11540246>
- Canfield, D. E., & Thamdrup, B. (1996). Fate of elemental sulfur in an intertidal sediment. In *FEMS Microbiology Ecology* (Vol. 19, Issue 2, pp. 95–103). Oxford University Press (OUP). <https://doi.org/10.1111/j.1574-6941.1996.tb00202.x>
- Carrión, O., Pratscher, J., Richa, K., Rostant, W. G., Farhan Ul Haque, M., Murrell, J. C., & Todd, J. D. (2019). Methanethiol and Dimethylsulfide Cycling in Stiffkey Saltmarsh. In *Frontiers in Microbiology* (Vol. 10). Frontiers Media SA. <https://doi.org/10.3389/fmicb.2019.01040>
- Charbonnier, F., Forterre, P., Erauso, G. and Prieur, D., 1995. Purification of plasmids from thermophilic and hyperthermophilic archaeobacteria. In: *Archaea: A Laboratory Manual*. Robb, F. T. (Editor in Chief), A. R. Place, S. DasSarma, H. J. Schreier and E. M. Fleischmann (eds). Cold Spring Harbor Laboratory Press, NY. Thermophiles pp 87-90 (1995)
- Charlson, R. J., Lovelock, J. E., Andreae, M. O., & Warren, S. G. (1987). Oceanic phytoplankton, atmospheric sulphur, cloud albedo and climate. In *Nature* (Vol. 326, Issue 6114, pp. 655–661). Springer Science and Business Media LLC. <https://doi.org/10.1038/326655a0>
- Chaumeil, P.-A., Mussig, A. J., Hugenholtz, P., & Parks, D. H. (2019). GTDB-Tk: a toolkit to classify genomes with the Genome Taxonomy Database. In J. Hancock (Ed.), *Bioinformatics*. Oxford University Press (OUP). <https://doi.org/10.1093/bioinformatics/btz848>
- Chavagnac, V., Leleu, T., Fontaine, F., Cannat, M., Ceuleneer, G., & Castillo, A. (2018). Spatial variations in vent chemistry at the Lucky Strike hydrothermal field, mid-Atlantic ridge (37°N): Updates for subsurface flow geometry from the newly discovered Capelinhos vent. *Geochemistry, Geophysics, Geosystems*, 19, 4444–4458. <https://doi.org/10.1029/2018GC007765>



Chen, Q., & Chen, C. (2005). The Role of Inorganic Compounds in the Prebiotic Synthesis of Organic Molecules. In *Current Organic Chemistry* (Vol. 9, Issue 10, pp. 989–998). Bentham Science Publishers Ltd. <https://doi.org/10.2174/1385272054368394>

Chen, I. A., Markowitz, V. M., Chu, K., Palaniappan, K., Szeto, E., Pillay, M., Ratner, A., Huang, J., Andersen, E., Huntemann, M., Varghese, N., Hadjithomas, M., Tennessen, K., Nielsen, T., Ivanova, N. N., & Kyrpides, N. C. (2017). IMG/M: integrated genome and metagenome comparative data analysis system. *Nucleic acids research*, 45(D1), D507–D516. <https://doi.org/10.1093/nar/gkw929>

Chen, S., Zhou, Y., Chen, Y., & Gu, J. (2018). fastp: an ultra-fast all-in-one FASTQ preprocessor. In *Bioinformatics* (Vol. 34, Issue 17, pp. i884–i890). Oxford University Press (OUP). <https://doi.org/10.1093/bioinformatics/bty560>

Chen, X., Liu, L., Gao, X., Dai, X., Han, Y., Chen, Q., & Tang, K. (2021). Metabolism of chiral sulfonate compound 2,3-dihydroxypropane-1-sulfonate (DHPS) by *Roseobacter* bacteria in marine environment. *Environment international*, 157, 106829. <https://doi.org/10.1016/j.envint.2021.106829>

Connelly, D. P., Copley, J. T., Murton, B. J., Stansfield, K., Tyler, P. A., German, C. R., Van Dover, C. L., Amon, D., Furlong, M., Grindlay, N., Hayman, N., Hühnerbach, V., Judge, M., Le Bas, T., McPhail, S., Meier, A., Nakamura, K., Nye, V., Pebody, M., ... Wilcox, S. (2012). Hydrothermal vent fields and chemosynthetic biota on the world's deepest seafloor spreading centre. In *Nature Communications* (Vol. 3, Issue 1). Springer Science and Business Media LLC. <https://doi.org/10.1038/ncomms1636>

Corliss, J. B., & Ballard, R. D. (1977). Oasis of life in the cold abyss. *National Geographic Magazine*, 152.

Corliss, J. B., Lyle, M., Dymond, J., & Crane, K. (1978). The chemistry of hydrothermal mounds near the Galapagos Rift. In *Earth and Planetary Science Letters* (Vol. 40, Issue 1, pp. 12–24). Elsevier BV. [https://doi.org/10.1016/0012-821x\(78\)90070-5](https://doi.org/10.1016/0012-821x(78)90070-5)

Corliss, J. B., Dymond, J., Gordon, L. I., Edmond, J. M., von Herzen, R. P., Ballard, R. D., Green, K., Williams, D., Bainbridge, A., Crane, K., & van Andel, T. H. (1979). Submarine Thermal Springs on the Galápagos Rift. In *Science* (Vol. 203, Issue 4385, pp. 1073–1083). American Association for the Advancement of Science (AAAS). <https://doi.org/10.1126/science.203.4385.1073>

Couvin, D., Bernheim, A., Toffano-Nioche, C., Touchon, M., Michalik, J., Néron, B., Rocha, E. P. C., Vergnaud, G., Gautheret, D., & Pourcel, C. (2018). CRISPRCasFinder, an update of CRISRFinder, includes a portable version, enhanced performance and integrates search for Cas proteins. In *Nucleic Acids Research* (Vol. 46, Issue W1, pp. W246–W251). Oxford University Press (OUP). <https://doi.org/10.1093/nar/gky425>

Crane, E. J., III. (2019). Sulfur-dependent microbial lifestyles: deceptively flexible roles for biochemically versatile enzymes. In *Current Opinion in Chemical Biology* (Vol. 49, pp. 139–145). Elsevier BV. <https://doi.org/10.1016/j.cbpa.2018.12.015>

Curson, A. R. J., Liu, J., Bermejo Martínez, A., Green, R. T., Chan, Y., Carrión, O., Williams, B. T., Zhang, S.-H., Yang, G.-P., Bulman Page, P. C., Zhang, X.-H., & Todd, J. D. (2017). Dimethylsulfoniopropionate biosynthesis in marine bacteria and identification of the key gene in this process. In *Nature Microbiology* (Vol. 2, Issue 5). Springer Science and Business Media LLC. <https://doi.org/10.1038/nmicrobiol.2017.9>

Cypionka, H., Smock, A. M., & Böttcher, M. E. (1998). A combined pathway of sulfur compound disproportionation in *Desulfovibrio desulfuricans*. In *FEMS Microbiology Letters* (Vol. 166, Issue 2, pp. 181–186). Oxford University Press (OUP). <https://doi.org/10.1111/j.1574-6968.1998.tb13888.x>

## D

Dahl, C., & Friedrich, C. G. (Eds.). (2008). *Microbial Sulfur Metabolism*. Springer Berlin Heidelberg. <https://doi.org/10.1007/978-3-540-72682-1>

De Anda, V., Zapata-Peñasco, I., Eguiarte, L. E., & Souza, V. (2018). The Sulfur Cycle as the Gear of the “Clock of Life”: The Point of Convergence Between Geological and Genomic Data in the Cuatro Ciénegas Basin. In *Cuatro Ciénegas Basin: An Endangered Hyperdiverse Oasis* (pp. 67–83). Springer International Publishing. [https://doi.org/10.1007/978-3-319-95855-2\\_6](https://doi.org/10.1007/978-3-319-95855-2_6)

de Zwart, J. M. M., & Kuenen, J. G. (1992). C1-cycle of sulfur compounds. In *Biodegradation* (Vol. 3, Issue 1, pp. 37–59). Springer Science and Business Media LLC. <https://doi.org/10.1007/bf00189634>

Dhanasekaran, D., Paul, D., Amaresan, N., Sankaranarayanan, A., & Shouche, Y.S. (Eds.). (2021). *Microbiome-Host Interactions* (1st ed.). CRC Press. <https://doi.org/10.1201/9781003037521>

Dias, D., do Nascimento, P. C., Jost, C. L., Bohrer, D., de Carvalho, L. M., & Koschinsky, A. (2010). Voltammetric Determination of Low-Molecular-Weight Sulfur Compounds in Hydrothermal Vent Fluids - Studies with Hydrogen Sulfide, Methanethiol, Ethanethiol and Propanethiol. In *Electroanalysis* (Vol. 22, Issue 10, pp. 1066–1071). Wiley. <https://doi.org/10.1002/elan.200900472>

Dick G. J. (2019). The microbiomes of deep-sea hydrothermal vents: distributed globally, shaped locally. *Nature reviews. Microbiology*, 17(5), 271–283. <https://doi.org/10.1038/s41579-019-0160-2>

## F

Fakraee, M., & Katsev, S. (2019). Organic sulfur was integral to the Archean sulfur cycle. *Nature communications*, 10(1), 4556. <https://doi.org/10.1038/s41467-019-12396-y>

Fike, D. A., Bradley, A. S., & Rose, C. V. (2015). Rethinking the Ancient Sulfur Cycle. In *Annual Review of Earth and Planetary Sciences* (Vol. 43, Issue 1, pp. 593–622). Annual Reviews. <https://doi.org/10.1146/annurev-earth-060313-054802>

Findlay A. J. (2016). Microbial impact on polysulfide dynamics in the environment. *FEMS microbiology letters*, 363(11), fnw103. <https://doi.org/10.1093/femsle/fnw103>



Finster, K. (2008). Microbiological disproportionation of inorganic sulfur compounds. In *Journal of Sulfur Chemistry* (Vol. 29, Issues 3–4, pp. 281–292). Informa UK Limited. <https://doi.org/10.1080/17415990802105770>

Finster, K. W., Kjeldsen, K. U., Kube, M., Reinhardt, R., Mussmann, M., Amann, R., & Schreiber, L. (2013). Complete genome sequence of *Desulfocapsa sulfexigens*, a marine deltaproteobacterium specialized in disproportionating inorganic sulfur compounds. In *Standards in Genomic Sciences* (Vol. 8, Issue 1, pp. 58–68). Springer Science and Business Media LLC. <https://doi.org/10.4056/sigs.3777412>

Florentino, A. P., Brienza, C., Stams, A. J. M., & Sánchez-Andrea, I. (2016). *Desulfurella amilsii* sp. nov., a novel acidotolerant sulfur-respiring bacterium isolated from acidic river sediments. In *International Journal of Systematic and Evolutionary Microbiology* (Vol. 66, Issue 3, pp. 1249–1253). Microbiology Society. <https://doi.org/10.1099/ijsem.0.000866>

Florentino, A. P., Stams, A. J. M., & Sánchez-Andrea, I. (2017). Genome Sequence of *Desulfurella amilsii* Strain TR1 and Comparative Genomics of Desulfurellaceae Family. In *Frontiers in Microbiology* (Vol. 8). Frontiers Media SA. <https://doi.org/10.3389/fmicb.2017.00222>

Florentino, A. P., Pereira, I. A. C., Boeren, S., van den Born, M., Stams, A. J. M., & Sánchez-Andrea, I. (2019). Insight into the sulfur metabolism of *Desulfurella amilsii* by differential proteomics. In *Environmental Microbiology* (Vol. 21, Issue 1, pp. 209–225). Wiley. <https://doi.org/10.1111/1462-2920.14442>

Flores, G. E., & Reysenbach, A.-L. (2011). Hydrothermal Environments, Marine. In *Encyclopedia of Geobiology* (pp. 456–467). Springer Netherlands. [https://doi.org/10.1007/978-1-4020-9212-1\\_113](https://doi.org/10.1007/978-1-4020-9212-1_113)

Fouquet, Y., Auclair, G., Cambon, P., & Etoubleau, J. (1988). Geological setting and mineralogical and geochemical investigations on sulfide deposits near 13°N on the East Pacific Rise. In *Marine Geology* (Vol. 84, Issues 3–4, pp. 145–178). Elsevier BV. [https://doi.org/10.1016/0025-3227\(88\)90098-9](https://doi.org/10.1016/0025-3227(88)90098-9)

Francois D. Dynamique spatiale et temporelle des communautés microbiennes dans les édifices hydrothermaux actifs / Spatial and temporal dynamics of microbial communities in active hydrothermal vents. 2021. PhD Thesis, Université de Bretagne Occidentale. <https://archimer.ifremer.fr/doc/00690/80209/>

Frederiksen, T.-M., & Finster, K. (2003). In *Biodegradation* (Vol. 14, Issue 3, pp. 189–198). Springer Science and Business Media LLC. <https://doi.org/10.1023/a:1024255830925>

Frolova, A. A., Slobodkina, G. B., Baslerov, R. V., Novikov, A. A., Bonch-Osmolovskaya, E. A., & Slobodkin, A. I. (2018). *Thermosulfurimonas marina* sp. nov., an Autotrophic Sulfur-Disproportionating and Nitrate-Reducing Bacterium Isolated from a Shallow-Sea Hydrothermal Vent. In *Microbiology* (Vol. 87, Issue 4, pp. 502–507). Pleiades Publishing Ltd. <https://doi.org/10.1134/s0026261718040082>

## G

German, C.R. and Von Damm, K.L. (2004) Hydrothermal processes. In, Holland, H.D., Turekian, K.K. and Elderfield, H. (eds.) Treatise on geochemistry, Vol. 6. The oceans and marine geochemistry. Oxford, UK. Elsevier-Pergamon, pp. 181-222.

Gilhooly, W. P., Fike, D. A., Druschel, G. K., Kafantaris, F. C., Price, R. E., & Amend, J. P. (2014). Sulfur and oxygen isotope insights into sulfur cycling in shallow-sea hydrothermal vents, Milos, Greece. *Geochemical transactions*, 15, 12. <https://doi.org/10.1186/s12932-014-0012-y>

Godfroy, A., François, D., Hartunians, J., Moalic, Y. & Alain, K. (in press). Physiology, metabolism and ecology of thermophiles from deep-sea vents. In Vetriani, C., Giovannelli, D. (eds.), *The Microbiology of Deep-Sea*. Editions Springer International.

Goldford, J. E., Hartman, H., Marsland, R., 3rd, & Segrè, D. (2019). Environmental boundary conditions for the origin of life converge to an organo-sulfur metabolism. *Nature ecology & evolution*, 3(12), 1715–1724. <https://doi.org/10.1038/s41559-019-1018-8>

González, J. M., Kiene, R. P., Joye, S. B., Sorokin, D. Yu., & Moran, M. A. (2002). Oxidation of organic and inorganic sulfur compounds by aerobic heterotrophic marine bacteria. In *Progress in Industrial Microbiology* (pp. 291–310). Elsevier. [https://doi.org/10.1016/s0079-6352\(02\)80016-9](https://doi.org/10.1016/s0079-6352(02)80016-9)

Greene, B. L., Vansuch, G. E., Chica, B. C., Adams, M., & Dyer, R. B. (2017). Applications of Photogating and Time Resolved Spectroscopy to Mechanistic Studies of Hydrogenases. *Accounts of chemical research*, 50(11), 2718–2726. <https://doi.org/10.1021/acs.accounts.7b00356>

Gregersen, L. H., Bryant, D. A., & Frigaard, N.-U. (2011). Mechanisms and Evolution of Oxidative Sulfur Metabolism in Green Sulfur Bacteria. In *Frontiers in Microbiology* (Vol. 2). Frontiers Media SA. <https://doi.org/10.3389/fmicb.2011.00116>

Guiral, M., Prunetti, L., Aussignargues, C., Ciaccafava, A., Infossi, P., Ilbert, M., Lojou, E., & Giudici-Orticoni, M.-T. (2012). The Hyperthermophilic Bacterium *Aquifex aeolicus*. In *Advances in Microbial Physiology* (pp. 125–194). Elsevier. <https://doi.org/10.1016/b978-0-12-394423-8.00004-4>

## H

Haymon, R. M. (1983). Growth history of hydrothermal black smoker chimneys. In *Nature* (Vol. 301, Issue 5902, pp. 695–698). Springer Science and Business Media LLC. <https://doi.org/10.1038/301695a0>

Heinen, W., & Lauwers, A. M. (1996). Organic sulfur compounds resulting from the interaction of iron sulfide, hydrogen sulfide and carbon dioxide in an anaerobic aqueous environment. In *Origins of Life and Evolution of the Biosphere* (Vol. 26, Issue 2, pp. 131–150). Springer Science and Business Media LLC. <https://doi.org/10.1007/bf01809852>

Holm, N. G. (Ed.). (1992). *Marine Hydrothermal Systems and the Origin of Life*. Springer Netherlands. <https://doi.org/10.1007/978-94-011-2741-7>

Houghton, J. L., Gilhooly, W. P., III, Kafantaris, F.-C. A., Druschel, G. K., Lu, G.-S., Amend, J. P., Godelitsas, A., & Fike, D. A. (2019). Spatially and temporally variable sulfur cycling in shallow-sea hydrothermal vents, Milos, Greece. In *Marine Chemistry* (Vol. 208, pp. 83–94). Elsevier BV. <https://doi.org/10.1016/j.marchem.2018.11.002>

Huber, C., & Wächtershäuser, G. (1997). Activated Acetic Acid by Carbon Fixation on (Fe,Ni)S Under Primordial Conditions. In *Science* (Vol. 276, Issue 5310, pp. 245–247). American Association for the Advancement of Science (AAAS). <https://doi.org/10.1126/science.276.5310.245>

Hügler, M., Gärtner, A., & Imhoff, J. F. (2010). Functional genes as markers for sulfur cycling and CO<sub>2</sub> fixation in microbial communities of hydrothermal vents of the Logatchev field. In *FEMS Microbiology Ecology* (p. no-no). Oxford University Press (OUP). <https://doi.org/10.1111/j.1574-6941.2010.00919.x>

Hügler, M., & Sievert, S. M. (2011). Beyond the Calvin Cycle: Autotrophic Carbon Fixation in the Ocean. In *Annual Review of Marine Science* (Vol. 3, Issue 1, pp. 261–289). Annual Reviews. <https://doi.org/10.1146/annurev-marine-120709-142712>

Humphris, S. E., & Klein, F. (2018). Progress in Deciphering the Controls on the Geochemistry of Fluids in Seafloor Hydrothermal Systems. *Annual review of marine science*, 10, 315–343. <https://doi.org/10.1146/annurev-marine-121916-063233>

## I

Ihara, H., Hori, T., Aoyagi, T., Hosono, H., Takasaki, M., & Katayama, Y. (2019). Stratification of Sulfur Species and Microbial Community in Launched Marine Sediment by an Improved Sulfur-Fractionation Method and 16S rRNA Gene Sequencing. *Microbes and environments*, 34(2), 199–205. <https://doi.org/10.1264/jsme2.ME18153>

Ilbert, M., Méjean, V., Giudici-Orticoni, M.-T., Samama, J.-P., & Iobbi-Nivol, C. (2003). Involvement of a Mate Chaperone (TorD) in the Maturation Pathway of Molybdoenzyme TorA. In *Journal of Biological Chemistry* (Vol. 278, Issue 31, pp. 28787–28792). Elsevier BV. <https://doi.org/10.1074/jbc.m302730200>

Jordan, S. L., Kraczkiewicz-Dowjat, A. J., Kelly, D. P., & Wood, A. P. (1995). Novel eubacteria able to grow on carbon disulfide. In *Archives of Microbiology* (Vol. 163, Issue 2, pp. 131–137). Springer Science and Business Media LLC. <https://doi.org/10.1007/bf00381787>

## J

Jackson, B. E., & McInerney, M. J. (2000). Thiosulfate Disproportionation by *Desulfotomaculum thermobenzoicum*. In *Applied and Environmental Microbiology* (Vol. 66, Issue 8, pp. 3650–3653). American Society for Microbiology. <https://doi.org/10.1128/aem.66.8.3650-3653.2000>

Johnston, D. T., Wing, B. A., Farquhar, J., Kaufman, A. J., Strauss, H., Lyons, T. W., Kah, L. C., & Canfield, D. E. (2005). Active Microbial Sulfur Disproportionation in the Mesoproterozoic. In *Science* (Vol. 310, Issue 5753, pp. 1477–1479). American Association for the Advancement of Science (AAAS). <https://doi.org/10.1126/science.1117824>

Jørgensen, B. B. (1990). The sulfur cycle of freshwater sediments: Role of thiosulfate. In *Limnology and Oceanography* (Vol. 35, Issue 6, pp. 1329–1342). Wiley. <https://doi.org/10.4319/lo.1990.35.6.1329>

Jørgensen, B. B., & Bak, F. (1991). Pathways and Microbiology of Thiosulfate Transformations and Sulfate Reduction in a Marine Sediment (Kattegat, Denmark). In *Applied and Environmental Microbiology* (Vol. 57, Issue 3, pp. 847–856). American Society for Microbiology. <https://doi.org/10.1128/aem.57.3.847-856.1991>

Jørgensen, B. B., Findlay, A. J., & Pellerin, A. (2019). The Biogeochemical Sulfur Cycle of Marine Sediments. In *Frontiers in Microbiology* (Vol. 10). Frontiers Media SA. <https://doi.org/10.3389/fmicb.2019.00849>

Jørgensen, B. B. (2021). Sulfur Biogeochemical Cycle of Marine Sediments. *Geochemical Perspectives*, 145–307. <https://doi.org/10.7185/geochempersp.10.2>

## K

Kanao, T., Sharmin, S., Tokuhisa, M., Otsuki, M., & Kamimura, K. (2020). Identification of a gene encoding a novel thiosulfate:quinone oxidoreductase in marine *Acidithiobacillus* sp. strain SH. *Research in microbiology*, 171(7), 281–286. <https://doi.org/10.1016/j.resmic.2020.09.004>

Kawai, S., Kamiya, N., Matsuura, K., & Haruta, S. (2019). Symbiotic Growth of a Thermophilic Sulfide-Oxidizing Photoautotroph and an Elemental Sulfur-Disproportionating Chemolithoautotroph and Cooperative Dissimilatory Oxidation of Sulfide to Sulfate. In *Frontiers in Microbiology* (Vol. 10). Frontiers Media SA. <https://doi.org/10.3389/fmicb.2019.01150>

Kelley, D. S., Baross, J. A., & Delaney, J. R. (2002). Volcanoes, Fluids, and Life at Mid-Ocean Ridge Spreading Centers. In *Annual Review of Earth and Planetary Sciences* (Vol. 30, Issue 1, pp. 385–491). Annual Reviews. <https://doi.org/10.1146/annurev.earth.30.091201.141331>

Kelley, D. S., Karson, J. A., Früh-Green, G. L., Yoerger, D. R., Shank, T. M., Butterfield, D. A., Hayes, J. M., Schrenk, M. O., Olson, E. J., Proskurowski, G., Jakuba, M., Bradley, A., Larson, B., Ludwig, K., Glickson, D., Buckman, K., Bradley, A. S., Brazelton, W. J., Roe, K., ... Sylva, S. P. (2005). A Serpentinite-Hosted Ecosystem: The Lost City Hydrothermal Field. In *Science* (Vol. 307, Issue 5714, pp. 1428–1434). American Association for the Advancement of Science (AAAS). <https://doi.org/10.1126/science.1102556>

Kieft, K., Zhou, Z., Anderson, R. E., Buchan, A., Campbell, B. J., Hallam, S. J., Hess, M., Sullivan, M. B., Walsh, D. A., Roux, S., & Anantharaman, K. (2021). Ecology of inorganic sulfur auxiliary metabolism in widespread bacteriophages. *Nature communications*, 12(1), 3503. <https://doi.org/10.1038/s41467-021-23698-5>

- Kiene, R. P., Oremland, R. S., Catena, A., Miller, L. G., & Capone, D. G. (1986). Metabolism of Reduced Methylated Sulfur Compounds in Anaerobic Sediments and by a Pure Culture of an Estuarine Methanogen. In *Applied and Environmental Microbiology* (Vol. 52, Issue 5, pp. 1037–1045). American Society for Microbiology. <https://doi.org/10.1128/aem.52.5.1037-1045.1986>
- Kletzin, A. (1989). Coupled enzymatic production of sulfite, thiosulfate, and hydrogen sulfide from sulfur: purification and properties of a sulfur oxygenase reductase from the facultatively anaerobic archaeobacterium *Desulfurolobus ambivalens*. In *Journal of Bacteriology* (Vol. 171, Issue 3, pp. 1638–1643). American Society for Microbiology. <https://doi.org/10.1128/jb.171.3.1638-1643.1989>
- Kletzin, A., Urich, T., Müller, F., Bandejas, T. M., & Gomes, C. M. (2004). Dissimilatory Oxidation and Reduction of Elemental Sulfur in Thermophilic *Archaea*. In *Journal of Bioenergetics and Biomembranes* (Vol. 36, Issue 1, pp. 77–91). Springer Science and Business Media LLC. <https://doi.org/10.1023/b:jobb.0000019600.36757.8c>
- Klimmek O. et al. (2004) Chapter 10: Sulfur Respiration. In: Zannoni D. (eds) Respiration in *Archaea* and *Bacteria*. Advances in Photosynthesis and Respiration, vol 16. Springer, Dordrecht. [https://doi.org/10.1007/978-1-4020-3163-2\\_10](https://doi.org/10.1007/978-1-4020-3163-2_10)
- Klotz, M. G., Bryant, D. A., & Hanson, T. E. (2011). The Microbial Sulfur Cycle. In *Frontiers in Microbiology* (Vol. 2). Frontiers Media SA. <https://doi.org/10.3389/fmicb.2011.00241>
- Kojima, H., Umezawa, K., & Fukui, M. (2016). *Caldimicrobium thiodismutans* sp. nov., a sulfur-disproportionating bacterium isolated from a hot spring, and emended description of the genus *Caldimicrobium*. In *International Journal of Systematic and Evolutionary Microbiology* (Vol. 66, Issue 4, pp. 1828–1831). Microbiology Society. <https://doi.org/10.1099/ijsem.0.000947>
- Konstantinidis, K. T., Rosselló-Móra, R., & Amann, R. (2017). Uncultivated microbes in need of their own taxonomy. In *the ISME Journal* (Vol. 11, Issue 11, pp. 2399–2406). Springer Science and Business Media LLC. <https://doi.org/10.1038/ismej.2017.113>
- Krämer, M., & Cypionka, H. (1989). Sulfate formation via ATP sulfurylase in thiosulfate- and sulfite-disproportionating bacteria. In *Archives of Microbiology* (Vol. 151, Issue 3, pp. 232–237). Springer Science and Business Media LLC. <https://doi.org/10.1007/bf00413135>
- Kröber, E., & Schäfer, H. (2019). Identification of Proteins and Genes Expressed by *Methylophaga thiooxydans* During Growth on Dimethylsulfide and Their Presence in Other Members of the Genus. In *Frontiers in Microbiology* (Vol. 10). Frontiers Media SA. <https://doi.org/10.3389/fmicb.2019.01132>
- Kublanov, I. V., Perevalova, A. A., Slobodkina, G. B., Lebedinsky, A. V., Bidzhieva, S. K., Kolganova, T. V., Kaliberda, E. N., Rumsh, L. D., Haertlé, T., & Bonch-Osmolovskaya, E. A. (2009). Biodiversity of thermophilic prokaryotes with hydrolytic activities in hot springs of Uzon Caldera, Kamchatka (Russia). *Applied and environmental microbiology*, 75(1), 286–291. <https://doi.org/10.1128/AEM.00607-08>



Kushkevych, I., Cejnar, J., Treml, J., Dordević, D., Kollar, P., & Vítězová, M. (2020). Recent Advances in Metabolic Pathways of Sulfate Reduction in Intestinal Bacteria. *Cells*, 9(3), 698. <https://doi.org/10.3390/cells9030698>

## L

Lagostina, L., Frandsen, S., MacGregor, B. J., Glombitza, C., Deng, L., Fiskal, A., Li, J., Doll, M., Geilert, S., Schmidt, M., Scholz, F., Bernasconi, S. M., Jørgensen, B. B., Hensen, C., Teske, A., & Lever, M. A. (2021). Interactions between temperature and energy supply drive microbial communities in hydrothermal sediment. *Communications biology*, 4(1), 1006. <https://doi.org/10.1038/s42003-021-02507-1>

Lahme, S., Callbeck, C. M., Eland, L. E., Wipat, A., Enning, D., Head, I. M., & Hubert, C. (2020). Comparison of sulfide-oxidizing *Sulfurimonas* strains reveals a new mode of thiosulfate formation in subsurface environments. *Environmental microbiology*, 22(5), 1784–1800. <https://doi.org/10.1111/1462-2920.14894>

Lai, Q., Cao, J., Dupont, S., Shao, Z., Jebbar, M., & Alain, K. (2016). *Thermodesulfatator autotrophicus* sp. nov., a thermophilic sulfate-reducing bacterium from the Indian Ocean. In *International Journal of Systematic and Evolutionary Microbiology* (Vol. 66, Issue 10, pp. 3978–3982). Microbiology Society. <https://doi.org/10.1099/ijsem.0.001297>

Langwig, M. V., De Anda, V., Dombrowski, N., Seitz, K. W., Rambo, I. M., Greening, C., Teske, A. P., & Baker, B. J. (2021). Large-scale protein level comparison of *Deltaproteobacteria* reveals cohesive metabolic groups. *The ISME journal*, 10.1038/s41396-021-01057-y. Advance online publication. <https://doi.org/10.1038/s41396-021-01057-y>

LaRowe, D. E., Carlson, H. K., & Amend, J. P. (2021). The Energetic Potential for Undiscovered Manganese Metabolisms in Nature. *Frontiers in microbiology*, 12, 636145. <https://doi.org/10.3389/fmicb.2021.636145>

Lee, I., Ouk Kim, Y., Park, S.-C., & Chun, J. (2016). OrthoANI: An improved algorithm and software for calculating average nucleotide identity. In *International Journal of Systematic and Evolutionary Microbiology* (Vol. 66, Issue 2, pp. 1100–1103). Microbiology Society. <https://doi.org/10.1099/ijsem.0.000760>

Lepot, K., Williford, K. H., Philippot, P., Thomazo, C., Ushikubo, T., Kitajima, K., Mostefaoui, S., & Valley, J. W. (2019). Extreme <sup>13</sup>C-depletions and organic sulfur content argue for S-fueled anaerobic methane oxidation in 2.72 Ga old stromatolites. In *Geochimica et Cosmochimica Acta* (Vol. 244, pp. 522–547). Elsevier BV. <https://doi.org/10.1016/j.gca.2018.10.014>

Lezcano, M. Á., Moreno-Paz, M., Carrizo, D., Prieto-Ballesteros, O., Fernández-Martínez, M. Á., Sánchez-García, L., Blanco, Y., Puente-Sánchez, F., de Diego-Castilla, G., García-Villadangos, M., Fairén, A. G., & Parro, V. (2019). Biomarker Profiling of Microbial Mats in the Geothermal Band of Cerro Caliente, Deception Island (Antarctica): Life at the Edge of Heat and Cold. *Astrobiology*, 19(12), 1490–1504. <https://doi.org/10.1089/ast.2018.2004>

Li, Y., Tang, K., Zhang, L., Zhao, Z., Xie, X., Chen, C. A., Wang, D., Jiao, N., & Zhang, Y. (2018). Coupled Carbon, Sulfur, and Nitrogen Cycles Mediated by Microorganisms in the Water Column of a Shallow-Water Hydrothermal Ecosystem. *Frontiers in microbiology*, 9, 2718. <https://doi.org/10.3389/fmicb.2018.02718>

Liu, Y., Beer, L. L., & Whitman, W. B. (2012). Sulfur metabolism in archaea reveals novel processes. In *Environmental Microbiology* (Vol. 14, Issue 10, pp. 2632–2644). Wiley. <https://doi.org/10.1111/j.1462-2920.2012.02783.x>

Loison, A., Dubant, S., Adam, P., & Albrecht, P. (2010). Elucidation of an Iterative Process of Carbon–Carbon Bond Formation of Prebiotic Significance. In *Astrobiology* (Vol. 10, Issue 10, pp. 973–988). Mary Ann Liebert Inc. <https://doi.org/10.1089/ast.2009.0441>

Lomans, B. P., Smolders, A., Intven, L. M., Pol, A., Op, D., & Van Der Drift, C. (1997). Formation of dimethyl sulfide and methanethiol in anoxic freshwater sediments. In *Applied and Environmental Microbiology* (Vol. 63, Issue 12, pp. 4741–4747). American Society for Microbiology. <https://doi.org/10.1128/aem.63.12.4741-4747.1997>

Longnecker, K., Sievert, S. M., Sylva, S. P., Seewald, J. S., & Kujawinski, E. B. (2018). Dissolved organic carbon compounds in deep-sea hydrothermal vent fluids from the East Pacific Rise at 9°50'N. In *Organic Geochemistry* (Vol. 125, pp. 41–49). Elsevier BV. <https://doi.org/10.1016/j.orggeochem.2018.08.004>

Lonsdale, P. (1977). Clustering of suspension-feeding macrobenthos near abyssal hydrothermal vents at oceanic spreading centers. In *Deep Sea Research* (Vol. 24, Issue 9, pp. 857–863). Elsevier BV. [https://doi.org/10.1016/0146-6291\(77\)90478-7](https://doi.org/10.1016/0146-6291(77)90478-7)

Lovelock, J. E., Maggs, R. J., & Rasmussen, R. A. (1972). Atmospheric Dimethyl Sulphide and the Natural Sulphur Cycle. In *Nature* (Vol. 237, Issue 5356, pp. 452–453). Springer Science and Business Media LLC. <https://doi.org/10.1038/237452a0>

## M

Madigan, M. T., Martinko, J. M., Bender, K. S., Buckley, D. H., & Stahl, D. A. (2015). Brock biology of microorganisms (Fourteenth edition.). Boston: Pearson.

Manan, N. S., Aldous, L., Alias, Y., Murray, P., Yellowlees, L. J., Lagunas, M. C., & Hardacre, C. (2011). Electrochemistry of sulfur and polysulfides in ionic liquids. *The journal of physical chemistry. B*, 115(47), 13873–13879. <https://doi.org/10.1021/jp208159v>

Mardanov, A. V., Beletsky, A. V., Kadnikov, V. V., Slobodkin, A. I., & Ravin, N. V. (2016). Genome Analysis of *Thermosulfurimonas dismutans*, the First Thermophilic Sulfur-Disproportionating Bacterium of the Phylum *Thermodesulfobacteria*. In *Frontiers in Microbiology* (Vol. 7). Frontiers Media SA. <https://doi.org/10.3389/fmicb.2016.00950>

Marietou, A., Røy, H., Jørgensen, B. B., & Kjeldsen, K. U. (2018). Sulfate Transporters in Dissimilatory Sulfate Reducing Microorganisms: A Comparative Genomics Analysis. *Frontiers in microbiology*, 9, 309. <https://doi.org/10.3389/fmicb.2018.00309>

- Martin, W., & Russell, M. J. (2007). On the origin of biochemistry at an alkaline hydrothermal vent. In *Philosophical Transactions of the Royal Society B: Biological Sciences* (Vol. 362, Issue 1486, pp. 1887–1926). The Royal Society. <https://doi.org/10.1098/rstb.2006.1881>
- Martin, W., Baross, J., Kelley, D., & Russell, M. J. (2008). Hydrothermal vents and the origin of life. In *Nature Reviews Microbiology* (Vol. 6, Issue 11, pp. 805–814). Springer Science and Business Media LLC. <https://doi.org/10.1038/nrmicro1991>
- Maugeri, T. L., Lentini, V., Gugliandolo, C., Italiano, F., Cousin, S., & Stackebrandt, E. (2009). Bacterial and archaeal populations at two shallow hydrothermal vents off Panarea Island (Eolian Islands, Italy). *Extremophiles: life under extreme conditions*, 13(1), 199–212. <https://doi.org/10.1007/s00792-008-0210-6>
- McCollom, T. M. (2000). Geochemical constraints on primary productivity in submarine hydrothermal vent plumes. In *Deep Sea Research Part I: Oceanographic Research Papers* (Vol. 47, Issue 1, pp. 85–101). Elsevier BV. [https://doi.org/10.1016/s0967-0637\(99\)00048-5](https://doi.org/10.1016/s0967-0637(99)00048-5)
- McDermott, J. M., Seewald, J. S., German, C. R., & Sylva, S. P. (2015). Pathways for abiotic organic synthesis at submarine hydrothermal fields. In *Proceedings of the National Academy of Sciences* (Vol. 112, Issue 25, pp. 7668–7672). Proceedings of the National Academy of Sciences. <https://doi.org/10.1073/pnas.1506295112>
- Mehta D., Satyanarayana T. (2013) Diversity of Hot Environments and Thermophilic Microbes. In: Satyanarayana T., Littlechild J., Kawarabayasi Y. (eds) *Thermophilic Microbes in Environmental and Industrial Biotechnology*. Springer, Dordrecht. [https://doi.org/10.1007/978-94-007-5899-5\\_1](https://doi.org/10.1007/978-94-007-5899-5_1)
- Meier-Kolthoff, J. P., Auch, A. F., Klenk, H.-P., & Göker, M. (2013). Genome sequence-based species delimitation with confidence intervals and improved distance functions. In *BMC Bioinformatics* (Vol. 14, Issue 1). Springer Science and Business Media LLC. <https://doi.org/10.1186/1471-2105-14-60>
- Merkel, A. Y., Pimenov, N. V., Rusanov, I. I., Slobodkin, A. I., Slobodkina, G. B., Tarnovetskii, I. Y., Frolov, E. N., Dubin, A. V., Perevalova, A. A., & Bonch-Osmolovskaya, E. A. (2017). Microbial diversity and autotrophic activity in Kamchatka hot springs. *Extremophiles: life under extreme conditions*, 21(2), 307–317. <https://doi.org/10.1007/s00792-016-0903-1>
- Meyer, B. (1976). The Structures of Elemental Sulfur (H. J. Emeléus & A. G. B. T.-A. in I. C. and R. Sharpe, eds.). [https://doi.org/https://doi.org/10.1016/S0065-2792\(08\)60032-1](https://doi.org/https://doi.org/10.1016/S0065-2792(08)60032-1)
- Meyer-Dombard, D.R., Shock, E.L. and Amend, J.P. (2005), Archaeal and bacterial communities in geochemically diverse hot springs of Yellowstone National Park, USA. *Geobiology*, 3: 211-227. <https://doi.org/10.1111/j.1472-4669.2005.00052.x>
- Moeller, T., & Shellman, R. W. (1953). The Iron(III)-Phenol Complex in Aqueous Solution. *Science (New York, N.Y.)*, 118(3064), 327–328. <https://doi.org/10.1126/science.118.3064.327>



Moran, J. J., Beal, E. J., Vrentas, J. M., Orphan, V. J., Freeman, K. H., & House, C. H. (2008). Methyl sulfides as intermediates in the anaerobic oxidation of methane. In *Environmental Microbiology* 10, 162–173. Wiley. <https://doi.org/10.1111/j.1462-2920.2007.01441.x>

Morrison, P. R., & Mojzsis, S. J. (2020). Tracing the Early Emergence of Microbial Sulfur Metabolisms. In *Geomicrobiology Journal* (Vol. 38, Issue 1, pp. 66–86). Informa UK Limited. <https://doi.org/10.1080/01490451.2020.1812773>

Moussard, H., L'Haridon, S., Tindall, B. J., Banta, A., Schumann, P., Stackebrandt, E., Reysenbach, A.-L., & Jeanthon, C. (2004). *Thermodesulfatator indicus* gen. nov., sp. nov., a novel thermophilic chemolithoautotrophic sulfate-reducing bacterium isolated from the Central Indian Ridge. In *International Journal of Systematic and Evolutionary Microbiology* (Vol. 54, Issue 1, pp. 227–233). Microbiology Society. <https://doi.org/10.1099/ijs.0.02669-0>

Müller, H., Marozava, S., Probst, A. J., & Meckenstock, R. U. (2020). Groundwater cable bacteria conserve energy by sulfur disproportionation. *The ISME journal*, 14(2), 623–634. <https://doi.org/10.1038/s41396-019-0554-1>

## N

Nakagawa, S., & Takai, K. (2008). Deep-sea vent chemoautotrophs: diversity, biochemistry and ecological significance. *FEMS microbiology ecology*, 65(1), 1–14. <https://doi.org/10.1111/j.1574-6941.2008.00502.x>

Neukirchen, S., & Sousa, F. L. (2021). DiSCo: a sequence-based type-specific predictor of Dsr-dependent dissimilatory sulphur metabolism in microbial data. *Microbial genomics*, 7(7), 10.1099/mgen.0.000603. <https://doi.org/10.1099/mgen.0.000603>

## O

Obraztsova, A. Y., Francis, C. A., & Tebo, B. M. (2002). Sulfur Disproportionation by the Facultative Anaerobe *Pantoea agglomerans* SP1 as a Mechanism for Chromium(VI) Reduction. In *Geomicrobiology Journal* (Vol. 19, Issue 1, pp. 121–132). Informa UK Limited. <https://doi.org/10.1080/014904502317246219>

Ollivier, B., Zeyen, N., Gales, G., Hickman-Lewis, K., Gaboyer, F., Benzerara, K., & Westall, F. (2018). Importance of Prokaryotes in the Functioning and Evolution of the Present and Past Geosphere and Biosphere. In *Prokaryotes and Evolution* (pp. 57–129). Springer International Publishing. [https://doi.org/10.1007/978-3-319-99784-1\\_3](https://doi.org/10.1007/978-3-319-99784-1_3)

Oró, J., & Mills, T. (1989). Sulfur metabolism: An anaerobic strategy for microbial life on europa. In *Origins of Life and Evolution of the Biosphere* (Vol. 19, Issues 3–5, pp. 479–480). Springer Science and Business Media LLC. <https://doi.org/10.1007/bf02388960>

## P

- Paschinger, H., Paschinger, J., & Gaffron, H. (1974). Photochemical disproportionation of sulfur into sulfide and sulfate by *Chlorobium limicola formathiosulfatophilum*. In *Archives of Microbiology* (Vol. 96, Issue 1, pp. 341–351). Springer Science and Business Media LLC. <https://doi.org/10.1007/bf00590189>
- Pelletier, N., Leroy, G., Guiral, M., Giudici-Ortoni, M.-T., & Aubert, C. (2008). First characterisation of the active oligomer form of sulfur oxygenase reductase from the bacterium *Aquifex aeolicus*. In *Extremophiles* (Vol. 12, Issue 2, pp. 205–215). Springer Science and Business Media LLC. <https://doi.org/10.1007/s00792-007-0119-5>
- Pereira, I. A., Ramos, A. R., Grein, F., Marques, M. C., da Silva, S. M., & Venceslau, S. S. (2011). A comparative genomic analysis of energy metabolism in sulfate reducing bacteria and archaea. *Frontiers in microbiology*, 2, 69. <https://doi.org/10.3389/fmicb.2011.00069>
- Peters, J. W., Miller, A. F., Jones, A. K., King, P. W., & Adams, M. W. (2016). Electron bifurcation. *Current opinion in chemical biology*, 31, 146–152. <https://doi.org/10.1016/j.cbpa.2016.03.007>
- Philippot, P., Van Zuilen, M., Lepot, K., Thomazo, C., Farquhar, J., & Van Kranendonk, M. J. (2007). Early Archaean Microorganisms Preferred Elemental Sulfur, Not Sulfate. In *Science* (Vol. 317, Issue 5844, pp. 1534–1537). American Association for the Advancement of Science (AAAS). <https://doi.org/10.1126/science.1145861>
- Poddar, A., & Das, S. K. (2018). Microbiological studies of hot springs in India: a review. *Archives of microbiology*, 200(1), 1–18. <https://doi.org/10.1007/s00203-017-1429-3>
- Pommier, J., Méjean, V., Giordano, G., & Iobbi-Nivol, C. (1998). TorD, A Cytoplasmic Chaperone That Interacts with the Unfolded Trimethylamine N-Oxide Reductase Enzyme (TorA) in *Escherichia coli*. In *Journal of Biological Chemistry* (Vol. 273, Issue 26, pp. 16615–16620). Elsevier BV. <https://doi.org/10.1074/jbc.273.26.16615>
- Poser, A., Lohmayer, R., Vogt, C., Knoeller, K., Planer-Friedrich, B., Sorokin, D., Richnow, H.-H., & Finster, K. (2013). Disproportionation of elemental sulfur by haloalkaliphilic bacteria from soda lakes. In *Extremophiles* (Vol. 17, Issue 6, pp. 1003–1012). Springer Science and Business Media LLC. <https://doi.org/10.1007/s00792-013-0582-0>
- Power, J. F., Carere, C. R., Lee, C. K., Wakerley, G., Evans, D. W., Button, M., White, D., Climo, M. D., Hinze, A. M., Morgan, X. C., McDonald, I. R., Cary, S. C., & Stott, M. B. (2018). Microbial biogeography of 925 geothermal springs in New Zealand. *Nature communications*, 9(1), 2876. <https://doi.org/10.1038/s41467-018-05020-y>
- Price, R. E., & Giovannelli, D. (2017). A Review of the Geochemistry and Microbiology of Marine Shallow-Water Hydrothermal Vents. In *Reference Module in Earth Systems and Environmental Sciences*. Elsevier. <https://doi.org/10.1016/b978-0-12-409548-9.09523-3>

## R

Rabus, R., Hansen, T. A., & Widdel, F. (2013). Dissimilatory Sulfate- and Sulfur-Reducing Prokaryotes. In *The Prokaryotes* (pp. 309–404). Springer Berlin Heidelberg. [https://doi.org/10.1007/978-3-642-30141-4\\_70](https://doi.org/10.1007/978-3-642-30141-4_70)

Raulin, F., & Toupance, G. (1977). The role of sulphur in chemical evolution. In *Journal of Molecular Evolution* (Vol. 9, Issue 4, pp. 329–338). Springer Science and Business Media LLC. <https://doi.org/10.1007/bf01796095>

Renshaw, J. (2007). Introduction to Geomicrobiology - by K. Konhauser. In *European Journal of Soil Science* (Vol. 58, Issue 5, pp. 1215–1216). Wiley. [https://doi.org/10.1111/j.1365-2389.2007.00943\\_4.x](https://doi.org/10.1111/j.1365-2389.2007.00943_4.x)

Reigstad, L. J., Jorgensen, S. L., & Schleper, C. (2010). Diversity and abundance of *Korarchaeota* in terrestrial hot springs of Iceland and Kamchatka. *The ISME journal*, 4(3), 346–356. <https://doi.org/10.1038/ismej.2009.126>

Richter, M., & Rosselló-Móra, R. (2009). Shifting the genomic gold standard for the prokaryotic species definition. In *Proceedings of the National Academy of Sciences* (Vol. 106, Issue 45, pp. 19126–19131). Proceedings of the National Academy of Sciences. <https://doi.org/10.1073/pnas.0906412106>

Rodriguez-R, L. M., & Konstantinidis, K. T. (2016). The Enveomics collection: a toolbox for specialized analyses of microbial genomes and metagenomes. *PeerJ*. <https://doi.org/10.7287/peerj.preprints.1900v1>

Rogers, K. L., & Schulte, M. D. (2012). Organic Sulfur Metabolisms in Hydrothermal Environments. In *Geobiology* (Vol. 10, Issue 4, pp. 320–332). Wiley. <https://doi.org/10.1111/j.1472-4669.2012.00324.x>

Rogers, A. D., Tyler, P. A., Connelly, D. P., Copley, J. T., James, R., Larter, R. D., Linse, K., Mills, R. A., Garabato, A. N., Pancost, R. D., Pearce, D. A., Polunin, N. V. C., German, C. R., Shank, T., Boersch-Supan, P. H., Alker, B. J., Aquilina, A., Bennett, S. A., Clarke, A., ... Zwirgmaier, K. (2012). The Discovery of New Deep-Sea Hydrothermal Vent Communities in the Southern Ocean and Implications for Biogeography. In J. A. Eisen (Ed.), *PLoS Biology* (Vol. 10, Issue 1, p. e1001234). Public Library of Science (PLoS). <https://doi.org/10.1371/journal.pbio.1001234>

Rosenberg, N. K., Lee, R. W., & Yancey, P. H. (2006). High contents of hypotaurine and thiotaurine in hydrothermal-vent gastropods without thiotrophic endosymbionts. In *Journal of Experimental Zoology Part A: Comparative Experimental Biology* (Vol. 305A, Issue 8, pp. 655–662). Wiley. <https://doi.org/10.1002/jez.a.316>

Rushdi, A. I., & Simoneit, B. R. T. (2005). Abiotic Synthesis of Organic Compounds from Carbon Disulfide Under Hydrothermal Conditions. In *Astrobiology* (Vol. 5, Issue 6, pp. 749–769). Mary Ann Liebert Inc. <https://doi.org/10.1089/ast.2005.5.749>

## S

Sako, Y., Nakagawa, S., Takai, K., & Horikoshi, K. (2003). *Marinithermus hydrothermalis* gen. nov., sp. nov., a strictly aerobic, thermophilic bacterium from a deep-sea hydrothermal vent chimney. In *International Journal of Systematic and Evolutionary Microbiology* (Vol. 53, Issue 1, pp. 59–65). Microbiology Society. <https://doi.org/10.1099/ijs.0.02364-0>

Sánchez-Andrea, I., Guedes, I. A., Hornung, B., Boeren, S., Lawson, C. E., Sousa, D. Z., Bar-Even, A., Claassens, N. J., & Stams, A. (2020). The reductive glycine pathway allows autotrophic growth of *Desulfovibrio desulfuricans*. *Nature communications*, *11*(1), 5090. <https://doi.org/10.1038/s41467-020-18906-7>

Santos, A. A., Venceslau, S. S., Grein, F., Leavitt, W. D., Dahl, C., Johnston, D. T., & Pereira, I. A. (2015). A protein trisulfide couples dissimilatory sulfate reduction to energy conservation. *Science (New York, N.Y.)*, *350*(6267), 1541–1545. <https://doi.org/10.1126/science.aad3558>

Savojardo, C., Martelli, P. L., Fariselli, P., Profiti, G., & Casadio, R. (2018). BUSCA: an integrative web server to predict subcellular localization of proteins. In *Nucleic Acids Research* (Vol. 46, Issue W1, pp. W459–W466). Oxford University Press (OUP). <https://doi.org/10.1093/nar/gky320>

Schäfer, H., Myronova, N., & Boden, R. (2010). Microbial degradation of dimethylsulphide and related C1-sulphur compounds: organisms and pathways controlling fluxes of sulphur in the biosphere. In *Journal of Experimental Botany* (Vol. 61, Issue 2, pp. 315–334). Oxford University Press (OUP). <https://doi.org/10.1093/jxb/erp355>

Schäfer, H., & Eyice, Ö. (2019). Microbial Cycling of Methanethiol. In *Methylotrophs and Methylotroph Communities*. Caister Academic Press. <https://doi.org/10.21775/9781912530045.09>

Schuler, C. G., Havig, J. R., & Hamilton, T. L. (2017). Hot Spring Microbial Community Composition, Morphology, and Carbon Fixation: Implications for Interpreting the Ancient Rock Record. In *Frontiers in Earth Science* (Vol. 5). Frontiers Media SA. <https://doi.org/10.3389/feart.2017.00097>

Schulte, M. D., & Rogers, K. L. (2004). Thiols in hydrothermal solution: standard partial molal properties and their role in the organic geochemistry of hydrothermal environments. In *Geochimica et Cosmochimica Acta* (Vol. 68, Issue 5, pp. 1087–1097). Elsevier BV. <https://doi.org/10.1016/j.gca.2003.06.001>

Schulte, M. (2010). Organic Sulfides in Hydrothermal Solution: Standard Partial Molal Properties and Role in Organic Geochemistry of Hydrothermal Environments. In *Aquatic Geochemistry* (Vol. 16, Issue 4, pp. 621–637). Springer Science and Business Media LLC. <https://doi.org/10.1007/s10498-010-9102-3>

Seemann, T. (2014). Prokka: rapid prokaryotic genome annotation. In *Bioinformatics* (Vol. 30, Issue 14, pp. 2068–2069). Oxford University Press (OUP). <https://doi.org/10.1093/bioinformatics/btu153>

Suzuki, I. (1999). Oxidation of inorganic sulfur compounds: Chemical and enzymatic reactions. *Canadian Journal of Microbiology*, 45(2), 97–105. <https://doi.org/10.1139/w98-223>

Slobodkin, A. I., Tourova, T. P., Kuznetsov, B. B., Kostrikina, N. A., Chernyh, N. A., & Bonch-Osmolovskaya, E. A. (1999). *Thermoanaerobacter siderophilus* sp. nov., a novel dissimilatory Fe(III)-reducing, anaerobic, thermophilic bacterium. In *International Journal of Systematic and Evolutionary Microbiology* (Vol. 49, Issue 4, pp. 1471–1478). Microbiology Society. <https://doi.org/10.1099/00207713-49-4-1471>

Slobodkin, A. I., Reysenbach, A.-L., Slobodkina, G. B., Baslerov, R. V., Kostrikina, N. A., Wagner, I. D., & Bonch-Osmolovskaya, E. A. (2012). *Thermosulfurimonas dismutans* gen. nov., sp. nov., an extremely thermophilic sulfur-disproportionating bacterium from a deep-sea hydrothermal vent. In *International Journal of Systematic and Evolutionary Microbiology* (Vol. 62, Issue Pt\_11, pp. 2565–2571). Microbiology Society. <https://doi.org/10.1099/ijs.0.034397-0>

Slobodkin, A. I., Reysenbach, A.-L., Slobodkina, G. B., Kolganova, T. V., Kostrikina, N. A., & Bonch-Osmolovskaya, E. A. (2013). *Dissulfuribacter thermophilus* gen. nov., sp. nov., a thermophilic, autotrophic, sulfur-disproportionating, deeply branching deltaproteobacterium from a deep-sea hydrothermal vent. In *International Journal of Systematic and Evolutionary Microbiology* (Vol. 63, Issue Pt\_6, pp. 1967–1971). Microbiology Society. <https://doi.org/10.1099/ijs.0.046938-0>

Slobodkin, A. I., Slobodkina, G. B., Panteleeva, A. N., Chernyh, N. A., Novikov, A. A., & Bonch-Osmolovskaya, E. A. (2016). *Dissulfurimicrobium hydrothermale* gen. nov., sp. nov., a thermophilic, autotrophic, sulfur-disproportionating deltaproteobacterium isolated from a hydrothermal pond. *International journal of systematic and evolutionary microbiology*, 66(2), 1022–1026. <https://doi.org/10.1099/ijsem.0.000828>

Slobodkin, A. I., & Slobodkina, G. B. (2019). Diversity of Sulfur-Disproportionating Microorganisms. In *Microbiology* (Vol. 88, Issue 5, pp. 509–522). Pleiades Publishing Ltd. <https://doi.org/10.1134/s0026261719050138>

Slobodkina, G. B., Kolganova, T. V., Kopitsyn, D. S., Viryasov, M. B., Bonch-Osmolovskaya, E. A., & Slobodkin, A. I. (2016). *Dissulfurirhabdus thermomarina* gen. nov., sp. nov., a thermophilic, autotrophic, sulfite-reducing and disproportionating deltaproteobacterium isolated from a shallow-sea hydrothermal vent. In *International Journal of Systematic and Evolutionary Microbiology* (Vol. 66, Issue 7, pp. 2515–2519). Microbiology Society. <https://doi.org/10.1099/ijsem.0.001083>

Slobodkina, G. B., Reysenbach, A.-L., Kolganova, T. V., Novikov, A. A., Bonch-Osmolovskaya, E. A., & Slobodkin, A. I. (2017). *Thermosulfuriphilus ammonigenes* gen. nov., sp. nov., a thermophilic, chemolithoautotrophic bacterium capable of respiratory ammonification of nitrate with elemental sulfur. In *International Journal of Systematic and Evolutionary Microbiology* (Vol. 67, Issue 9, pp. 3474–3479). Microbiology Society. <https://doi.org/10.1099/ijsem.0.002142>



Slobodkina, G. B., Mardanov, A. V., Ravin, N. V., Frolova, A. A., Chernyh, N. A., Bonch-Osmolovskaya, E. A., & Slobodkin, A. I. (2017). Respiratory Ammonification of Nitrate Coupled to Anaerobic Oxidation of Elemental Sulfur in Deep-Sea Autotrophic Thermophilic *Bacteria*. In *Frontiers in Microbiology* (Vol. 8). Frontiers Media SA. <https://doi.org/10.3389/fmicb.2017.00087>

Smeulders, M. J., Barends, T. R. M., Pol, A., Scherer, A., Zandvoort, M. H., Udvarhelyi, A., Khadem, A. F., Menzel, A., Hermans, J., Shoeman, R. L., Wessels, H. J. C. T., van den Heuvel, L. P., Russ, L., Schlichting, I., Jetten, M. S. M., & Op den Camp, H. J. M. (2011). Evolution of a new enzyme for carbon disulphide conversion by an acidothermophilic archaeon. In *Nature* (Vol. 478, Issue 7369, pp. 412–416). Springer Science and Business Media LLC. <https://doi.org/10.1038/nature10464>

Smith, J. W. (2000). Isotopic fractionations accompanying sulfur hydrolysis. In *Geochemical journal* (Vol. 34, Issue 1, pp. 95–99). Geochemical Society of Japan. <https://doi.org/10.2343/geochemj.34.95>

Smith, J. A., Aklujkar, M., Risso, C., Leang, C., Giloteaux, L., & Holmes, D. E. (2015). Mechanisms involved in Fe(III) respiration by the hyperthermophilic archaeon *Ferroglobus placidus*. *Applied and environmental microbiology*, 81(8), 2735–2744. <https://doi.org/10.1128/AEM.04038-14>

Stackebrandt, E. & Ebers, J. (2006). Taxonomic parameters revisited: tarnished gold standards.

Stockdreher, Y., Sturm, M., Josten, M., Sahl, H. G., Dobler, N., Ziggan, R., & Dahl, C. (2014). New proteins involved in sulfur trafficking in the cytoplasm of *Allochromatium vinosum*. *The Journal of biological chemistry*, 289(18), 12390–12403. <https://doi.org/10.1074/jbc.M113.536425>

Szynkiewicz, A., Goff, F., Vaniman, D., & Pribil, M. J. (2019). Sulfur cycle in the Valles Caldera volcanic complex, New Mexico – Letter 1: Sulfate sources in aqueous system, and implications for S isotope record in Gale Crater on Mars. In *Earth and Planetary Science Letters* (Vol. 506, pp. 540–551). Elsevier BV. <https://doi.org/10.1016/j.epsl.2018.10.036>

## T

Takai, K., Nakagawa, S., Reysenbach, A.-L., & Hoek, J. (2006). Microbial ecology of mid-ocean ridges and back-arc basins. In *Back-Arc Spreading Systems: Geological, Biological, Chemical, and Physical Interactions* (pp. 185–213). American Geophysical Union. <https://doi.org/10.1029/166gm10>

Tanaka, S., & Lee, Y.-H. (1997). Control of sulfate reduction by molybdate in anaerobic digestion. In *Water Science and Technology* (Vol. 36, Issue 12, pp. 143–150). IWA Publishing. <https://doi.org/10.2166/wst.1997.0441>

Tanizawa, Y., Fujisawa, T., & Nakamura, Y. (2017). DFAST: a flexible prokaryotic genome annotation pipeline for faster genome publication. In J. Hancock (Ed.), *Bioinformatics* (Vol. 34, Issue 6, pp. 1037–1039). Oxford University Press (OUP). <https://doi.org/10.1093/bioinformatics/btx713>

- Tang, W. T., Hao, T. W., & Chen, G. H. (2021). Comparative metabolic modeling of multiple sulfate-reducing prokaryotes reveals versatile energy conservation mechanisms. *Biotechnology and bioengineering*, 118(7), 2676–2693. <https://doi.org/10.1002/bit.27787>
- Tanimoto, Y., & Bak, F. (1994). Anaerobic degradation of methylmercaptan and dimethyl sulfide by newly isolated thermophilic sulfate-reducing bacteria. In *Applied and Environmental Microbiology* (Vol. 60, Issue 7, pp. 2450–2455). American Society for Microbiology. <https://doi.org/10.1128/aem.60.7.2450-2455.1994>
- Tarasov, V. G., Gebruk, A. V, Mironov, A. N., & Moskalev, L. I. (2005). Deep-sea and shallow-water hydrothermal vent communities: Two different phenomena? *Chemical Geology*, 224(1), 5–39. <https://doi.org/https://doi.org/10.1016/j.chemgeo.2005.07.021>
- Tasaki, M., Kamagata, Y., Nakamura, K., & Mikami, E. (1991). Isolation and characterization of a thermophilic benzoate-degrading, sulfate-reducing bacterium, *Desulfotomaculum thermobenzoicum* sp. nov. In *Archives of Microbiology* (Vol. 155, Issue 4). Springer Science and Business Media LLC. <https://doi.org/10.1007/bf00243454>
- Tatusova, T., DiCuccio, M., Badretdin, A., Chetvernin, V., Nawrocki, E. P., Zaslavsky, L., Lomsadze, A., Pruitt, K. D., Borodovsky, M., & Ostell, J. (2016). NCBI prokaryotic genome annotation pipeline. In *Nucleic Acids Research* (Vol. 44, Issue 14, pp. 6614–6624). Oxford University Press (OUP). <https://doi.org/10.1093/nar/gkw569>
- Thamdrup, B., Finster, K., Hansen, J. W., & Bak, F. (1993). Bacterial Disproportionation of Elemental Sulfur Coupled to Chemical Reduction of Iron or Manganese. In *Applied and Environmental Microbiology* (Vol. 59, Issue 1, pp. 101–108). American Society for Microbiology. <https://doi.org/10.1128/aem.59.1.101-108.1993>
- Thorup, C., Schramm, A., Findlay, A. J., Finster, K. W., & Schreiber, L. (2017). Disguised as a Sulfate Reducer: Growth of the Deltaproteobacterium *Desulfurivibrio alkaliphilus* by Sulfide Oxidation with Nitrate. In D. K. Newman (Ed.), *mBio* (Vol. 8, Issue 4). American Society for Microbiology. <https://doi.org/10.1128/mbio.00671-17>
- Tsallagov, S. I., Sorokin, D. Y., Tikhonova, T. V., Popov, V. O., & Muyzer, G. (2019). Comparative Genomics of *Thiohalobacter thiocyanaticus* HRh1T and *Guyparkeria* sp. SCN-R1, Halophilic Chemolithoautotrophic Sulfur-Oxidizing *Gammaproteobacteria* Capable of Using Thiocyanate as Energy Source. In *Frontiers in Microbiology* (Vol. 10). Frontiers Media SA. <https://doi.org/10.3389/fmicb.2019.00898>
- Tsola, S. L., Zhu, Y., Ghurnee, O., Economou, C. K., Trimmer, M., & Eyice, Ö. (2021). Diversity of dimethylsulfide-degrading methanogens and sulfate-reducing bacteria in anoxic sediments along the Medway Estuary, UK. *Environmental microbiology*, 23(8), 4434–4449. <https://doi.org/10.1111/1462-2920.15637>

## V

Vallenet, D., Calteau, A., Cruveiller, S., Gachet, M., Lajus, A., Josso, A., Mercier, J., Renaux, A., Rollin, J., Rouy, Z., Roche, D., Scarpelli, C., & Médigue, C. (2017). MicroScope in 2017: an expanding and evolving integrated resource for community expertise of microbial genomes. In *Nucleic Acids Research* (Vol. 45, Issue D1, pp. D517–D528). Oxford University Press (OUP). <https://doi.org/10.1093/nar/gkw1101>

Van Dover (2000). *The ecology of Deep-Sea Hydrothermal Vents*. Princeton University Press.

Van Leerdam, R. C., de Bok, F. A. M., Bonilla-Salinas, M., van Doesburg, W., Lomans, B. P., Lens, P. N. L., Stams, A. J. M., & Janssen, A. J. H. (2008). Methanethiol degradation in anaerobic bioreactors at elevated pH ( $\geq 8$ ): Reactor performance and microbial community analysis. In *Bioresource Technology* (Vol. 99, Issue 18, pp. 8967–8973). Elsevier BV. <https://doi.org/10.1016/j.biortech.2008.05.007>

Van Vliet, D. M., von Meijenfildt, F., Dutilh, B. E., Villanueva, L., Sinninghe Damsté, J. S., Stams, A., & Sánchez-Andrea, I. (2021). The bacterial sulfur cycle in expanding dysoxic and euxinic marine waters. *Environmental microbiology*, 23(6), 2834–2857. <https://doi.org/10.1111/1462-2920.15265>

Vanwonterghem, I., Evans, P. N., Parks, D. H., Jensen, P. D., Woodcroft, B. J., Hugenholtz, P., & Tyson, G. W. (2016). Methylotrophic methanogenesis discovered in the archaeal phylum *Verstraetearchaeota*. In *Nature Microbiology* (Vol. 1, Issue 12). Springer Science and Business Media LLC. <https://doi.org/10.1038/nmicrobiol.2016.170>

Vincent, K. A., Belsey, N. A., Lubitz, W., & Armstrong, F. A. (2006). Rapid and reversible reactions of [NiFe]-hydrogenases with sulfide. *Journal of the American Chemical Society*, 128(23), 7448–7449. <https://doi.org/10.1021/ja061732f>

Visscher, P. T., Baumgartner, L. K., Buckley, D. H., Rogers, D. R., Hogan, M. E., Raleigh, C. D., Turk, K. A., & Des Marais, D. J. (2003). Dimethyl sulphide and methanethiol formation in microbial mats: potential pathways for biogenic signatures. In *Environmental Microbiology* (Vol. 5, Issue 4, pp. 296–308). Wiley. <https://doi.org/10.1046/j.1462-2920.2003.00418.x>

Von Damm, K. L. (1995). Temporal and compositional diversity in seafloor hydrothermal fluids. In *Reviews of Geophysics* (Vol. 33, Issue S2, pp. 1297–1305). American Geophysical Union (AGU). <https://doi.org/10.1029/95rg00283>

## W

Wacey, D., Kilburn, M. R., Saunders, M., Cliff, J., & Brasier, M. D. (2011). Microfossils of sulphur-metabolizing cells in 3.4-billion-year-old rocks of Western Australia. In *Nature Geoscience* (Vol. 4, Issue 10, pp. 698–702). Springer Science and Business Media LLC. <https://doi.org/10.1038/ngeo1238>



- Waite, D. W., Chuvochina, M., Pelikan, C., Parks, D. H., Yilmaz, P., Wagner, M., Loy, A., Naganuma, T., Nakai, R., Whitman, W. B., Hahn, M. W., Kuever, J., & Hugenholtz, P. (2020). Proposal to reclassify the proteobacterial classes *Deltaproteobacteria* and *Oligoflexia*, and the phylum *Thermodesulfobacteria* into four phyla reflecting major functional capabilities. *International journal of systematic and evolutionary microbiology*, 70(11), 5972–6016. <https://doi.org/10.1099/ijsem.0.004213>
- Wang, L., Cheung, M. K., Liu, R., Wong, C. K., Kwan, H. S., & Hwang, J. S. (2017). Diversity of Total Bacterial Communities and Chemoautotrophic Populations in Sulfur-Rich Sediments of Shallow-Water Hydrothermal Vents off Kueishan Island, Taiwan. *Microbial ecology*, 73(3), 571–582. <https://doi.org/10.1007/s00248-016-0898-2>
- Wang, R., Lin, J. Q., Liu, X. M., Pang, X., Zhang, C. J., Yang, C. L., Gao, X. Y., Lin, C. M., Li, Y. Q., Li, Y., Lin, J. Q., & Chen, L. X. (2019). Sulfur Oxidation in the Acidophilic Autotrophic *Acidithiobacillus* spp. *Frontiers in microbiology*, 9, 3290. <https://doi.org/10.3389/fmicb.2018.03290>
- Wang, S., Jiang, L., Hu, Q., Liu, X., Yang, S., & Shao, Z. (2021). Elemental sulfur reduction by a deep-sea hydrothermal vent *Campylobacterium Sulfurimonas* sp. NW10. *Environmental microbiology*, 23(2), 965–979. <https://doi.org/10.1111/1462-2920.15247>
- Ward, L. M., Bertran, E., & Johnston, D. T. (2020a). Draft Genome Sequence of *Desulfovibrio sulfodismutans* ThAc01, a Heterotrophic Sulfur-Disproportionating Member of the *Desulfobacterota*. *Microbiology resource announcements*, 9(13), e00202-20. <https://doi.org/10.1128/MRA.00202-20>
- Ward, L. M., Bertran, E., & Johnston, D. T. (2020b). Genomic sequence analysis of *Dissulfurirhabdus thermomarina* SH388 and proposed reassignment to *Dissulfurirhabdaceae* fam. nov. *Microbial genomics*, 6(7), mgen000390. <https://doi.org/10.1099/mgen.0.000390>
- Ward, L. M., Bertran, E., & Johnston, D. T. (2021). Expanded Genomic Sampling Refines Current Understanding of the Distribution and Evolution of Sulfur Metabolisms in the *Desulfobulbales*. *Frontiers in microbiology*, 12, 666052. <https://doi.org/10.3389/fmicb.2021.666052>
- Wasmund, K., Mußmann, M., & Loy, A. (2017). The life sulfuric: microbial ecology of sulfur cycling in marine sediments. In *Environmental Microbiology Reports* (Vol. 9, Issue 4, pp. 323–344). Wiley. <https://doi.org/10.1111/1758-2229.12538>
- Wayne, L. G., Moore, W. E. C., Stackebrandt, E., Kandler, O., Colwell, R. R., Krichevsky, M. I., Truper, H. G., Murray, R. G. E., Grimont, P. A. D., Brenner, D. J., Starr, M. P., & Moore, L. H. (1987). Report of the Ad Hoc Committee on Reconciliation of Approaches to Bacterial Systematics. In *International Journal of Systematic and Evolutionary Microbiology* (Vol. 37, Issue 4, pp. 463–464). Microbiology Society. <https://doi.org/10.1099/00207713-37-4-463>
- Wemheuer, B., Taube, R., Akyol, P., Wemheuer, F., & Daniel, R. (2013). Microbial diversity and biochemical potential encoded by thermal spring metagenomes derived from the Kamchatka Peninsula. *Archaea* (Vancouver, B.C.), 2013, 136714. <https://doi.org/10.1155/2013/136714>

Wheat, C. G., Mottl, M. J., Fisher, A. T., Kadko, D., Davis, E. E., & Baker, E. (2004). Heat flow through a basaltic outcrop on a sedimented young ridge flank. In *Geochemistry, Geophysics, Geosystems* (Vol. 5, Issue 12, p. n/a-n/a). American Geophysical Union (AGU). <https://doi.org/10.1029/2004gc000700>

Weiss, M. C., Sousa, F. L., Mrnjavac, N., Neukirchen, S., Roettger, M., Nelson-Sathi, S., & Martin, W. F. (2016). The physiology and habitat of the last universal common ancestor. In *Nature Microbiology* (Vol. 1, Issue 9). Springer Science and Business Media LLC. <https://doi.org/10.1038/nmicrobiol.2016.116>

Wick, R. R., Schultz, M. B., Zobel, J., & Holt, K. E. (2015). Bandage: interactive visualization of de novo genome assemblies. In *Bioinformatics* (Vol. 31, Issue 20, pp. 3350–3352). Oxford University Press (OUP). <https://doi.org/10.1093/bioinformatics/btv383>

Wick, R. R., Judd, L. M., Gorrie, C. L., & Holt, K. E. (2017). Unicycler: Resolving bacterial genome assemblies from short and long sequencing reads. In A. M. Phillippy (Ed.), *PLoS Computational Biology* (Vol. 13, Issue 6, p. e1005595). Public Library of Science (PLoS). <https://doi.org/10.1371/journal.pcbi.1005595>

Wilkins, L., Ettinger, C. L., Jospin, G., & Eisen, J. A. (2019). Metagenome-assembled genomes provide new insight into the microbial diversity of two thermal pools in Kamchatka, Russia. *Scientific reports*, 9(1), 3059. <https://doi.org/10.1038/s41598-019-39576-6>

Wójcik-Augustyn, A., Johansson, A. J., & Borowski, T. (2021). Reaction mechanism catalyzed by the dissimilatory adenosine 5'-phosphosulfate reductase. Adenosine 5'-monophosphate inhibitor and key role of arginine 317 in switching the course of catalysis. *Biochimica et biophysica acta. Bioenergetics*, 1862(1), 148333. <https://doi.org/10.1016/j.bbabi.2020.148333>

Wood, P. M. (1981). The redox potential for dimethyl sulphoxide reduction to dimethyl sulphide. In *FEBS Letters* (Vol. 124, Issue 1, pp. 11–14). Wiley. [https://doi.org/10.1016/0014-5793\(81\)80042-7](https://doi.org/10.1016/0014-5793(81)80042-7)

Wu, C. H., Schut, G. J., Poole, F. L., 2nd, Haja, D. K., & Adams, M. (2018). Characterization of membrane-bound sulfane reductase: A missing link in the evolution of modern day respiratory complexes. *The Journal of biological chemistry*, 293(43), 16687–16696. <https://doi.org/10.1074/jbc.RA118.005092>

Wu, B., Liu, F., Fang, W., Yang, T., Chen, G. H., He, Z., & Wang, S. (2021). Microbial sulfur metabolism and environmental implications. *The Science of the total environment*, 778, 146085. <https://doi.org/10.1016/j.scitotenv.2021.146085>

## Y

Yao, X.-Z., Chu, Y.-X., Wang, C., Li, H.-J., Kang, Y.-R., & He, R. (2019). Enhanced removal of methanethiol and its conversion products in the presence of methane in biofilters. In *Journal of Cleaner Production* (Vol. 215, pp. 75–83). Elsevier BV. <https://doi.org/10.1016/j.jclepro.2019.01.019>

Yarza, P., Yilmaz, P., Pruesse, E., Glöckner, F. O., Ludwig, W., Schleifer, K.-H., Whitman, W. B., Euzéby, J., Amann, R., & Rosselló-Móra, R. (2014). Uniting the classification of cultured and uncultured bacteria and archaea using 16S rRNA gene sequences. In *Nature Reviews Microbiology* (Vol. 12, Issue 9, pp. 635–645). Springer Science and Business Media LLC. <https://doi.org/10.1038/nrmicro3330>

Yoon, S.-H., Ha, S., Lim, J., Kwon, S., & Chun, J. (2017). A large-scale evaluation of algorithms to calculate average nucleotide identity. In *Antonie van Leeuwenhoek* (Vol. 110, Issue 10, pp. 1281–1286). Springer Science and Business Media LLC. <https://doi.org/10.1007/s10482-017-0844-4>

## Z

Zeng, X., Alain, K. & Shao, Z. Microorganisms from deep-sea hydrothermal vents. *Mar Life Sci Technol* 3, 204–230 (2021). <https://doi.org/10.1007/s42995-020-00086-4>

Zhang, J., Liu, R., Xi, S., Cai, R., Zhang, X., & Sun, C. (2020). A novel bacterial thiosulfate oxidation pathway provides a new clue about the formation of zero-valent sulfur in deep sea. *The ISME journal*, 14(9), 2261–2274. <https://doi.org/10.1038/s41396-020-0684-5>

Zhang, L., Qiu, Y. Y., Zhou, Y., Chen, G. H., van Loosdrecht, M., & Jiang, F. (2021). Elemental sulfur as electron donor and/or acceptor: Mechanisms, applications and perspectives for biological water and wastewater treatment. *Water research*, 202, 117373. <https://doi.org/10.1016/j.watres.2021.117373>

**Titre :** Études physiologiques et multi-omiques de métabolismes du soufre présents dans les écosystèmes hydrothermaux

**Mots clés :** Cycle du soufre, Dismutation, Comproportionnement, Composés organiques soufrés, Hydrothermal

**Résumé :** Les cheminées hydrothermales hébergent une vaste diversité microbienne, tant au niveau taxonomique qu'au niveau métabolique. Ces écosystèmes sont qualifiés d'extrêmes, en raison des très larges gradients physico-chimiques qu'ils abritent. Le soufre y est un élément omniprésent, il peut être utilisé par une large diversité de microorganismes pour des réactions d'oxydations ou de réductions. Cependant, le cycle du soufre reste partiellement méconnu au sein de ces écosystèmes. L'objectif de cette thèse était d'étudier les métabolismes du cycle du soufre peu documentés ou simplement prédits par la thermodynamique, au sein des écosystèmes hydrothermaux, à savoir la dismutation des composés inorganiques soufrés, le catabolisme des composés organosoufrés et le comproportionnement du soufre. Quatre nouveaux taxons dismutant les composés inorganiques soufrés ont été découverts au cours de cette étude et des analyses génomiques approfondies ont été menées pour décrypter les voies de la dismutation des composés inorganiques soufrés. Des analyses en génomique comparative ont permis d'identifier un cluster de gènes potentiellement impliqué dans la dismutation du soufre élémentaire chez des bactéries hydrothermales marines, mais ce résultat nécessitera d'être confirmé par des approches fonctionnelles. Enfin, les communautés microbiennes de sources chaudes des îles Kerguelen très isolées géographiquement ont été étudiées par métagénomique, ce qui a révélé la présence de nombreuses nouvelles lignées de bactéries et d'archées dans ces habitats jamais étudié auparavant.

---

**Title:** Physiological and multi-omics studies of microbial sulfur metabolisms present in hydrothermal ecosystems

**Keywords:** Sulfur cycle, Disproportionation, Comproportionation, Organic sulfur compounds, Hydrothermal

**Abstract:** Hydrothermal vents host a vast microbial diversity, both at the taxonomic and metabolic levels. These ecosystems are qualified as extreme, because they harbor harsh physico-chemical gradients. Sulfur is omnipresent in these environments, and it can be used by a large diversity of microorganisms for oxidation or reduction reactions. However, the sulfur cycle remains partially unknown in these ecosystems. The objective of this thesis was to study the poorly documented or thermodynamically predicted metabolisms of the sulfur cycle in hydrothermal ecosystems, namely the dismutation of inorganic sulfur compounds, the catabolism of organosulfur compounds and the comproportionation of sulfur. Four new inorganic sulfur compound disproportionating taxa were discovered during this study and extensive genomic analyses were conducted to decipher the pathways of inorganic sulfur compound dismutation. Comparative genomics analyses identified a gene cluster potentially involved in elemental sulfur dismutation in marine hydrothermal bacteria, but this result will need to be confirmed by functional approaches. Finally, the microbial communities of the geographically isolated hot springs from the Kerguelen Islands were studied by metagenomics, revealing the presence of many new lineages of bacteria and archaea in these previously unstudied habitats.